The Role of Macrophage Steroid Metabolism in Chronic Inflammation

By

Claire Syme Martin

A thesis submitted to the University of Birmingham for the degree of

DOCTOR OF PHILOSOPHY

Institute of Metabolism and Systems Research

College of Medical and Dental Sciences

University of Birmingham

April 2023

Abstract

Macrophages are central to both the pathology and resolution of chronic inflammatory diseases such as rheumatoid arthritis (RA). Steroid hormones such as glucocorticoids (GCs) and androgens are reported to be important modulators of macrophage functions. However, the role of intracrine and paracrine steroid metabolism in the regulation of macrophage inflammatory function in RA remains poorly understood. Using transcriptional analysis of human RA synovial macrophages, we showed that differential expression of steroidogenic enzymes: the GC-activating enzyme 11β-HSD1 and late androgen activating enzyme SRD5A1, expressed within pathogenic macrophage subsets, increased with inflammation, while the early androgen activator AKR1C3, expressed by protective macrophages, decreased with inflammation. In vitro monocyte-derived macrophages were used to interrogate steroidogenesis and effects of intracrine steroid metabolism on inflammatory functions relevant to RA. Intracrine GC metabolism increased with inflammatory polarisation, enabling acquisition of a pro-resolution phenotype at the expense of inflammatory functions on GC stimulation. Therapeutic targeting of this pathway to promote anti-inflammatory actions of GCs was assessed using sheared gellan hydrogels, with proof of principle studies showing selective inflammatory macrophage GC-mediated regulation. Androgen metabolism was strongly increased by pro-inflammatory polarisation of macrophages. Although intracrine androgen metabolism did not regulate inflammation, our data suggest a role for inflammatory macrophages as paracrine androgen activators. This thesis describes distinct patterns of inflammation-induced steroid metabolism in RA synovial macrophage subsets that could be exploited by novel therapeutics for inflammatory diseases.

For my gran, Eileen Martin, thank you for always reminding me to have fun

Q. Do you think the scientific world is too solemn?

A. Oh, no. Not true science. It's art. Actually, it's a sandbox and scientists get to play all of our lives.

– Polly Matzinger, 1998

Acknowledgements

I would first like to thank my supervisors. Here, Dr Rowan Hardy was a perfectly cromulent supervisor; thank you for your boundless enthusiasm and support, particularly during the many difficult times in this PhD. Thank you to Professor Martin Hewison for your guidance, insight and motivation that kept reminding me of the bigger picture. Thank you to the MIDAS programme leads and my funders, the Wellcome Trust. I'm grateful to all the NHS Blood and Transplant staff and donors and QEUHB rheumatology staff and patients, who made this research possible. Parts of Figures were created using images from Servier Medical Art by Servier, licensed under a Creative Commons Attribution 3.0 Unported Licence.

I am very grateful to Professor Andy Clark, Dr John O'Neil, and Dr Sally Clayton, who provided invaluable macrophage insights, advice and help with experiments. Thank you to everyone involved in the Accelerating Medicines Partnership RA phase 1 programme (study accession: SDY998), in particular Professor Andrew Filer and Dr Jason Turner for generating the R script that provided access to the bulk RNA-seq data. The scRNA-seq analysis was kindly carried out by the research group of Professor Mariola Kurowska-Stolarska at the University of Glasgow. Thank you to Hardy group members Ana Crastin and Matthew Singh Kalirai for the incredible work you contributed to this thesis, I wish you both the very best of luck with your careers. The hydrogel work in this thesis was greatly supported by Professor Liam Grover's team, especially Dr Richard Moakes. Thank you to the good Drs Slater and Williams of the Gkoutos group for stats advice, computational analysis (and script debugging) and for always surmounting the biology-computer science binary.

I would like to thank everyone in the IMSR who gave their support, whether practical, emotional or (often) both. Especially to my Hardy group alumni Chloe and Justine, and to Kat and Becky. Thank you to my fellow MIDAS cohort: Laura B, Ailbhe, Laura H, Veronika and Alex. Also thank you to everyone at my new lab home in the ODDI for making me feel welcome.

Thank you to my family for your support and for not asking me “are you still doing the PhD?” too many times. I hope my nephews Eli and Arthur have the same opportunities to be inspired by science that I had when I was younger. I’m so grateful to my Glasgow friends Amber, Elliot, Jonny, Kenny, Matt, Nicole, Stu and Rix. Thank you so much for all the board games and hours of highly tangential chat, and for always making me feel like I’m home again. Thank you to my ACORN comrades, especially James and Patrick, for the jazz punk discourse and radical friendship. Thank you also to my London friends Adam, Alex, Brian, Ellie, Farah and Seb for your daily love and encouragement from across the world.

Finally thank you to my wonderful partner Karin for your endless support, proof-reading, but above all the joy you bring to my life.

Table of Contents

List of Figures

List of Tables

Abbreviations

11β-HSD1	11β-hydroxysteroid dehydrogenase type 1
11β-HSD2	11β-hydroxysteroid dehydrogenase type 2
^{3}H	Tritium
5α-dione	Androstanedione
A4	Androstenedione
ACTH	Adrenocorticotropic hormone
AKR1C3	Aldo-keto reductase family 1 member C3
AIA	Antigen induced arthritis
AMP	Accelerating Medicines Partnership
AP-1	Activator protein 1
AR	Androgen receptor
AU	Arbitrary unit
BSA	Bovine serum albumin
CAIA	Collagen antibody-induced arthritis
CBG	Corticosteroid-binding globulin
cDNA	Complementary deoxyribonucleic acid
CIA	Collagen induced arthritis
COPD	Chronic obstructive pulmonary disease
CRP	C-reactive protein
Ct	Cycle threshold
CVD	Cardiovascular disease
DAMP	Damage-associated molecular marker
DAS28	Disease activity score
DAS28-CRP	Disease activity score 28-C reactive protein
DHEA	Dehydroepiandrosterone

DHT	Dihydrotestosterone
DMARD	Disease-modifying antirheumatic drug
E	Cortisone
ECM	Extracellular matrix
ELISA	Enzyme-linked immunosorbent assay
ESR	Erythrocyte sedimentation rate
EULAR	European League Against Rheumatism
F	Cortisol
FACS	Fluorescence-activated cell sorting
FCS	Foetal calf serum
FLS	Fibroblast-like synoviocytes
GC	Glucocorticoid
GILZ	Glucocorticoid-induced leucine zipper
GM-CSF	Granulocyte macrophage colony-stimulating factor
GR	Glucocorticoid receptor
GRE	Glucocorticoid-response element
H6PDH	Hexose-6-phosphate dehydrogenase
HIFα	Hypoxia-inducible factor alpha
HLA	Human leukocyte antigen
HPA	Hypothalamic-pituitary-adrenal
HRP	Horseradish peroxidase
HSC	Haematopoietic stem cell
IFNγ	Interferon gamma
IA	Intra-articular
IL	Interleukin
LC-MS/MS	Liquid chromatography with tandem mass spectrometry
LPS	Lipopolysaccharide
M-CSF	Macrophage colony-stimulating factor

MAPK	Mitogen-activated protein kinase
MHCII	Major histocompatibility complex II
MMP	Matrix metalloproteinase
MPS	Mononuclear phagocyte system
MR	Mineralocorticoid receptor
mRNA	Messenger ribonucleic acid
NAD	Nicotinamide adenine dinucleotide
NADPH	Nicotinamide adenine dinucleotide phosphate
NFκB	Nuclear factor kappa-light-chain-enhancer of activated B cells
NOS	Nitric oxide synthase
OA	Osteoarthritis
OD	Optical density
OPG	Osteoprotegerin
PAMP	Pathogen-associated molecular marker
PBMC	Peripheral blood mononuclear cell
PBS	Phosphate buffered saline
Pen/strep	Penicillin/streptomycin
qPCR	Quantitative polymerase chain reaction
RA	Rheumatoid arthritis
RANK	Receptor activator of nuclear factor kappa-B
RANKL	Receptor activator of nuclear factor kappa-B ligand
ROS	Reactive oxygen species
RNA-seq	RNA sequencing
SRD5A1	Steroid 5α-reductase 1
T	Testosterone
Th cell	T helper cell
THE	Tetrahydrocortisone
THF	Tetrahydrocortisol

TLC	Thin layer chromatography
TLR	Toll-like receptor
TNF-tg	TNF-transgenic
TPM	Transcripts per million
TNFα	Tumour necrosis factor alpha
VEGF	Vascular endothelial growth factor
WT	Wildtype

Chapter 1 INTRODUCTION:

1.1 Rheumatoid arthritis

1.1.1 Clinical manifestations and diagnosis

Rheumatoid arthritis (RA) is an autoimmune inflammatory disease of the joints which has an overall prevalence of around 1% in Western countries. The lifetime risk of developing RA is 3.6% in females and 1.7% in males in the US (1). RA mainly targets the proximal interphalangeal and metacarpophalangeal joints of the hands, metatarsophalangeal joints of the feet, and joints of the wrists and knees. The arthritic joint is characterised by synovial hyperplasia, degradation of cartilage, and erosion of bone, which collectively lead to painful progressive disability through joint deformity and loss of function. As well as directly hampering quality of life by damage to joints, RA is linked to systemic comorbidities including increased risk of cardiovascular disease (CVD), muscle wasting, osteoporosis, and cancer (2). The strong inflammatory profile of RA, including high systemic levels of the cytokines interleukin 6 (IL-6) and tumour necrosis factor α (TNFα), and inflammatory marker C-reactive protein (CRP), have been linked to the inherent increased mortality of RA and its associated comorbidities (3, 4).

The diagnostic criteria of RA includes the number of affected joints, duration of symptoms, serology (rheumatoid factor and anti-citrullinated protein antibodies) and acute-phase reactants (CRP and erythrocyte sedimentation rate [ESR]) (5). Severity and progression of disease is assessed by measures such as Disease Activity Score 28 (DAS28), which charts

changes in number of affected joints, severity of systemic inflammation and patient-reported measures of health (6).

RA is often compared to osteoarthritis (OA), a more common inflammatory disease of the joints, which is also characterised by erosion of the bones and cartilage of the joints, pain, and disability. However, they have different aetiologies and mechanisms of disease. In contrast to the autoimmune and auto-inflammatory components of RA, OA is more associated with degeneration of joints with age or wear and tear (7). The joint destruction associated with OA results in a local chronic inflammatory response that can also spill over into systemic inflammation as measured by factors such as CRP, despite OA's earlier classification as a "noninflammatory" arthritis (8).

1.1.2 Physiology of the healthy joint

Under normal homeostatic conditions, the joint has a tightly controlled and compartmentalised structure to allow mobility, depicted in Figure 1-1 A. Each end of bone in a synovial joint is covered with a layer of articular cartilage, to absorb shock and reduce friction. The joint capsule extends from the periosteum of articulating bones to surround the joint and is composed of two layers. The outer fibrous layer or capsular ligament connects the bones and the inner synovial layer or synovium, which is highly vascularised and serves as a source of synovial fluid and nutrient exchange for the joint. The joint cavity is filled with hyaluronan-rich synovial fluid which provides shock absorption and lubrication for the moving joint, as well as nutrients for the largely non-vascularised cartilage (9, 10).

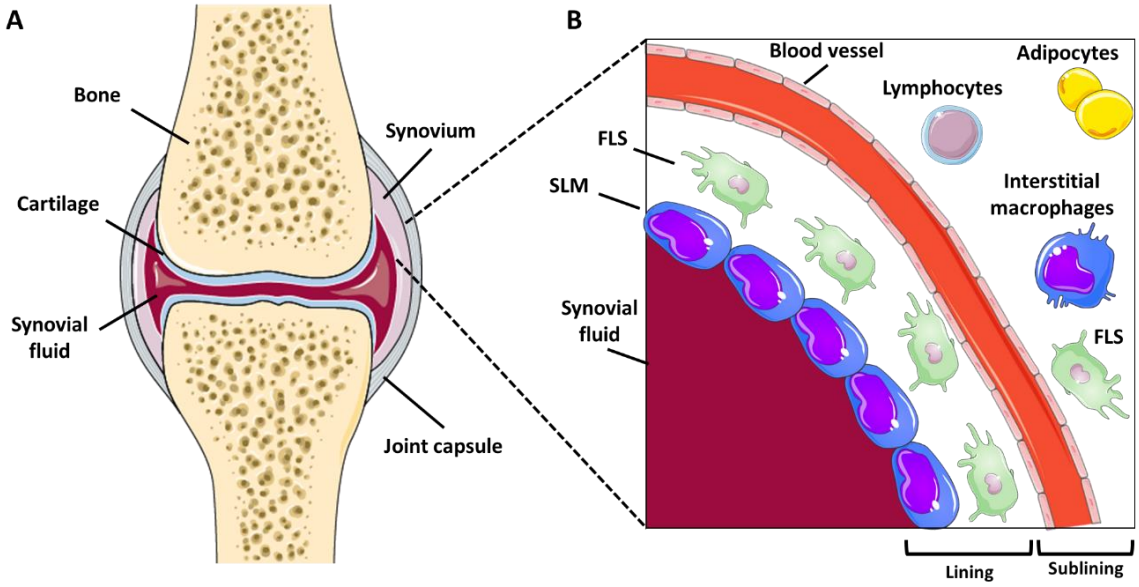

Figure 1-1 Structure of the healthy joint and synovium

(A) The synovial joint is composed of a fibrous joint capsule connecting adjacent bones, whose ends are covered in cartilage. Within the joint capsule is synovial fluid encased by the synovial membrane. (B) The intimal or lining layer of the synovium is composed of a tightly connected protective barrier of synovial lining macrophages (SLM) that sequesters the synovial fluid. SLM interact closely with fibroblast like synoviocytes (FLS). The sublining is a sparse layer of blood vessels, adipocytes, FLS and immune cells such as interstitial macrophages and lymphocytes.

The synovial membrane itself is composed of two layers: an outer sublining layer and an inner lining or intimal layer, depicted in Figure 1-1 B. The lining layer is composed of type A synoviocytes, fibroblast-like synoviocytes (FLS), and type B synoviocytes, synovial macrophages. FLS produce hyaluronic acid and lubricin for lubricating synovial fluid and extracellular matrix (ECM). FLS maintain healthy synovial fluid and ECM through a careful balance of matrix-targeting enzymes such as the matrix metalloproteinases (MMPs) and their inhibitors, tissue inhibitors of MMPs (TIMPs) (11, 12). Synovial macrophages have a high phagocytic capacity for clearance of dead cells and debris and also form an immunoprotective physical barrier, thus they help maintain a healthy joint environment (13). The sublining of the synovia has minimal cells. It is a sparse layer formed of blood vessels, fibroblasts,

adipocytes and quiescent immune cells, such as macrophages and lymphocytes. There is also a careful balance of cytokines and growth factors in the healthy joint, with pro-inflammatory cytokines outweighed by anti-inflammatory cytokines and the osteoclast activator receptor activator of nuclear factor κ-B ligand (RANKL) blocked by presence of its inhibiting decoy receptor osteoprotegrin (OPG) (9).

1.1.3 Pathophysiology of RA

RA is a complex and heterogenous disease, with different genetic and environmental influences, rates of progression, and clinical presentations. This complexity is also seen in disease pathophysiology, with numerous stromal and immune cell types, both local and recruited, identified as contributing to joint destruction and inflammation.

RA is characterised by synovitis, the inflammation of the synovial lining of a joint. This dramatically changes the structure and composition of the affected joint, as shown in Figure 1-2. An increase in synovial fibroblasts and macrophages, termed hyperplasia, transforms this usually thin and stable lining. The increased inflammatory cell mass forms a growth in the joint called a pannus (2). The macrophage population expands due to increased recruitment of circulating monocytes into the inflammatory site, where they are activated into macrophages. Macrophages in the RA joint are some of the main producers of inflammatory factors and cytokines, and therefore help to drive the inflammatory activation and joint destructive properties of neighbouring cells (discussed further in section 1.2 Macrophages).

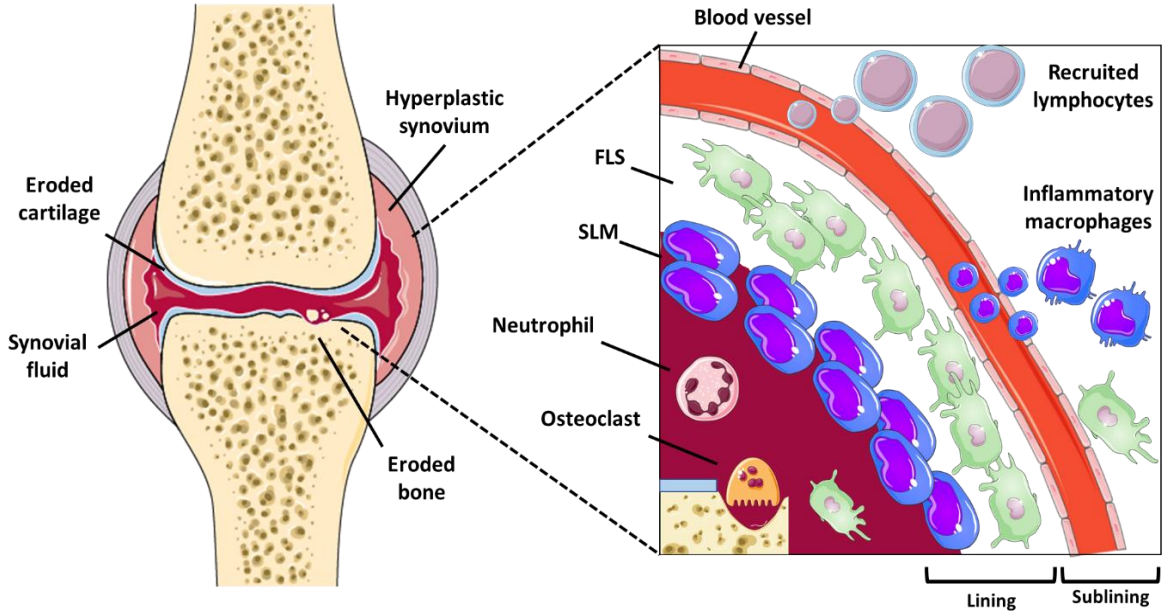

Figure 1-2 Structure of the RA joint

In RA, the bone and cartilage of the joint are degraded by inflammatory erosion and the synovium becomes a hyperplastic pannus characterised by influx of inflammatory cells. Immune cells such as neutrophils, lymphocytes and inflammatory monocyte-derived macrophages are recruited, and the layers of resident synovial lining macrophages (SLM) and fibroblast-like synoviocytes (FLS) are massively expanded with inflammatory activated cells. They secrete inflammatory factors which promote further immune cell recruitment and osteoclast erosion of bone.

Resident FLS undergo a process of pathological reprogramming, where they transform into destructive inflammatory cells (14). FLS acquire insensitivity to apoptosis-inducing factors such as inflammatory cytokines and free radicals present in the inflamed synovium, which leads to a hyperplastic pannus saturated with FLS. RA FLS also gain invasive and migratory abilities, enabling them to directly damage local cartilage and spread disease to unaffected joints. The homeostatic regulation of lubricating synovial fluid is lost and instead RA FLS metabolism shifts towards catabolism of ECM via increase in expression of MMPs and downregulation of inhibitory TIMPs (15).

In addition to direct destruction of the joint, aggressive RA FLS produce inflammatory mediators such as prostaglandins and cytokines to further promote inflammatory activation

of immune and stromal cells in the synovium. For example, FLS produce chemokines, such as CCL2, which recruit inflammatory monocytes to the joint, as well as RANKL which activates bone eroding osteoclasts, while production of vascular endothelial factor (VEGF) promotes vascularisation in the joint that promotes T and B cell influx (11). FLS also directly communicate with the endothelial cells of the joint, with IL-6 signalling from FLS promoting activated endothelial cell recruitment of lymphocytes (14, 16).

T cells and B cells are the main lymphocytes found in the arthritic joint, with CD4+ helper T cells (Th cells), particularly of the pro-inflammatory Th1 and Th17 subsets, forming the majority. These T cells release pro-inflammatory cytokines such as interferon gamma (IFNγ) and IL-17, respectively, as well as osteoclast activating RANKL to promote inflammatory joint destruction. In addition, autoreactive Th cells activate cognate B cells to form ectopic lymphoid structures, similar to germinal centres of lymph nodes, in the synovium for the local production of autoantibodies (17). Neutrophils dominate the synovial fluid and release tissue destructive factors and inflammatory mediators such as reactive oxygen species (ROS), prostaglandins and proteases (18). Many of the major pro-inflammatory cytokines in the RA joint, including TNFα, IL-1 and IL-17a, promote osteoclast differentiation via upregulation of pro-osteoclastogenic RANKL on FLS, osteoblasts and Th17 cells (19, 20). These inflammatory cytokines inhibit differentiation and promote apoptosis of osteoblasts, thereby skewing bone remodelling towards catabolic metabolism and destruction of bone driven by activated osteoclasts at the pannus (21). Similarly, the production of the cartilaginous matrix by chondrocytes becomes dysregulated, with chondrocytes being both targets and effectors of joint inflammation. Destruction of cartilage is driven by inflammatory-mediated apoptosis of chondrocytes as well as chondrocyte upregulation of collagen and proteoglycan proteinases (22, 23).

In addition to destruction and inflammation at the local synovial level, RA pathophysiology is characterised by profound systemic effects. RA patients suffer not only local juxta articular and subchondral bone loss, but also systemic osteoporosis, with low bone mineral density and a higher risk of fractures. Fat and muscle metabolism are also affected by systemic inflammation, leading to insulin resistance and cachexia (2). Collectively, these local and systemic inflammatory processes drive a vicious cycle of destruction and progression of clinical RA symptoms.

1.1.4 Insights from murine models of RA

Mouse models of arthritis have contributed greatly to understanding the mechanisms underpinning human RA. These include induced arthritis models, such as collagen-induced arthritis (CIA), in which inoculation of type II heterologous collagen in complete Freund's adjuvant triggers an arthritis-like disease. The CIA model mimics breach of tolerance and autoantibodies seen in human disease, mediated by collagen-specific T cells and anti-collagen type II antibodies from autoreactive B cells, and Th1 cytokines such as IFNγ dominate. Therefore, some key cellular characteristics of human disease are replicated in this model, such as polyarthritis with synovial hyperplasia and a bone eroding immune infiltrate. However, a single injection of heterologous collagen leads to monophasic polyarthritis with remission after around 35 days of disease (24). A more accurate representation of human disease can be obtained using further immunisation with homologous murine type II collagen, which drives chronic and relapsing arthritis (25). This model of arthritis was found to be effectively treated with blockade of TNFα, leading to the development and use of clinical TNFα inhibition through biologic drugs (26).

Genetically manipulated mouse models, in which onset of disease can be driven spontaneously, allowed a more systemic model of the cells and processes involved in inflammatory arthritis. One of the most widely used genetic models of inflammatory arthritis is the TNFα transgenic (TNF-Tg) mouse model, in which chronic overexpression of human TNFα drives disease. This model is characterised by erosive polyarthritis with a chronic relapsing progression as seen in human RA. The model also shares histological features of the inflamed synovium, including polymorphonuclear and lymphocytic immune cell infiltrate, pannus formation and erosion of cartilage and bone (27, 28). The TNF-Tg model has elucidated the regulation and functions of pro-inflammatory cytokines in RA, including the central role of TNFα as an "apex" inflammatory cytokine and its downstream mediators. It was found that blocking the actions of IL-1α and IL-1β at the IL-1 receptor prevented arthritis development in the TNF-Tg model, highlighting the importance of IL-1 cytokines as a downstream target of TNFα signalling in disease (29). Similarly, the TNF-Tg model has been used to identify the role of TNFα in inducing tissue destructive MMPs (30). The TNF-tg mouse also highlighted that marked destruction of juxta-articular cartilage and bone was identified to occur early in disease, prior to development of clinical symptoms such as paw swelling (31).

The spontaneous K/BxN mouse model was generated by crossing the T cell receptor transgenic KRN line with NOD mice that express the MHCII loci A^{g7}, each providing immune specificity for the enzyme glucose-6-phosphate isomerase (GPI) (32, 33). Transfer of serum from K/BxN mice, containing autoantibodies specific to GPI, can induce a resolving arthritic disease in several susceptible mouse strains. This model has proven useful for studying the regulation of arthritis by IL-1 and TNFα, and the roles of the complement system in joint damage (34).

Mouse models have provided extensive preclinical translational insight in the development of therapeutics aimed at management of RA and its systemic complications. These included potent biological interventions such as infliximab and etanercept which target TNFα.

1.1.5 Treating RA

Disease-modifying antirheumatic drugs (DMARDs) are a broad class of drugs that target the various processes behind RA pathology, with the aim of reducing inflammatory tissue damage. The variety of DMARDs available reflects the vast heterogeneity of RA, with patients often requiring "multiple successive therapies throughout life" with different regimens (35). Current clinical guidelines are to begin DMARD treatment as soon as possible after diagnosis, given extensive evidence that early therapeutic intervention is vital to limit progression of disease (36, 37).

Initial DMARD treatment includes nonsteroidal anti-inflammatory drugs (NSAIDs), such as ibuprofen, and the antimetabolite methotrexate (MTX), which is thought to inhibit adaptive immune cell activation. If initial treatment does not successfully reduce symptoms, patients can then be treated with biological DMARDs for more precise targeting of synovial inflammatory processes. These drugs block key inflammatory cytokines such as TNFα and IL-6. Newer small molecule inhibitor formulations, termed targeted synthetic DMARDs, are now also used to inhibit the JAK-STAT inflammatory signalling pathway (35).

Therapeutic glucocorticoids (GCs), such as prednisolone and dexamethasone, are synthetic steroid hormones with potent immunomodulatory and anti-inflammatory properties (reviewed in section 1.3 Glucocorticoids). Their application in RA is associated with rapid disease suppression and a reduction in joint degradation and pain (38). However, due to

severe off-target side effects, their use in RA is reserved for symptomatic flares and initial "bridging" therapy when time is needed for effects of DMARDs such as MTX to build (39). Current European League Against Rheumatism (EULAR) recommendations state that GC treatment should be "tapered as rapidly as clinically feasible" following bridging therapy due to these systemic effects, but may be given for prolonged periods at low doses (35). A recent study highlighted the benefits of low dose short term prednisone therapy in RA, finding that treatment of newly diagnosed RA patients could induce remission, where disease progression and symptoms are halted, in around 50% of patients (40).

Although DMARDs can be used to great effect in reducing symptoms, and can in some cases remission, they cannot cure RA. In addition they commonly drive adverse effects in patients; MTX can cause nausea, vomiting and depression, while the immunoinhibitory effects of biological and targeted synthetic DMARDs increase the risk of tuberculosis, urogenital tract infections and opportunistic infections (41).

For a proportion of patients, treatment with numerous DMARDs will fail to manage symptoms and progression of disease. This is defined by EULAR as "difficult-to-treat" RA, although other terms such as refractory, severe and treatment resistant are used in the clinic and literature (42). However even in refractory RA, there is considerable heterogeneity of disease presentation across patients. Patients with refractory RA may not show high levels of systemic inflammation, as measured by CRP and ESR. Similarly, serology measures, such as presence of autoantibodies, did not vary between patients with refractory or "treatment amenable" RA. The strongest predictor of advancement to refractory RA was found to be severity of disease activity at first presentation, emphasising the importance of rapid diagnosis and treatment (43).

As discussed above, macrophages are prominent cells in the synovial joint with defined roles in synovial homeostasis and progression of inflammatory arthritic disease. As such, successful therapeutic interventions in RA are often linked to their effects on macrophages (44, 45).

1.2 Macrophages

Macrophages are cells of the innate immune system which encompass a broad and dynamic range of cells with vital roles in maintaining homeostasis of tissues and immunity. They possess a remarkable level of plasticity, in which their function is dictated by a broad range of activating stimuli. Macrophage phenotype and function is also defined by their particular niche within the body, including the microglia of the brain, Kupffer cells of the liver and Hofbauer cells of the placenta. Macrophages function as immune cells, but also as key tissue remodellers during growth and maintain tissue homeostasis through close interaction with stromal cells.

Macrophages were first identified by Metchnikoff in the 19th century, who termed them after the Greek for “large eater” for their powerful phagocytic capabilities. Metchnikoff was also the first to define phagocytosis as an important method of immune defence against microorganisms (46). Macrophages can phagocytose a wide range of material, enabling destruction of microorganisms in immunity and clearance of dead or dying cells for tissue growth or resolution of inflammation. Macrophages are also professional antigen presenters, able to present fragments of engulfed material to T and B cells and thereby activate the adaptive immune response against phagocytosed particles (47).

1.2.1 Macrophage ontogeny

Macrophages are part of the mononuclear phagocyte system (MPS), which also includes monocytes and dendritic cells, a classification defined by similar morphology, phagocytic capabilities and roles including immune defence and activation of the adaptive immune system (48). Therefore, the criteria that defines whether a cell is a macrophage and not a

monocyte or dendritic cell is a topic of sometimes heated debate in immunology. Under the widely accepted classification of the MPS by Guilliams et al, monocytes, macrophages and dendritic cells can be discriminated into distinct cell types based on their cellular origin. In this model, macrophages derive from embryonic precursors, and monocytes and dendritic cells from distinct precursors of adult haematopoietic stem cell (HSC) origin (49). However, despite their ontogenic differences, these cells collectively form a vast variety of immune populations necessary for host defence and homeostasis.

Macrophage populations were originally believed to all derive from circulating monocytes, which seed tissues during both homeostasis and inflammation. In the 1960s, experiments utilising labelling of rat blood cells with tritiated thymidine (thymidine-H^3) suggested that the thymidine-H^3-enriched macrophages of the skin and peritoneal cavity were derived from HSC progenitors in the bloodstream. Labelled peritoneal macrophages were said to be “end stage cells” with no proliferative activity or capacity to self-renew. Under conditions of inflammation, labelled blood monocytes were seen to rapidly migrate into the peritoneal cavity and were thus concluded to be the sources of resident macrophage populations. Full or partial irradiation of mice to ablate bone marrow stem cell populations revealed that these monocytes originated from the bone marrow (50-52).

However, this pervasive theory did not go entirely unchallenged. Induction of monocytopenia in mice using the bone-seeking radioactive isotope strontium-89 revealed that numbers of tissue resident macrophage populations in the peritoneum, lung and liver were unaffected by the loss of their apparent source. Collectively, these data implied local self-renewal of tissue resident populations (53, 54). Genetic fate-mapping studies, involving tracking of markers such as the chemokine receptor CX_3CR1 expressed across MPS cells, identified waves of early

progenitor cells originating from the yolk-sac seeded tissues early in embryogenesis. These populations give rise to tissue macrophage populations across the body, including the Kupffer cells of the liver, alveolar cells of the lungs, microglial cells of the brain and Langerhans cells in the skin (55-58). Later, it was found that tissue resident macrophages are capable of self-renewal, despite being terminally differentiated through downregulation of the transcription factors MafB and c-Maf, which typically block the enhancers of proliferation c-Myc and Klf2 (59, 60).

Further phenotypic characterisation revealed a greater level of complexity and diversity in monocyte populations, and their connections to macrophages. Flow cytometric analysis showed that human monocytes can be classified phenotypically based on differential expression of the surface markers CD14 and CD16, which represent a lipopolysaccharide-(LPS-) binding co-receptor and an IgG antibody low affinity Fc receptor respectively (61). These monocyte subsets are classical (CD14++ CD16-), intermediate (CD14++CD16+) and nonclassical (CD14+CD16++), with monocytes first entering circulation from the bone marrow as the CD14++CD16- classical subset and then developing into the intermediate and nonclassical subsets sequentially (62, 63).

The main function of monocytes is patrol of the endothelium and some tissues, serving as rapid responders to inflammation on injury or pathogen insult to a tissue. Different subsets of monocytes display different patrolling behaviour. Classical (CD14++) monocytes circulate rapidly through the bloodstream whilst primed for rapid homing to inflammatory tissues by constitutive inflammatory chemokine receptor expression, while nonclassical monocytes are “resident” cells of the vasculature, performing a slow patrol crawling across the endothelium (64-66).

Endothelial cells activated by inflammatory stimuli express a panel of adhesion markers and chemokines to recruit monocytes from the blood. Although commonly thought of as the precursors to macrophages, monocytes can perform immune functions within tissues while retaining a monocyte transcriptional identity (67, 68). These functions include phagocytosis of pathogens, release of pro-inflammatory cytokines and chemokines and antigen presentation, however the classical subset of monocytes can also play roles in tissue repair during resolution of an inflammatory response (69, 70) Additionally, monocytes can give rise to populations of dendritic cells and osteoclasts, with distinct lymph node-homing and bone resorptive functions respectively (71, 72).

Following the original hypothesis of macrophage origin, monocytes have been identified to differentiate into macrophages which fully "integrate" into the tissue resident compartment in the peritoneal cavity, as seen by acquisition of a distinct phenotype and longevity in tissue after resolution of inflammation (73). These monocyte-derived macrophages show acquisition of macrophage-associated gene profiles, such as expression of c-Maf and Maf-B, which regulate tissue macrophage self-renewal (65). Although tissue resident macrophages self-renew under homeostatic conditions, many populations rely on contributions from monocytes during inflammatory insult. For example, the tissue macrophages of the heart have been found to be replenished by local self-renewal solely during homeostasis, but during cardiac inflammation tissue resident populations are replenished by both this process and recruitment of circulating monocytes (74).

However, this monocyte-lead replenishment is not limited to extreme conditions such as inflammation. Recent research has identified two distinct populations of macrophages in the peritoneal cavity: a population of small peritoneal macrophages derived from bone marrow

progenitors and another population of large peritoneal tissue resident macrophages which instead derive from precursors seeded during embryogenesis (73, 75). The larger tissue resident macrophage population is characterised by the GATA6 transcription factor, whose expression is driven by exposure to retinoic acid in the peritoneum and regulates expression of many genes specific to this subset (76). However, despite their distinct ontogeny to small peritoneal macrophages and self-renewal in situ, it was found that the GATA6+ subset was increasingly replenished by monocytes with age. These monocyte-derived GATA6+ macrophages emulate distinct features of this tissue resident subset such as longevity, but show some heterogeneity in other key features such as expression of ICAM2 (77). There is therefore a complex level of macrophage heterogeneity that varies greatly between tissues, including in the incorporation of monocytes into the tissue resident compartment.

Monocytes contribute to distinct short-lived subsets of inflammatory macrophages within tissues following extravasation. These monocytes rapidly acquire macrophage-like morphology and surface marker expression, such as the murine macrophage marker F4/80. Monocytes recruited to the peritoneum during an inflammatory zymosan challenge were seen to differentiate into “inflammatory macrophages” phenotypically distinct from resident macrophages. These inflammatory macrophages declined after resolution of inflammation, while resident macrophages proliferated to replenish the peritoneal compartment (78). Inflammatory monocyte derived macrophages may also undergo apoptosis which aids inflammatory resolution (79).

In addition to inflammatory functions, monocyte-derived macrophages can also perform anti-inflammatory and tissue reparative functions, such as in skeletal muscle regeneration after injury (70, 80). Importantly, while the recruitment of monocytes and their differentiation into

macrophages is beneficial in the context of acute inflammatory insult and pathogen invasion, monocyte-derived macrophages have been implicated in the pathogenesis of several inflammatory diseases. This includes atherosclerosis and inflammatory bowel disease, where they contribute to harmful inflammatory responses, and pro-fibrotic responses in idiopathic pulmonary fibrosis (81-83).

Macrophages comprise a variety of different populations across various tissues, which includes distinct subsets of tissue resident cells derived from embryonic origin and monocyte derived cells. This broad scope facilitates their function as central drivers of the inflammatory response, discussed in more detail below.

1.2.2 Macrophages in onset & resolution of inflammation

Inflammation is a vital response which allows the immune system to identify and remove harmful stimuli and repair any damage caused to the host. The initial trigger for an acute inflammatory response, whether sterile tissue damage or presence of or destruction by microbial threats, is the release of soluble vasoactive products, such as the lipid mediator prostaglandin, complement and cytokines, from activated resident cells adjacent to the threat. These cells can include the endothelial cells of the vasculature, tissue supporting fibroblasts and resident tissue immune cells such as macrophages, dendritic cells and lymphocytes. This stage is known as the vascular phase, characterised by rapidly increased blood flow and permeability of blood vessels adjacent to damaged tissue, which also causes swelling by oedema (84). The release of chemokines such as CXCL8 and upregulation of cell adhesion molecules by the inflammatory activated endothelial cells recruits the “first responders” of the innate immune system: neutrophils. In the next stage of inflammation,

termed the cellular phase, waves of neutrophils cross the endothelium in a process via extravasation and neutralise pathogens through release of powerful inflammatory mediators and engulfment of microbes and debris into phagolysosomes and neutrophil extracellular traps (85).

Monocytes, as discussed above, are typically the next immune cell recruited to the inflammatory site, where they can differentiate into macrophages, dendritic cells or osteoclasts. Macrophages contribute to the pro-inflammatory destruction and engulfment of pathogens, and aid recruitment and activation of cells of the adaptive immune system. Their exact roles in an inflammatory response are dictated by the activating stimuli, which include cytokines, pathogen-associated molecular markers (PAMPs) and damage-associated molecular markers (DAMPs), leading to specific functional programming known as polarisation, discussed in detail in section 1.2.3.

Resolution, the final stage of an acute inflammatory response, is vital to limit the damage caused by the antecedent inflammatory processes and enables repair of the host tissue. Although initially thought to be a “passive” process following removal of microbial or inorganic threats and cessation of inflammatory signalling, resolution is now understood to be as dynamic and active as inflammation itself (86). Just as the initiation of an inflammatory response is driven by pro-inflammatory mediators, resolution is initiated by its own class of pro-resolving mediators. This diverse range of molecules includes lipoxins, resolvins, maresins and protectins (87). Inflammatory leukocytes, including macrophages, in the damaged site undergo “lipid mediator class switching” to promote resolution through downregulation of pro-inflammatory mediators and upregulation of pro-resolving mediators (88). Pro-resolving mediators also promote further recruitment of macrophages (89). Macrophages play a vital

role in initiation of the resolution stage of inflammation by efferocytosis: the phagocytosis of apoptotic neutrophils. As neutrophils possess destructive inflammatory molecules that could contribute to bystander tissue damage, they have a short lifespan in tissues and undergo apoptosis, which maintains compartmentalisation of cell contents and targets them for uptake by macrophages (90). Efferocytosis promotes the release of anti-inflammatory cytokines such as transforming growth factor beta (TGFβ) and IL-10 by macrophages, and therefore promotes a feedforward loop of resolution of inflammation (91).

In the final stage of inflammatory resolution, the damaged tissue is repaired by regrowth or replacement of lost cells and structure. This process varies depending on the site of inflammation and typically involves the formation of “granulation tissue” as connective tissue cells such as endothelial cells, fibroblasts and myofibroblasts attempt to heal the damaged site with scar tissue. Following resolution of inflammation is the “post-resolution phase”, during which further macrophages are recruited to aid generation of adaptive immune responses to the causative pathogenic agent of the inflammatory response (92).

Chronic inflammation is the result of an inflammatory response without successful resolution and has been implicated in countless diseases in a vast variety of tissues, each with unique mechanisms of pathophysiology. Generally, chronic inflammation is more persistent and of lower intensity than acute inflammation and promotes accumulating tissue degeneration. Fibroblasts have been implicated as a key cell type involved in the failure of resolution of inflammation due to their central function as recruiters and activators of leukocytes to inflamed tissue (93). One mechanism of chronic inflammation is the persistence of the initial trigger of the inflammatory response, such as the bacterium *Mycobacterium tuberculosis,* which evades macrophage destruction on phagocytosis, instead establishing itself within

these host cells and causing formation of a destructive inflammatory granuloma (94). Persistence and accumulation of intrinsic inflammatory activators, such as the self-debris of damaged cells, may also drive chronic inflammation. For example, the DAMP high-mobility group box 1 (HMGB1), which is present at high levels in the RA synovia, could be successfully targeted in a rat model of RA, implying an important role in driving and sustaining chronic destructive inflammation (95). The uptake of apoptotic cells by macrophages has been hypothesised to be an important signal for resolution of inflammation, as this process both removes potentially harmful material and drives a positive feedback loop of pro-resolution programming of macrophages (96). Due to this key function and their role as a central coordinator of the inflammatory response, macrophages are often regarded as the driver of chronic inflammation.

1.2.3 Macrophage polarisation

A feature unique to macrophages as cells of the MPS is their ability to polarise, in which they acquire vastly different phenotypic, metabolic and functional profiles depending on the activating stimuli. This enables them to carry out the seemingly conflicting roles of both destructive anti-microbial immune defence and anti-inflammatory tissue repair.

The paradigm of differential macrophage polarisation is often presented as the simple binary of M1 and M2. Whilst this has been shown to be an oversimplification of their diverse phenotypic states in vivo, it has proven a useful tool for understanding the extremes of their polarisation states in in vitro studies. The M1-M2 binary names originated in experiments by Mills etc all in which macrophages from Th1-prone C57BL/6 mice were more readily activated by IFNγ and LPS to induce T cell IFNγ production, whereas macrophages from the Th2-prone

BALB/c strain were less so (97). The Th2 cytokine IL-4 was found to activate macrophages to a different functional profile, characterised by upregulation of the mannose receptor (CD206) and decreased pro-inflammatory cytokine release (98). A dichotomy in metabolism of arginine was identified that neatly classified these cells in mice: Th1-activated macrophages upregulated inducible nitric oxide synthase (NOS) to break down arginine into microbicidal ROS while Th2-activated macrophages instead upregulated arginase which generates polyamines required for tissue repair (99). These M1 "classically activated" macrophages and M2 "alternatively activated" macrophages have since been cemented as the archetypal pro- and anti-inflammatory representations of macrophage function (Figure 1-3 A).

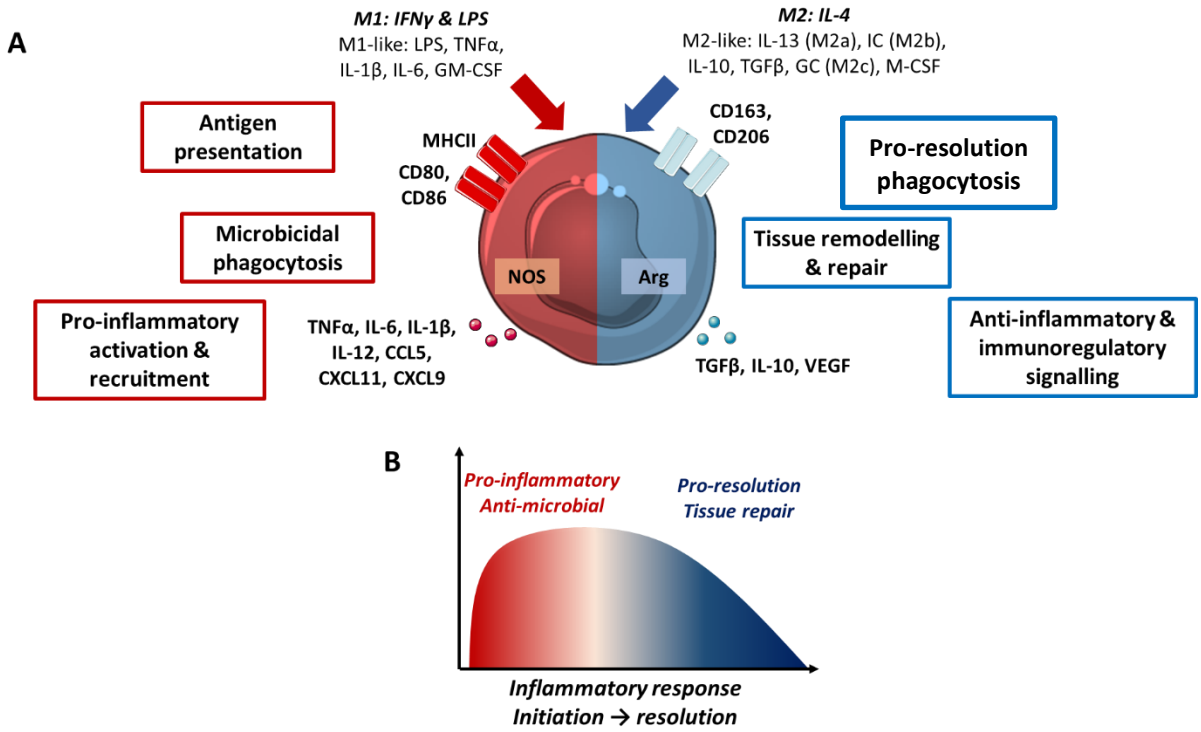

Figure 1-3 The M1-M2 polarisation axis

(A) The phenotype and function of M1-like and M2-like macrophages. (B) Schematic of the shift in polarisation from M1-like to M2-like polarised macrophages in an acute resolving inflammatory response. Arg, arginase; GC, glucocorticoid; IC, immune complex; NOS, nitric oxide synthase; VEGF, vascular endothelial growth factor.

A further commonly used method of polarisation involves in vitro differentiation of blood-derived monocytes into macrophages using the cytokines macrophage colony-stimulating factor (M-CSF) or granulocyte-macrophage colony-stimulating factor (GM-CSF) (100). M-CSF is a growth factor which is ubiquitously expressed across many tissues at a low level and promotes macrophage survival and differentiation, whereas GM-CSF concentrations are elevated during inflammation. Therefore, macrophage cultures generated from these methods can differ in phenotype and functional response to stimuli, with GM-CSF-derived macrophages being more prone to inflammatory responses (101, 102).

M1 macrophages, activated with IFNγ and LPS, dramatically upregulate pro-inflammatory cytokines such as TNFα, IL-1β and IL-12 and inflammatory chemokines including CXCL11, CXCL9, CCL19 and CCL5. They are characterised by strong microbicidal activity, enabled by production of reactive nitrogen and oxygen intermediates to destroy phagocytosed pathogens. Inflammatory polarisation also increases expression of the antigen presentation molecule MHCII as well as its costimulatory markers, such as CD80 and CD86, which enable activation of T cells on presentation of cognate antigen (103, 104). Glucose tracer experiments have shown inflammatory macrophages downregulate mitochondrial oxidative phosphorylation and instead rely on ATP rapidly generated by aerobic glycolysis (105). Oxidation of glucose also supplies nicotinamide adenine dinucleotide phosphate (NADPH) which is utilised for generation of ROS by NADPH oxidase (106). Central transcriptional drivers of the M1 pro-inflammatory phenotype in humans include STAT1 and IRF5, which is induced by signalling via the IFNγ and TLR receptors (107). Importantly, the inflammatory transcriptional cascade triggered by cytokine receptor or pattern recognition receptor activation in macrophages is under tight regulatory control to ensure inflammatory damage to the host is limited. This is ensured via upregulation of inhibitory transcription factors during

inflammatory signalling, such as suppressor of cytokine signalling 1 (SOCS1), which is induced by IFNγ signalling and acts to inhibit STAT1 (108). Numerous other stimuli can drive an M1-like pro-inflammatory polarisation state, including TNFα in combination with IFNγ, GM-CSF, IL-6 and IL-1β (109).

IL-4 activated M2 macrophages are characterised by expression of anti-inflammatory cytokines such as TGFβ and IL-10, and upregulation of scavenger receptors such as CD163, CD204 and CD206 for binding and clearance of endogenous or foreign particles via phagocytosis (103). These transcriptional changes are mediated by the transcription factor STAT6 (107). IL-4 is produced by basophils, eosinophils and Th2 cells and is associated with allergic inflammation. However, regulatory T cells, which suppress immune responses, can also polarise macrophages with IL-4, as well as the other M2-like inducing cytokines IL-10 and IL-13 (110). M2 macrophages possess enhanced phagosomal proteolysis, a targeted mechanism for degradation of proteins taken up during tissue homeostasis and repair (111). This alternative activation of macrophages also drives a distinct metabolic programme in these cells compared to M1 polarised cells. Oxidative phosphorylation is preferred by M2 macrophages as it utilises fatty acids taken up by scavenger receptors, which provide cellular fuel while facilitating breakdown of material (105). Similarly, arginine metabolism is directed towards generation of polyamine precursors such as ornithine, allowing M2 macrophages to facilitate wound repair (99). M2 macrophages are therefore considered pro-resolution cells, acting to dampen down inflammatory signalling and clear up damaged and dead cells and repair damage. Unified classifications of M2-like polarised macrophage subsets have been proposed, with IL-4 or IL-13-induced alternatively activated known as M2a, immune complex-Fcγ receptor-induced “type II activated” as M2b and glucocorticoid-, IL-10- or TGFβ-induced “deactivated” as M2c (112). M-CSF differentiation drives a transcriptome similar to that of IL-

4 polarisation, including macrophage scavenger receptor 1 (MRS1/CD204) and CD206 scavenger receptors, implying that this is a default homeostatic phenotype for macrophages under normal conditions of basal M-CSF levels in tissues (113).

Macrophages possess remarkable plasticity, enabling them to rapidly switch from a basal "M2-like" homeostatic state to a pro-inflammatory "M1-like" state after encountering inflammatory or pathogen-specific signals. This plasticity also enables a functional shift in M1 macrophages to a more pro-resolution phenotype when they encounter signals indicative of the cessation of an inflammatory response, such as apoptotic cells or ligation of the inactivating Fcγ receptor (Figure 1-3 B) (114, 115). This plasticity goes beyond mere suppression or "switching off" of pro-inflammatory functions, as there is an active reprogramming to differential functions, such as phagocytosis or anti-inflammatory cytokine release. Although the M1-M2 framework has provided vital insight into the role of macrophages in immunity and homeostasis, this binary representation does not fully encapsulate the vast variety of macrophage identity in vivo. RNA-seq analysis of tissue macrophages has revealed that macrophage polarisation states are better represented as a broad functional spectrum with a high level of plasticity and dynamism (109, 116).

1.2.4 Synovial macrophages in health and RA

1.2.4.1 Macrophages in the healthy synovial joint

The normal healthy synovial joint contains two populations of macrophages: intimal lining layer macrophages that coexist with FLS in the intimal lining, as well as a sparse number of resident macrophages in the sublining amongst the fibroblasts, adipocytes and blood vessels of the connective tissue. The proximity of synovial macrophages and FLS reflects their shared

functions in maintenance of tissue homeostasis, and each population provides growth factors to sustain the other. Macrophages can produce the fibroblast sustaining platelet-derived growth factor (PDGF), while fibroblasts are the major source of M-CSF in tissues (12, 117). As M-CSF has been identified to have anti-inflammatory and pro-resolution polarisation effects on macrophages in vitro, the secretion of this growth factor by fibroblasts likely not only promotes synovial macrophage survival but also quiescent homeostatic functions.

Intimal macrophages stain positive for the scavenger receptor CD163, the activating IgG Fc receptor FcγRIIIa, CD14 and the IL-1 receptor antagonist (IL-1RA), suggesting an important role in maintaining healthy tissue homeostasis while remaining primed for detection of inflammatory signals. Intimal macrophages also express high levels of the RANKL decoy receptor OPG and therefore help downregulate osteoclast survival and activity to prevent excess bone erosion. Sublining macrophages express lower levels of FcγRIIIa and distinct populations adjacent to venules are enriched for CD14 and the high affinity IgG receptor FcγRI (9, 10, 118, 119). As they are equipped with scavenger receptors and high phagocytic activity, synovial tissue resident macrophages are hypothesised to “scavenge” damaged cells and debris such as hyaluronan, resulting from the mechanical stress of joint movement to prevent accumulation of inflammatory DAMPs (12).

Later research identified that the healthy murine joint is populated with both embryonic precursor derived tissue resident macrophages, which are predominantly MHCII- and have a slow rate of self-renewal during homeostasis, and lower numbers of short-lived MHCII+ bone marrow derived macrophages (120). These can be thought of as more M2-like and M1-like respectively, as pro-inflammatory M1-like macrophages are more equipped for antigen presentation via MHCII. In addition to promoting an anti-inflammatory quiescent

environment, a subset of tissue resident lining TREM2+ macrophages expressing tight-junction proteins form an epithelial tight junction-like barrier thought to protect the delicate intraarticular structures from inflammatory insult (13).

1.2.4.2 Macrophages in RA

Macrophages are well-established in the pathogenesis of RA. They are one of the most abundant cell types identified in synovial inflammation, with a dramatic expansion of intimal lining and sublining populations (9). The number of both lining and sublining macrophages has been shown to strongly positively correlate with radiologic severity of local joint destruction and overall disease DAS28 score (44, 121). Many of the more successful RA therapies are seen to have direct effects on macrophages or their functions, and novel cell-specific therapies are being developed to target this key pathogenic cell (41).

Dramatic changes in macrophage numbers and phenotypes can be seen from early established RA, in both mouse models and human disease. The expansion in macrophage numbers occurs as a key part of the mononuclear cell infiltrate that predominates synovial inflammation, along with CD4+ T cells and FLS. These inflammatory macrophages are thought to derive from recruitment of monocytes, in addition to the proliferation of resident macrophages, via the inflammatory macrophage expressed chemokines CXCL4 and CXCL7 in an inflammatory recruitment positive feedback loop that begins early in RA establishment (120, 122, 123). The protective barrier formed by TREM2+ macrophages is damaged in RA, and macrophage numbers increase massively as part of synovial hyperplasia, with most of the lining layer being composed of macrophages (9, 13). The loss of this protective barrier may

be a key opening of the floodgates, exposing the joint to accumulated peripheral autoimmunity.

These inflammatory monocyte-derived macrophages are archetypal pro-inflammatory M1-like cells. They are a major source of the pro-inflammatory cytokines TNFα, IL-1β and IL-6 as well as the inflammatory chemokines CCL2 and CXCL8 and ROS in the synovial fluid (118, 124-126). They are therefore key cells in the recruitment and inflammatory activation of leukocytes, lymphocytes and stromal cells in RA.

In a process analogous to their crosstalk in synovial homeostasis, macrophages of the RA synovial membrane closely interact with the expanded inflammatory FLS layer, and their crosstalk is a known driver of many key pathogenic processes. Similar to macrophages, synovial fibroblasts have profound functional heterogeneity with distinct phenotypical and functional subsets identified to drive or protect against RA. The HAS1+ PRG4+ lining layer subset of fibroblasts, which produce lubricin and hyaluronic acid for healthy joint lubrication, closely interact with the TREM2+ macrophage barrier layer. It has been hypothesised that these resident synovial populations regulate each other via these interactions, with this immunosuppressive regulation lost on damage of the protective barrier and induction of inflammatory arthritis (13, 127). Fibroblast activation protein α (FAPα), absent in homeostatic fibroblast populations, has been identified as a marker of pathogenic RA FLS. Sublining FAPα+ Thy1+ fibroblasts and lining FAPα+ Thy1- fibroblasts were found to drive inflammatory infiltration and bone and cartilage destruction respectively. Injection of FAPα+ Thy1+ FLS into the ankles of CIA model mice was seen to increase macrophage infiltration, suggesting that this subset could serve as a potent inflammatory macrophage activator in RA (128).

The release of pro-inflammatory factors by transformed RA FLS such as RANKL and IL-6 can promote inflammatory activation of macrophages. Conditioned media from inflammatory FLS was found to be sufficient to drive M1-like polarisation of macrophages in vitro, characterised by a marked increase in glycolytic metabolism and production of TNFα (129). In turn, inflammatory RA macrophages further drive FLS cartilage invasion and tissue destruction, via release of inflammatory cytokines and growth factors, such as heparin binding EGF-like growth factor (HBEGF) (130).

Sublining macrophages are found in lymphoid aggregates with lymphocytes and so appear to function more as antigen presenters (131). Macrophages may be involved in the initial induction of immune targeting of the joint in RA through antigen presentation. They can present collagen and cartilage glycoprotein autoantigens to activate autoreactive T cells (132, 133). Additionally, they are activated via Fc receptors by immune complexes of neoantigens, such as citrullinated fibrinogen, and their autoantibodies, thus they perpetuate inflammatory autoimmune reactions (134, 135). Macrophages can promote activation of CD4+ T cells into the highly inflammatory Th17 subset associated with RA progression, via production of IL-6 and IL-1β (136).

Macrophages are also found at the cartilage-pannus and bone-pannus junctions in RA, where they contribute to cartilage and bone erosion. RA macrophages express some MMPs, but are thought to contribute to tissue destruction more indirectly, via inflammatory activation of FLS and osteoclasts (137). Inflammatory cytokines such as IL-6 and TNFα from activated macrophages help to promote osteoclast RANKL-mediated differentiation and bone resorptive activity (138).

Many of these inflammatory macrophage functions are successfully targeted by biologic DMARDs, validating their contribution to severe RA disease. Macrophage costimulatory molecules CD80 and CD86, required for CD4+ T cell activation on antigen presentation, are targeted with the costimulatory inhibitor CTLA4 in the drug abatacept (139). Treatment with the anti-TNFα antibody infliximab reduces inflammatory macrophage recruitment to the synovium and therefore synovial inflammation (140).

Macrophages with a "homeostatic" phenotype and transcriptomic profile can be identified in the RA synovium even during severe inflammatory flare. CD163+ synovial macrophages, with roles in homeostasis of healthy synovium as discussed previously, have been identified in RA synovium, typically distal to IFNγ-producing Th1 cells and are not removed by anti-TNFα treatment, and thus have been suggested to retain anti-inflammatory tissue reparative functions (141-143). Depletion of MHCII- tissue resident macrophages exacerbated inflammatory disease in the K/BxN serum transfer model of arthritis, suggesting they retain a pro-resolution and tissue reparative phenotype (120).

Single cell RNA sequencing (scRNA-seq) analysis of the RA synovium has proven to be an invaluable technique for elucidating the complex heterogeneous populations of macrophages in the inflamed joint, and how they vary with disease state and severity (144, 145). This in-depth transcriptomic analysis has validated previous findings on homeostatic tissue resident populations, identifying distinct clusters of macrophages expressing *CD163*, *CD206* and the transmembrane receptor tyrosine kinase *MerTK*, associated with phagocytosis of apoptotic cells, are all enriched in synovial macrophages from healthy donors or RA patients in clinical remission. Ex vivo analysis of this macrophage subset found that they released pro-resolving lipoxins, which stimulate inflammatory RA FLS to acquire an anti-inflammatory pro-reparative

phenotype on co-culture. Patients with treatment-naïve and treatment-resistant active RA showed a marked reduction in these homeostatic MerTK+ clusters, and an increase in distinct inflammatory clusters enriched in osteopontin or alarmins (146).

Similarly, pro-resolving subsets of synovial fibroblasts have been identified which interact with macrophages to regulate inflammatory processes and resolve arthritic disease. This includes a CXCL14+ sublining fibroblast subset which release the MerTK ligand GAS6, driving MerTK+ macrophage resolvin production (146). Furthermore, DKK3+ sublining fibroblasts have been hypothesised to help repair the TREM2+ macrophage protective joint barrier via expression of proteins such as CADM1, linked to restoration of intestinal barrier function in inflammatory bowel disease (127, 147).

This increased resolution of macrophage complexity and heterogeneity in the RA synovium has revealed new possibilities for macrophage-targeted therapeutics, where destructive inflammation could be alleviated by both reducing pro-inflammatory macrophages but also promoting pro-resolution populations. Glucocorticoids, as key regulators of macrophage resolution of inflammation, are attractive targets for exploiting macrophage anti-inflammatory and pro-resolution polarisation.

1.3 Glucocorticoids

Glucocorticoids (GCs) are steroid hormones with vital roles in development, glucose and lipid metabolism, and the stress response. GC signalling is necessary for development and maturation of various tissues in utero, such as the lung, as seen in the lethally underdeveloped lungs of glucocorticoid receptor (GR) knockout mice (148). GCs are named for their function of promoting liver gluconeogenesis and regulation of glucose metabolism both homeostatically and under conditions of stress, where additional glucose may be required by the brain. In response to stress signals such as starvation, GCs act to antagonise the actions of the pancreatic hormone insulin to increase serum glucose levels, while uptake of glucose by white adipose tissue and skeletal muscle is suppressed to maximise glucose uptake and use by the brain. Glucose production is promoted by upregulation of gluconeogenesis and glycogen storage in the liver, as well as an increase in the pancreatic hormone glucagon (149-151). GCs also maintain epidermal development and skin barrier integrity (152). Finally, GCs have roles in regulating blood pressure by increasing sodium retention through activation of the kidney mineralocorticoid receptor (MR) and also through enhancing vascular tone by acting directly on vascular smooth muscle, both of which raise blood pressure (153).

In addition to these myriad roles throughout the body, GCs possess potent anti-inflammatory activity, which was first discovered on therapeutic administration of “compound E” to RA patients in 1949 (154). This substance is now known as cortisone, the main inactive GC in humans. In humans the main endogenous GC is cortisol, and in rodents it is corticosterone. Their desirable anti-inflammatory functions have been replicated for clinical use in countless synthetic GCs, including prednisolone and dexamethasone.

1.3.1 Endogenous glucocorticoid physiology

Systemic levels of GCs are regulated by the hypothalamic-pituitary-adrenal (HPA) axis under a circadian rhythm with a peak of cortisol levels in humans seen in the early morning. However, production can also be induced by physiological stressors (Figure 1-4) (155).

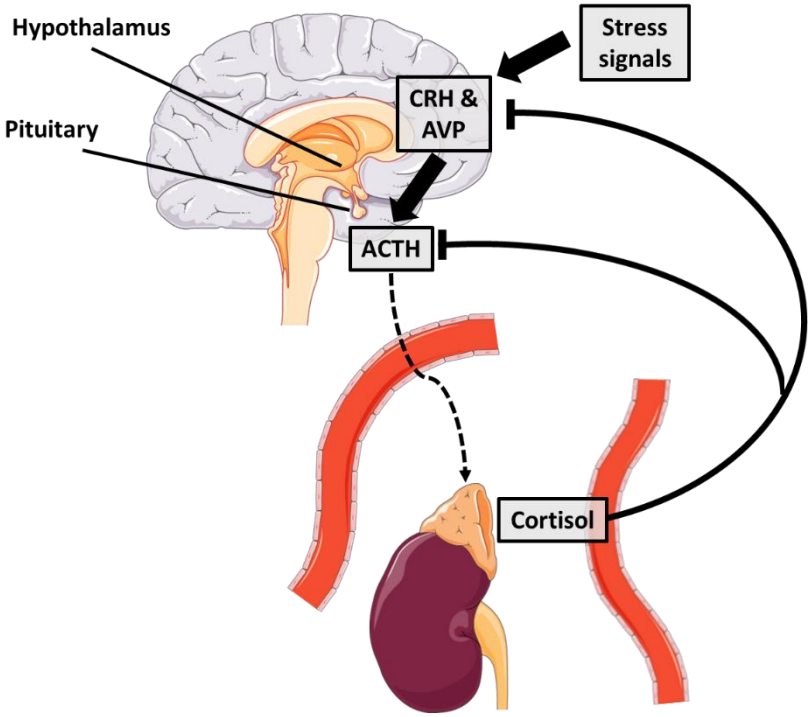

Figure 1-4 The HPA axis

Stress signals such as inflammatory cytokines activate neurons in the hypothalamus to release corticotrophin releasing hormone (CRH) and arginine vasopressin (AVP). These activate cells of the anterior pituitary to release adrenocorticotrophic hormone (ACTH) into systemic circulation. ACTH activates cortisol synthesis in the adrenal cortex. Cortisol is released into the circulation and downregulates its own production in a negative feedback loop by inhibiting CRH, AVP and ACTH release.

Following stimulation of the hypothalamus by agents such as IL-1 or IL-6, the hypothalamic paraventricular nucleus produces corticotrophin-releasing hormone (CRH) and arginine vasopressin (AVP) (156-158). These induce the pituitary gland to release adrenocorticotrophic hormone (ACTH) into the circulation. ACTH acts on the adrenal cortex to drive synthesis of cortisol, along with the mineralocorticoid aldosterone and the androgen precursor

dehydroepiandrosterone (DHEA) from cholesterol in different regions of the cortex (Figure 1-5).

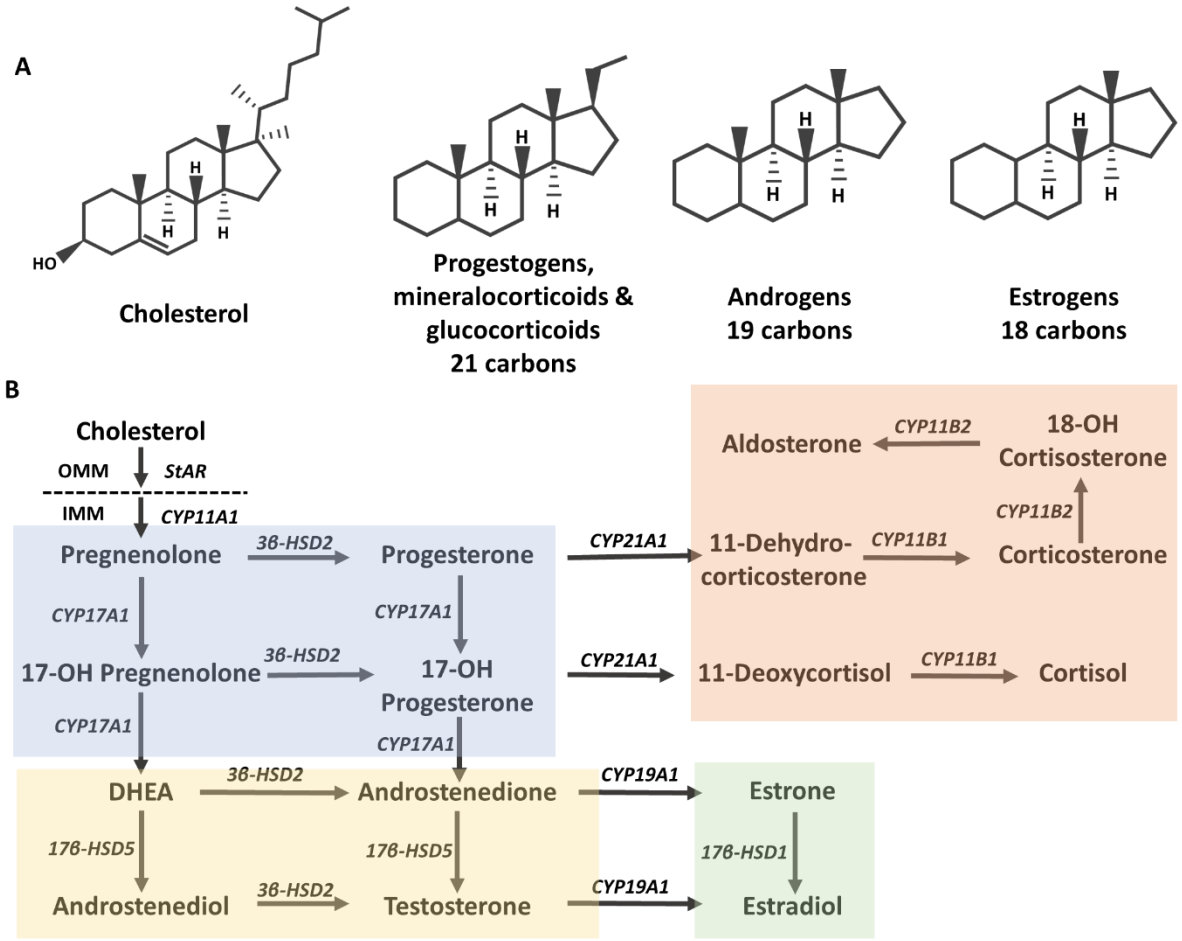

Figure 1-5 Adrenal steroidogenesis

A) Chemical structures of cholesterol and the major groups of derived steroids. (B) Steroid biosynthesis in the adrenal glands. Progestogens (highlighted in blue) are generated from cholesterol and are the precursors of other steroids: mineralocorticoids & glucocorticoids (orange), androgens (yellow) and estrogens (green).

Steroidogenic adrenal cells are enriched with cytosolic cholesterol ester droplets, which supply stores of cholesterol in the outer mitochondrial membrane (OMM). During steroidogenesis, cholesterol is transferred from the OMM to the inner mitochondrial membrane (IMM) by steroidogenic acute regulatory protein (StAR). In the IMM, the side-chain cleavage enzyme CYP11A1 synthesises the precursor steroid pregnenolone from

cholesterol. Progesterone is then generated from pregnenolone by the enzyme 3β-hydroxysteroid dehydrogenase type 2 (3β-HSD2) (159). Pregnenolone and progesterone undergo 17α-hydroxylation by CYP17A1 to form cortisol which is released into the circulation (160).

Levels of active and inactive GCs are regulated by the 11β-hydroxysteroid dehydrogenase (11β-HSD) enzymes. Hepatic 11β-HSD1 activates cortisone into cortisol to replenish systemic levels of GCs, while renal 11β-HSD2 carries out the opposing inactivating reaction to spare GC action at the MR (161). The 11β-HSD enzymes are also involved in tissue specific regulation of GC levels across the body, including in the regulation of GC levels during inflammation.

GCs are lipophilic molecules, and therefore exert effects on target cells by diffusing through cell membranes and bind to intracellular receptors. The intracellular GR, encoded by the gene *NR3C1*, is highly evolutionarily conserved and expressed in the majority of tissues in the body, where it confers the broad physiological effects of GCs (162-164). These include the PVN and pituitary gland, where GC signalling downregulates its own production, thus keeping the HPA axis under strict feedback mediated control under healthy conditions (165). The HPA axis also follows a circadian rhythm, with peak cortisol levels seen in the early morning and a nadir at night (155). The effects of which can be clearly seen in the classic “morning joint stiffness” symptoms of RA, in which rise in pro-inflammatory IL-6 levels precedes morning peak cortisol production (166).

About 90% of circulating GCs are bound by transport proteins such as corticosteroid-binding globulin (CBG). Steroids can also be more loosely bound to albumin, to which they have a low binding affinity. However, albumin is the most abundant serum protein, and so this provides a reservoir of around 10% of all bound GCs (167). Binding GCs to transport proteins is

hypothesised to prevent constitutive crossing of the cell membrane and activation of the GR and MR by lipophilic GCs (168). Transport proteins can also act to "deliver" GCs to sites of inflammation, for example CBG is cleaved by the elastase released by activated neutrophils, therefore providing a source of free GCs available to sites of inflammation (169).

Cortisone and cortisol are excreted in urine as 5α-tetrahydrocortisone (THE) and 5α-tetrahydrocortisol (THF) following metabolism by 5α- and 5β-reductases and 3α-hydroxysteroid dehydrogenases (170).

1.3.2 GC signalling

GC signalling via the GR is essential for survival. GR knockout mice die shortly after birth due to severely impaired lung development, but also present with impaired HPA axis function due to high levels of ACTH and corticosterone, enlarged adrenal glands and paucity of gluconeogenesis in the liver (148). The GR, first cloned in 1985, presents as two major isoforms, GRα and GRβ (163). GRα, which represents around 90% of GR transcripts, binds GCs and acts to positively drive GC-sensitive gene expression. GRβ does not bind GCs and instead negatively regulates GRα, and is upregulated by the cytokines IL-2 and IL-4 (171). Further GR isoforms have been identified, such as GRγ, which appears to be involved in mitochondrial function, however these are expressed at far lower levels and their functions are less well understood (172).

The GR is a nuclear receptor consisting of a C-terminal ligand binding domain (LBD), a central zinc-finger DNA-binding domain (DBD) and N-terminal modulating domain (NTD). The LBD activation function 2 (AF-2) region facilitates conformational change on ligand binding and binds transcriptional coactivators to promote GR activity (173). The DBD enables dimerization

of the GR as part of cytoplasmic activation, and contains sequences which bind the receptor-ligand complex to GC-response elements (GRE) present in promoter regions of genes (174). The modulating NTD contains the activation function 1 (AF-1) region, shared by the nuclear hormone receptor superfamily. This is a transactivation domain which facilitates interactions with basal transcription factors and chromatin modifiers during GRE binding to promote transcription (175). Nuclear localisation is facilitated by nuclear localisation signals (NLS), NL1 and NL2, located in the DBD and LBD respectively (176)

At basal level, the GR is sequestered in the cytoplasm within a multiprotein complex formed of the heat shock protein 90 (hsp90) and the immunophilin FK506-binding protein 52 (FKBP52). This conformation keeps the receptor unable to migrate to the nucleus through blocking of the NL1 and NL2, but the ligand-binding domain remains accessible (176, 177). On binding of GCs such as cortisol to the GR ligand binding domain, conformational change occurs. This allows release of the GR and ligand from the inhibitory complex, allowing rapid translocation to the nucleus (178).

On ligand binding, the GR can function as a transcription factor with multiple distinct functions. It can function via transactivation, where the GR complex homodimerises and binds directly to GREs on genes such as glucocorticoid induced leucine zipper (*GILZ*), *annexin-A1* and dual specificity phosphatase 1 (*DUSP1*), where it recruits transcriptional coactivators including histone acetyltransferases to mark active chromatin and induce transcription (179, 180). The GR has also been found to drive gene expression in monomeric form binding to “half site motifs”, and it was identified that this monomeric binding form is more prevalent than the dimeric form. Here it may be more reliant on stabilisation by further transcription

factors, such as tissue-specific lineage-determining transcription factors, which may explain its more tissue specific regulation in sites such as the liver (181).

The GR can also drive direct transrepression, in which the GR binds to “negative GREs” (nGREs) in order to transcriptionally repress expression. These have been identified in the gene for the ACTH-precursor pro-opiomelanocortin in corticotropic cells of the anterior pituitary, therefore these nGRE can act to regulate the HPA axis (182). This nGRE is also present in the thymic stromal lymphopoietin (TSLP) cytokine gene (183). However, the functional importance of this mechanism is disputed, as more recent transcriptome profiling identified that only 20% of GR-dependent downregulation of gene expression could be explained by tethering and nGREs. For many key inflammatory genes, such *IL-6* and *CCL2*, it was “canonical” GREs that the GR interacted with to drive transrepression via recruitment of the corepressor GRIP1 to inhibit transcriptional activation (184). The GR can also bind directly to inflammatory response elements, such as the activator protein 1 (AP-1) TRE response element present in promoter regions of the *IL-6*, *IL-11* and *VCAM1* genes to inhibit transcription (185).

These transcriptional effects can also occur more indirectly, via tethering of the GR dimer to other transcription factors bound to DNA to induce or repress gene expression. This mechanism was originally believed to be the main manner in which GCs suppressed inflammatory gene transcription. The GR monomer directly binds to and sequesters inflammatory transcription factors nuclear factor kappa-light-chain-enhancer of activated B cells (NFκB) and AP-1 using this tethering mechanism (186, 187). Finally, the GR can also inhibit transcription by modifying chromatin structure (188).

GCs can also function more rapidly via non-genomic effects, with responses seen after a very short incubation period of less than 30 minutes or even instantaneously after GC treatment. These effects are often insensitive to treatment with the GR antagonist RU486 and inhibitors of transcription such as actinomycin D. The GR-ligand complex has been found to sequester key intracellular signalling molecules such as phosphoinositide 3-kinase to prevent downstream signalling (189). These nongenomic effects also include interactions of GC with cellular membranes, where they can regulate cholesterol synthesis, ion transporters and cyclic AMP signalling (190). GCs may also interact with membrane-associated GC receptors to regulate downstream signalling (191). These diverse signalling responses shape a myriad of cell and tissue specific responses by GCs, including immunoregulation and resolution of the inflammatory response.

1.3.3 Immune modulatory and anti-inflammatory regulation by GCs

Due to the ubiquitous expression of *NR3C1* across cells and tissues, GCs are able to affect numerous cell types involved in an inflammatory response. Microarray analysis of human peripheral blood mononuclear cells treated with dexamethasone revealed that a vast range of genes were affected by GC stimulation. In addition to anti-inflammatory cytokines and regulators such as IL-10 and IL-1RA, GCs also upregulate genes involved in scavenger receptors, TLRs and complement. GC treatment potently downregulated genes involved in antigen presentation, implying a transcriptomic shift away from adaptive activating immune responses and towards clearance of antigens and debris (192).

As NFκB is a central driver of the inflammatory response to many DAMPs and PAMPs, it is a key target of suppression by GCs. This occurs both by transrepression via tethering

mechanisms and also by upregulating the IκBα inhibitory protein which sequesters inactivate NFκB in the cytoplasm (186, 193). These mechanisms can be cell-type specific, as induction of IκBα was identified to be the primary method of NFκB suppression in leukocytes, while in endothelial cells NFκB was instead inhibited via tethering mechanisms (194). GCs interfere with many other key pro-inflammatory transcriptional regulators, such as the transcription factor AP-1, which drives expression of inflammatory cytokines including CXCL8 via transrepression (195). Finally, the mitogen-activated protein kinase (MAPK) family is involved in numerous inflammatory and immune signalling processes and is thus targeted at many points by GCs. The MAPK family members extracellular regulated kinases (Erk)-1 and -2 regulate several pathways in immune cells such as production of the inflammatory secondary messenger arachidonic acid and release of TNFα and are downregulated by GCs (196).

In addition to direct negative regulation of inflammatory genes, GCs upregulate expression of several anti-inflammatory regulators. These include GILZ, which interacts with and inhibits the transcriptional activity of inflammatory transcriptional regulators such as NFκB, AP-1 and MAPK1 (197-199). Annexin A1 similarly has potent anti-inflammatory roles upon its induction by GCs, such as inhibition of phospholipase A_2, which generates prostaglandins and leukotrienes, and promotion of apoptosis and efferocytosis of apoptotic cells to aid inflammatory resolution (200). Treatment with GCs stimulates both expression and secretion of annexin A1 and expression of its receptor in leukocytes (201). DUSP1 is upregulated by GCs and its proteosomal degradation is prevented, allowing it to potently inhibit the MAPK pathway (202). Further anti-inflammatory genes induced by GCs include the anti-inflammatory cytokine *IL-10* (203). Many of these processes are shared across cells involved in immune and inflammatory responses, however GCs have distinct effects depending on cell type and context (204).

The vasoactive properties of GCs enable them to regulate key microcirculatory changes that occur early in an inflammatory response. GCs limit leukocyte migration into sites of inflammatory activation by suppressing vasodilation, decreasing vascular permeability and limiting leukocyte extravasation (205, 206).

Within the innate immune system, GCs suppress TLR signalling and activation in mast cells, including their inflammatory allergic functions of degranulation and histamine release (207, 208). GCs decrease neutrophil extravasation into tissues, but also promote their survival by inhibiting apoptosis in a similar method to pro-inflammatory factors, although without the corresponding inflammatory activation of these cells (209, 210). Similarly, GCs have immunomodulatory effects on monocytes beyond straightforward suppression. Although GC treatment suppresses monocyte expression of inflammatory factors such as IL-12 p70, it can also activate them to a distinct “anti-inflammatory subtype” characterised by increased survival, expression of IL-10 and the decoy IL-1 receptor IL-1R2, and enhanced phagocytosis and chemotaxis (211-213).

GCs inhibit not only antigen presentation by dendritic cells through downregulation of MHCII and associated costimulatory molecules required to activate an adaptive immune response, but also limit their maturation from precursors (214). However, GCs also increase antigen uptake by these cells and promote their acquisition of a “tolerogenic” activating profile, in which they promote anergy of T cells or generation of regulatory T cells which suppress inflammatory immune responses to the antigen presented (215).

GCs target many processes within the adaptive immune system, generally downregulating inflammatory antigen specific responses and promoting resolution of responses either through suppression of the inflammatory populations or increasing regulatory lymphocytes.

The activation of the adaptive immune system is repressed by GC signalling, which disrupts signal transduction at both the T cell and B cell receptors (216, 217). GCs promote Th2 differentiation and cytokine production, such as IL-4 and IL-10, while suppressing Th1 and Th17 activation and cytokines and cytotoxic T cell function (218, 219). Treatment with GCs also promotes apoptosis in helper T cells, cytotoxic T cells and B cells, which may function as a mechanism of clearance of these potentially harmful inflammatory cells as part of the resolution stage of an immune response (220-222).

1.3.4 Actions of GCs on macrophages

Macrophages, as key drivers of inflammation, are prime targets of GCs, and their responses to treatment are highly context specific. GC-polarised macrophages, sometimes called M2c macrophages, are M2-like with immunoregulatory properties distinct to the other M2 and M2-like subsets. They are a source of the immunosuppressive cytokine IL-10 and possess specialised phagocytic activity for clearance of apoptotic cells via increased cytoskeletal activity and upregulation of unmodified phosphatidylserine receptor MerTK (223, 224). They are therefore primed for aiding resolution of the inflammatory response through removal of apoptotic cells and suppression of pro-inflammatory factors.

The GRα gene *NR3C1* has been found to be constitutively expressed in both primary murine bone marrow derived macrophages and macrophage cell lines, with its expression being increased upon inflammatory stimulation with LPS or IFNγ (225). Inflammatory activated macrophages are therefore equipped with heightened ability to respond to active GCs in the environment. In vitro studies identified robust suppression of inflammatory cytokines such as IL-1β, IL-6 and TNFα, and downregulation of ROS production, MHCII and costimulatory

markers (226-229). Similarly, pre-treatment of macrophages prior to LPS or IFNγ stimulation suppressed adaptive immune associated genes, including MHCII and costimulatory marker expression, but maintained or promoted those associated with innate functions, such as phagocytosis and phagocyte recruiting chemokines CCL7 and CCL8. This was transcriptomically more similar to a GC-only treated state than that of an LPS-treated state (230). As with other innate immune cells detailed in section 1.3.3 above, GC treatment of macrophages does not seem to drive the more generalised suppression and induction of apoptosis seen in adaptive immune cells, but instead more of a modulation of immune functions.

In vitro studies have highlighted biphasic effects of GC stimulation on macrophages: high doses in the micromolar range suppress inflammatory activated cells, while lower doses in the nanomolar range instead promoted TNFα production, phagocytosis and chemotaxis. This immunostimulatory effect was hypothesised to promote host immune function during periods of stress, when GC production would be triggered (231, 232).

These GC-induced phenotypic changes are driven by many of the mechanisms discussed in section 1.3.2 above and vary based on the transcriptional context of inflammatory macrophage activation. The inflammatory profiles of LPS-activated macrophages, driven by TLR4, were restrained by GC induction of DUSP1 and inhibition of p38 MAPK, but not the other MAPKs ERK and Janus kinase (233). However, in macrophages activated by double stranded RNA (TLR3) or unmethylated DNA (TLR9) the major target of GC-mediated suppression of inflammatory function was the kinase TAK1, upstream of NFκB and MAPK (234). Inflammatory activation driven by IFNγ was suppressed by GC targeting of the major downstream signalling molecule, and driver of M1 polarisation, STAT1 (235). More recently it

has been confirmed that GCs also drive metabolic changes in macrophages. Metabolomic analysis identified a decrease in LPS-induced inflammatory glycolysis when macrophages were treated with dexamethasone, resulting in a decrease in production of ROS (236).

The physiological significance of these phenotypic effects has been validated in mouse models of injury and disease. GC signalling appears to be important for the maintenance of homeostasis by tissue resident macrophages, such as the promotion of neuroprotective anti-inflammatory functions of microglia in the brain (237). This is true also for macrophages derived from recruited blood monocytes, as seen in a model of myocardial infarction where GC signalling was required for the differentiation of blood monocytes into anti-inflammatory tissue reparative macrophages (238). In models of tissue injury, endogenous GCs suppressed macrophage inflammatory functions including production of ROS, microbicidal phagocytosis and TNFα and IL-6 release, therefore allowing successful tissue repair (239). GC signalling via the myeloid GR has been shown to be important for resolution of inflammatory disease in several mouse models, including colitis, sepsis and lung injury, for both endogenous and therapeutic GCs (240-242).

1.3.5 Therapeutic GCs

Synthetic GCs have been used in countless inflammatory conditions for over 70 years due to their affordability and broad immunosuppressive functions. Their indications include inflammatory bowel disease, asthma, graft-versus-host disease and RA, in addition to other conditions including cortisol deficiency due to adrenocortical insufficiency and congenital adrenal hyperplasia. However, for effective anti-inflammatory treatment they must be taken

long-term, and their use is often contraindicated or discontinued in patients due to harmful metabolic side effects (243).

Hydrocortisone is a synthetic form of cortisol, and so acts on both the GR and MR, and can be administered orally, intravenously or topically depending on the condition and patient need. Other common therapeutic GCs include prednisolone and prednisone, modified variations of cortisol and cortisone respectively. Analogous to cortisone, prednisone is a prodrug which must be converted to its active form (prednisolone) by hydrogenation of the 11-keto residue by hepatic 11β-HSD1. These drugs have 4x higher affinity for the GR and around 20% reduced affinity for the MR, due to the removal of an acetyl group at carbon-11 of the steroid ring and introduction of a double bond in steroid ring A (244). Methylprednisolone is a modified form of prednisolone with a methyl group added to carbon 6. This modification gives methylprednisolone 5x higher affinity than hydrocortisone for the GR and minimal affinity for the MR, and in addition makes it resistant to binding by CBG and resistant to metabolism by the 11β-HSD enzymes, thus decreasing its metabolic clearance (245). Dexamethasone is a highly potent GC generated by the addition of 9α-fluoro- and 16α-methyl groups to prednisolone, with similar insensitivity to 11β-HSDs (246). Additionally, different formulations of synthetic GCs have been optimised for different routes of administration. For example esterification of GCs, such as methylprednisolone acetate, decreases their solubility in water, which optimises them for intra-articular (IA) injection into inflamed sites as these compounds are retained in tissues for longer (247).

The side effects associated with long-term GC therapy for inflammatory conditions are similar to that of disorders of endogenous GC excess: osteoporosis, glucose intolerance, hypertension and increased risk of cardiovascular mortality (248). Many of these side effects

represent the “extreme” unchecked side of the physiological effects of GCs. Under homeostatic conditions, GCs help regulate bone metabolism by managing the balance of osteoblasts and osteoclasts. However therapeutic GCs decrease osteoblast differentiation and release of RANKL decoy receptor OPG while promoting RANKL-mediated osteoclast differentiation and bone resorption (249, 250). Similarly, GCs regulate muscle mass as a source of nutrients during a stress response. Cachexia is induced by the effects of GCs on increasing proteolysis and autophagy in myoblasts and myotubes of muscles (251).

Although many of the modifications detailed above reduce synthetic GCs affinity for the MR, the necessity of long-term treatment to manage inflammatory conditions often means that MR-associated side effects are still induced. Additionally, the higher potency of some synthetic GCs, dexamethasone in particular, precludes their long-term use due to suppression of the HPA axis and endogenous GC production (252).

Due to their widespread mechanism of action in suppression of inflammation, discussed previously in section 1.3.3, therapeutic GCs target many different cell types in RA. In RA GCs can be administered systemically, by the oral or intravenous route, or more locally via intramuscular injections or into the inflamed joints by IA injections. IA injection of GCs is commonly used in combination with other DMARDs in RA for symptom relief as it reduces the risk of systemic side effects compared to oral or intravenous route, or the direct risk to muscle metabolism on intramuscular injection (253). IA GCs were found to decrease numbers of synovial T cells and inflammatory mediators such as TNFα and IL-1β (254). Importantly, though IA GCs did not change numbers of synovial macrophages, a study of IA GCs in rheumatoid and non-rheumatoid arthritis found that pre-treatment levels of total synovial macrophage numbers correlated positively with successful clinical outcome (45). Therefore,

therapeutic GCs likely work to alleviate RA inflammation and symptoms by modifying polarisation of macrophages towards a more anti-inflammatory phenotype, rather than simply suppressing numbers of inflammatory macrophages. IA GCs were also found to decrease synovial levels of MMPs and RANKL, which can help slow bone and cartilage erosion in patients (255, 256).

1.3.6 GC metabolism by the 11β-HSD enzymes

While the HPA axis regulates the day-to-day circadian rhythm of GCs and systemic stress responses, levels of active and inactive GCs and their local tissue-specific availability are regulated by the 11β-HSD enzymes (Figure 1-6).

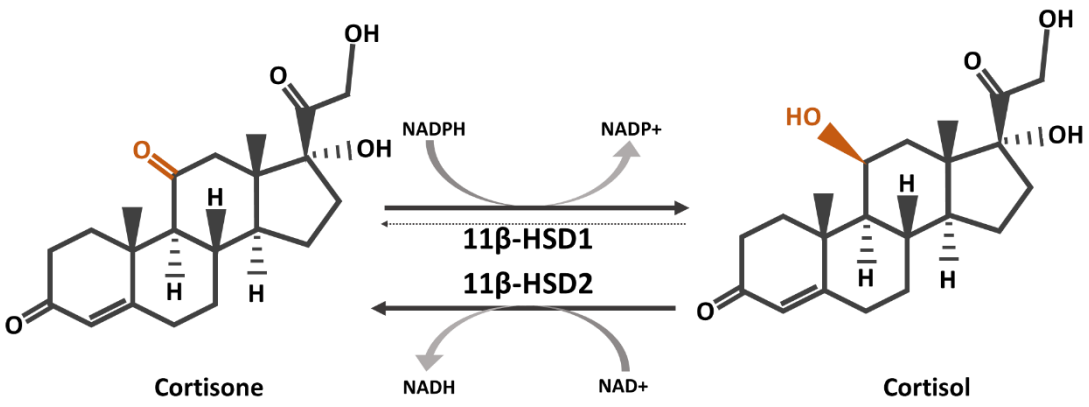

Figure 1-6 The cortisone-cortisol shuttle

The keto group (in red) of cortisone is reduced to a hydroxy group (in red) to form the active glucocorticoid cortisol by 11β-HSD1, which uses NADPH as an electron donor. 11β-HSD2 catalyses the reverse reaction, using NAD+ as an electron acceptor.

As 11β-HSD metabolism defines the ability of GCs to bind to and activate the GR within a cell, this is referred to as pre-receptor or intracrine metabolism. Intracrine metabolism differs

from autocrine as the receptor is located within the cell, such as the nuclear GR, rather than on the cell membrane (257).

Cortisone, and synthetic derivatives such as prednisone are intrinsically inert, with low affinity for the GR, and so must be converted into their biologically active counterparts, cortisol and prednisolone, in order to bind the GR. The activating reaction is carried out by 11β-HSD1 which reduces the “inactive” 11-oxo group in the steroid C ring into an “active” 11β-hydroxyl with increased affinity for the GR. This reaction requires the use of nicotinamide adenine dinucleotide phosphate (NAPDH) as a cofactor and electron donor (161). 11β-HSD1 is an intracellular enzyme localised in the endoplasmic reticulum, which is rich in NADPH generated by the pentose phosphate pathway enzyme hexose-6-phosphate (H6PDH) (258). Although 11β-HSD1 is predominantly a reductase, it can act as a dehydrogenase, carrying out the same NAD^+-dependent reaction as 11β-HSD2, detailed below, in the absence of H6PDH (259, 260). 11β-HSD1 is most highly expressed in the liver, where activated GCs regulate glucose metabolism by upregulating key gluconeogenic enzymes (261). Hepatic 11β-HSD1 also provides a considerable proportion of circulating cortisol, thus participating in endocrine function (262). As cortisone can travel through the plasma not bound to protein, it can freely enter cells, whereas cortisol is bound by CBG and albumin. Therefore cortisone’s effects on activation to cortisol are “targeted” by the intracellular expression of 11β-HSD1, acting in intracrine fashion (263). Through supply of active steroid, 11β-HSD1 mediates the local metabolic functions of GCs and so is expressed in key metabolic tissues.

The 11β-HSD2 isozyme inactivates GCs by converting the 11β-hydroxyl group to an 11-oxo group through dehydrogenase activity, using NAD^+ as a cofactor and electron acceptor. As this inactivation of GCs limits their binding to the highly GC-sensitive MR, 11β-HSD2 is

expressed at high levels in mineralocorticoid-sensitive tissues such as the kidneys, placenta, and colon, as well as epithelial tissues including the colon (264, 265). A systemic balance of active and inactive GCs is therefore maintained through activation of GCs by hepatic 11β-HSD1 and inactivation by renal 11β-HSD2.

Under physiological conditions the provision of active GCs by 11β-HSD1 in adipose tissue and muscle helps regulate glucose and lipid metabolism. However, this enzyme has been identified as a key driver of insulin resistance and dyslipidaemia in these tissues, with inhibition or knockout in mouse models protecting from diabetes and metabolic syndrome associated with excess endogenous or therapeutic GCs (266-268). 11β-HSD1 inhibitors are therefore being assessed in these conditions, and phase II trials have produced mostly positive outcomes including improved hyperglycaemia, reduction in plasma cholesterol and triglycerides, and reduced hypertension (269, 270). However, 11β-HSD1 is also upregulated under conditions of inflammation, where it can provide active GCs necessary for resolution of inflammation, as detailed below. These effects could preclude the use of 11β-HSD1 inhibitors in cases where inflammation drives pathophysiology alongside GC excess (271).

1.3.6.1 11β-HSD1 as a regulator of inflammation

In addition to its expression in metabolic tissues, 11β-HSD1 is expressed by a variety of immune and stromal cells. As GCs are vital to the resolution of inflammation, expression of 11β-HSD1 enables these cells to regulate inflammatory functions in response to freely circulating cortisone. This is highlighted in mouse models of acute inflammation such as peritonitis and pleurisy, where 11β-HSD1 knockout (*Hsd11b1*$^{-/-}$) mice exhibited increased inflammatory infiltrates and delayed resolution of inflammation (272).

In vitro analysis of rodent and human peripheral blood mononuclear cells (PBMCs) identified that 11β-HSD1 was expressed in many different immune cell types, with upregulation commonly seen on inflammatory stimulation, while the GC-inactivating 11β-HSD2 was not expressed on circulating leukocytes (273, 274). 11β-HSD1 mediates many of the GC-mediated effects on immune cells as discussed above in section 1.3.3. GCs inhibit mast cell degranulation and thus allergic inflammation, and 11β-HSD1 is required to mediate these effects in response to inactive GCs (275). Similarly, neutrophils treated with LPS upregulate 11β-HSD1, and this was found to be essential for resolution of inflammation in a model of sterile peritonitis (276). However, this enzyme can also drive distinct context-dependent effects in cell populations, in particular myeloid cells.

Although circulating monocytes do not express 11β-HSD1, this enzyme is dramatically upregulated upon their differentiation to macrophages or dendritic cells (273, 277). Briefly, macrophage 11β-HSD1 has been proposed to be central to the induction of inflammatory resolution as it drives macrophage efferocytosis and associated anti-inflammatory regulation, although it has further roles which will be discussed in section 1.3.6.2 below (278). The metabolism of endogenous GCs by 11β-HSD1 was found to negatively regulate immature dendritic cell survival and immune functions, maintaining them in an inactive state until their activation by TLR ligation overrides this inhibition (279). Dendritic cells activated solely by innate immune signals, such as TLR ligation, maintained or increased expression of 11β-HSD1, thus retaining the ability to respond to inactive GCs and generate cortisol. However, dendritic cells which have successfully presented cognate antigen to T cells to drive adaptive immunity instead downregulate 11β-HSD1 and thus bioavailability of GCs (277). This mechanism allows for the GC-mediated restraint of inflammatory innate reactions, while permitting dendritic cells carrying relevant antigen a release from the GC-mediated suppression of adaptive

functions as discussed previously. This fine-tuning of intracrine and paracrine GC responses by 11β-HSD1 in myeloid cells thus enables regulation of their immune and inflammatory functions.

11β-HSD1 is also expressed by lymphocytes including CD4+ and CD8+ T cells and B cells. A marked increase in expression of 11β-HSD1 can be seen on activation of the T cell receptor and polarisation to Th1 and Th2 subsets. Stimulation with the inactive murine GC 11-deoxycortisosterone (11-DHC) drives induction of GILZ and IL-7Rα, which both protect T cells against GC-induced apoptosis (274). Although a model of atopic dermatitis has revealed a role for 11β-HSD1 in inhibiting T cell acquisition of an allergic Th2 phenotype, there is relatively little evidence of the importance of 11β-HSD1 in adaptive immune cells compared with its role in cells of the innate immune system (280).

In addition, 11β-HSD1 expression is induced or upregulated on inflammatory stimulation of stromal cells, and mesenchymal-derived stromal cells present with distinct differences in regulation of GC metabolism to lymphoid and myeloid cells. Osteoblasts and osteoclasts both express 11β-HSD1, and this expression is increased on stimulation with inflammatory factors such as TNFα (281). Whereas in myeloid-derived osteoclasts, treatment with inactive GCs downregulates inflammation-induced 11β-HSD1 expression, in osteoblasts cortisone treatment synergises with TNFα to potently upregulate 11β-HSD1 in a positive feedback loop (282, 283). Fibroblasts and myocytes similarly undergo this synergistic induction of 11β-HSD1 expression and activity when stimulated simultaneously with GCs and inflammatory cytokines, which has been hypothesised to be a stromal cell mechanism of dramatically increasing local GC levels to suppress inflammation (284). Interestingly, this synergistic induction was found to centre on NFκB signalling, with this transcription factor being

necessary for the continued expression of 11β-HSD1 and release of active GCs. This mechanism may allow continued release of GCs while an NFκB-stimulating inflammatory signal remains in tissue, however it could also be a driver of excess GC-associated pathology such as muscle wasting and bone erosion (285, 286).

Given the broad range of expression of 11β-HSD1, and its induction or enhancement on inflammatory stimulation, it is unsurprising that this enzyme is upregulated in many chronic inflammatory diseases. This includes the inflamed colon in ulcerative colitis and Crohn's disease, and the inflamed synovium in RA (287-289). Additionally, the activity of 11β-HSD1 was recently found to be vital for mediating the anti-inflammatory effects of therapeutic GCs, highlighting the potential for specific targeting of therapeutic GCs to this enzyme to augment anti-inflammatory actions (290).

1.3.6.2 11β-HSD1 in macrophages

11β-HSD1 was first identified in macrophages in 2001, where it was revealed that differentiation of blood monocytes into macrophages by passive adherence and stimulation of the monocyte/macrophage THP-1 cell line with LPS drove potent induction of 11β-HSD1 expression (273). This has been corroborated in further cell lines such as the murine macrophage J774.1 cell line, which has some baseline *HSD11B1* mRNA expression, though both expression and enzyme activity were dramatically upregulated by LPS stimulation (291). M1-polarisation of human blood monocyte derived macrophages with IFNγ and LPS similarly upregulates 11β-HSD1 expression, and this was found to be 9-fold higher than its induction in IL-4 polarised M2 macrophages (104). This disparity is also seen in M1-like and M2-like macrophages generated from human blood monocytes using GM-CSF and M-CSF respectively

(292). The inflammation-induced upregulation of 11β-HSD1 in macrophages thus primes them for anti-inflammatory regulation by GCs, just as the similar inflammatory-mediated induction of GRα does (225). Inflammatory macrophages are therefore equipped with the ability to respond to both active and inactive GCs.

However, in vitro analysis of macrophages is complicated by the broad range of techniques used to generate and stimulate these cells, as highlighted in section 1.2.2. Contrary to their findings in inflammatory macrophages, Thieringer at al did not find significant upregulation of 11β-HSD1 in freshly isolated monocytes activated with inflammatory factors such as LPS or TNFα. Anti-inflammatory activation of monocytes using IL-4 and IL-13 instead elicited 11β-HSD1 expression and activity (273). Similarly, studies involving direct stimulation of monocytes with macrophage polarising factors during differentiation (LPS for M1-like or IL-4 for M2), reported higher 11β-HSD1 expression in M2 macrophages compared to M1-like (293).

There are species-specific differences in 11β-HSD1 expression, as human circulating leukocytes do not express basal 11β-HSD1, while those of mice do (278). Nevertheless, mouse models have provided important data on the functions and regulation of 11β-HSD1 in macrophages in vivo, within the context of systemic GC metabolism. Tissue resident macrophages isolated from the adipose tissue of non-obese mice were found to express very low levels of 11β-HSD1 (294). Similarly, so do CD11b+ splenic populations of macrophages, although at a relatively high level compared to that of B and T lymphocytes of the spleen (274). However, other papers have identified that while 11β-HSD1 can be induced on inflammatory stimulation of recruited monocyte-derived macrophages, such as in the sterile inflammation induced by intraperitoneal thioglycolate injection, tissue resident macrophage

populations in this site did not upregulate 11β-HSD1 (278). This fits with in vitro differentiation of monocytes into M2-like macrophages with M-CSF driving only moderate levels of 11β-HSD1 expression and activity, as this growth factor is associated with maintenance of a homeostatic M2-like tissue resident macrophage phenotype (292).

11β-HSD1 has been found to have functions in regulation of inflammation in macrophages. Thioglycolate-elicited peritoneal macrophages and splenic macrophages from *Hsd11b1*$^{-/-}$ mice both dramatically overproduce inflammatory cytokines such as TNFα, IL-6 and IL-12 p40 on LPS stimulation compared to wild type macrophages. This was found to be due to unrestrained activation of the MAPK and NFκB signalling pathways, which are targeted by active GCs in macrophages (295). Similarly, Gilmour et al noted an increase in IL-6 release from LPS-treated thioglycolate-induced peritoneal macrophages from *Hsd11b1*$^{-/-}$ mice, and also identified a key role for 11β-HSD1 in the acquisition of a pro-resolution phenotype in macrophages. 11β-HSD1 was found to be rapidly upregulated by macrophages recruited to the peritoneum by intraperitoneal thioglycolate, and *Hsd11b1*$^{-/-}$ mice showed a delay in macrophage phagocytosis of apoptotic neutrophils (278). Although this deficiency did not delay overall resolution of peritonitis, this was an acute resolving animal model of inflammation which highlights some of the processes that could be affected in more chronic inflammatory diseases where GC metabolism becomes dysregulated. Macrophage phagocytosis of apoptotic neutrophils downregulates 11β-HSD1 activity, which shows that GC metabolism is acutely linked to macrophage phenotypic and functional state (296).

In addition to modulating inflammatory functions via intracrine metabolism, GCs generated by 11β-HSD1 have been shown to influence neighbouring cells in a paracrine fashion. Previous work in the Hardy group found conditioned supernatant from wild-type inflammatory

activated macrophages treated with the inactive murine GC 11-DHC could drive GC-inducible responses in FLS from *Hsd11b1*$^{-/-}$ mice. Inflammatory activated FLS upregulated *GILZ* expression and suppressed IL-6 secretion in response to GCs in conditioned media that could only have been activated by 11β-HSD1-compentent macrophages (290).

Despite the evidence in support of a role for 11β-HSD1 in driving an M1-like to M2-like polarisation shift in macrophages during an inflammatory response, further mouse models of acute inflammatory insult have highlighted that this process is far more complex and likely highly context specific. Although *Hsd11b1*$^{-/-}$ mice suffer worse inflammatory influx than wild type mice in a model of myocardial infarction (MI), they also show improved infarct healing and cardiac function on recovery. Increased numbers of M2-like Ym1+ macrophages expressing pro-angiogenic and pro-inflammatory CXCL8 could be seen in the hearts of *Hsd11b1*$^{-/-}$ mice following MI, and this was associated with increased vessel formation required for healing (297). Further work highlighted that this increased inflammatory neutrophil influx seen in *Hsd11b1*$^{-/-}$ mice likely served to polarise macrophages towards this pro-reparative profile as macrophages phagocytosed the excess apoptotic neutrophils (298).

This pro-angiogenic programming has also been seen on inflammatory challenge of mice with specific knockout of 11β-HSD1 in macrophages utilising Cre-Lox recombination. Crossing mice with the Cre recombinase gene inserted under the key myeloid cell anti-microbial enzyme lysozyme (LysM; *LysM-Cre*) to those with the Cre-targeted Lox sequences "floxed" on either end of the Hsd11b1 gene (*Hsd11b1*$^{f/f}$) results in offspring with a deficiency of 11β-HSD1 selectively in myeloid cells (*11βflx/LysMcre*), which includes macrophages but also neutrophils (299). Assessment of wound healing using the subcutaneous sponge implantation model found that *11βflx/LysMcre* mice had greater inflammatory angiogenesis, characterised

by increased vessel density and expression of pro-inflammatory cytokines with pro-angiogenic functions such as IL-1β, although the cellular source of these cytokines was not identified (300). It may be that while 11β-HSD1 functions as an inflammatory brake in M1-like macrophages, its absence does not prevent macrophages polarising to a final tissue reparative phenotypic stage of resolution. Alternatively, it could be that while macrophages are unable to fully repolarise from M1-like to M2-like, as seen by the increased expression of macrophage associated inflammatory cytokines such as IL-1β and CXCL8, this does not impede reparative functions required for repair of sterile acute tissue injuries, such as MI.

Additionally, the molecular regulation of 11β-HSD1 expression in macrophages has not been fully ascertained. The nuclear receptor peroxisome proliferator-activated receptor-γ (PPARγ), which binds a range of natural and synthetic ligands, promotes anti-inflammatory functions and M2-like polarisation in macrophages by repressing NFκB-mediated induction of inflammatory gene expression (301). Activation of PPARγ with synthetic ligands has been found to directly induce 11β-HSD1 transcription in human macrophages via binding at a PPARγ response element in the *Hsd11b1* promoter. However, although PPARγ ligand binding induced 11β-HSD1 gene expression in both M1-like and M2-like macrophages, enzyme activity was only upregulated in M2-like macrophages, with no induction seen in M1-like macrophages (293). As of yet, no similar response elements have been identified for M1-like inflammatory macrophage induction of *Hsd11b1* expression. NFκB signalling may play a role as this transcription factor mediates activation following macrophage stimulation with numerous TLR ligands, and it has been found to mediate 11β-HSD1 upregulation in mesenchymal cells in a manner involving the *Hsd11b1* P2 promoter (285, 302). Likewise, the transcription factor CCAAT/enhancer binding protein-β (C/EBPβ) is involved in induction of *HSD11B1* expression, in response to GC and inflammatory stimulation in adipose cells and

fibroblasts via balance of its isoforms liver-enriched inhibitor protein (LIP) and liver-enriched activator protein (LAP), which have inhibitory and stimulatory functions respectively (303-305). C/EBPβ has been hypothesised to play a role in induction of 11β-HSD1 expression in macrophages, as this transcription factor has been linked to both pro-inflammatory and pro-reparative macrophage functions, perhaps driven by a linking of the balance of LIP:LAP isoforms and the metabolic state of macrophages (306-308).

The differential metabolic programming of polarised macrophages may provide an additional non-genomic layer of regulation of 11β-HSD1, as the glycolytic metabolism of M1-like macrophages may favour 11β-HSD1 reductase activity by providing more NADPH cofactor via H6PDH than the oxidative phosphorylation preferred by M2-like macrophages (308). However, this regulation, and whether 11β-HSD1 itself can affect macrophage polarisation via metabolism, has not yet been fully explored.

1.3.6.3 11β-HSD1 in RA synovial macrophages

Initial studies suggested a reduction in the conversion of cortisone to cortisol mediated by 11β-HSD1 in the synovia of RA patients compared to OA patients. However, the level of inflammatory synovitis in RA patients strongly correlated with GC reactivation ratio, in line with earlier in vitro studies on the inflammatory induction of 11β-HSD1 (309). More recent analysis similarly identified that higher levels of 11β-HSD1 reductase activity, as measured by urinary corticosteroid metabolites, predicted progression to more persistent disease in newly diagnosed RA patients. 11β-HSD1 activity levels also correlated with systemic inflammation measures of CRP and ESR, whereas lower 11β-HSD1 levels were associated with resolving disease (310). This is in contrast to the levels of systemic GCs in RA patients, which are often

reduced compared to healthy individuals, implying a general suppression of the HPA axis despite high systemic levels of inflammatory cytokines which would be expected to promote HPA activation (311).

Immunohistochemistry analysis of synovial samples from RA patients showed expression of 11β-HSD1 was localised to FLS, with some expression on T cells and dendritic cells, while synovial macrophages were initially found to instead express the GC-inactivating enzyme 11β-HSD2 (289). It has been hypothesised that the induction of 11β-HSD2 in macrophages could occur as a response to persisting chronic inflammation, in contrast to its downregulation in other cell types during acute inflammatory stimulation (281, 308). Microarray analysis of PBMCs in RA patients conflicts with this theory in RA as HSD11B2, encoding 11β-HSD2, was upregulated significantly in early RA compared to established RA, implying that this enzyme profoundly decreases in expression with progressive chronic inflammation (312). However, this study only assessed circulating PBMCs, not tissue synovial macrophages, and within a small relatively unrepresentative sample group. As such, no functional significance has been ascertained for 11β-HSD2 in synovial macrophages.

Interestingly, although there are more limited reports of 11β-HSD1 staining of RA synovial macrophages, this has been identified in both total CD68+ lining macrophages and within CD163+ macrophages (309, 313). This isozyme has also been found to be more important in the context of disease according to animal models. While *Hsd11b1*$^{-/-}$ mice suffered worse disease on induction of the K/BxN serum transfer model of arthritis, *Hsd11b2*$^{-/-}$ mice had no differences in disease development or progression (272).

The LysM-cre mediated knockout of *Hsd11b1* in myeloid cells in mouse models of inflammatory arthritis have revealed important roles for macrophage pre-receptor GC

metabolism in disease. Loss of macrophage *Hsd11b1* in the acute resolving K/BxN serum transfer model of arthritis leads to a delay in resolution of disease and worse histopathological scoring compared to wild-type animals. An increase in expression of endothelial cell markers highlighted that macrophage 11β-HSD1 acts to repress inflammatory angiogenesis in response to endogenous GCs, with its loss driving inflammatory cell recruitment and the resulting increased synovial hyperplasia and bone erosion seen in LysM-cre mice (300). In the chronic TNF-tg mouse model of polyarthritis, global knockout of 11β-HSD1 not only worsened disease severity and joint destruction but also promoted an increase in number and M1-like inflammatory polarisation of synovial macrophages (314). This increase in MHCII+ macrophages came with a loss of the MHCII- synovial macrophage population that had previously been shown to be associated with protection from severe disease in the K/BxN model of arthritis (120). Additionally, while deletion of *Hsd11b1* in stromal cells such as FLS and osteoblasts using floxed *Hsd11b1* crossed with cre recombinase under the mesenchymal lineage transcription factor Twist2 (*11βflx/Tw2cre*) did not exacerbate clinical scores or bone erosion compared to *Hsd11b1*-competent TNF-tg mice, there was a reduction in joint inflammation and paw swelling (314). This may be due to a greater level of endogenous inactive GCs being targeted to synovial macrophage 11β-HSD1 and driving a decrease in inflammatory angiogenesis.

In addition to endogenous GCs, macrophage 11β-HSD1 has also been strongly implicated in the anti-inflammatory actions of therapeutic GCs. Fenton et al identified that active therapeutic GCs require local reactivation at the inflamed site by 11β-HSD1 for effective function, as TNF-tg *Hsd11b1*$^{-/-}$ mice lost therapeutic responsiveness to corticosterone (290). GC treatment of TNF-tg mice reduced numbers of both total F4/80+ synovial macrophages and MHCII+ M1-like polarisation as well as levels of the M1-associated pro-inflammatory

cytokines TNFα and IL-1β, and this was lost on global 11β-HSD1 knockout. While *11βflx/Tw2cre* mice retained therapeutic responses to GCs, including reduced clinical scores, joint inflammation and destruction and bone erosion, *11βflx/LysMcre* mice partially phenocopied *Hsd11b1*$^{-/-}$ mice. Although *11βflx/LysMcre* mice showed a reduction in joint inflammation scores and serum IL-6 levels, total clinical score was not reduced and there was greater evidence of persistent joint destruction. Loss of 11β-HSD1 activity was confirmed in both in vitro differentiated monocyte-derived macrophages and peritoneal macrophages, thus it can be assumed that 11β-HSD1 was targeted in both tissue resident and circulating monocyte-derived synovial macrophage populations.

Importantly, while macrophage 11β-HSD1 has been found to mediate anti-inflammatory actions of therapeutic GCs in polyarthritis, it does not appear to drive the GC-mediated bone erosion commonly seen as side effects of therapy. Therapeutic GCs drive bone erosion through promotion of osteoclast survival and activity at the expense of that of osteoblasts, in addition to downregulation of pathways responsible for inflammatory bone loss such as TNFα and RANKL, which are upregulated in RA synovial macrophages (138, 315). *11βflx/LysMcre* mice display a partial loss of the bone protective effects of therapeutic GCs, and in vitro analysis of osteoclasts identified a role for 11β-HSD1-activated GCs in downregulating catabolic metabolism. However, targeting myeloid-derived cells via LysM expression will also have targeted 11β-HSD1 in macrophage populations. This implies that macrophage 11β-HSD1 could have a role in the bone protective effects of therapeutic GCs (282).

As synovial macrophages potently upregulate 11β-HSD1 in response to inflammatory factors in polyarthritis, and their pre-receptor metabolism of GCs mediates anti-inflammatory functions shown to be beneficial in models of disease, there is rationale for targeting GCs to

macrophages more specifically via this enzyme to better promote these functions. More specific targeting of inactive GCs to macrophages would allow intracrine GC regulation of a key inflammatory player in RA, while also reducing the exposure of stromal cells such as osteoblasts and myocytes, where therapeutic GCs drive catabolic effects. Importantly however it is not yet known whether macrophage GC metabolism is involved in the muscle wasting associated with GC treatment of polyarthritis, which itself has recently been shown to be dependent on 11β-HSD1 by Webster et al (316).

1.4 Androgens

Androgens are steroid hormones with diverse roles in development and maintenance of male characteristics including primary sex organs and secondary sex characteristics. In addition, they have several roles in female sexual function and are the precursors to estrogens. Further research has identified vital functions for these hormones in immunity and inflammation. However, they are also implicated in the pathology of chronic inflammatory and autoimmune diseases, many of which present with markedly skewed sex ratios which could imply a protective role for androgens. This includes RA, where the ratio of female:male patients can be as high as 3:1, and others with far higher sex disparity such as systemic lupus erythematosus (7:1) and primary Sjögren syndrome (10:1) (317, 318).

The four main androgens in order of increasing potency are DHEA, androstenedione, testosterone and dihydrotestosterone (DHT), with DHEA possessing only weak androgenic effects. These steroids exert androgenic effects by binding the intracellular androgen receptor (AR), part of the nuclear receptor family. Although DHT is far more potent than testosterone, testosterone is the main androgen present in serum in males, and in females this is DHEA. However DHT is considered a “true” androgen as it cannot be converted to estrogen by the enzyme aromatase, as testosterone can (319).

The adrenal glands are the main source of DHEA and androstenedione, however they also provide around 1% of circulating testosterone in males and 30-50% in females (320, 321). As with cortisol, these androgens are generated from the metabolism of cholesterol, as shown previously in Figure 1-5, with the 19-carbon steroid DHEA forming the precursor for subsequent androgens. Serum DHEA derives from the zona reticularis of the adrenal cortex in response to ACTH, with around 10% secreted from gonads in response to gonadotrophin-

releasing hormone (GnRH). Most serum DHEA exists as the inactive sulfate ester form DHEA-sulfate (DHEAS), which is generated in the adrenals by the enzyme steroid sulfotransferase 2A1 (SULT2A1) (320). The adrenal gland also generates the 11-oxygenated androgen precursors 11OH-androstenedione and 11OH-testosterone, which can be converted in the periphery to active 11-oxygenated androgens. 11-oxygenation has roles in androgen metabolism and diseases of androgen excess, as reviewed by Turcu et al (322). There has been limited research on the role of these androgens in immunoregulation, however recently Schiffer et al identified that natural killer cells could metabolise these steroids, implying they may have a role in regulating immune function (323).

Most circulating androgens are bound by serum proteins including albumin and sex hormone binding globulin (SHBG), with around 1% existing in serum as free steroid (167). This regulates their ability to cross cell membranes and exert effects by binding the AR. As with other nuclear receptor family members such as the GR, the AR has NTD, DBD and LBD regions, which dictate its retention in the cytoplasm by heat shock proteins and chaperone proteins until ligand binding induces a conformational change, permitting nuclear translocation. The AR-ligand complex binds to androgen response elements (ARE) on androgen-inducible genes with regulation by cofactors to directly drive gene transcription. The AR gene itself is a target of androgen stimulation, with androgens either downregulating or upregulating its expression depending on cell type (324). All active androgens can activate the AR, however the more potent ones such as DHT are characterised by enhanced binding and retention at the AR with slower dissociation rate (325).

Similar to GCs, androgens have been found to exert effects via both genomic and non-genomic routes. Rapid induction of calcium flux in response to androgen stimulation has been

identified in macrophages and T cells. This has been hypothesised to be induced by putative membrane ARs, however evidence for this is controversial (326, 327). SHBG bound androgens have also been shown to mediate nongenomic effects such as increases in cyclic AMP levels via interactions with membrane receptors (328).

1.4.1 Extragonadal androgen synthesis and metabolism

In addition to endocrine action of androgens produced by the adrenal glands and gonads, androgens can be generated at the tissue level to exert local effects. Although unbound steroids can freely cross the plasma membrane, conjugated steroids such as DHEAS must be transported via transmembrane proteins, such as organic anion-transporting polypeptides (OATPs) expressed across tissues (329). Once taken up by OATPs, DHEAS can be converted back to DHEA through desulfation by steroid sulfatase (STS), which generates the majority of circulating DHEA (330). This also provides the precursor for androgen synthesis in peripheral tissues as detailed in Figure 1-7 Intracrine androgen synthesis.

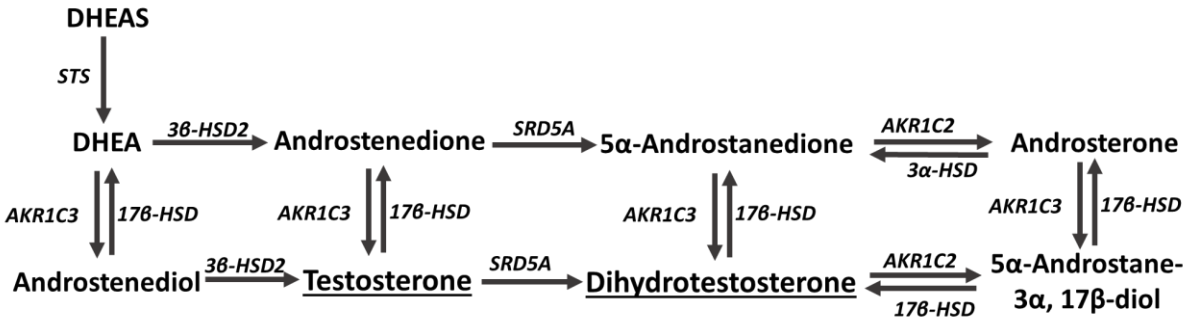

Figure 1-7 Intracrine androgen synthesis

Active androgens (underlined) can be generated from precursors such as DHEA in peripheral tissues. Adapted from Schiffer et al (336)

Testosterone is generated mainly in gonads, the testes and ovaries. However, extragonadal testosterone metabolism plays fundamental roles in various organs such as the development of kidneys and maintenance of muscle. Aldo-keto reductase 1C3 (AKR1C3) is a reductive 17β-HSD enzyme, which is expressed at low levels in the adrenal glands and also primarily functions as a nongonadal androgen activator in the periphery. As seen in Figure 1-7 it catalyses several reactions to generate active androgens from precursors, in particular via the conversion of androstenedione to testosterone (160). DHT is solely generated locally, mainly through 5α-reduction of testosterone by the steroid 5α-reductase type A (SRD5A) enzymes (160, 331). This occurs in peripheral tissues that are the main target of androgens during development such as the prostate but also in the adult skin and liver (332).

AKR1C3 and SRD5A therefore act as the rate limiting enzymes for androgen activation within cells in the periphery, enabling generation of androgens that can act via AR within the cell. This extragonadal activation of steroid precursors is called intracrine metabolism, as it acts within a cell and does not involve secretion of the product for receptor binding (333). Intracrine metabolism of sex steroids has been hypothesised to be important in regulation of immune cells such as macrophages (334).

There are multiple pathways of extragonadal androgen activation that have been identified in humans. However, some, such as the "backdoor pathway" which uses 17α-hydroxyprogesterone instead of DHEA or androstenedione, have only been found to be relevant in conditions of progestogen excess, such as with deficiencies of various cytochrome P5450 enzymes (335). In the classical androgen pathway, DHT is generated directly from testosterone via SRD5A type 1 (SRD5A1), however this has been noted to not be the preferred route of DHT synthesis from DHEA(S) in the periphery and is instead is more relevant for

metabolism of circulating testosterone (336). The alternate pathway does not use testosterone, instead androstenedione is catalysed by SRD5A1 into 5α-androstanedione which is then converted to DHT by AKR1C3 (337). As SRD5A1 has a higher binding affinity for androstenedione than testosterone, this pathway is the major generator of active androgens in the periphery within cells expressing these enzymes (336).

1.4.2 Androgens as immunomodulators

In addition to serving as a precursor for more potent androgens, DHEA has immunomodulatory functions on binding AR or a hypothesised unique DHEA-specific receptor, which include reducing levels of inflammatory cytokines such as IL-6 and direct negative regulation of inflammatory transcriptional regulators such as NFκB (338, 339). These functions are reviewed extensively by Prall and Muehlenbein, while this thesis will instead consider the role of DHEA as an androgen precursor (340).

The AR is expressed widely across the body, including on immune cells. T cells have been identified to express both the classical intracellular AR as well as membrane associated androgen receptors, while B cells appear to express only the intracellular AR (326). Similarly, the AR is expressed across innate immune cell populations, including neutrophils, monocytes, dendritic cells and macrophages (341).

Androgens possess generally anti-inflammatory and immunosuppressive effects, although this specificity depends on cell type and context. They have been strongly implicated in promotion of neutrophil differentiation and survival, with neutropenia seen in $AR^{-/-}$ mice, however stimulation of neutrophils with testosterone downregulates pro-inflammatory cytokines and anti-microbial functions in favour of IL-10 secretion (342, 343). Androgens have

similar context-specific effects on macrophage survival and function, discussed in more detail below. Dendritic cells subjected to androgen treatment show impaired activation of Th1 or Th2 T cells during antigen presentation (344). Many of these anti-inflammatory and immunosuppressive effects could be explained by the AR-induced maintenance of expression of the NFκB inhibitor IκBα, which was found to inhibit IL-6 expression and secretion (345).

Androgens also regulate several other stages of adaptive immunity. T and B cells express *HSD17B1* and *SRD5A1* and can generate testosterone from androstenedione and DHT from testosterone (346). Lymphopoiesis of both B and T cells is negatively regulated by androgens, with reversal seen on gonadectomy or AR deficiency (347). Interestingly in T cells this involves an androgen-driven increase in expression of the autoimmune regulatory element (Aire) gene in the thymus, which aids removal of self-antigen specific developing T cells (348). Therefore, androgens have many functions in immunoregulation, many of which begin to explain some of the sex differences with autoimmune and inflammatory disease.

1.4.3 Dysregulation of androgens in RA

Due to its immunosuppressive effects on immune cells, detailed above, there are strong associations between lower androgen levels and increased risk of developing chronic inflammatory disease including atherosclerosis, type 2 diabetes and RA (349-351). Androgens have long been implicated in the pathogenesis of RA, as the disease is more prevalent in females, with an all age F:M patient sex ratio of 2.3:1, which dramatically decreases following average age of menopause. The peak incidence of RA in females occurs post-menopause (352). Serum testosterone levels have been found to significantly negatively correlate with ESR in male RA patients (353).

Although it is beyond the scope of this thesis, it is important to note that estrogens have been strongly implicated in the pathogenesis of RA and its associated patient sex ratio. As reviewed extensively by Islander et al, estrogens regulate bone metabolism and so have protective effects on bone in models of RA, which may explain the increased incidence of RA post-menopause. However, estrogen metabolites have been shown to have distinct pro-inflammatory effects on synoviocytes in RA (354, 355). Therefore, both excess and deficiency of estrogens can have roles in driving RA pathology.

Dysregulation of androgens can be seen further upstream in RA. Lower serum levels of DHEA are commonly seen in chronic inflammatory diseases, as well as an increased DHEAS/DHEA ratio. Inflammatory bowel disease patients have been found to possess increased ratios of cortisol/DHEA and lower ratios of DHEA/androstenedione, highlighting that steroid metabolism shifts towards preferential generation of GCs over androgens. Multiple linear regression analysis identified serum TNFα levels as the mostly likely key driver of this skewed ratio (356). RA patients also produce far less adrenal androgens such as DHEA on ACTH stimulation test, while normal cortisol levels were seen (357). Neutralisation of TNFα or IL-6 has been shown to normalise this skewed GC/androgen ratio in RA patients. Anti-TNFα and anti-IL-6 therapy each increased the ratio of serum androstenedione/cortisol while anti-IL-6 therapy also decreased DHEAS/DHEA, thus dysregulation in androgen levels is mediated by inflammatory cytokine levels in chronic inflammatory diseases (358, 359). These findings were attributed to inhibitory actions of inflammatory cytokines on adrenal androgen secretion. However, they likely also have effects at the intracrine level within immune cells. IA GC injections were found to decrease expression of steroid receptors, including the AR, on synovial cells (360). This highlights that a complex regulation of steroid levels occurs at the local synovial level.

Androgens in synovial fluid have been hypothesised to exert immunosuppressive effects, as discussed in section 1.4.2 above, particularly on monocytes, macrophages, T cells and B cells (361). The anti-inflammatory effects of DHT, acting via AR-dependent NFκB inhibition, were noted in an RA FLS-like cell line, therefore synovial stromal cells are likely also a target of regulation (362). However it appears this immunoregulation is lost in RA, as low levels of androgens have been identified in the synovial fluid of RA patients, with a corresponding increase in estrogens (363). This is likely driven by the action of pro-inflammatory cytokines such as TNFα and IL-6 in increasing expression of aromatase (364). Aromatase expression has been identified in the sublining and lining of RA synovium, which was thought to drive the observed higher levels of estrogens to androgens in the tissue. The same findings were seen in OA synovial tissue, although no comparison to healthy synovium was made, but it could be that local inflammation drives this skewing towards estrogen production in both diseases. Interestingly however, analysis of steroid conversion in mixed synovial cells in this study found that while conversion of DHEA into estrogens was similar in RA and OA, RA mixed synovial cells converted androstenedione and testosterone into DHT at a far greater level (365). This implies higher expression or activity of SRD5A in RA cells, despite the dominance of estrogens in the synovium. Additionally, androgen treatment inhibited the action of aromatase in these mixed cells, as seen in a reduction of estrogens produced from androgen treatment. This implies that therapeutic androgens could be able to exert anti-inflammatory effects without conversion to estrogens (365).

This shift from androgens to estrogens has been proposed to drive loss of the anti-inflammatory functions of androgens, such as the inhibition of the RA-associated inflammatory cytokine IL-6 and IL-1β by PBMCs (345, 366). The effects of this shift in sex steroids has been detailed in mouse models of CIA using expression of the shared epitope,

*DRB1*04*, to recapitulate features of sex disparity seen in human disease but not mouse models (367). Female mice showed a stronger T cell response to the arthritis-inducing collagen peptide than male mice, with a greater number of splenic and activated T cells and increased IFNγ production. Similarly, estrogen has been found to enhance autoantibody production by B cells, while androgens suppress this (368). Estrogen also has stimulatory effects on FLS proliferation and secretion of MMPs in a cartilage invasion assay (369). Together, these data have supported the hypothesis that dysregulated sex steroid ratios in RA, characterised by decreased androgens and increased estrogens, promote inflammatory pathology.

1.4.4 Androgen action in macrophages

Expression of the classical nuclear AR has been identified in human blood monocytes, as well as numerous macrophage populations, including monocyte-derived and tissue resident (370, 371). There have been fewer studies into expression of the non-classical membrane AR on macrophages, however it has been identified so far on murine bone marrow derived macrophages and peritoneal macrophages, implying it may be present on human macrophage populations (327, 371). Expression of the AR on macrophages appears to be negatively regulated by androgen stimulation (372). Macrophages also express STS and can convert DHEAS to DHEA, though inflammatory activation was found to decrease this ability (373).

Additionally, macrophages possess the enzymes required for intracrine generation of active androgens. Human macrophages have been found to generate testosterone and DHT from androstenedione, and testosterone, DHT and androstenedione from DHEA, therefore they

express *SRD5A1* and *AKR1C3* (374, 375). However, it is unknown how expression of androgen activating enzymes changes with macrophage differentiation and polarisation. Human blood monocytes were recently found to express minimal AKR1C3 on analysis of PBMCs, therefore implying it could be induced only on differentiation to macrophages (323).

Macrophages also express the estrogen-generating enzyme aromatase, with an upregulation in expression seen on differentiation of both human blood monocytes and THP-1 monocytes to macrophages (375). Macrophages both respond to and generate estrogens, and these have been shown to have diverse, though generally pro-inflammatory and immunostimulatory, effects depending on dose and cell context, as reviewed by Batty et al (376). Interestingly, unlike in other cell types, inflammatory activation of macrophages with TNFα, IL-1β or IL-6 did not induce aromatase. Nevertheless, pro-inflammatory cytokines did slightly downregulate the dramatic induction of aromatase seen on dexamethasone treatment (377, 378). DHEA treatment conversely decreased aromatase expression in human blood-monocyte derived macrophages (375). Therefore, macrophages have the capacity not only to respond to paracrine androgens but also to modulate local androgen levels via intracrine metabolism, and this process is regulated by androgen availability.

As with other immune cells, androgens have generally anti-inflammatory and immunosuppressive actions on macrophages. Testosterone suppresses LPS activation of macrophages both by downregulating expression of TLR4 and inhibiting downstream p38 MAPK signalling via increased intracellular calcium (379, 380). The latter effect occurred in a rapid apparent AR-independent mechanism. Androgens also suppress NFκB signalling in macrophages in an AR-dependent mechanism involving promotion of IκBα stability and inhibitory function (381). This results in a downregulation of inflammatory cytokine output in

macrophages, such as TNFα and NO production on LPS challenge, when exposed to physiological levels of testosterone (382, 383). Testosterone treated macrophages also release cytokines such as IL-10, highlighting a shift towards a more M2-like pro-resolution state (372). Similarly, DHT was found to enhance the acquisition of M2-like markers such as *Agr1* expression in IL-4 polarised murine bone marrow derived macrophages (371). Longer term stimulation with testosterone has also been found to promote apoptosis of macrophages (381, 384).

There have been fewer studies on the effects of androgen precursors on macrophage functions. Recently, DHEA has been found to repress LPS-induced activation of MAPK, NFκB and AKT and inhibit NLRP3 inflammasome activation in RAW264.7 macrophages (385, 386). DHEA treatment has also reduced superoxide anion production in alveolar macrophages (387). However, it is unknown whether this is due to the conversion of DHEA into active androgens or separate actions of DHEA itself as a steroid.

1.4.5 Androgen metabolism in RA synovial macrophages

Despite the prominent role of macrophages in the inflammatory pathology of RA and studies on the response to and metabolism of androgens in other macrophage populations, little is known about the metabolism of androgens within RA synovial macrophages. They are known to express the AR in both healthy and RA human synovium, with higher expression seen on cells from RA patients (388, 389). Additionally, synovial macrophages can metabolise testosterone into DHT in vitro, a process which also resulted in decreased IL-1β release (390). Therefore, they must express SRD5A, or perhaps use a more complex pathway, and androgens may exert anti-inflammatory functions in RA via synovial macrophages. Synovial

macrophages isolated from RA patients were also found to generate small amounts of androstenedione from testosterone, however this was not compared to healthy synovial macrophages so it is unknown whether this back-conversion of androgen precursors from active androgens is a feature of RA pathology (391).

Synovial macrophages were hypothesised to be central to the anti-inflammatory effects of DHEA treatment in a mouse model of AIA, where a significant reduction in paw swelling was seen, however this was not tested directly (392). Similarly, IA injections of androgens were found to decrease synovial hyperplasia and cartilage erosion, both effects which RA synovial macrophages are known to drive, but again macrophages were not assessed in detail (393). Treatment of RA patients with the immunosuppressant cyclosporin is associated with androgenising side effects such as excess hair growth and increased serum levels of androgen metabolites. The metabolism of testosterone by isolated RA synovial macrophages into DHT via SRD5A was found to be increased on stimulation with cyclosporin (394). This was hypothesised to be driven by direct pro-androgenising effects of cyclosporin, however may be due to previously identified anti-inflammatory actions of cyclosporin on macrophages (395). The inhibition of inflammatory signalling may counteract the upregulation of enzymes such as aromatase driven by cytokines in the RA synovia or may instead directly enhance androgen metabolism further upstream.

In summary, there is limited research into intracrine metabolism of androgens in RA synovial macrophages, despite suggestions that this metabolism is an important regulator of inflammatory function in other macrophage populations. It is therefore unknown how androgen metabolism differs in the distinct pathological and protective subsets of macrophages identified in RA, and how this intersects with GC metabolism in these cells.

Functional analyses of steroid metabolism in these cells would offer vital insight into targeting metabolism with novel therapeutics to overcome the dysregulation of steroid hormones seen in RA.

1.5 Hypothesis

I hypothesise that macrophage function in inflammatory disease is associated with dynamic changes in intracrine and paracrine metabolism of GCs and androgens. I further hypothesise that the enzymes associated with this macrophage-specific steroidogenesis could be important new targets for treatment of inflammatory diseases such as RA.

1.6 Aims

This thesis investigates these hypotheses by:

1. Characterising global steroid metabolism profiles in synovial macrophages in human inflammatory disease (Chapter 3)
2. Exploring macrophage metabolism of glucocorticoids and functional effects on inflammatory profiles (Chapter 4)
3. Exploring macrophage metabolism of androgens and functional effects on inflammatory profiles (Chapter 5)
4. Investigating novel targeting of glucocorticoids to macrophages using inflammatory glucocorticoid metabolism to improve anti-inflammatory therapeutics (Chapter 6)

Chapter 2 GENERAL METHODS

2.1 Rheumatoid arthritis RNA-seq analysis

RNA-seq is a technique in which next generation sequencing (NGS) is used to identify the transcriptome of cells. One of the most common techniques is Illumina® sequencing, in which amplification of sequences on flow cells allows massive parallel sequencing. RNA extracted from samples is reverse transcribed and complementary DNA (cDNA) transcripts are tagged with adaptors to allow hybridisation to the flow cell. Following clonal amplification, "sequencing by synthesis" is carried out, in which these fragments are sequenced through the addition of nucleotides by a polymerase, with each of the four nucleobases is labelled with a different fluorophore. The fluorescent emission readout of each cycle of amplification provides the sequencing of that transcript. During data analysis, reads of forward and reverse transcripts are paired to provide the complete sequence aligned to a reference genome for the species (396).

2.1.1 Bulk RNA-seq analysis of synoviocytes

Bulk RNA-seq data was generated by the National Institute for Health (NIH) Accelerating Medicines Partnership (AMP) RA Network (study accession code SDY998) (397). In this multicentre study, synovial tissue samples acquired from OA or RA patients undergoing joint biopsy or arthroplasty were sorted by fluorescence-activated cell sorting (FACS) into macrophage (CD45+ CD14+), fibroblast (CD45- CD31+ PDPN+), T cell (CD45+ CD3+) and B cell (CD45+ CD3- CD19+) populations and analysed by low-input bulk RNA-seq using Illumina®

Smart-seq2 (145). RNA expression of at least 1,000 cells per cell type for each sample was recorded as log_2 transcripts per million (log_2(TPM)). Low-quality samples were removed, including those with low cell counts (<1,000) and where <99% of common genes for that cell type were not expressed in that sample. Data for select genes and clinical data was accessed as a comma-separated values (CSV) file using an R script written by Dr Jason Turner at the Rheumatology Research Group, University of Birmingham Queen Elizabeth Hospital.

A panel of 109 key genes involved in steroid metabolism was developed by Dr Rowan Hardy and Dr Paul Foster (Supplementary Table 1 Steroid metabolism genes analysed in AMP RNA-seq dataset). The effects of local inflammation on expression of these genes were assessed in macrophages, fibroblasts, T cells and B cells by comparing leukocyte-poor and leukocyte-rich samples, as previously defined by Zhang et al in their dataset and related paper. These classifications have been found to correlate with Krenn histopathological measures of local synovial inflammation (145, 398).

2.1.2 Single-cell RNA-seq analysis of synovial tissue macrophage clusters

Single-cell RNA-seq (scRNA-seq) enables transcriptomic analysis of individual cells in order to capture the heterogeneity of cells such as synovial macrophages. Professor Mariola Kurowska-Stolarska analysed the expression of HSD11B1, AKR1C3 and SRD5A1 in a previously generated scRNA-seq dataset of human healthy and RA-affected synovial tissue macrophage (STM) subsets (146).

2.2 Serum and synovial fluid analysis

Blood serum and synovial fluid samples were taken by clinical staff at the Queen Elizabeth University Hospitals Birmingham Rheumatology Unit. Samples were collected, with informed consent, from adult patients with hip OA or RA undergoing elective joint replacement surgery. This study was carried out with ethical approval (REC 14/ES/1044 and NRES 16/SS/0172). Samples were stored at -80°C within 2 hours of collection.

2.2.1 Luminex

Luminex allows the quantification of multiple cytokines present in a sample using sets of beads labelled with fluorophores and antibodies specific for the cytokines of interest. Samples are incubated with the labelled beads, and the amount of fluorescence measured in a flow-based assay from the beads in each sample is proportional to the level of cytokine, and quantified with a standard curve (399).

Levels of inflammatory cytokines in synovial fluid samples were assessed using an Inflammation 20-Plex Human ProcartaPlex™ Panel (Thermo Fisher, UK) according to manufacturer's instructions. Magnetic antibody-labelled beads were added to the samples and antigen standards and incubated for 2h. Samples were incubated with detection antibody for 30min and then streptavidin-PE for 30min before resuspension in reading buffer and analysis on a Bio-Plex® instrument (Bio-Rad Laboratories Inc, USA). Each incubation stage was carried out on a rocker and samples washed in between each incubation.

2.3 Macrophage cultures

Although tissue resident macrophages can be isolated directly from sites such as the synovium, this is a laborious process that results in few cells. Additionally, methods of isolation using enzymatic digestion have been found to cause inflammatory activation (400). Differentiation of macrophages from peripheral blood derived monocytes enables culture of high number of cells and polarisation towards different pro- and anti-inflammatory phenotypes.

2.3.1 Blood monocyte derived macrophage culture

Macrophages were generated using monocytes obtained from blood cones from healthy fully anonymised donors, from the NHS Blood and Transplant Centre, Birmingham. This was approved by the University of Birmingham Ethics Committee, under ethical agreement ERN_14-0446.

2.3.1.1 Monocyte isolation

CD14+ monocytes were isolated from blood using by RosetteSep™ Human Monocyte Enrichment Cocktail (Stem Cell, UK), as per manufacturer's guidelines in a sterile environment at room temperature. This protocol isolates monocytes by negative selection, in which antibodies targeting non-monocyte cell surface markers bind and crosslink unwanted cells with red blood cells, forming "immunorosettes." Therefore when centrifuged over a density gradient medium, red blood cells and unwanted cells both pellet, leaving unlabelled monocytes at the blood plasma:density gradient medium interface. Blood was mixed with

ethylenediaminetetraacetic acid (EDTA) (Sigma-Aldrich, UK) to a final concentration of 1 mM and incubated with 75 µl RosetteSep™ Human Monocyte Enrichment Cocktail per 1ml of blood for 20 minutes. Blood was then diluted 1/4 in wash buffer (PBS, 2% v/v foetal bovine serum (FBS) and 1 mM EDTA), layered over Lymphoprep™ density gradient medium (Stem Cell Technologies, UK) and centrifuged at 1200g for 30 minutes with low acceleration and brake off. The interface layer of monocytes was pipetted off, resuspended in wash buffer and spun down at 300g for 10 minutes 5 times, until supernatant was clear. Isolated monocytes were counted and resuspended in Roswell Park Memorial Institute medium (RPMI 1640), supplemented with 10% v/v FBS, 100 U/ml penicillin and 100 µg/ml streptomycin (all Sigma Aldrich, UK) and 20 ng/ml human recombinant M-CSF (PeproTech, UK) and plated out at a concentration of $1x10^6$ cells/ml for 24-well plates or T75 flasks, or $0.2x10^6$ cells/ml for 96-well plates (plasticware all from Greiner, UK unless stated).

2.3.1.2 Macrophage differentiation and polarisation

In vitro differentiated macrophages were obtained by culturing monocytes with 20 ng/ml M-CSF for 6 days, with media changes on day 2 (d2) and d5. Macrophages were polarised as shown in Table 2-1. All cytokines were purchased from PeproTech, UK.

Macrophage polarisation type	Treatment cytokines	Concentration
M0	M-CSF	20 ng/ml
M1	M-CSF	20 ng/ml
	IFNγ	20 ng/ml
	Lipopolysaccharide (LPS)	10 ng/ml
M1-like	M-CSF	20 ng/ml
	IFNγ	20 ng/ml
	TNFα	10 ng/ml
M2	M-CSF	20 ng/ml
	IL-4	20 ng/ml

Table 2-1 Macrophage polarisation treatments

To assess active and inactive steroid stimulation, macrophages were treated with cortisol or cortisone respectively (Sigma-Aldrich, UK) at either 100 nM (equivalent to endogenous dose) or 1000 nM (equivalent to therapeutic dose).

2.3.2 Alveolar macrophages

Alveolar macrophages were provided by Dr Rahul Mahida and Lauren Davies at the Institution of Inflammation and Ageing at the Queen Elizabeth Hospital Birmingham. Lung tissue samples were taken from consenting never-smoker or long-term ex-smoker patients undergoing

surgical resection of lung tissue for mild chronic obstructive pulmonary disease (COPD). Alveolar macrophages were isolated by saline perfusion of lung tissue and density gradient centrifugation of lavage fluid, and samples assessed for purity by cytospin(401). Cells were seeded on 24-well plates at a density of 250,000 cells/ml in RPMI supplemented with 10% v/v FBS, 100 U/ml penicillin and 100 µg/ml streptomycin (all Sigma-Aldrich, UK).

Alveolar macrophages were inflammatory activated by treatment with 1 µg/ml LPS (PreproTech, UK) and responses to steroid stimulation assessed by treatment with cortisone or cortisol (Sigma-Aldrich, UK).

2.4 mRNA expression analysis

The expression of individual genes was investigated using TaqMan® quantitative polymerase chain reaction (qPCR) probes. TaqMan® probes contain a sequence complementary to the gene of interest along with a fluorescent probe that is normally inhibited by a quencher. During amplification of the cDNA by Taq® polymerase, the fluorescent probe is released from suppression by the quencher and a fluorescent signal is generated. This fluorescence is measured at each cycle of amplification and the intensity of the signal is proportional to the amount of that specific gene present in the sample. Relative quantification can be calculated by comparing the cycle threshold (CT), the cycle of amplification in which the fluorescent signal crosses a set threshold, of genes of interest to a housekeeping gene.

2.4.1 RNA extraction

RNA was isolated using the innuPREP RNA Mini Kit, following the manufacturer's protocol for extraction from eukaryotic cells (Analytik Jena, Germany). Briefly, cells were lysed in RL lysis buffer at room temperature before removal of DNA and cell debris by centrifugation at 10,000g on silica membrane. RNA was precipitated using 70% ethanol at room temperature and purified by centrifugation at 10,000g at 4°C on silica membrane. RNA was eluted in 30 µl RNase-free water (Promega, UK) by centrifuging at 8,000g and samples were stored at -80°C.

Concentration and purity of samples were determined using a NanoDrop™ ND-1000 spectrophotometer (Wilmington, USA). Absorbance at 260 nm was measured to calculate RNA concentration. Absorbance ratios at 260/280 and 260/230 were assessed to determine contamination by genomic DNA, phenol, protein and carbohydrates.

2.4.2 Reverse transcription

350 ng of RNA per sample was reversed transcribed to cDNA for qPCR analysis using a GeneAmp® PCR System 27000 machine (Applied Biosystems, UK), following manufacturer's instructions (Tables 2-2 and 2-3). cDNA samples were stored at -20°C until analysis by qPCR. All reagents were purchased from Applied Biosystems, UK.

Reagent	Volume per sample (µl)
10X Reverse transcriptase buffer	2
10mM dNTPs	0.8
Random primers	2
Multiscribe™ reverse transcriptase	1
RNase-free water	7.2

Table 2-2 Reverse transcription mastermix

Temperature (°C)	Time (minutes)
25	10
37	60
48	30
95	5
4	∞

Table 2-3 Reverse transcription PCR conditions

2.4.3 qPCR

The mRNA expression of key genes was assessed by qPCR analysis of cDNA and normalised to expression of the housekeeping gene 18S. 7 ng cDNA (1µl) of each sample was loaded with 9 µl qPCR mastermix containing appropriate gene probe, as detailed in Table 2-4 and 2-5 below.

Reagent	Volume per sample (µl)
SensiFAST™ Probe Lo-ROX (Bioline, UK)	5
RNase-free water	3.5
Gene probe (as below)	0.5

Table 2-4 qPCR mastermix

Target gene	Applied Biosystems reference number
18S	431943E
HSD11B1	Hs01547870_m1
HSD11B2	Hs00388669_m1
CD64	Hs00417598_m1
CD68	Hs02836816_g1
CD163	Hs00174705_m1
GILZ	Hs00608272_m1
NR3C1	Hs00353740_m1
H6PD	Hs00188728_m1
AKR1C3	Hs00366267_m1
SRD5A1	Hs00602694_mH
IL-6	Hs00985639_m1
IL-10	Hs00961622_m1
IL-12A (p35)	Hs01073447_m1
TNFα	Hs01113624_g1

Table 2-5 qPCR probes used for analysis

All reactions were carried out in a 96-well 0.1 ml microarray reaction plate (MicroAmp™, Applied Biosystems, UK). Plates were ran on the QuantStudio™ 5 Real-Time PCR System (Applied Biosystems, UK), as detailed in Table 2-6:

Cycles	Temperature (°C)	Time
X1	50	2 min
	95	1 min
X40	95	15 sec
	60	1 min

Table 2-6 qPCR cycle conditions

Abundance of specific mRNAs analysed, in CT, were normalised to that of the housekeeping gene 18S to determine ΔCT. mRNA expression (in arbitrary units, AU) was calculated through log transformation as:

$$Expression\ (AU) = 1000\ \times 2^{-\Delta CT}$$

All analysis of statistical significance in mRNA expression changes was carried out using ΔCT values.

2.5 Steroid quantification

2.5.1 11β-HSD1 enzyme activity assay

The conversion of the inactive steroid cortisone into its active form cortisol by the enzyme 11β-HSD1 was assessed using scanning thin layer chromatography (TLC). TLC allows separation of a sample into constituent compounds based on their differences in solubility. This is achieved through loading the samples onto an absorbent silica TLC plate (the stationary phase) that is placed in a tank containing a solvent such as ethanol and chloroform (the mobile phase). The samples are incubated for a set amount of time in the tank. As the more water-soluble compounds will travel up the TLC plate at a slower rate, they are therefore separated from less water-soluble compounds which will have travelled further. For example, cortisone is slightly less water-soluble than cortisol, and so travels further up the TLC plate (402). The conversion of cortisone to cortisol is quantified by use of tritiated (^{3}H) steroid tracer. On conversion of ^{3}H-cortisone into cortisol the ^{3}H group is retained, and so the level of radioactivity detected at each of the cortisone and cortisol bands in the TLC plate is proportional to the amount of each steroid.

2.5.2 Scanning thin layer chromatography

Macrophage 11β-HSD oxoreductase activity was quantified by incubating cells with 100nM cortisone (Sigma-Aldrich, UK) and 2 µl/ml ^{3}H-cortisone tracer (Perkin Elmer, UK) for 18 hours. Steroids were then extracted from culture media in 5 ml dichloromethane. Samples were centrifuged at 1400 rpm for 10 minutes to separate aqueous and dichloromethane phases before aspiration of the aqueous phase. Dichloromethane phases were evaporated at 50°C

for 40 minutes. Steroid extracts were resuspended in 70 µl dichloromethane, spotted into silica plates and separated by TLC using 92:8 chloroform:ethanol. TLC plates were analysed with the Bioscan 200 Imaging scanner (Bioscan, USA) to give fractional conversion of cortisone to active cortisol (Figure 2-1). Steroid running distances on traces were confirmed using UV imaging of non-radiolabelled steroid controls.

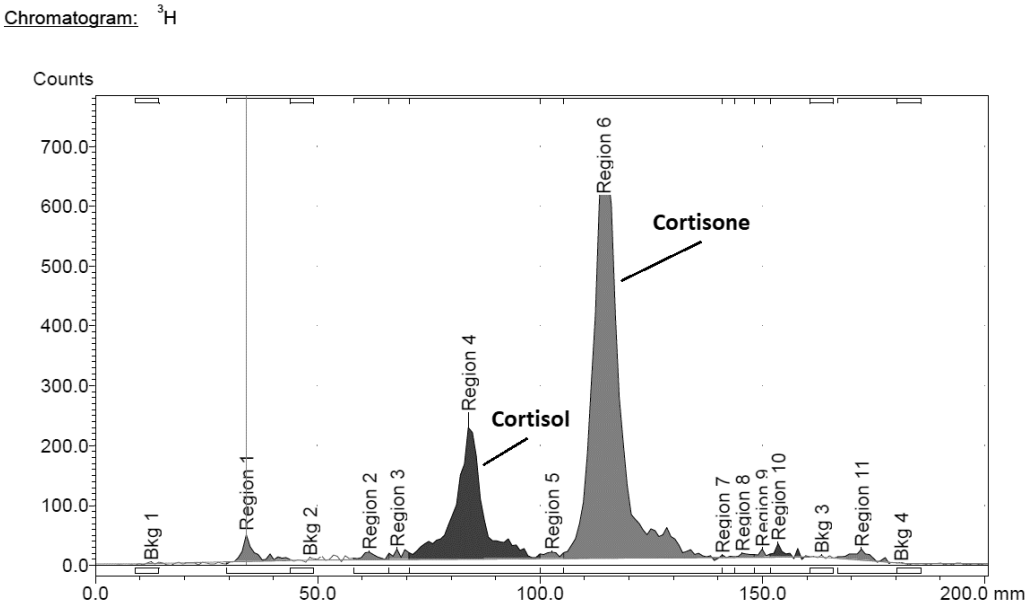

Figure 2-1 Representative radioactivity peaks for cortisol and cortisone on a TLC plate

2.5.3 Protein assay

To normalise steroid fractional conversion, protein concentrations of samples were determined by detergent compatible (DC) Protein assay as per manufacturer's instructions (BioRad, UK). Cells were resuspended in RNase-free water, scraped and frozen at -20°C for at least 24h to lyse contents. 5 µl of each sample was incubated in duplicate in a 96-well plate with 25 µl Reagent A* (20 µl Reagent S per 1 ml Reagent A) and 200µl Reagent B for 15 min on a rocker. Bovine serum albumin (BSA; Sigma-Aldrich, UK) in RNase-free water was used as

a protein standard, with concentrations spanning the range 0-2 mg/ml. Concentration of protein was measured as absorbance at 750 nm using a Wallac Victor3 1420 multilabel counter (PerkinElmer, UK). The BSA standards were used to plot a standard curve with a linear trendline. The equation of this straight line (y = mx + c) was used to formulate the equation shown below, which was used to calculate the protein concentration of the samples in Microsoft® Excel® v2208:

$$p = (m\ x\ OD) + c$$

In which p = sample protein concentration (mg/ml), m = the gradient of the linear trendline, OD = the optical density of the absorbance at 750 nm, c = the y-intercept of the linear trendline.

2.5.4 Calculation of 11β-HSD1 enzyme activity

11β-HSD1 enzyme activity, expressed as picomoles product per milligram protein per hour (pmol/mg/hr), was calculated in Microsoft® Excel® v2208 as shown:

$$Enzyme\ activity = \left(\frac{E}{E+F}\right) \times S_E \times \left(\frac{1}{p}\right) \times \left(\frac{1}{t}\right)$$

In which E = cortisone (area of trace peak in counts), F = cortisol (area of trace peak in counts), S_E = substrate amount (pmol), p = sample protein concentration (mg/ml), t = incubation time (hours).

2.5.5 LC-MS/MS

Liquid chromatography-tandem mass spectrometry (LC-MS/MS) is a commonly used technique for quantification of multiple steroids with a high level of sensitivity and specificity. LC-MS/MS allows for multiplex analysis of metabolites in a solution using liquid chromatography to first separate out individual metabolites based on their differing affinity for the water-solvent mobile phase and a linear gradient stationary matrix. After separation, the metabolites are ionised, and their mass-to-charge ratios measured by a mass analyser. This mass-to-charge ratio is based on the unique chemical composition of each metabolite and so allows their identification and quantification (403).

Steroids from cell culture supernatants were extracted using liquid/liquid extraction. 3 ml of the solvent methyl tert-butyl ether (MTBE) was added to each 1 ml of supernatant in silane-treated borosilicate glass tubes (Fisherbrand, Germany) with internal standards for each steroid assessed and vortexed for 15 seconds. Samples were centrifuged at 1500 rpm for 10min and the upper organic layer containing steroids was collected into new glass tubes. Steroid extracts were evaporated for 15 min at 55°C under a nitrogen evaporator (Gebrüder Liebisch Labortechnik GmbH, Germany) and then reconstituted in 50/50 methanol/water for analysis by LC-MS/MS.

Quantification of steroids by LC-MS/MS was carried out by Dr Angela Taylor using a Waters Xevo® mass spectrometer with ACQUITY ultra performance liquid chromatography system with HSS T3 1.2 x 50 mm column (Waters Corporation, UK).

2.6 ELISA

Production of the pro-inflammatory M1 macrophage associated cytokines TNFα, IL-6 and IL-12 p70 and the anti-inflammatory M2 associated cytokine IL-10 were assessed using enzyme-linked immunosorbent assay (ELISA) analysis of cell culture supernatants. Cytokine levels are typically measured using sandwich ELISA assays. An absorbent microtiter plate is coated with polyclonal capture antibody specific to the cytokine of interest. Then the sample is added and incubated such that cytokine present in the sample will bind to the capture antibody. A "sandwich" is built with an enzyme labelled-detection antibody also specific to the cytokine, and then a substrate for that enzyme. This enzyme reaction is chromogenic and so produces a coloured product with an optical density proportional to the amount of cytokine present. A standard curve is generated using known concentrations of cytokine to calculate the concentration of the sample.

Cytokine production was quantified using Invitrogen Human Uncoated ELISA Kits for TNFα, IL-12 p70 and IL-10 (all Thermo Fisher Scientific, USA) and Precoated Quantikine® Human IL-6 ELISA Kit (R&D Systems, USA), following manufacturers' protocols. Samples were added in duplicate and diluted as appropriate in assay diluent. All stages performed at room temperatures on a shaker. Colorimetric changes were stopped with 25 µl of 2N H_2S0_4 prior to being read at 450 nm on a FLUOstar® Omega Microplate Reader (BMG Labech, Germany). The cytokine standards of each plate were used to plot an asymmetric (five parameter) standard curve in GraphPad Prism and this was used to interpolate sample cytokine concentrations from optical density at 450 nm.

2.7 Flow cytometry for surface marker expression

Macrophages were detached from wells using Accutase™ (BioLegend, UK), washed and resuspended in PBS supplemented with 0.5% w/v bovine serum albumin (BSA) (Sigma-Aldrich, UK) and 2mM EDTA with 10 µg/ml human IgG and incubated at 4°C for 30min to block Fc receptors. Cells were washed in PBS, centrifuged at 400g and resuspended in BD Horizon™ Fixable Viability Stain 780 (BD Biosciences, UK) diluted 1/1000 in PBS and incubated at room temperature for 15 min. A sample of cells was killed by sonication for a positive stain in the live/dead control. Cells were washed in PBS, spun down at 400g and resuspended in BD Horizon™ Brilliant Stain Buffer (BD Biosciences, UK) and an antibody mix as detailed in Table 2-7 below (all antibodies from BD Biosciences, UK). Single stained controls and isotype controls were prepared at the same concentration, following Fc blocking. Cells were incubated with antibodies for 30min at room temperature, in 96-well plates at a concentration of $1x10^6$ cells/ml. After staining, cells were washed in PBS, spun down at 400g and resuspended in 4% v/v formaldehyde in PBS and incubated at room temperature for 15 min to fix. Fixed cells were washed in PBS, spun down at 400g and resuspended in PBS with 0.5% BSA and 2mM EDTA. Prior to analysis on a LSRFortessa™ flow cytometer (BD Biosciences, UK) samples were filtered through a cell strainer. Data were acquired using DIVA software and analysed with FlowJo v10 (both BD Biosciences, UK).

Marker	Fluorochrome	Clone	Isotype	Dilution
CD16	FITC	3G8	Mouse IgG1 κ	1/100
CD64	PE-Cy7	10.1	Mouse IgG1 κ	1/100
CD86	BV510	2331 (FUN-1)	Mouse IgG1 κ	1/100
CD163	PE-CF594	GHI/61	Mouse IgG1 κ	1/100
CD206	BV421	19.2	Mouse IgG1 κ	1/100
HLA-DR	BV605	G46-6	Mouse IgG2a κ	1/100

Table 2-7 Flow cytometry antibody staining panel

Antibody dilutions were optimised using stain index calculations. M1 and M2 macrophages were individually stained with 1 µl (1/100), 2.5 µl (1/40) or 5 µl (1/20) of antibody or isotype control per 100 µl stain volume. The median fluorescence intensity (MFI) of the antibody-stained population ($MFI_{positive}$) and the isotype control-stained population ($MFI_{negative}$) and the standard deviation (SD) of the negative population were calculated from FlowJo and used to find the stain index as shown in the equation below. The antibody dilution that gave the highest stain index was chosen as this gave the best separation between positive and negative staining (Table 2-8).

$$Stain\ index = \frac{MFI_{positive} - MFI_{negative}}{(2xSD_{negative})}$$

Marker	Fluorochrome	Dilution	$MFI_{positive}$	$MFI_{negative}$	$SD_{negative}$	Stain index
CD16	FITC	**1/100**	**13000**	**3126**	**1010**	**4.888119**
		1/40	17100	3310	3934	1.752669
		1/20	14200	3665	1876	2.807836
CD64	PE-Cy7	**1/100**	**16500**	**864**	**3254**	**2.4025814**
		1/40	19600	1485	5964	1.5186955
		1/20	19700	2323	7864	1.1048449
CD86	BV510	**1/100**	**15900**	**4934**	**12400**	**0.442177**
		1/40	15500	5572	17300	0.286936
		1/20	16700	5929	19000	0.283447
CD163	PE-CF594	**1/100**	**11200**	**567**	**649**	**8.191834**
		1/40	11400	784	908	5.845815
		1/20	11700	1129	1983	2.665406
CD206	BV421	**1/100**	**15500**	**184**	**377**	**20.313**
		1/40	15000	207	5904	1.252795
		1/20	16800	238	551	15.02904
HLA-DR	BV605	**1/100**	**220000**	**52800**	**67200**	**1.244048**
		1/40	153000	81900	64700	0.549459
		1/20	136000	135000	79200	0.006313

Table 2-8 Flow cytometry antibody stain index calculation

2.8 Phagocytosis assay

Phagocytic capacity of macrophages was analysed with the Vybrant™ Phagocytosis Assay kit (Thermo Fisher, UK) according to manufacturer's instructions. Polarised macrophages with or without glucocorticoid treatment were incubated with fluorescein-labelled *Escherichia coli* (*E. coli*) particles for 2h. Particles were removed, cells washed, and then trypan blue solution added for 1 min to quench non-internalised fluorescent particles. Samples were read on a PHERAstar® Omega microplate reader (BMG LabTech, Germany) to measure fluorescence at an excitation of 480 nm and emission of 520 nm.

2.9 Viability assay

Macrophage viability was assessed using an ApoLive-Glo® Multiplex assay (Promega, UK). This assay uses two reagents to measure cell viability and apoptosis. Cells are incubated first with GF-AFC, a peptide substrate which is broken down by proteases in live cells to release a fluorescent product. This fluorescence intensity of this product is proportional to the number of viable cells. Cells are then incubated with Caspase-Glo®, a luminogenic caspase-3/7 substrate. These caspases are activated during apoptosis, therefore a luminescent signal proportional to the number of apoptotic cells in the sample is generated.

RosetteSep™-isolated human blood monocytes were plated on Eppendorf® Cell Imaging 96 well glass bottom plates (Sigma-Aldrich, UK) at a concentration of $0.2x10^6$ cells/ml for differentiation into macrophages. On d6 macrophages were polarised and treated for 24h with steroids. Then 20 µl Viability Reagent (10 µl GF-AFC substrate and 2 ml Assay Buffer) was added, plate was mixed gently on a rocker and cells were incubated at 37°C for 2h. Fluorescence at 400 nm excitation and 505 nm emission was measured using a PHERAstar® Omega microplate reader (BMG LabTech, Germany). Immediately after this, 100 µl Caspase-Glo® 3/7 Reagent was added to each well. The plate was gently mixed on a rocker and incubated for 2h at room temperature before luminescence was read on the PHERAstar® Omega plate reader.

2.10 Sheared hydrogel GC formulations

2.10.1 Sheared hydrogel generation

1% w/v low acyl gellan gum (KELCOGEL®, USA) was added to 17 ml deionised sterile water with 5% v/v PBS and 10mM sodium chloride (NaCl) crosslinker (Sigma-Aldrich, UK) in a Wheaton™ borosilicate glass spinner flask (Thermo Fisher, UK) and autoclaved to dissolve and sterilise.

Once cooled to room temperature, the flask was heated on a magnetic stirrer at 100°C for 15 minutes, stirring at 500 rpm for the final 10 minutes once the bottom layer of the gel melted. Once the gel was molten, 1 ml cortisone (at a concentration of 10 mM in ethanol) or ethanol vehicle was added drop-by-drop using a 2 ml syringe through one of the arms of the flask. The heating was turned off and the mix was left to gel under constant shear rate of 500 rpm for 2h until fully gelled. Gels were stored at 4°C until testing on cells or rheology.

2.10.2 Rheological analysis

Rheology concerns the deformation properties of a material and therefore these attributes can be analysed to assess how a material would behave under conditions of applied stress such as when being injected. Shear stress is the amount of force that must be exerted on a fluid to induce shear flow, where the top layer of a fluid moves at “maximum velocity” while the bottom layer “remains stationary”. This deformation in the fluid layers is termed shear strain, and its change can be measured over the time a shear stress is applied, resulting in a shear rate. The shear rate is the velocity of the uppermost layer of fluid (m/s) divided by the distance of this layer from the stationary layer (m) to give the unit 1/s or s^{-1}. Viscosity is the

resistance of a fluid to be induced to flow and can be calculated by dividing the shear stress by the shear rate (to give Pa/s^{-1} or Pa·s). For simple Newtonian fluids such as water viscosity does not change with shear stress or rate, and the relationship between these variables is linear. However, shear-thinning liquids show decreasing viscosity with increasing shear rate (404). This allows shear-thinning materials to be more easily injected, as they become less viscous when injection stress is applied.

Rheological properties of gels were measured using a Kinexus rheometer and analysed with rSpace software v1.175.2326 (both Malvern Instruments, UK). Shear-thinning properties of gels were assessed using the Viscometry Shear Rate Ramp programme, where an applied shear rate was increased (ramp up) and then decreased (ramp down) in logarithmic increments to cover the range $0.01\text{-}500s^{-1}$.

2.10.3 Macrophage treatments

Macrophages were polarised for 24h into unpolarised M0, M1-like (IFNγ/TNFα) or M2 (IL-4) and then treated with 1 μM cortisone, 5 μM cortisone in gel or blank gel for 24h. RNA and supernatants were collected and analysed by qPCR or ELISA respectively.

2.11 Statistical analysis

All data were analysed using IBM SPSS Statistics v28.0.1.0 (IBM Analytics, USA) and GraphPad Prism v5.03 and v9.5 (GraphPad Software, USA), with a P-value of ≤ 0.05 considered to be statistically significant. Normality of data was confirmed using the Shapiro-Wilk normality test. AMP dataset RNA-seq and synovial fluid LC-MS/MS correlations were assessed with Pearson correlation for parametric data or Spearman correlation for non-parametric data and corrected for multiple comparisons with a Bonferroni post-test. Data were analysed using Student's t-test, or one-way ANOVA with post hoc Tukey's test or two-way ANOVA with Tukey correction as appropriate. Experiments were carried out with sample sizes of n ≥ 3, defined as independent primary cell cultures from different donors, unless stated otherwise in figure legend. * denotes P≤0.05, ** denotes P≤0.01, *** denotes P≤0.001 and **** denotes P≤0.0001.

Chapter 3 CHARACTERISATION OF GLOBAL STEROID METABOLISM PROFILES IN SYNOVIAL MACROPHAGES IN HUMAN DISEASE:

3.1 Introduction

There is a strong body of evidence that supports a dysregulation of circulating GC and androgen levels in chronic inflammatory diseases such as RA. This has been implicated in disease pathology and inflammation, with an inflammation-induced steroidogenic shift towards increased production of GCs at the expense of androgens linked to worse disease (357-359). However, in addition to circulating serum levels of steroid determining tissue exposure, local steroid metabolism plays a central role in mediating their actions at a tissue and cellular level. This intracrine and paracrine activation of steroids has been implicated to facilitate anti-inflammatory functions of GCs and androgens on synovial cells (290, 314, 390). Previous studies of steroid dysregulation at the local synovial level in RA have focused on the balance of estrogens and androgens, however the interplay between synovial GCs and androgens has not been addressed (363).

Several studies have demonstrated the expression and activity of key rate-limiting steroid activating enzymes within macrophages which are predicted to possess immunomodulatory potential and define the local levels of active steroids in peripheral tissues. These include GC activation by the enzyme 11β-HSD1 and androgen activation by the enzymes SRD5A1 and AKR1C3 (278, 290, 295, 314, 374, 375, 390). However, how these enzymes, in particular SRD5A1 and AKR1C3, are regulated in chronic inflammatory diseases such as RA remains

poorly defined. Similarly, it is unknown how expression and activity may change in macrophages with inflammation or whether there is differential steroid metabolism across the distinct macrophage subtypes that have been found to contribute to protection from or promotion of severe arthritic disease (120, 146). Therefore, the expression of these and related steroidogenic enzymes in synovial macrophages may have significant implications for the dysregulation of GCs and androgens seen in RA, and thereby contribute to disease pathophysiology.

Thus, in this chapter we used a bulk RNA-seq dataset to explore how steroid metabolism changed at the cellular level in macrophages across RA disease severity and inflammation. We then examined whether these changes are reflected in the local synovial steroid metabolome profile using LC-MS/MS analysis of synovial fluid from RA and OA patients.

3.2 Materials and methods

3.2.1 Bulk RNA-seq analysis of synoviocytes

Bulk RNA-seq analysis was carried out as described in section 2.1 using data from the NIH AMP RA Network study (accession code SDY998) (145). The characteristics and demographics of the patients in this study are shown in Table 3-1.

Demographic category		**Mean (± standard deviation)**
Age	**At sample collection**	61 (± 10.48)
	At diagnosis	51.1 (± 13.18)
Demographic category		**Number (% of total, n = 30)**
Sex	**Female**	23 (76.67%)
	Male	7 (23.33%)
Ethnicity	**White**	20 (66.67%)
	Black	6 (20.0%)
	Asian	2 (6.67%)
	Other	2 (6.67%)

Table 3-1 AMP RNA-seq study patient characteristics and demographics

Differential steroid metabolism gene expression in high and low DAS28-CRP RA patient samples was assessed by BMedSci student Matthew Singh Kalirai a research project under my

co-supervision. Cut-offs of DAS28-CRP <2.6 and DAS28-CRP >5.1 for low and high inflammatory disease activity respectively were defined according to accepted clinical thresholds in the literature and validated by assessment of differential inflammatory gene expression in macrophages. DAS28-CRP <2.6 is usually defined as disease in remission, while >5.1 is usually defined as severe disease (6). Characteristics of low and high DAS28-CRP groups are shown in Table 3-2. Statistical significance of categorical characteristics was assessed by Chi-squared test and numerical characteristics assessed by unpaired Student's t-test. Due to low sample numbers, it was not possible to exclude patients who were currently taking therapeutic GCs at the time of synovial tissue sample collection. However, a brief analysis of differential gene expression between therapeutic groups identified no differences in the expression of DAS28-CRP-associated differentially expressed genes identified.

Categorical characteristics		DAS28-CRP <2.6 (n=8, 40%)	DAS28-CRP >5.1 (n=12, 60%)	p-value
		Number (% total)		
Sex	Female	7 (87.5%)	8 (66.67%)	0.2918
	Male	1 (12.5%)	4 (33.33%)	
Leukocyte infiltrate	Leukocyte rich	1 (12.5%)	12 (100%)	**0.0009 (***)**
	Leukocyte poor	7 (87.5%)	0 (0%)	
Taking oral steroids at time of sample collection	Yes	3 (37.5%)	3 (25%)	0.6590
	No	3 (37.5%)	7 (58.33%)	
	Unknown	2 (25%)	2 (16.67%)	
Numerical characteristics		Mean (± SD)		
Age	At sample collection	61.714 (± 1.658)	57.417 (± 8.826)	0.4181
	At diagnosis	41.833 (± 18.472)	54.167 (± 12.298)	0.1730
DAS28-CRP		0.496 (± 0.926)	6.184 (± 0.968)	**6.78E-10 (****)**
Krenn inflammation score		0.625 (± 0.744)	1.431 (± 1.292)	0.0947

Table 3-2 DAS28-CRP low and high patient characteristics

3.2.2 Single-cell RNA-seq analysis of synovial tissue macrophage clusters

The expression of *HSD11B1*, *SRD5A1* and *AKR1C3* was assessed in healthy and RA synovial macrophages by Professor Mariola Kurowska-Stolarska and her lab group, using a previously published single-cell RNA-seq (scRNA-seq) dataset (146). Synovial tissue samples were

acquired from RA patients and healthy donors using ultrasound-guided biopsy (n=27; 4 healthy, 4 undifferentiated peripheral inflammatory arthritis, 6 treatment-naïve active RA, 6 treatment-resistant active RA and 7 RA in remission). CD11b+ and CD64+ synovial myeloid cells were sorted by FACS and 2,000-10,000 cells per sample were sequenced using 10X Genomics. Synovial tissue macrophages were clustered by principal component analysis (PCA) and uniform manifold approximation and projection (UMAP). The following previously defined synovial tissue macrophage clusters were analysed: $TREM2^{low}$, $TREM2^{high}$, FOLR2+ ID2+, $FOLR2^{high}$ LYVE1+, HLA^{high} $CLEC10A^{high}$, $CD48^{high}$ S100A12+, CD48+ SPP1+, HLA^{high} ISG15+ and FOLR2+ ICAM1+ (146).

3.2.3 Synovial fluid and serum analysis

Synovial fluid samples were collected from patients with hip OA or RA as described in section 2.2. Matched blood serum samples were collected from OA patients by venous draw. Measures of disease severity and inflammation were correlated by Pearson or Spearman correlation to synovial fluid steroid and inflammatory cytokine levels.

Patient characteristics are shown in the Table 3-3. Significance was assessed with unpaired Student's t-test (age) or Chi-square test (sex).

Characteristics		OA (n=27)	RA (n=17)
Age at sample collection	**Years (± SD)**	69.8 (± 9.5)	55.2 (± 13.8)
	P-value	**0.0003 (***)**	
Sex	**Number female (%)**	16 (59.23%)	12 (70.59%)
	P-value	0.09592	

Table 3-3 OA and RA patient characteristics

The clinical characteristics of RA patients, DAS28-CRP and CRP, are shown in Table 3-4. Significance was assessed using unpaired Student's t-test.

Clinical characteristic		Mean	SD (±)	p-value
CRP	**Total**	**28.36**	**23.313**	
	Female	26.73	25.769	0.487
	Male	34.33	12.014	
DAS28-CRP	**Total**	**4.72**	**0.774**	
	Female	4.65	0.702	0.693
	Male	4.96	1.149	

Table 3-4 RA patient clinical characteristics

Due to low sample numbers, it was not possible to exclude patients who were actively currently taking therapeutic GCs at the time of synovial fluid sample collection. The effect of GC treatment on readouts assessed in this chapter were calculated as shown in Table 3-5,

where statistical significance was assessed with Chi-square test (categorical variable; sex) or unpaired two-tailed Student's t-test (numerical variables).

		Currently taking GCs		
		Yes	**No**	**P-value**
N (%)	**Total**	**3 (17.65%)**	**14 (82.35%)**	
	Female	1 (8.33%)	11 (91.67%)	0.1186
	Male	2 (40%)	3 (60%)	
CRP (± SD)		31.33 (± 25.70)	25.58 (± 23.78)	0.7488
DAS28-CRP (± SD)		3.78 (± 0.20)	4.87 (± 0.72)	**0.0032 (**)**
Cortisol (average nM, ± SD)		109.82 (± 57.88)	182.72 (± 63.75)	0.1430
Cortisone (average nM, ± SD)		6.56 (± 2.71)	16.42 (± 6.48)	**0.0029 (**)**
Cortisol/cortisone		17.48 (± 7.15)	12.79 (± 5.55)	0.3759
TNFα (average pg/ml, ± SD)		41.04 (± 37.86)	96.98 (± 62.11)	0.2673

Table 3-5 Characteristics of RA patients associated with therapeutic GC use

3.2.3.1 Inflammatory cytokine quantification

Levels of inflammatory cytokines in synovial fluid samples of 27 OA patients and 6 RA patients was measured by Luminex analysis using an Inflammation 20-Plex Human ProcartaPlex™ Panel (Thermo Fisher, UK) as described in section 2.2.1. The average levels of TNFα measured in synovial fluid of patients is shown in Table 3-6. No significant differences in synovial TNFα were found between disease groups, as assessed by unpaired two-tailed Student's t-test.

	n	Synovial TNFα (pg/ml)	SD (±)	P-value
OA	27	15.434	10.711	0.0636
RA	6	69.008	55.274	

Table 3-6 Synovial TNFα levels in OA and RA patients

3.2.3.2 Steroid hormone quantification

Steroids were extracted from synovial fluid and serum samples by Dr Angela Taylor using liquid/liquid extraction and run on a Waters Xevo® mass spectrometer as detailed in section 2.5.5. The concentration of 25 steroids involved in GC and androgen metabolism (Supplementary Table 2) were quantified relative to a calibration series spanning the range 0.5-1000 ng/ml for each steroid.

3.2.4 Comparison of AMP RNA-seq and synovial fluid RA samples

The demographics and characteristics of RA patients from the AMP RNA-seq and the synovial fluid studies used in this chapter are shown in Table 3-7. Statistical significance of numerical variables (age and DAS28-CRP) was assessed by unpaired Student's t-test and categorical variable (sex) by Chi-square test.

Characteristics	RA patients		P-value
	AMP study (n=30)	Synovial fluid study (n=17)	
Age at sample collection (years ± SD)	61 (± 10.6)	55.2 (± 13.8)	0.155
DAS28-CRP (± SD)	3.936 (± 2.451)	4.716 (± 0.774)	0.121
Female sex (n, %)	23 (76.67%)	12 (70.59%)	0.646

Table 3-7 Characteristics of RA patients in the AMP RNA-seq and synovial fluid studies

3.2.5 Statistical analysis

Statistical significance was assessed with IBM SPSS Statistics v28.0.1.0 (IBM Analytics, USA) and GraphPad Prism v5.03 and v9.5 (GraphPad Software, USA). Normality of data was tested using the Shapiro-Wilk normality test. Linear correlation was assessed using Pearson correlation for normally distributed data and Spearman correlation for nonparametric data with two-tailed P-value computed. Further statistical tests are detailed in Figure legends. Statistical significance is presented as follows: * P≤0.05, ** P≤0.01, *** P≤0.001 and **** P≤0.0001.

3.3 Results

3.3.1 Synovial macrophage steroid metabolism gene expression correlates with disease activity and inflammation

We initially examined differential gene expression of the global steroidogenic metabolism profile of RA synovial macrophages using the AMP bulk RNA-seq dataset of FACS-sorted synoviocytes (145). Of the 109 steroid metabolism genes examined in RA macrophages (Supplementary Table 1), 6 were found to show significant differential expression of greater than 1.5-fold difference between high and low disease activity, as measured by DAS28-CRP (Table 3-8).

The genes that significantly increased with DAS28-CRP in synovial macrophages were the organic anion-transporting polypeptide *SLCO4A1*, the 11β-HSD1 gene *HSD11B1* and 5α-reductase *SRD5A1* (Table 3-8). The genes that significantly decreased in expression with higher DAS28-CRP were the estrogen inactivating 17β-HSD enzyme *HSD17B14*, the androgen inactivating aldo-keto reductase *AKR1C2* and androgen activating aldo-keto reductase *AKR1C3*. In the interests of time and to focus the study we chose to reduce the candidates to the known peripheral activators of GCs and androgens: the GC-activating enzyme *HSD11B1* and the rate-limiting androgen activating enzymes *SRD5A1* and *AKR1C3* (160, 336).

Gene	Log_2 fold change: DAS28-CRP high v low	P-value	Function
SLCO4A1	1.279	0.0109 (*)	Organic anion-transporting polypeptide: uptakes estrone-3-sulfate, estradiol-17β-glucuronide & prostaglandin E2 (405)
HSD11B1	1.156	0.0146 (*)	11β-hydroxysteroid dehydrogenase with oxo-reductase activity, GC activating: converts cortisone to active GC cortisol and 11-DHC to active GC corticosterone (406)
SRD5A1	0.906	0.0040 (**)	5α-reductase, androgen activating enzyme: converts testosterone to DHT (407)
HSD17B14	-1.578	0.0021 (**)	17β-hydroxysteroid dehydrogenase, estrogen inactivating: converts estrodiol to weaker estrogen estradiol estrone (408)
AKR1C2	-1.915	0.0013 (**)	Aldo-keto reductase, androgen inactivator: converts potent androgen DHT to weak androgen androstanediol (409)
AKR1C3	-2.059	0.0003 (***)	Aldo-keto reductase, androgen activator: converts DHEA to androstenediol, androstenedione to testosterone, and 5α-androstenedione to DHT (336)

Table 3-8 DAS28-CRP high-low separated steroid metabolism DEGs in RA synovial macrophages

Differentially expressed genes (DEGs) from a panel of steroid metabolism genes (supplementary table 1) identified as having a statistically significant magnitude $\log_2$ fold change > 0.58 (1.5-fold change) between DAS28-CRP high (>5.1) and DAS28-CRP low (<2.6) in RA synovial macrophages in the AMP bulk RNA-seq dataset (DAS28-CRP high n=12, DAS28-CRP low n=8). Significance of differential expression was assessed by two tailed unpaired Student's t-test or Mann-Whitney U-test, with Benjamini-Horchbeg correction for false discovery rate at 5%. (* p≤0.05, ** p≤0.01, *** p≤0.001, **** p≤0.0001).

To examine if this differential expression was a unique property of macrophages, or a shared change with inflammation across synoviocytes, expression of these genes was assessed in further synovial cell populations in the AMP dataset: fibroblasts, macrophages, T cells and B cells (Figure 3-1). This dataset includes the classification of each RA sample based on histological analysis of lymphocyte infiltration and thus intensity of local synovitis. Although each subset contained equivalent numbers of monocytes and macrophages, leukocyte rich RA tissues have high levels of infiltrating T and B cells while leukocyte poor tissues had fewer and were more similar to that of OA patients. Leukocyte rich samples were seen to correlate with the Krenn inflammation score, a histological measure of severity of inflammation (196). We also found leukocyte rich and poor samples significantly correlated with high (>5.1) and low (<2.6) DAS28-CRP measures of RA disease activity respectively (Table 3-2). Therefore, these categories were used to assess the differential expression of steroid metabolism genes across different intensities of local synovitis.

Although fibroblasts showed high expression of *HSD11B1*, macrophages were the only population to show significant difference in expression of these genes between leukocyte rich and leukocyte poor samples (Figure 3-1 A). *HSD11B1* (3.2-fold; P≤0.001) and *SRD5A1* (1.3-fold;

P≤0.01) both increased in expression with local synovial inflammation while *AKR1C3* decreased (2.0-fold; P≤0.001).

The expression of *HSD11B2*, encoding 11β-HSD2, was briefly assessed as previous reports identified this to be the predominant 11β-HSD isozyme expressed in human synovial macrophages (289). However, *HSD11B2* was only expressed at low levels in macrophages, with a nonsignificant slight increase in expression in the less inflamed leukocyte poor samples (P=0.1177; Figure 3-1 D).

Expression of the GR isozyme GRα, *NR3C1*, and the androgen receptor, *AR*, was examined to ascertain steroid-responsiveness of different cell types. *NR3C1* was expressed across all cells (Figure 3-1 E) while the *AR* was mainly expressed by fibroblasts (Figure 3-1 F). The expression of both *NR3C1* and *AR* was unchanged between leukocyte rich and poor samples.

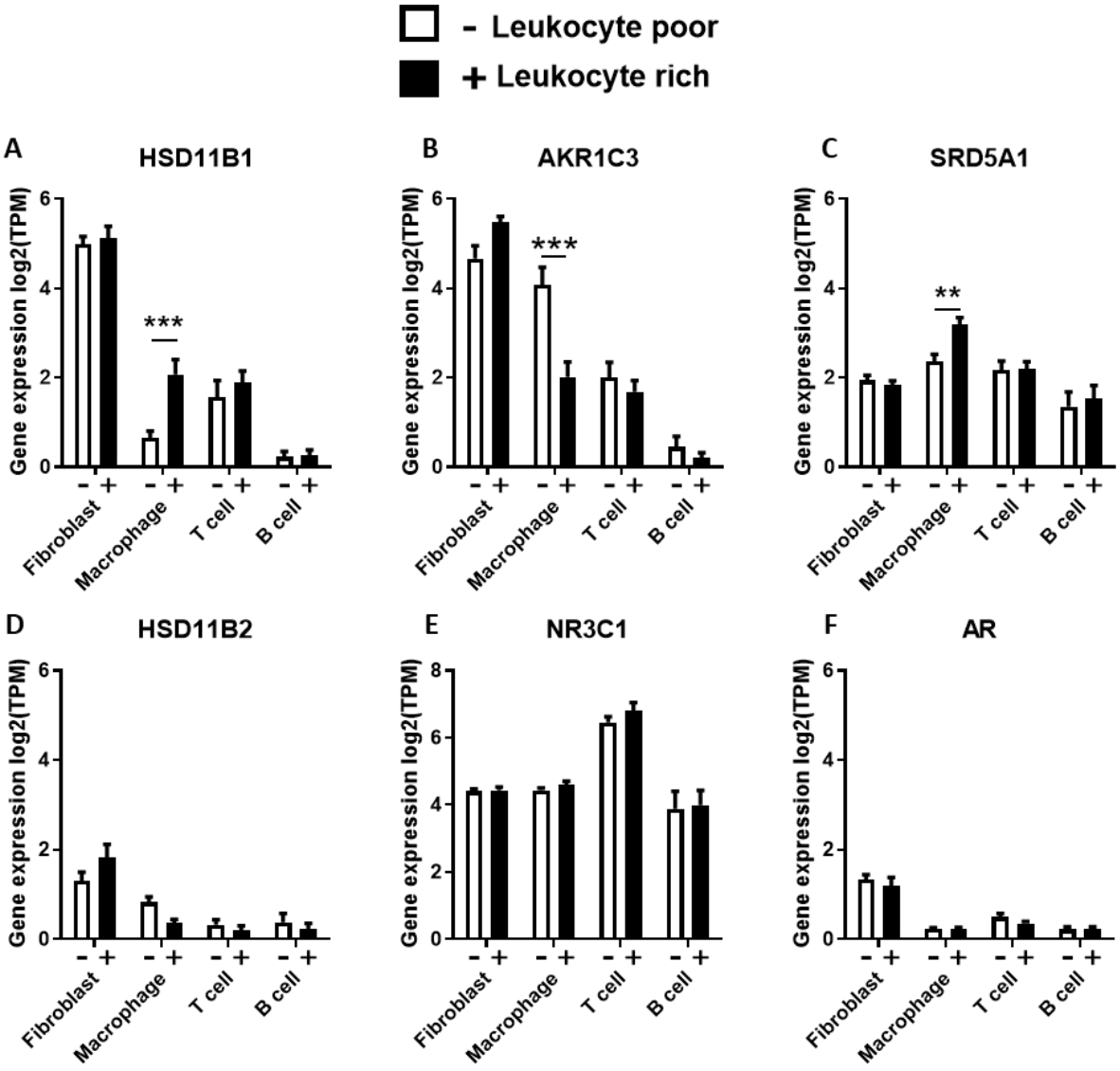

Figure 3-1 Glucocorticoid and androgen activating enzymes are differentially expressed with inflammation in RA synovial macrophages

RNA expression of (A) the GC activating enzyme *HSD11B1*, androgen-activating enzymes (B) *SRD5A1* and (C) *AKR1C3*, (D) GC inactivating enzyme *HSD11B2*, (E) glucocorticoid receptor *NR3C1* and (F) androgen receptor (*AR*) was assessed in leukocyte-poor (low synovial inflammation; - white bars) and leukocyte-rich (high synovial inflammation; + black bars) samples in the AMP RNA-seq dataset (leukocyte-poor n=12; leukocyte-rich n=11). Data are presented as mean ± SEM and statistical significance was determined using two-way ANOVA with Bonferroni's multiple comparisons test to compare leukocyte rich and poor (** p≤0.01, *** p≤0.001).

To assess whether there is an interaction between these changes in macrophage steroid metabolism and RA disease severity, the expression of *HSD11B1*, *AKR1C3* and *SRD5A1* was correlated to DAS28-CRP. As levels of GCs are unaffected by sex, whereas levels of androgens such as testosterone and DHT, generated by enzymes AKR1C3 and SRD5A1, are usually higher in males than females, samples were grouped for analysis of *HSD11B1* expression and sex-split for *AKR1C3* and *SRD5A1* (410) (Figure 3-2).

HSD11B1 RNA expression showed a moderate and significant positive correlation with DAS28-CRP (r=0.484; P=0.0068; Figure 3-2 A). Likewise, *AKR1C3* expression significantly decreased (r=-0.557; P=0.0058) and *SRD5A1* significantly increased (r=0.545; P=0.0072) with DAS28-CRP in female patients (Figure 3-2 A-C). These correlations matched the trends seen in expression for each gene with local synovial inflammation as characterised by level of leukocyte infiltration.

Although male patients followed the same trend for each enzyme, the correlations were not significant (*AKR1C3*: P=0.5187; *SRD5A1*: P=0.2759), likely due to the low male sample size.

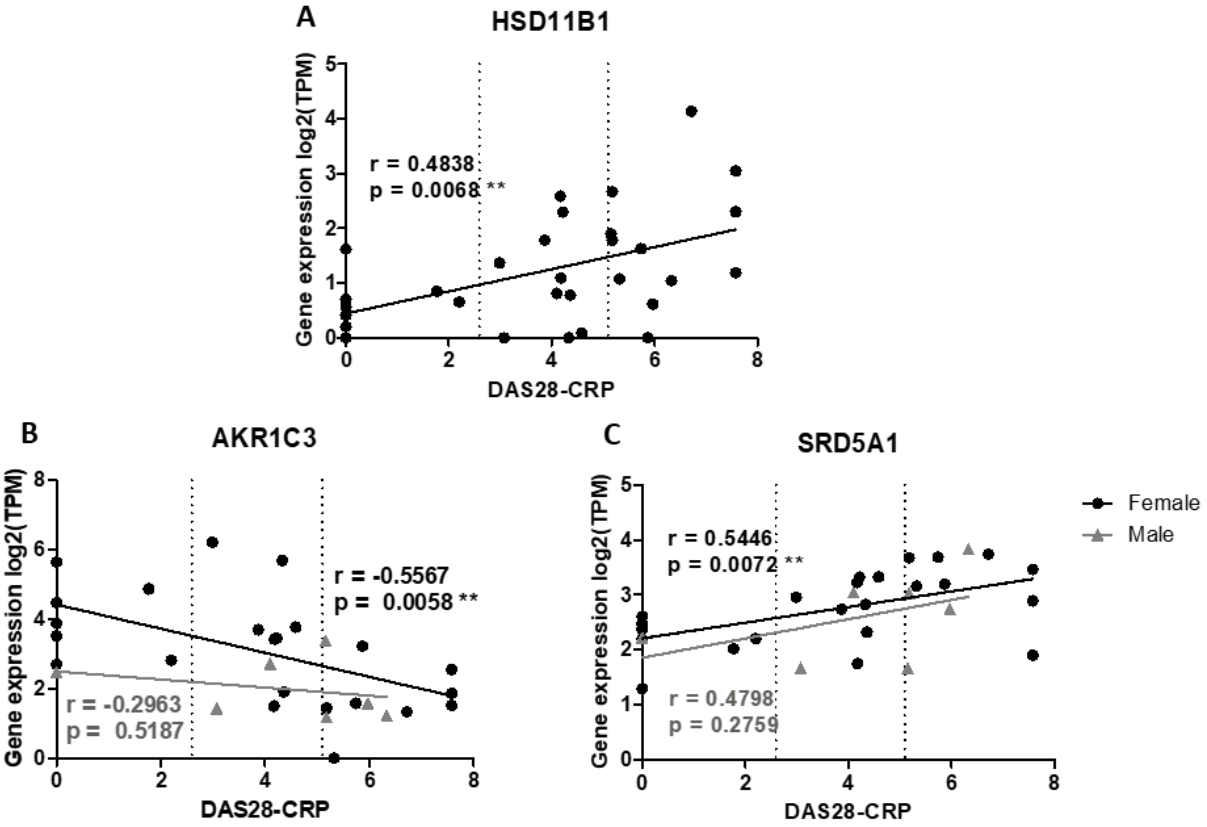

Figure 3-2 Macrophage expression of *HSD11B1*, *AKR1C3* and *SRD5A1* correlates with RA disease severity

Correlations of RA patient disease severity (DAS28-CRP) with macrophage RNA expression of (A) *HSD11B1*, (B) *AKR1C3* and (C) *SRD5A1* as measured by RNA-seq in the AMP dataset. DAS28-CRP severity cut-offs of DAS28-CRP > 2.8 for low disease activity and DAS28-CRP < 5.1 for high disease activity as shown by dotted vertical lines (n=30; female n=23; male n=7). Data are presented as individual values. Correlation and statistical significance were determined using Pearson or Spearman correlation coefficient (** p≤0.01).

3.3.2 Examination of changes in steroid metabolism genes across macrophage subsets

As RA synovial macrophages are highly heterogenous, with distinct subsets identified in protection from and pathology of severe disease, the expression of *HSD11B1*, *AKR1C3* and *SRD5A1* was examined in a previously published scRNA-seq dataset in collaboration with Professor Mariola Kurowska-Stolarska (146).

This dataset defined nine clusters of macrophages present across healthy and RA synovia (Figure 3-3 A). The TREM2^{high} subset of synovial tissue macrophages were identified by Alivernini et al to be associated with healthy synovial tissue and RA remission, as well as expression of pro-resolution markers such as CD163. Severe and treatment-resistant RA was instead associated with higher levels of the SPP1+ and S100A12+ subsets, which express high levels of osteopontin and alarmin respectively (146).

HSD11B1 expression was identified primarily within the SPP1+ subset of synovial tissue macrophages (Figure 3-3 B) and *SRD5A1* expression was particularly enriched within the S100A12+ subset. *AKR1C3* expression however was found at high levels in the pro-resolution TREM2^{high} subset (Figure 3-3 C).

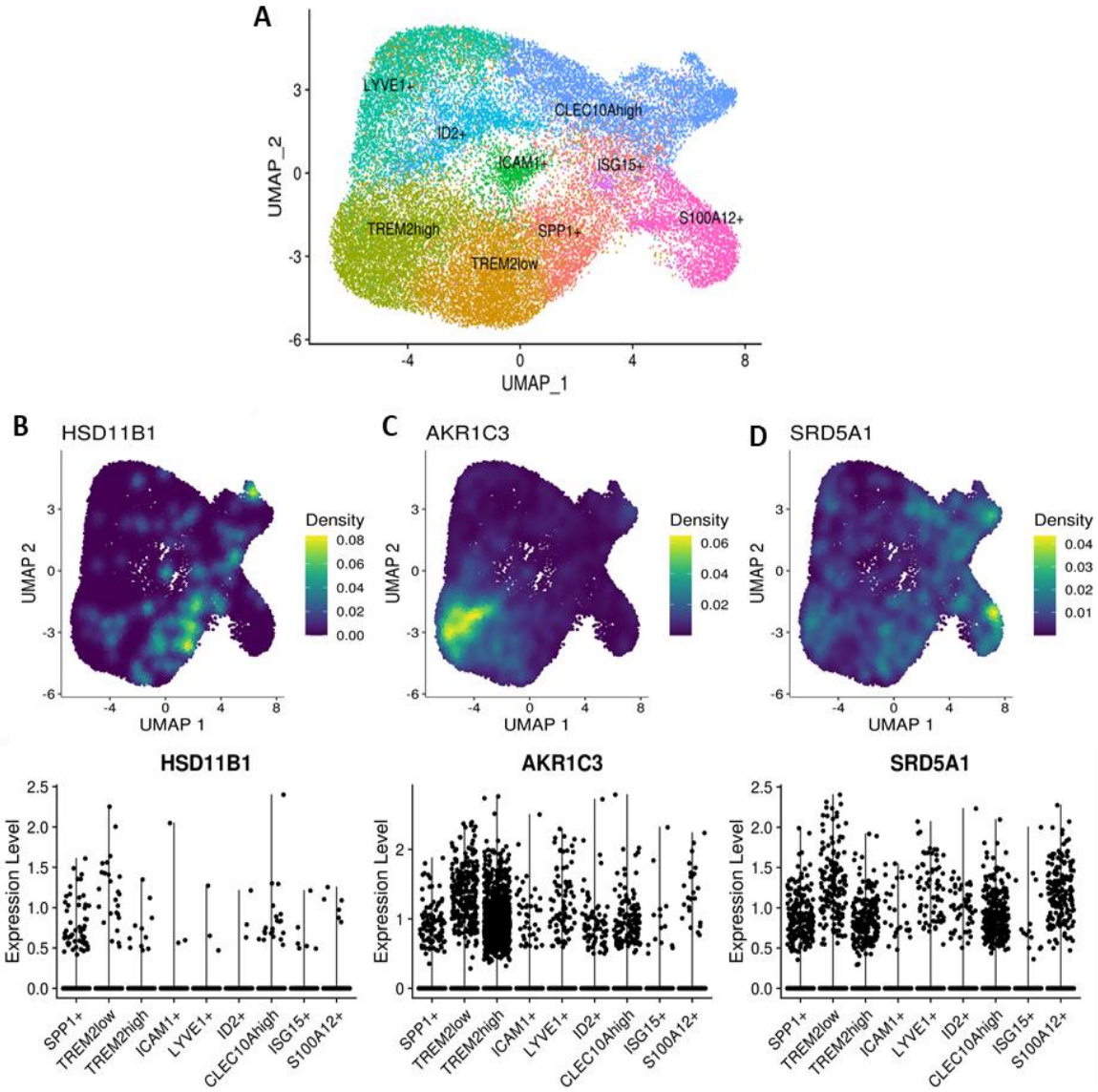

Figure 3-3 Steroid metabolism genes are expressed by functionally distinct synovial macrophage subsets

(A) Uniform manifold approximation and projection (UMAP) visualisation of transcriptomically- and functionally-distinct macrophage subset clusters identified by scRNA-seq of RA and healthy synovial macrophages by Professor Mariola Kurowska-Stolarska (146). UMAP visualisation of density (AU) and expression level (AU) for (B) *HSD11B1*, (C) *AKR1C3* and (D) *SRD5A1* according to clustering by subset. Data are presented as individual samples. n=27; 4 healthy, 4 undifferentiated peripheral inflammatory arthritis, 6 treatment-naïve active RA, 6 treatment-resistant active RA and 7 RA in remission.

3.3.3 Analysis of local synovial fluid steroid availability

To determine whether changes in local steroid metabolism drive differences in the local synovial micro-environment, we examined how steroid profiles compared between matched synovial fluid and blood serum samples by LC-MS/MS analysis of OA patients (Figure 3-4). As before, female and male samples were combined for GC analysis, but split for androgen analysis to avoid potential bias driven by differential adrenal-gonadal output.

There was an overall trend towards greater levels of steroid in blood serum of males and females relative to synovial fluid (Figure 3-4). Significantly higher levels of cortisol were found in OA patient serum compared to synovial fluid (1.9-fold; $P \leq 0.001$), while cortisone levels were equivalent ($P = 0.8610$; Figure 3-4 A). In female patients there was a higher level of both DHEA (0.8-fold; $P \leq 0.01$) and the precursor 11-oxygenated androgen 11β-hydroxyandrostenedione (11OHA4; 2.1-fold; $P \leq 0.001$) in serum (Figure 3-4 B). Meanwhile, male patients had higher serum 11OHA4 (2.2-fold; $P \leq 0.001$) and also higher testosterone (2.5-fold; $P \leq 0.001$; Figure 3-4 C). The data show that, although at a lower level than in serum, steroid metabolites are present in synovial fluid and are therefore readily available for conversion by steroidogenic cells, such as macrophages.

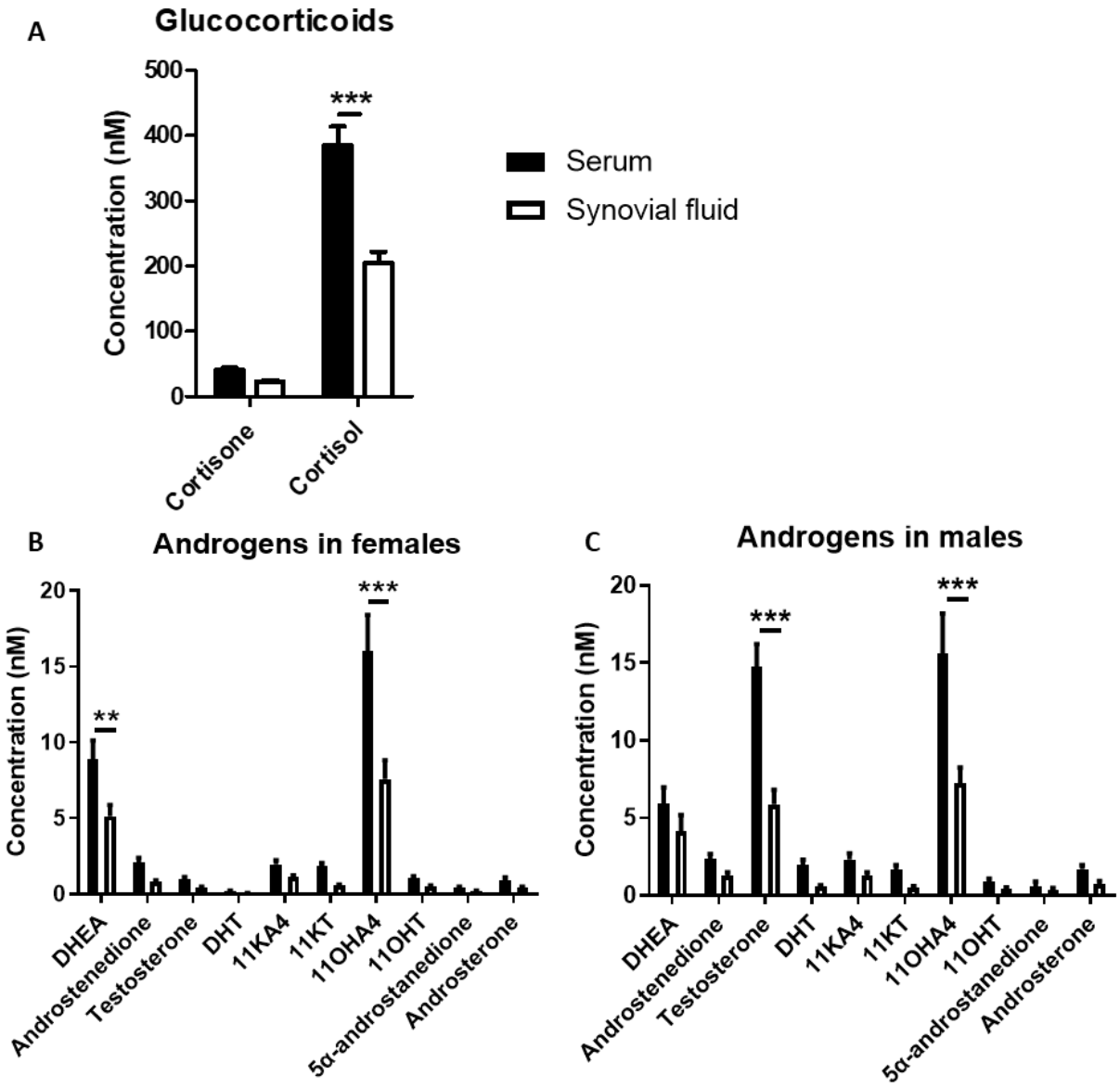

Figure 3-4 Blood serum has greater steroid levels than synovial fluid

LC-MS/MS was used to compare blood serum (black bars) and synovial fluid (white bars) levels of (A) glucocorticoids and androgens in (B) female and (C) male OA patients. n=27, female n=16, male n=11. Data are presented as mean ± SEM and statistical significance was determined using two-way ANOVA with Bonferroni's multiple comparisons test (** p≤0.01, *** p≤0.001).

Absolute steroid measurements can be confounded in singular spot samples by variation in diurnal and ultradian rhythms, and further variations of these rhythms identified between tissues, therefore we examined steroid ratios as an independent measure of relative enzyme activity (411).

On comparing the ratio of cortisol/cortisone, testosterone/androstenedione and DHT/5α-androstanedione as surrogates for 11β-HSD1 and AKR1C3 activity, no differences were found between synovial fluid and serum (Figure 3-5 A, C, D). Similarly, there was no difference in the ratio of total GCs (cortisone and cortisol) over androgens (DHT and testosterone) (Figure 3-4 E). The ratio of DHT/T, as catalysed by SRD5A1, was lower in the synovia of female patients (1.7-fold; $P \leq 0.05$; Figure 3-5 B). This may be due to low availability of the substrate testosterone (Figure 3-4 B), or lower expression of SRD5A1 compared to other tissues of the periphery.

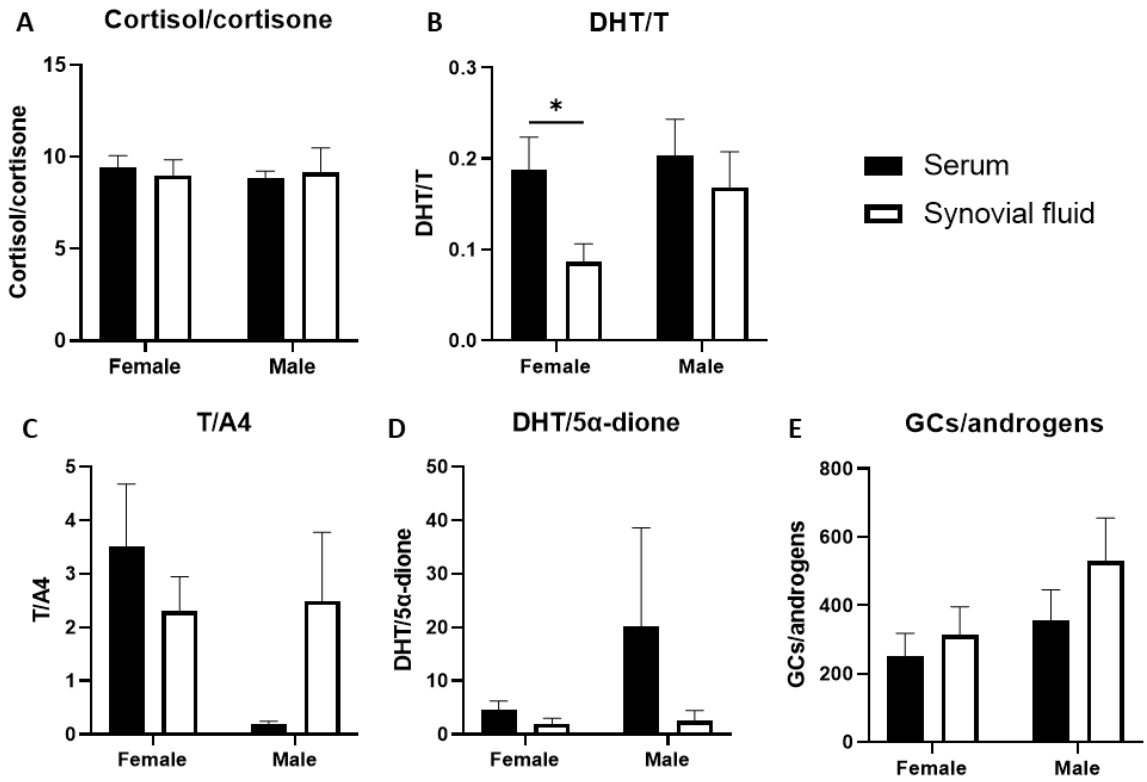

Figure 3-5 Serum and synovial fluid do not have differences in steroid enzymatic activation

LC-MS/MS was used to compare steroid ratios of blood serum (black bars) and synovial fluid (white bars) in OA patients: (A) cortisol/cortisone as mediated by 11β-HSD1, (B) DHT/testosterone as mediated by SRD5A1, and (C) testosterone/androstenedione and (D) DHT/5α-androstenedione as mediated by AKR1C3. (E) Levels of GCs (cortisol and cortisone) over androgens (DHT and testosterone). n=27, female n=16, male n=11. Data are presented as mean ± SEM and statistical significance was determined using two-way ANOVA with Bonferroni's multiple comparisons test (* p≤0.05).

In order to understand the effects of chronic inflammatory disease on relative levels of steroid hormones within the synovium, we examined the steroid metabolome profile in synovial fluid of OA and RA patients by LC-MS/MS (Figure 3-6). It has been previously reported that steroid dysregulation seen in RA has been associated with inflammatory factors such as TNFα, whereas the steroid dysregulation seen in OA is associated less with inflammation and more with age (358, 412). Therefore, it was expected that any steroid dysregulation would be more pronounced in RA.

As seen in serum, and based on expected adrenal output, total cortisol levels were higher than that of cortisone in synovial fluid of both RA and OA patients (Figure 3-6 A). Absolute levels of GCs did not differ between OA and RA synovial fluid samples. In both female and male patients, synovial androgens were broadly similar across OA and RA (Figure 3-6 B-C). However, there was a significantly higher level of 11OHA4 in the synovial fluid of OA patients than that of RA patients (female: 2.5-fold, $P \leq 0.0001$; male: 2.0-fold, $P \leq 0.01$). Androgen precursors such as DHEA, androstenedione and testosterone were identified in both RA and OA synovial fluid, although at low levels particularly in female patients.

Together these data indicate that the GC and androgen profiles of OA and RA synovial fluid are broadly similar, and that RA synovial fluid possesses inactive steroid metabolites, such as cortisone and androstenedione, which are available for local metabolism and activation.

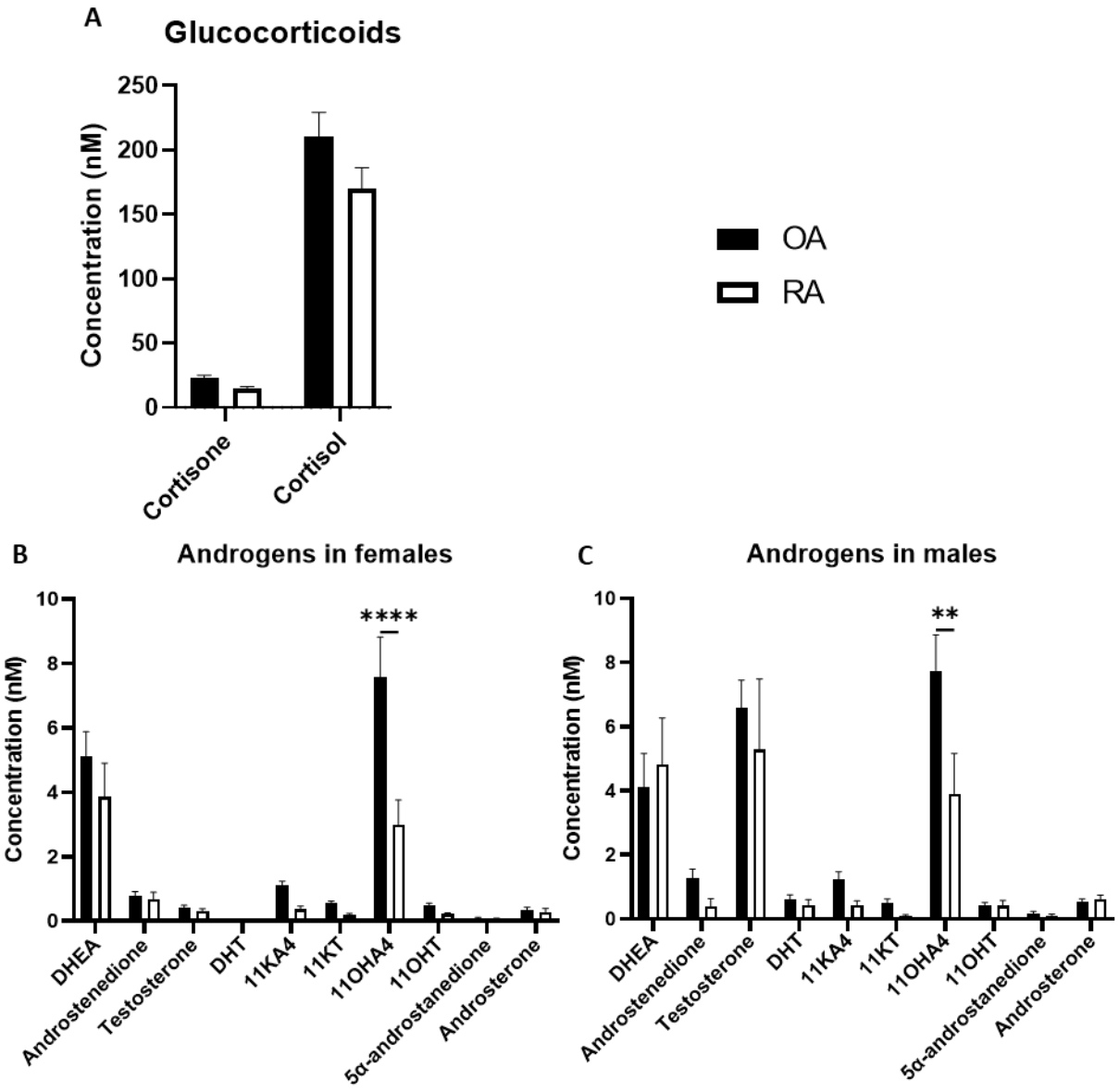

Figure 3-6 OA and RA synovial fluid have similar steroid profiles

LC-MS/MS was used to quantify steroids in synovial fluid of OA (black bars) and RA synovial fluid (white bars): levels of (A) glucocorticoids and androgens in (B) female and (C) male patients. OA female n=16, male n=11; RA female n=12, male n=5. Data are presented as mean ± SEM and statistical significance was determined using two-way ANOVA with Bonferroni's multiple comparisons test (** p≤0.01, **** p≤0.0001).

As before (Figure 3-5), we examined steroid ratios as an independent measure of relative enzyme activity to assess differences in metabolism between OA and RA synovial fluid (Figure 3-7).

No differences were seen in 11β-HSD1 (Figure 3-7 A) and SRD5A1 (Figure 3-7 B) activity, however sex differences were noticeable on assessing AKR1C3 activity. The ratios of testosterone/androstenedione (Figure 3-7 C) and DHT/5α-androstanedione (Figure 3-7 D) were significantly higher in male RA (T/A4 male RA v female RA: 19.7-fold, P≤0.01) and OA patients (DHT/5α-androstanedione male OA v female OA: 12.1-fold, P≤0.001), respectively, compared to their female counterparts. However, only DHT/5α-androstanedione was found to significantly differ with disease, with a lower level seen in male RA patients compared to OA patients (4.5-fold, P≤0.05; Figure 3-7 D).

The ratio of GCs/androgens was assessed as level of cortisol and cortisone over testosterone and DHT to measure the balance of metabolites at the final stages of each steroidogenic pathway, to assess whether local synovial steroid metabolism could recapitulate systemic adrenal GCs/androgen dysregulation seen previously in inflammatory disease (356). There was a trend towards higher levels of GCs/androgens in RA patients compared to OA patients, however this was not significant (Female OA v RA: 1.7-fold, P= 0.1876; male OA v RA: 12.4-fold, P= 0.5984; Figure 3-7 E).

Collectively, these data imply that while absolute levels of steroids may be broadly similar between OA and RA synovial fluid, the differential activity of AKR1C3 between them suggests that activity of steroidogenic enzymes may vary with disease severity and inflammation.

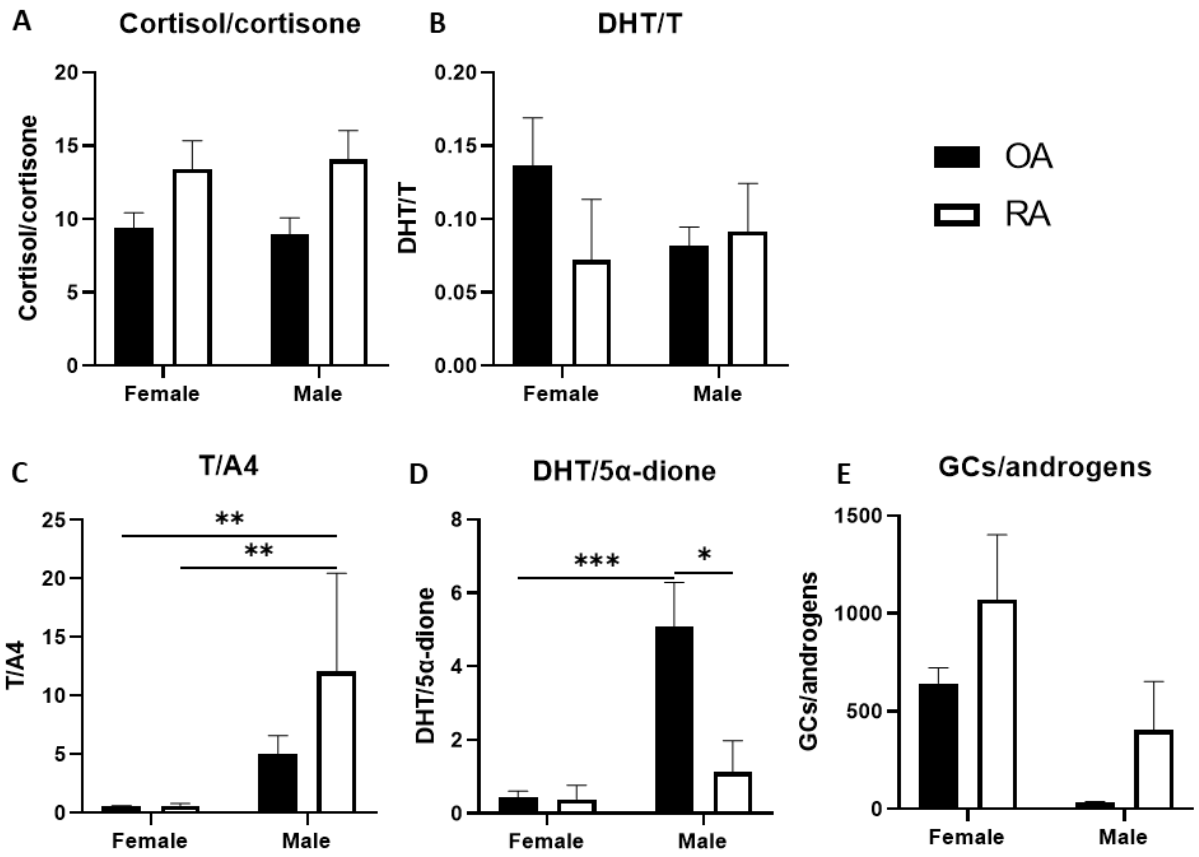

Figure 3-7 Sex- and disease-specific differences in androgen activation by AKR1C3 in OA and RA synovial fluid

LC-MS/MS was used to compare steroid ratios in synovial fluid of OA (black bars) and RA synovial fluid (white bars) female and male patients: (A) cortisol/cortisone as mediated by 11β-HSD1, (B) DHT/testosterone as mediated by SRD5A1, and (C) testosterone/androstenedione and (D) DHT/5α-androstenedione as mediated by AKR1C3. (E) Levels of GCs (cortisol and cortisone) over androgens (DHT and testosterone). OA female n=16, male n=11; RA female n=12, male n=5. Data are presented as mean ± SEM and statistical significance was determined using two-way ANOVA with Bonferroni's multiple comparisons test (* p≤0.05, ** p≤0.01, *** p≤0.001).

3.3.4 Correlation of steroidogenic enzyme activity with measures of disease severity

Using synovial steroid profiles as determined by LC-MS/MS, the enzyme activity of 11β-HSD1 (cortisol/cortisone), AKR1C3 (testosterone/androstenedione and DHT/5α-androstanedione) and SRD5A1 (DHT/testosterone) and the levels of total GCs relative to active androgens (cortisone + cortisol/testosterone + DHT) were calculated, and their correlation with markers of disease activity and inflammation in RA patients assessed.

A weak positive correlation between cortisol/cortisone and CRP was seen (r=0.342), implying higher 11β-HSD1 activity (Figure 3-8 A). There was a negative correlation between DHT/testosterone and CRP in both male (r=-0.999) and female patients (r=-0.474), which was also seen for DHT/5α-androstanedione (female: r=-0.943) and testosterone/androstenedione (female: r=-0.452; Figure 3-8 B-D). These changes would favour increased GC levels and reduced androgen activation with inflammation, which was supported by moderate positive correlations seen between levels of GCs/androgens and CRP (female: r=0.409; male: r=0.500; Figure 3-8 E). However, none of these correlations were statistically significant.

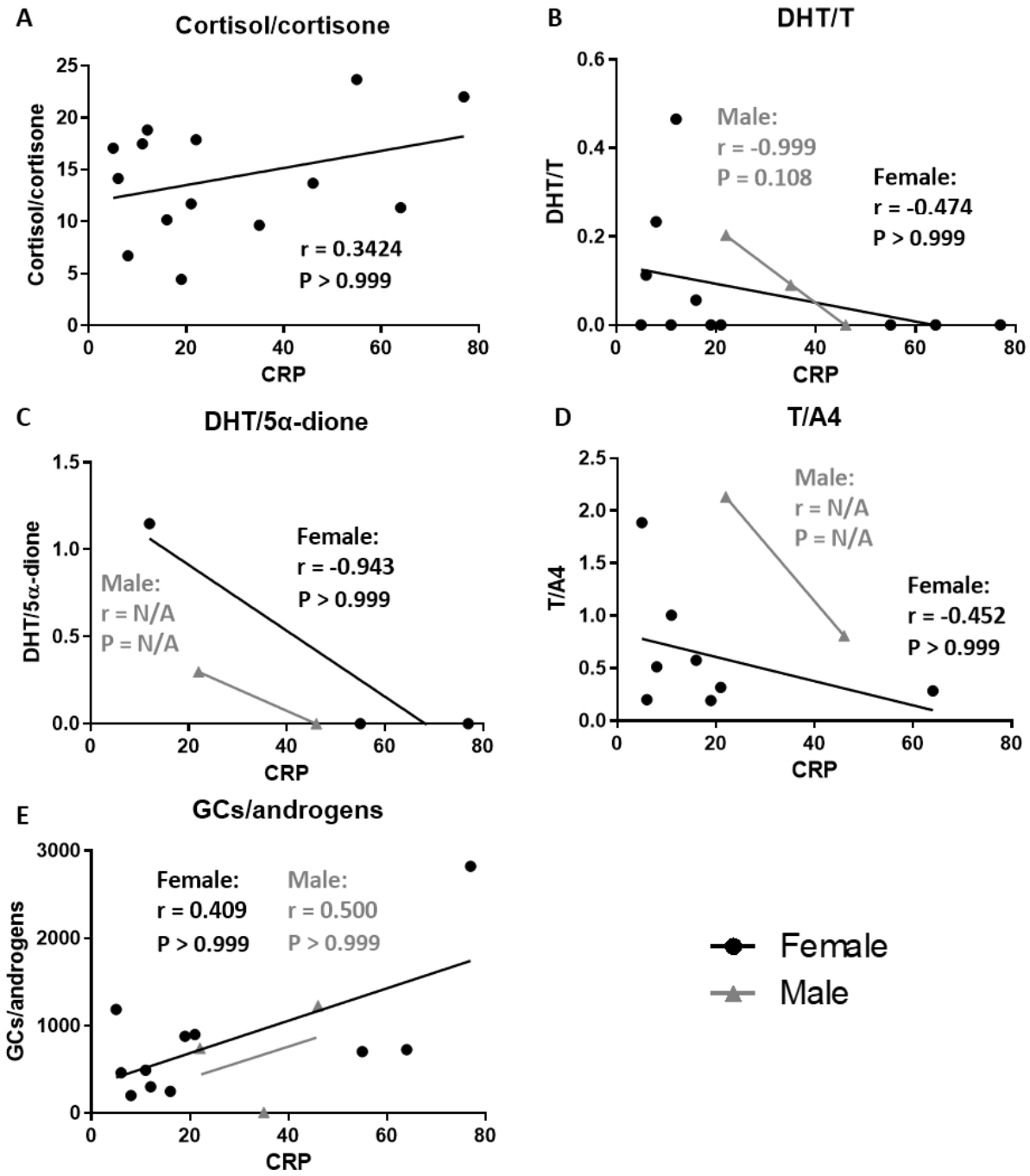

Figure 3-8 Ratios of synovial GCs and androgens do not correlate with RA patient CRP

Ratio of synovial fluid (A) cortisol over cortisone (n=14; female n=11; male n=3), (B) dihydrotestosterone (DHT) over testosterone (T) (n=14; female n=11; male n=3), (C) DHT over androstenedione (5α-dione) (n=5; female n=3; male n=2), (D) testosterone over androstenedione (A4) (n=10; female n=8; male n=2) and (E) cortisone and cortisol over testosterone and DHT (GCs/androgens) (n=14; female n=11; male n=3) calculated by LC-MS/MS and C-reactive protein (CRP). Female patients are represented by black circles and male patients by grey triangles. Data are presented as individual datapoints. Correlation and statistical significance were determined using Pearson or Spearman correlation with Bonferroni's post-test correction for number of repeated measures.

Ratios of GCs and androgens were then assessed against DAS28-CRP as a measure of global disease activity in RA patients. Here, synovial cortisol/cortisone was not found to correlate with DAS28-CRP (r=-0.080; Figure 3-9 A). Similarly, levels of active androgens over precursors did not correlate with DAS28-CRP, apart from a strong negative, though nonsignificant, correlation with AKR1C3 activity (DHT/5α-androstanedione: r=-0.999; testosterone/androstenedione: r=-0.997) and DAS28-CRP in male patients (Figure 3-9 C-D). As with CRP measurements, the GCs/androgens (cortisone and cortisol over testosterone and DHT) ratio positively correlated with DAS28-CRP, although far more so in male patients (r=0.999) than in female patients (r=0.255, Figure 3-9 E).

Together, these data show no significant correlation between synovial steroid levels and measures of inflammation (CRP) or disease activity (DAS28-CRP) in RA patients.

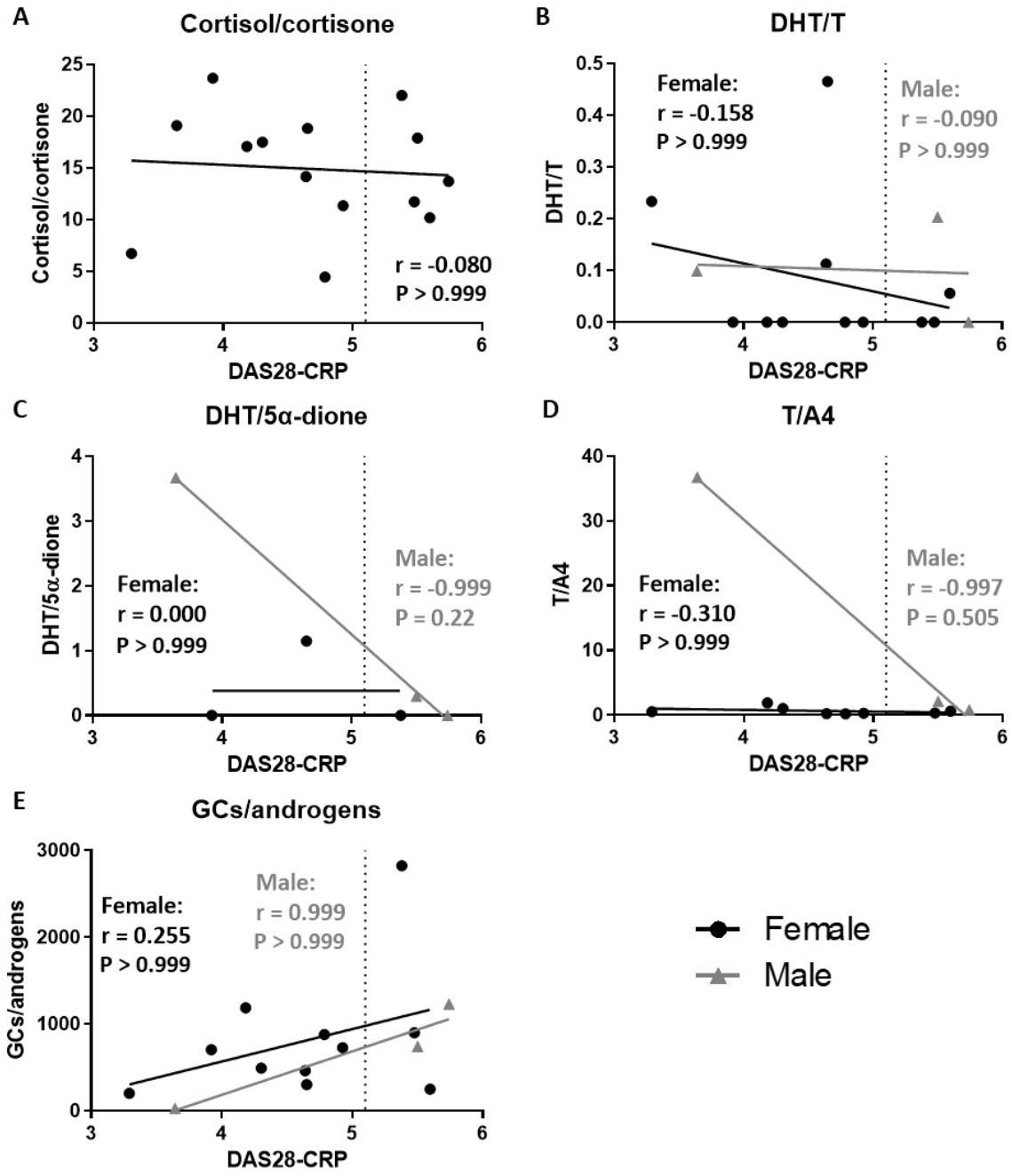

Figure 3-9 Ratios of synovial GCs and androgens do not correlate with RA patient DAS28-CRP

Ratio of synovial fluid (A) cortisol over cortisone (n=14; female n=11; male n=3), (B) dihydrotestosterone (DHT) over testosterone (T) (n=14; female n=11; male n=3), (C) DHT over androstenedione (5α-dione) (n=6; female n=3; male n=3), (D) testosterone over androstenedione (A4) (n=11; female n=8; male n=3) and (E) cortisone and cortisol over testosterone and DHT (GCs/androgens) (n=14; female n=11; male n=3) calculated by LC-MS/MS and patient DAS28-CRP. Female patients are represented by black circles and male patients by grey triangles. DAS28-CRP severity cut-offs of DAS28-CRP < 5.1 for high disease activity as shown by dotted vertical line. Data are presented as individual datapoints. Correlation and statistical significance were determined using Pearson or Spearman correlation with Bonferroni's post-test correction for number of repeated measures.

3.3.5 Correlation of steroidogenic enzyme activity with synovial TNFα

TNFα is a potent pro-inflammatory cytokine with defined roles in pathology of inflammatory diseases such as RA, particularly within macrophages, and strongly linked with systemic steroid dysregulation (356, 358). Therefore, the relationship between levels of synovial TNFα and steroids was investigated to determine if steroid dysregulation was similarly linked to local synovial inflammation. RA was compared to OA as an arthritic disease with less of an inflammation-induced steroid dysregulation component.

Synovial 11β-HSD1 activity was assessed using ratio of cortisol/cortisone (Figure 3-10). However, levels of cortisol/cortisone and TNFα did not correlate in RA or OA patients.

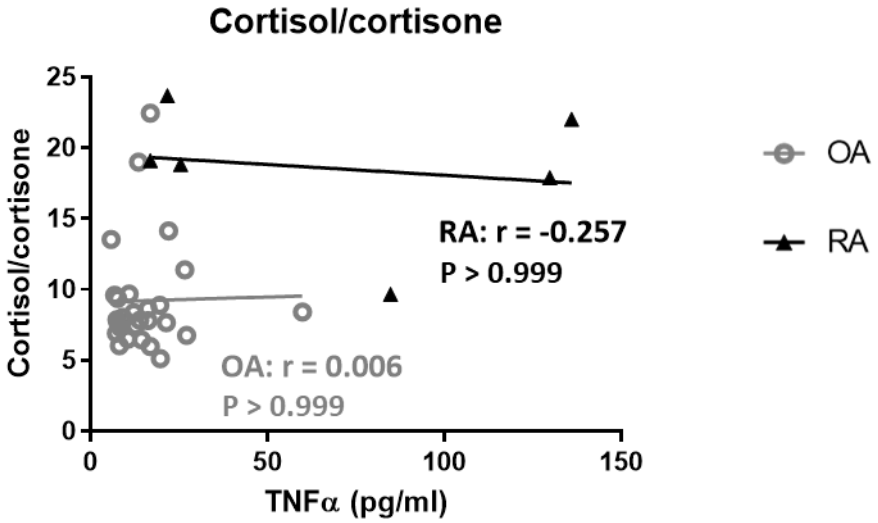

Figure 3-10 Synovial 11β-HSD1 activity does not correlate with TNFα levels

Ratio of synovial cortisol over cortisone calculated by LC-MS/MS and synovial TNFα as quantified by Luminex for OA patients (grey circle) and RA patients (black triangle) (n=38; OA=27; RA n=6). Data are presented as individual datapoints. Correlation and statistical significance were determined using Pearson or Spearman correlation with Bonferroni's post-test correction for number of repeated measures.

The activity of the enzyme SRD5A1 in local inflammation was investigated by assessing the ratio of DHT/testosterone against synovial TNFα (Figure 3-11). Male RA patients, but not OA patients, showed a moderate positive correlation between DHT/testosterone and TNFα (r=0.757, Figure 3-11 B), which corroborates the increased macrophage expression of SRD5A1 with synovial inflammation previously shown (Figure 3-1 C). In female RA patients this trend was negative (r=-0.475), likely due to low synovial levels of DHT, while female OA patients showed a weak positive trend between SRD5A1 activity and TNFα (r=0.221, Figure 3-11 A).

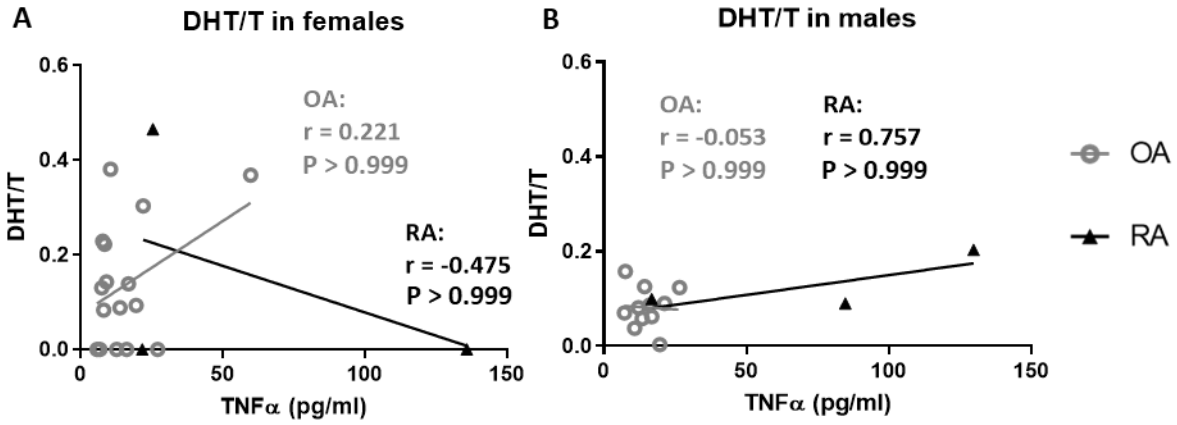

Figure 3-11 Synovial SRD5A1 activity does not correlate with TNFα levels

Steroid ratios as calculated by LC-MS/MS were correlated with synovial TNFα as quantified by Luminex for OA patients (grey circle) and RA patients (black triangle). The ratio of DHT over testosterone in (A) female and (B) male patients. Female OA n=16, RA n=3; male OA n=11, RA n=3. Data are presented as individual datapoints. Correlation and statistical significance were determined using Pearson or Spearman correlation with Bonferroni's post-test correction for number of repeated measures.

The activity of AR1C3 was assessed using the ratios of DHT/5α-androstanedione and testosterone/androstenedione (Figure 3-12). The ratio of DHT/5α-androstanedione was negatively correlated with synovial TNFα in OA patients (females: r=-0.423; males: r=-0.205) and female RA patients (r=-0.475, Figure 3-12 A-B). This is in line with the decreased macrophage expression of AKR1C3 seen with higher synovial inflammation (Figure 3-1 B), however this was not significant and could not be tested in male RA patients due to low sample numbers. Similarly, it was not possible to assess testosterone/androstenedione in RA patients due to low sample numbers, while OA patients showed weak positive correlations between testosterone/androstenedione and TNFα (females: r=0.132; males: r=0.371; Figure 3-12 C-D).

Collectively, these data do not show any significant relationship between ratios of active GCs, mediated by 11β-HSD1, and androgens, mediated by SRD5A1 and AKR1C3, and local levels of TNFα in either OA or RA.

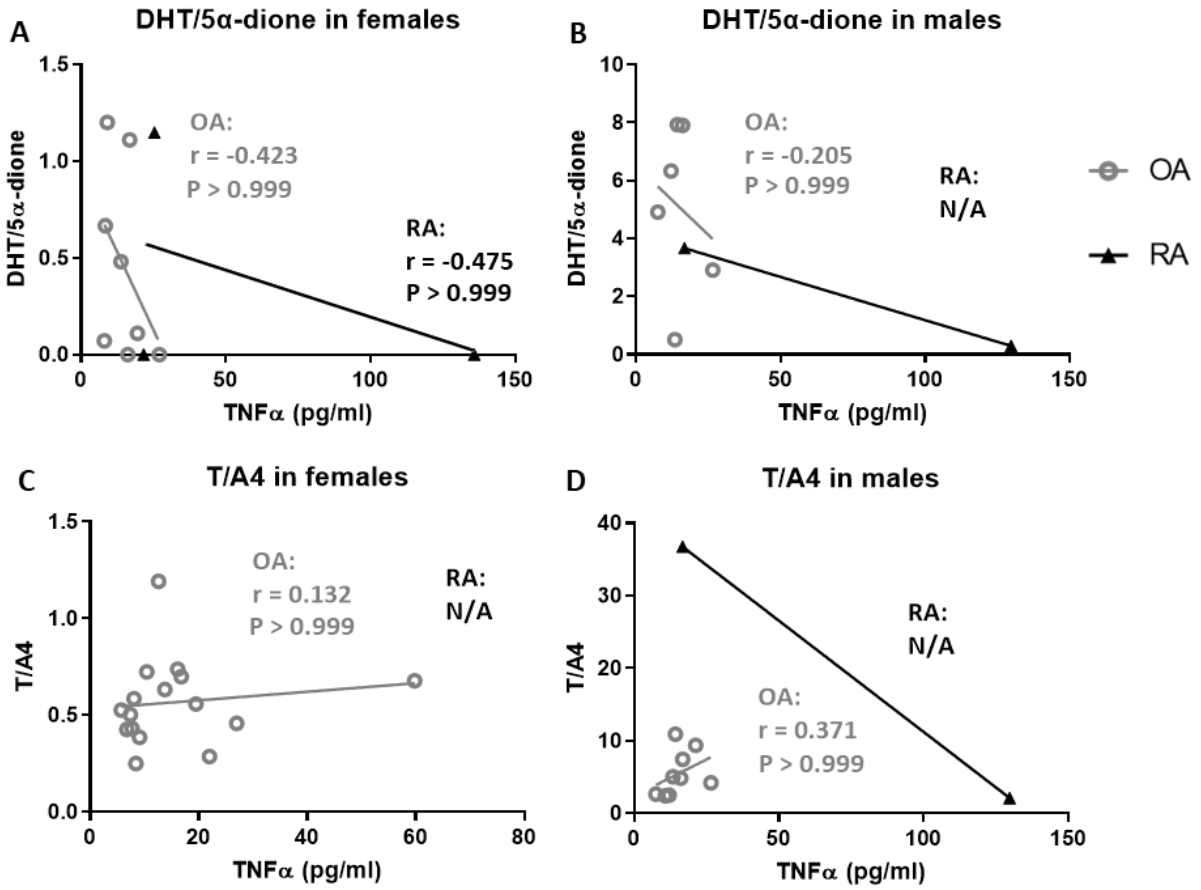

Figure 3-12 Synovial AKR1C3 activity does not correlate with TNFα levels

Steroid ratios as calculated by LC-MS/MS were correlated with synovial TNFα as quantified by Luminex for OA patients (grey circle) and RA patients (black triangle). The ratio of DHT over 5α-dione in (A) female (OA=8; RA n=3) and (B) male patients (OA=6; RA n=3). The ratio of testosterone (T) over androstenedione (A4) in (C) female (OA=16) and (D) male patients (OA=9; RA n=2). Data are presented as individual datapoints. Correlation and statistical significance were determined using Pearson or Spearman correlation with Bonferroni's post-test correction for number of repeated measures.

Finally, the balance of GCs (cortisone and cortisol) and androgens (testosterone and DHT) in synovial fluid was measured against TNFα levels (Figure 3-13). While RA patients showed positive correlations between GCs/androgens and TNFα (females: r=0.984; males: r=0.500) and this was not found in OA patients, these correlations were not significant.

Together these data do not show translation of changes identified in synovial macrophage steroidogenic gene expression with RA severity and inflammation to local changes in steroid metabolism identifiable at the synovial fluid level.

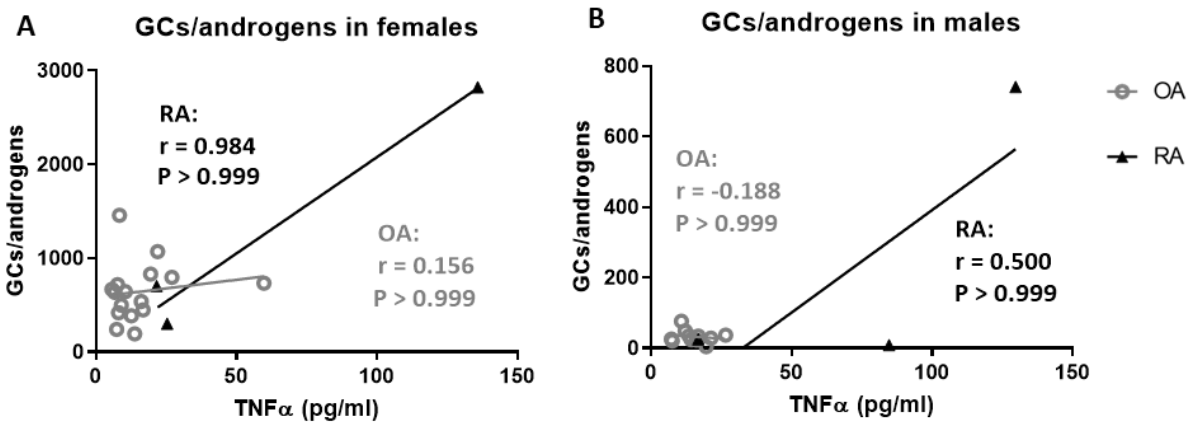

Figure 3-13 Synovial GCs/androgens do not correlate with TNFα levels

Ratio of synovial cortisone and cortisol (GCs) over DHT and testosterone (androgens) calculated by LC-MS/MS and synovial TNFα as quantified by Luminex for OA (grey circle) and RA (black triangle) (A) female (OA=16; RA n=3) and (B) male patients (OA=11; RA n=3). Data are presented as individual datapoints. Correlation and statistical significance were determined using Pearson or Spearman correlation with Bonferroni's post-test correction for number of repeated measures.

3.4 Discussion

Steroid dysregulation is a key feature of RA and is known to be driven by the chronic inflammatory backdrop of the disease. As macrophages are capable of metabolising both GCs and androgens, with resulting negative regulatory effects on inflammatory functions, the expression of steroid metabolising enzymes in synovial macrophages was examined. We have identified that three enzymes with rate-limiting roles in peripheral activation of GCs and androgens (*HSD11B1*, *AKR1C3* and *SRD5A1*) were among the most strongly differentially expressed, when we compared high and low DAS28-CRP disease activity, in RA synovial macrophages (Table 3-8). This implies that these cells are dynamically changing the metabolism and activation of GCs and androgens across inflammation and disease activity in RA. The significance of this is difficult to interpret, but we suspect it may underpin reported changes in steroid hormone profiles favouring increased GCs and decreased androgens that have been reported in RA and further chronic inflammatory diseases (356, 357).

Using further analysis of the AMP RNA-seq dataset, it was confirmed that this inflammation-mediated differential enzyme expression was unique to macrophages when compared to other major cell types in the inflamed synovia: fibroblasts, T cells and B cells (Figure 3-1). In leukocyte-rich samples, with higher synovitis and infiltrate, synovial macrophages upregulated *HSD11B1* and *SRD5A1,* but downregulated *AKR1C3* compared to those from less inflamed leukocyte-poor samples. This significant correlation was also seen with DAS28-CRP, suggesting that the dysregulation of steroid metabolism by macrophages in the local inflamed synovia had a global effect on disease severity. High expression of *HSD11B1* was also seen in fibroblasts, however this did not change between leukocyte rich and poor samples (Figure 3-

1 A). The former finding was expected, as RA FLS are known to express 11β-HSD1 and this contributes to protection from severe arthritic disease, as seen on mesenchymal knock out of 11β-HSD1 in murine polyarthritis (314). However, that RA fibroblast *HSD11B1* expression levels are not differentially regulated by local inflammation is noteworthy, as it suggests that macrophage pre-receptor GC metabolism is far more acutely regulated in inflammatory diseases such as RA. Importantly though, the activity of the 11β-HSD1 enzyme is regulated not only at the transcriptional level, but also through availability of its cofactor NAPDH, and similar posttranslational mechanisms of regulation are known for SRD5A1 and AKR1C3 (258).

Analysis of GC and androgen activating enzymes in the scRNA-seq dataset of synovial macrophages suggested an interesting functional link for this differential expression (Figure 3-3). *HSD11B1* and *SRD5A1* expression were both found within macrophage subsets previously associated with more severe RA, while *AKR1C3* expression was more found within pro-resolution subsets present in healthy and RA-remission synovia (146). This suggests a distinct shift in macrophage steroid metabolism as inflammatory disease progresses, with a loss of AKR1C3-mediated activation of earlier androgen precursors and the acquisition of a phenotype that preferentially activates GCs and later stage androgens via 11β-HSD1 and SRD5A1. Additionally, TREM2+ macrophages have previously been identified as a key tissue resident macrophage population for maintenance of synovial barrier integrity prior to the onset of arthritis (13). The expression of *AKR1C3* in these healthy- and remission-associated TREM2+ clusters implies that early stage activation of androgens by macrophages could be important in resolution of inflammation and disease activity.

The functional relevance of this dysregulated steroid metabolism transcriptome was assessed in synovial fluids from RA patients. It was expected that, were synovial macrophages contributing significantly to the local synovial fluid metabolome, we would find an increase in cortisol/cortisone and perhaps DHT/testosterone with local and systemic measures of inflammation and disease severity, due to inflammation-induced increases in *HSD11B1* and *SRD5A1* expression in macrophages. Moreover, total levels of androgens relative to GCs would decrease due to the inflammation-induced downregulation of *AKR1C3*, as this enzyme catalyses many key activation steps in androgen activation along the pathway, including testosterone/androstenedione and DHT/5α-androstanedione. It has been previously shown that 11β-HSD1 activity positively correlated with systemic inflammation, as measured by CRP and ESR, as well as levels of synovial infiltrate (309, 310). Although studies of steroid dysregulation in the synovial fluid have focused on the balance of estrogens/androgens, due to the reported inflammatory-mediated increase in serum GCs/androgens in RA, we expected a similar shift in the synovia (356-359). As inflammation drives further systemic and local generation of GCs, steroid biosynthesis may switch to preferentially generate GCs at the expense of androgens, which may contribute to the paucity of androgens in synovial fluid, in addition to the generation of estrogens via inflammation-induced aromatase upregulation on cells such as fibroblasts (364, 377). The balance of active androgens and GCs may therefore be reflected in measures of systemic inflammation and RA disease activity.

However, no significant correlations were identified with steroid ratios and measures of CRP, DAS28-CRP or synovial TNFα in this study. As synovial fluid steroids were seen to closely match the profiles of sera (Figure 3-4), it is likely that levels of steroids in synovial fluid represent only systemic serum changes, with any potential local metabolic differences being masked by this.

Synovial fluid is known to have a very high turnover and lipophilic steroids diffuse across the synovial membrane with ease (413, 414). The only steroid ratio that was found to be significantly different between synovial fluid and serum was DHT/testosterone, but only in female patients (Figure 3-5 B). Similarly, the level of DHT/5α-androstanedione was seen to be lower in male RA patients than OA patients, perhaps due to an inflammation-induced decrease in macrophage *AKR1C3* expression (Figure 3-7 D). However, neither of these changes were seen to be linked to inflammation or disease severity on closer analysis in RA patients.

This study was further limited due to the nature of sample collection, as it was not possible to control for the time of day, fasting state or other factors known to influence steroid availability. Circadian and ultradian rhythms drive steroid production from the adrenal glands, and further temporal variation can be seen even within peripheral tissues (411, 415). A further study controlling for this by taking synovial fluid and serum samples from patients at the same time of day would give a better representation of steroid availability, however singular "spot analysis" of steroid levels would not give an accurate representation of what is likely a dynamic metabolic process between multiple cell types. Additionally, it was not possible to exclude patients taking therapeutic GCs from these studies. Although these were only a minority of patients, it was seen that those taking GCs had significantly lower synovial cortisone and DAS28-CRP (Table 3-5).

Previous research has found stronger positive correlations between (THF+5aTHF)/THE, a urinary measure of 11β-HSD1 activity, and ESR and CRP in established RA, whereas early persistent RA and resolving arthritis showed little to no correlation (310). Unfortunately, it was not possible to stratify the serum and synovial fluid samples in this study in this manner

due to low sample numbers and unavailability of exact diagnoses. As shown in Table 3-7, RA patients in the synovial fluid study had an equivalent average DAS28-CRP score to the AMP study RA patients, 4.716 versus 3.936. This score is defined as moderate disease activity, however none of the patients in this study had a DAS28-CRP score lower than this moderate score range (≥3.2 to <5.1) and therefore our range of disease severity was limited (6). Further analysis with a larger sample of patients covering progression and resolution of disease, from remission/low activity through to high disease activity, could provide further insight into the relevance of steroid dysregulation to disease severity. Furthermore, the urinary metabolite study solely recruited GC- and DMARD-naïve patients to prevent interactions of synthetic steroids or anti-inflammatory agents on metabolism (310). Urine samples, used to calculate 11β-HSD1 activity, were collected from all patients in the mid-morning, following previous validation of this timepoint as an accurate representation of the GC ratios seen in a full 24-hour urine profile. A similar validation of synovial fluid steroid levels could identify the optimal timepoint for collection, however this would be far more invasive than urinary analysis. Additionally, this would likely not overcome the high turnover of synovial fluid and equilibration with serum obscuring local steroid metabolism.

Correlation of steroid ratios with disease activity and inflammation necessitated separation of the samples by sex, as sex-dependent differences were identified in both of the ratios assessed for AKR1C3 in OA and RA synovial fluid, where male patients were found to have higher ratios of testosterone/androstenedione and DHT/5α-androstanedione (Figure 3-7 C-D). However, despite similar measures of CRP and DAS28-CRP for male and female RA patients (Table 3-4), this reduced sample sizes for comparisons and so individual variability was not controlled for. This loss was particularly compounded on analysis of AKR1C3 activity as the precursors

androstenedione and 5α-androstanedione were found only at low levels, sometimes below the limit of detection, particularly in female patients. Finally, this study was limited by the age ranges of the patients. Whilst the significantly older average age of the OA patients compared to RA patients (69.8 v 55.2; Table 3-3) does accurately represent trends in disease presentation, age-matching would allow a better comparison of age-associated and inflammatory-associated steroid dysregulation between these diseases. Therefore, further analysis of a larger sample size for each disease, with age- and sex-matching, would provide a more accurate depiction of steroid dysregulation with disease and provide additional opportunities for variable control.

The identification of 11-oxygenated androgens in the synovial fluid was unexpected, and has not been previously reported. 11OHA4 and 11OHT, precursors with limited androgenic activity, are both mainly produced in the adrenal glands from CYP11B1-hydroxylation of androstenedione and testosterone respectively and released into circulation (320). These can be converted to their keto forms, 11-ketoandrostenedione (11KA4) and 11-ketotestosterone (11KT) by 11β-HSD2, and 11KA4 into 11KT by AKR1C3, in the adrenals or, preferentially, the periphery (416). Although 11KA4 is largely inert as an androgen, 11KT has equivalent androgenicity to testosterone (322). PBMCs have recently been shown to convert 11KA4 into 11KT by AKR1C3, however this was found to be mainly by natural killer cells, with little to no activity in monocytes (323). As human RA synovial macrophages have been identified to express both 11β-HSD2, according to previously published immunohistochemistry analysis, and AKR1C3 in this study (Figure 3-1 C) it is an intriguing possibility that they could be catalysing both the reduction of 11-hydroxy androgens into keto forms and generation of active 11KT (289). With the reduction of *AKR1C3* expression seen with increasing local RA

inflammation and disease severity (Figure 3-1 and Figure 3-2) there could be a reduction in generation of 11KT, and therefore any potential anti-inflammatory effects from this active androgen. However, as of yet there has been no exploration of the effects of 11-oxygenated androgens on macrophages. Additionally, 11β-HSD2 was not among the genes seen to be significantly differentially regulated with RA severity and inflammation (Figure 3-1 D). Further analysis was beyond the scope of this thesis, as we sought to focus on androgens generated by the classical and alternate pathways only, though 11-oxygenated androgens may have roles in regulation of inflammation in the synovia.

Although synovial macrophages have previously been shown to convert testosterone into DHT, presumably by SRD5A1, and other human macrophage populations appear to express both *SRD5A1* and *AKR1C3*, there are other cells populations in the synovia that could also express these enzymes and contribute to synovial steroid levels (374, 375, 390). T cells and B cells have previously been found generate DHT via *SRD5A1* expression, and here it was found that RA synovial T and B cells both expressed *SRD5A1*, while T cells also expressed lower levels of *AKR1C3* (Figure 3-1 B, C) (346). Similarly, RA fibroblasts were found to express both *SRD5A1* and *AKR1C3*, which does not appear to have been reported before in the synovia (Figure 3-1 B, C). Although these expression levels did not change with leukocyte infiltration level, this does not rule out posttranslational regulation of enzyme activity by inflammation in arthritic disease, and so these cell types may contribute to the changes in androgen levels seen with RA. Finally, as fibroblasts were seen to be the main population expressing AR, with a far lower expression level in macrophages, it may be that while macrophages produce androgens locally, fibroblasts are the main androgen-responsive population. Given the rapid fluid

turnover of the synovium, our analysis will not have captured the intracrine and paracrine steroid metabolism present within and between these cells.

In conclusion, this study confirmed distinct regulation of GC and androgen steroid metabolism genes in macrophages, which may be linked to their function in the RA synovia. However, synovial analysis was insufficient to prove contribution to synovial fluid steroid levels and dysregulation with inflammatory disease. As macrophages express both the receptor and activating enzyme for GCs, they may contribute to both intracrine and paracrine GC-induced regulation of inflammation. Meanwhile, the expression of androgen activating enzymes, with lower levels of *AR*, imply a stronger role for synovial macrophages in increasing local paracrine availability of androgens. Unfortunately, the dynamic nature of synovial fluid turnover and the insufficient sample size and controls in our synovial fluid study meant that analysis was unable to capture a functional outcome of the transcriptional changes seen. These data also imply that intracellular levels of steroids could be more relevant for inflammatory disease, therefore the effects of intracrine and paracrine steroid metabolism of GCs and androgens is further investigated in macrophages in vitro in the following chapters of this thesis.

Chapter 4 MACROPHAGE METABOLISM OF GLUCOCORTICOIDS AND FUNCTIONAL EFFECTS ON INFLAMMATORY PROFILES

4.1 Introduction

As central drivers of the inflammatory response, macrophages are key targets of the anti-inflammatory properties of GCs. GC treatment of inflammatory-activated macrophages downregulates their anti-microbial and pro-inflammatory functions and influences their polarisation states, as reviewed in section 1.3.4 (226-229, 235, 236). The GC-activating enzyme 11β-HSD1 has previously been shown to be upregulated upon inflammatory activation of macrophages by factors such as IFNγ and LPS (104, 273, 291). This facilitates the intracrine activation of GCs within macrophages, influencing their cytokine release profiles and pro-resolution functions, evidenced in murine models of transgenic *Hsd11b1* deletion. In this context, murine macrophages show excessive production of pro-inflammatory cytokines upon stimulation and delayed phagocytosis of apoptotic neutrophils in models of sterile inflammation (278, 295). However, the regulation of 11β-HSD1 and its effects on inflammatory functions in human macrophages have not been fully ascertained.

Analysis of the AMP bulk RNA-seq dataset in Chapter 3 identified that synovial macrophage expression of the 11β-HSD1 gene *HSD11B1* significantly correlated with severity of inflammation and disease in RA patients, and scRNA-seq cluster analysis suggested that this expression was localised to a pro-inflammatory pathogenic synovial macrophage subset. Whilst measures of GC metabolism in the synovial fluid did not yield significant correlations

with synovial cytokine profiles or changes in disease severity, this experimental design was not sufficient to explore the role of local intracrine and paracrine GC metabolism on the inflammatory function of macrophages. Therefore, in this chapter we used in vitro cultures of macrophages polarised to distinct pro- and anti-inflammatory states to investigate the effect of intracrine GC metabolism by 11β-HSD1 on macrophage inflammatory profiles and function.

4.2 Materials and methods

4.2.1 Macrophage culture

4.2.1.1 Validation of monocyte sorting purity

Monocytes were isolated from human blood cones by RosetteSep™ as previously described (section 2.3.1). To compare isolation efficacy, PBMCs were isolated from blood cones by density gradient centrifugation. Blood was layered over Lymphoprep™ density gradient medium (Stem Cell Technologies, UK) and centrifuged at 1200g for 30 minutes with low acceleration and brake off.

Isolated PBMCs and RosetteSep™ isolated monocytes from matched samples were washed in PBS, stained with CD14+ PE antibody (clone MPHIP9, BD Biosciences, UK) diluted 1/100 in PBS for 30min and then washed in PBS and resuspended in PBS with 0.5% BSA and 2 mM EDTA (all Sigma-Aldrich, UK). Unstained PBMCs and monocytes from the same samples were ran as negative controls to set CD14+ gating. Cells were filtered through a 100 µm cell strainer before analysis and ran on a LSRFortessa™ flow cytometer (BD Biosciences, UK). Data were acquired using DIVA software and analysed with FlowJo v10 (both BD Biosciences, UK).

Monocytes isolated from blood with RosetteSep™ had a CD14+ purity of around 90% (Figure 4-1).

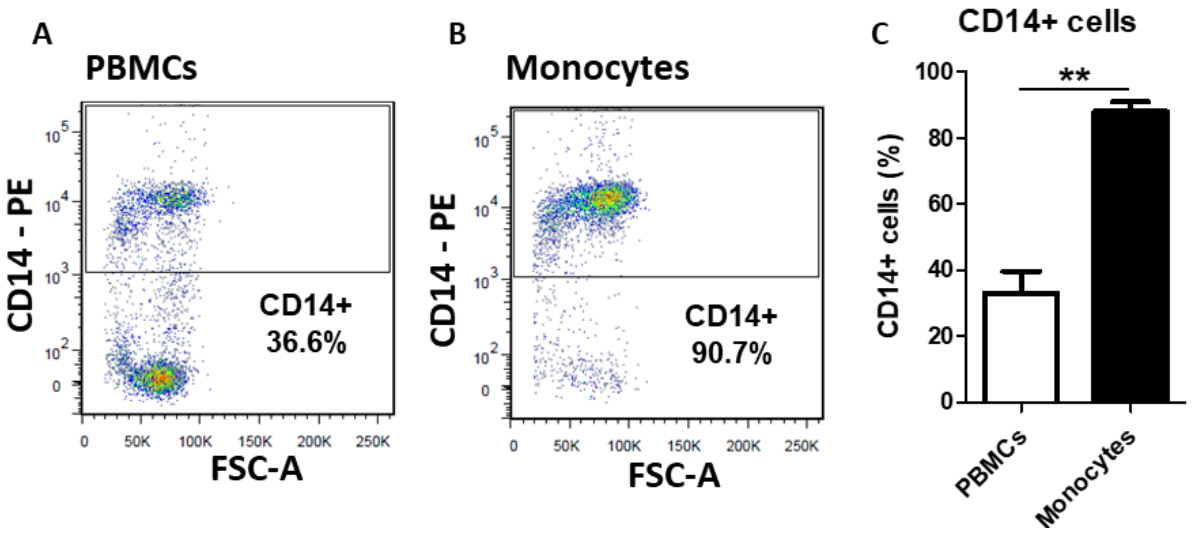

Figure 4-1 Purity of RosetteSep™ isolated blood monocytes

Representative scatter plots showing proportion of CD14+ cells as measured by flow cytometry in (A) peripheral blood mononuclear cells (PBMCs) isolated by density gradient centrifugation and (B) cells isolated from whole blood with RosetteSep™ Monocyte Enrichment kit. (C) Percentage of CD14+ cells in PBMCs and RosetteSep™-isolated monocytes (n=3). Data are presented as mean ± SEM and statistical significance was determined using Student's paired t-test (** p≤0.01).

4.2.1.2 Macrophage polarisation and validation

Macrophages were differentiated from CD14+ human blood monocytes, as detailed in section 2.3.1. After differentiation in 20 ng/ml M-CSF, macrophages were treated with polarising factors, as shown in Figure 4-2.

To validate M1 and M2 polarisation and assess differential GC metabolism, differentiated macrophages were treated with 20 ng/ml IFNγ and 10 ng/ml LPS (M1), 20 ng/ml IFNγ and 10 ng/ml TNFα (M1-like) or 20 ng/ml IL-4 (M2), or untreated (M0) for 24h in macrophage media (RPMI and 20 ng/ml M-CSF) before analysis by qPCR, ELISA or flow cytometry.

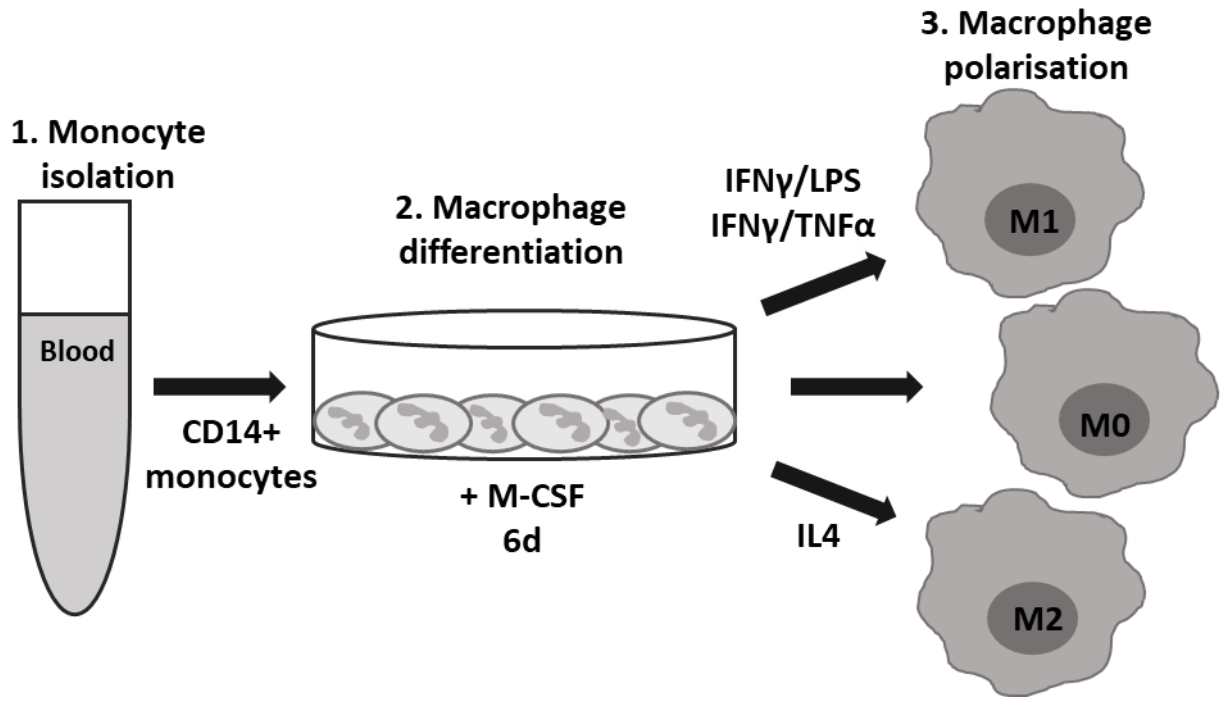

Figure 4-2 Generation of human blood monocyte-derived macrophages

1. Monocyte isolation – CD14+ monocytes isolated directly from whole blood with RosetteSep™ kit. 2. Macrophage differentiation – isolated monocytes differentiated into macrophages with d6 M-CSF treatment, with media changes on d2 and d5. 3. Macrophage polarisation – mature differentiated macrophages are polarised with cytokines into functionally distinct phenotypes.

4.2.1.3 Macrophage GC treatment during polarisation

To assess effects of GCs on polarisation, macrophages were concurrently treated with 1000 nM cortisol or cortisone, or ethanol vehicle control, during 24h polarisation as previously described. To assess the effect of PPARγ-agonism on HSD11B1 expression, macrophages were treated with 1 µM rosiglitazone (VWR International, UK) or DMSO vehicle control (Sigma-Aldrich, UK), with or without 1000 nM cortisol. Following 24h treatment, RNA was isolated for qPCR analysis and supernatants for ELISA analysis.

4.2.1.4 The effects of pre-receptor GC metabolism on macrophage inflammatory function

Macrophages were treated for 24h with 20 ng/ml IFNγ and 10 ng/ml TNFα (M1-like) or untreated (M0) in macrophage media (RPMI and 20 ng/ml M-CSF). After 24h, media was changed, and polarised macrophages were treated with 1000 nM cortisone or ethanol vehicle for a further 24h. 10 ng/ml LPS or vehicle was added for 8h before RNA and media collected for analysis.

4.2.1.5 Human alveolar macrophage isolation and culture

Alveolar macrophages were isolated by Dr Rahul Mahida and Lauren Davies at the Institution of Inflammation and Ageing at the Queen Elizabeth Hospital Birmingham as detailed in section 2.3.2. Macrophages were activated with 1 μg/ml LPS and treated with or without 100 nM or 1000 nM cortisol or 1000 nM cortisone during 24h polarisation to assess inflammatory activation and GC responses.

4.2.2 Gene expression analysis

Following appropriate treatment timepoint, RNA was isolated from macrophage cultures with an innuPREP RNA Mini kit (Analytik Jena, Germany), following manufacturer's protocol, as described in section 2.4.1. Yield and purity of samples, as determined by absorbance ratios at 260/280 and 260/230, was measured on a NanoDrop™ ND-1000 spectrophotometer (Wilmington, USA). 350 ng of RNA per sample was reverse transcribed using Applied Biosystems High-Capacity cDNA Reverse Transcription Kit and a GeneAmp® PCR System 27000 machine (Applied Biosystems, UK), following the protocol detailed in section 2.4.2. qPCR

analysis was carried out on a QuantStudio™ 5 Real-Time PCR System (Applied Biosystems, UK) with TaqMan probes, listed in section 2.4.3. Expression of genes of interest was normalised to that of 18S for quantification of relative expression.

4.2.3 Cytokine release analysis

Cytokine levels were measured by ELISA as detailed in section 2.6. Supernatants were collected from macrophage cultures following relevant stimulation time detailed in relevant figure legends. ELISAs were carried out using Invitrogen Human Uncoated ELISA Kits for TNFα, IL-12 p70 and IL-10 (all Thermo Fisher Scientific, USA) and Precoated Quantikine® Human IL-6 ELISA Kit (R&D Systems, USA), following manufacturers' protocols, and ran on a FLUOstar® Omega Microplate Reader (BMG Labtech, Germany).

4.2.4 Surface marker expression analysis

The expression of M1- and M2-associated cell surface markers was assessed by flow cytometry as detailed in section 2.7. After 24h polarisation, macrophages were stained with the following antibodies (all BD Biosciences, UK): CD16-FITC (clone 3G8), CD64-PE-Cy7 (clone 10.1), CD86-BV510 (clone 2331 [FUN-1]), CD163-PE-CF594 (clone GHI/61), CD206-BV421 (clone 19.2) and HLA-DR-BV605 (clone G46-6), all at 1/100 dilution as determined by staining index optimisation (section 2.7). Stained cells were ran on a LSRFortessa™ flow cytometer using DIVA software and analysed with FlowJo v10 (all BD Biosciences, UK). Expression of markers on M1- and M2-polarised macrophages was compared to nonspecific isotype controls for that antibody.

4.2.5 11β-HSD activity assays

GC-converting enzyme activity was assessed using scanning TLC (section 2.5.2) with normalisation determined by DC protein assay (section 2.5.3). Macrophages were polarised for 48h to ensure adequate protein expression of 11β-HSD enzymes, and then incubated with 100 nM cortisone (for oxo-reductase activity) or 100 nM cortisol (for dehydrogenase activity) with trace amounts of tritiated cortisone or cortisol respectively (all Perkin Elmer, UK) for 3h (oxo-reductase activity) or 18h (dehydrogenase activity). Steroids were extracted in dichloromethane, separated by TLC with 92:8 ratio of chloroform:ethanol and then analysed with a Bioscan 200 Imaging scanner (Bioscan, USA) and rate of steroid conversion calculated as detailed in section 2.5.4.

4.2.6 Phagocytosis assay

Macrophages were polarised to M2 macrophages with 20 ng/ml IL-4 for 24h in the presence of 1000 nM cortisol or ethanol vehicle. Phagocytosis was then assessed with the Vybrant™ *E. coli* Phagocytosis Assay kit (Thermo Fisher, UK) according to manufacturer's instructions, detailed in section 2.8. The fluorescence intensity of a linear dilution of fluorescent *E. coli* beads in assay buffer was measured to calculate the approximate level of beads phagocytosed by macrophages.

4.2.7 Cell viability assay

Viability was assessed using an ApoLive-Glo® Multiplex assay (Promega, UK) as detailed in section 2.9. Following differentiation from monocytes as before on Eppendorf® Cell Imaging

96 well glass bottom plates (Sigma-Aldrich, UK) macrophages were polarised to M0 (untreated) or M1-like (IFNγ and TNFα) for 24h with ethanol vehicle control or 1000 nM cortisone or cortisol and then assessed for viability and apoptosis according to manufacturer's guidelines. M0 macrophages were treated with 10 mM hydrochloric acid (HCl) 10min before assay as a positive control for cell death.

4.2.8 Statistical analysis

Statistical significance was assessed with IBM SPSS Statistics v28.0.1.0 (IBM Analytics, USA) and GraphPad Prism v5.03 and v9.5 (GraphPad Software, USA). Normality of data was tested using a Shapiro-Wilk test for Gaussian distribution. Paired Student's t-test was used to compare significance of two groups from same blood donors. When multiple treatment groups were present a one-way ANOVA with Tukey's post hoc analysis was used to test significance between all groups. Two-way ANOVA analysis with Bonferroni multiple comparison post-test was used to compare between macrophage polarisation subsets and treatment groups. Statistical significance is presented as follows: * $P \leq 0.05$, ** $P \leq 0.01$ and *** $P \leq 0.001$.

4.3 Results

4.3.1 Validation of M1 and M2 macrophage polarisation

To investigate the role of GC pre-receptor metabolism by 11β-HSD1 in regulation of macrophage inflammatory profiles, we generated M1 (IFNγ and LPS) and M2 (IL-4) polarised macrophages in vitro. The acquisition of expected distinct pro- and anti-inflammatory profiles was validated by analysis of morphology, gene expression, cytokine secretion and surface marker expression.

Following 24h of polarisation, microscopy of cultured macrophages confirmed acquisition of the expected distinct morphology: M1 macrophages had a rounder morphology while M2 macrophages had a more stromal-like spindle shape (Figure 4-3 A) (417). Analysis of mRNA expression by qPCR confirmed that both M1 and M2 macrophages expressed equivalent levels of the general human macrophage marker *CD68* (P=0.7409), while M1-polarised expressed significantly higher levels of the high affinity IgG receptor *CD64* (14.1-fold, P≤0.05), associated with M1 anti-microbial functions (Figure 4-3 B). There was a strong trend towards higher expression of the M2-associated pro-resolution scavenger receptor *CD163* in M2 macrophages (3.5-fold, P=0.0871; Figure 4-3 B).

High levels of TNFα secretion were seen in M1 macrophages, and these were significantly higher in M1 polarised macrophages than in M2 (249.2-fold, P≤0.05; Figure 4-3 C). IL-12 p70 levels also appeared greater in M1 macrophages relative to M2 polarised, although this was not significant (P=0.3460). The M2-associated anti-inflammatory cytokine IL-10 was secreted by both macrophage subsets, with a trend towards greater secretion in M1 polarised macrophages (9.0-fold, P=0.0896).

Brief analysis of cell surface marker expression by flow cytometry confirmed expression of macrophage polarisation associated markers compared to nonspecific antibody isotype controls. M1-polarised macrophages expressed markers associated with M1-like pro-inflammatory functions: high affinity IgG receptor CD64, co-stimulation marker CD86 and antigen presentation molecule HLA-DR (Figure 4-3 D). M2 macrophages expressed markers associated with M2-polarisation and anti-inflammatory function: the low affinity IgG receptor CD16 and scavenger receptors CD163 and CD206 (Figure 4-3 D).

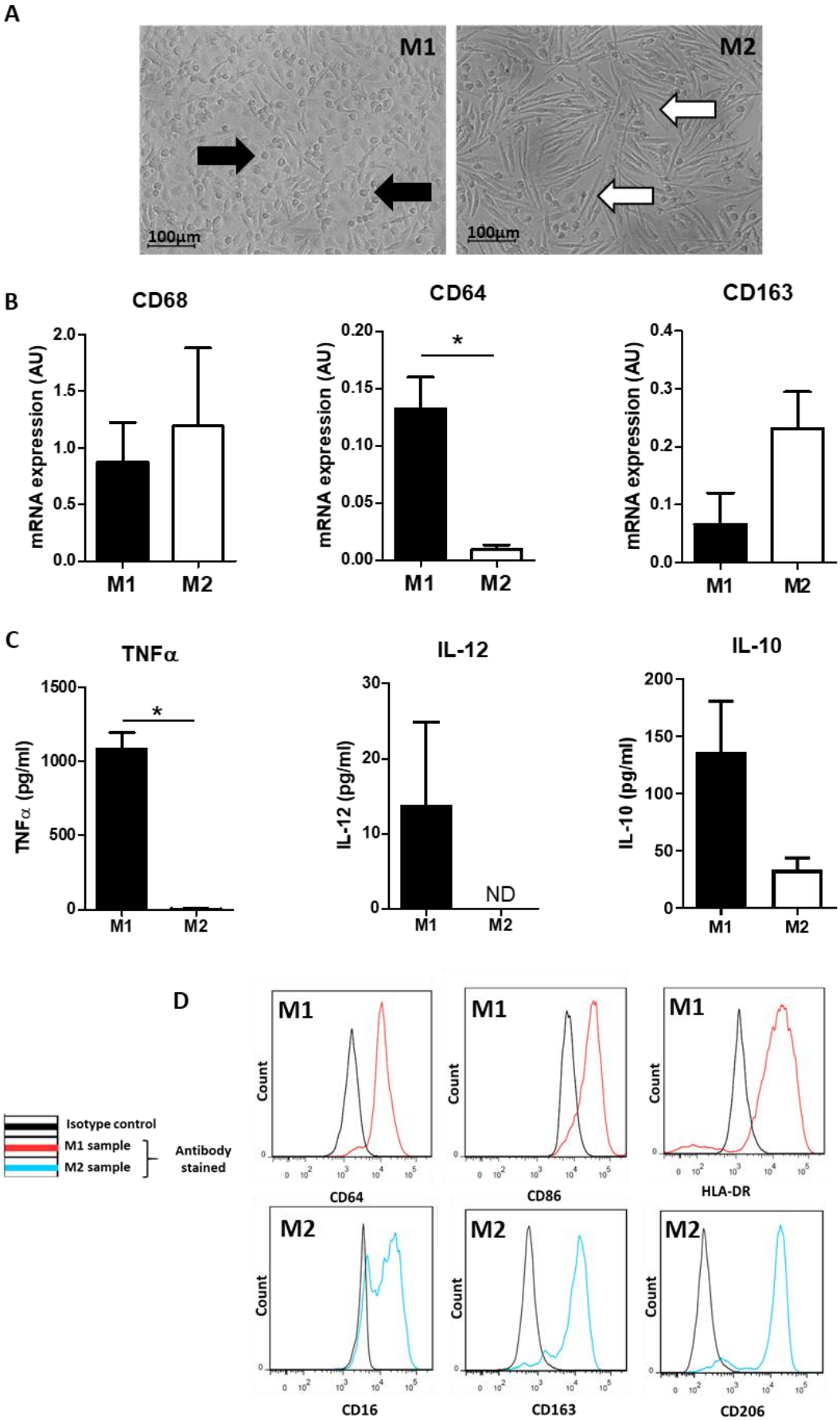
A
M1
M2
100µm
100µm
B
CD68
CD64
CD163
mRNA expression (AU)
2.0
1.5
1.0
0.5
0.0
0.20
0.15
0.10
0.05
0.00
0.4
0.3
0.2
0.1
0.0
*
M1
M2
C
TNFα
IL-12
IL-10
TNFα (pg/ml)
IL-12 (pg/ml)
IL-10 (pg/ml)
1500
1000
500
0
30
20
10
200
150
100
50
ND
D
Isotype control
M1 sample
M2 sample
Antibody stained
Count
CD64
CD86
HLA-DR
CD16
CD163
CD206

Figure 4-3 Validation of macrophage polarisation

Macrophages were polarised for 24h into M1 (IFNγ/LPS) or M2 (IL-4). (A) Microscopy images of macrophages at 10X magnification. Black arrows show cells with rounded and flat morphology, white arrows show cells with elongated processes. (B) RNA expression (AU) of the macrophage differentiation marker *CD68*, M1-associated gene *CD64* and M2-associated gene *CD163* as measured by qPCR (n=4). (C) Following 48h polarisation, concentration of the M1-associated cytokines TNFα and IL-12 p70 and M2-associated cytokine IL-10 were quantified by ELISA analysis of cell supernatants (n=3). (D) Representative histograms of M1 macrophage (red) expression of the M1-associated cell surface markers CD64, CD86 and HLA-DR and M2 macrophage (blue) expression of the M2-associated surface markers CD16, CD163 and CD206 compared to antibody isotype control (black), as measured by flow cytometry after 48h polarisation. Data are presented as mean ± SEM and statistical significance was determined using paired Student's t-test (* p≤0.05). ND, not detected.

4.3.2 GC pre-receptor activation is upregulated in pro-inflammatory macrophages

GC pre-receptor metabolism by the enzymes 11β-HSD1 and 11β-HSD2 was investigated in differentially polarised macrophages to assess the effects of inflammation on macrophage GC metabolism. We initially assessed further genes involved in GC signalling and metabolism to determine their contribution on inflammatory polarisation (Figure 4-4).

Following 24h M1 or M2 polarisation, the expression of the primary GC receptor *NR3C1* (Figure 4-4 A), acute GC signalling response transcript *GILZ* (Figure 4-4 B) and rate-limiting 11β-HSD1 oxo-reductase activity cofactor-generating enzyme *H6PDH* (Figure 4-4 C) were measured by qPCR. No difference in expression was identified for *NR3C1* or *H6PDH* between M1 and M2 polarised macrophages. Conversely, *GILZ* expression was higher in M1 polarised macrophages than M2 (2.2-fold, P≤0.05).

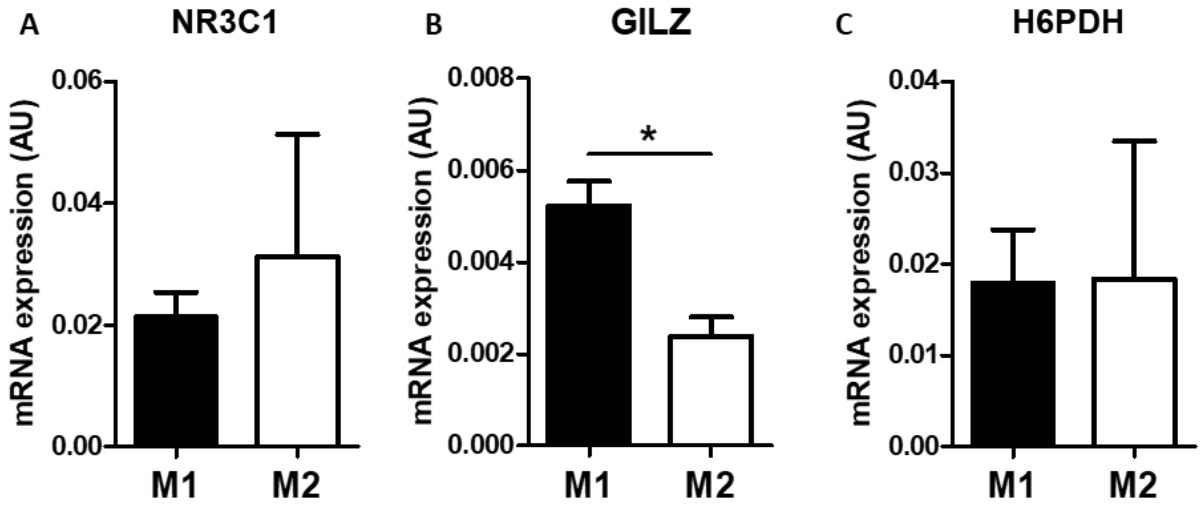

Figure 4-4 Polarised macrophage expression of glucocorticoid-associated genes

RNA expression (AU) of (A) the glucocorticoid receptor (*NR3C1*), (B) glucocorticoid-induced leucine zipper (*GILZ*) and (C) hexose-6-phosphate dehydrogenase (*H6PDH*) in M1 (IFNγ/LPS) and M2 (IL-4) polarised macrophages as measured by qPCR (n=4). Data are presented as mean ± SEM and statistical significance was determined using Student's paired t-test (* p≤0.05).

Pre-receptor GC metabolism was assessed in differentially polarised macrophages to confirm inflammatory induction of 11β-HSD1. We assessed 11β-HSD1 expression and activity across two well established protocols for M1-like polarisation using either IFNγ (20 ng/ml) and LPS (10 ng/ml) or IFNγ (20 ng/ml) and TNFα (10 ng/ml) for 24h, as well as establishing their independent action on 11β-HSD1 regulation (418).

Following 24h polarisation, *HSD11B1* mRNA expression was significantly increased in M1 and M1-like polarised macrophages using both protocols relative to unpolarised M0 controls (M1: 13.6-fold; M1-like: 12.7-fold; both P≤0.05), showing no significant difference between those polarised with IFNγ and LPS or IFNγ and TNFα (Figure 4-5 A). Individual inflammatory factors and IL-4 polarised M2 macrophages did not significantly upregulate *HSD11B1* expression compared to the unpolarised control.

We next examined *HSD11B2* mRNA expression to assess whether the GC-inactivating enzyme 11β-HSD2 was also differentially regulated by inflammatory polarisation. This appeared to be highest in unpolarised macrophages, however there were no significant differences in expression seen across macrophage subsets (Figure 4-5 B). There was a trend towards decreased *HSD11B2* expression in IFNγ/TNFα M1-like macrophages, but this was not significant (M0 vs IFNγ/TNFα M1: 6.6-fold, P=0.1191).

Oxo-reductase (cortisone to cortisol) enzyme activity assays supported these findings. The highest rate of cortisone to cortisol conversion by 11β-HSD1 was seen in IFNγ and TNFα M1-like polarised macrophages, being significantly greater than both M0 (25-fold, P≤0.001) and M2 polarised macrophages (3.3-fold, P≤0.05) as well as macrophages treated with LPS (2.5-fold, P≤0.05) or TNFα (5.3-fold, P≤0.01) alone (Figure 4-5 C). However, IFNγ and LPS M1 macrophages also had significantly higher oxo-reductase activity than unpolarised control (13-fold, P≤0.05). As seen in the gene expression analysis, there were no differences in dehydrogenase activity associated with the 11β-HSD2 isozyme (Figure 4-5 D).

Together these data show that 11β-HSD1 gene expression and cortisol-generating activity is most potently upregulated in pro-inflammatory M1-like polarised macrophages.

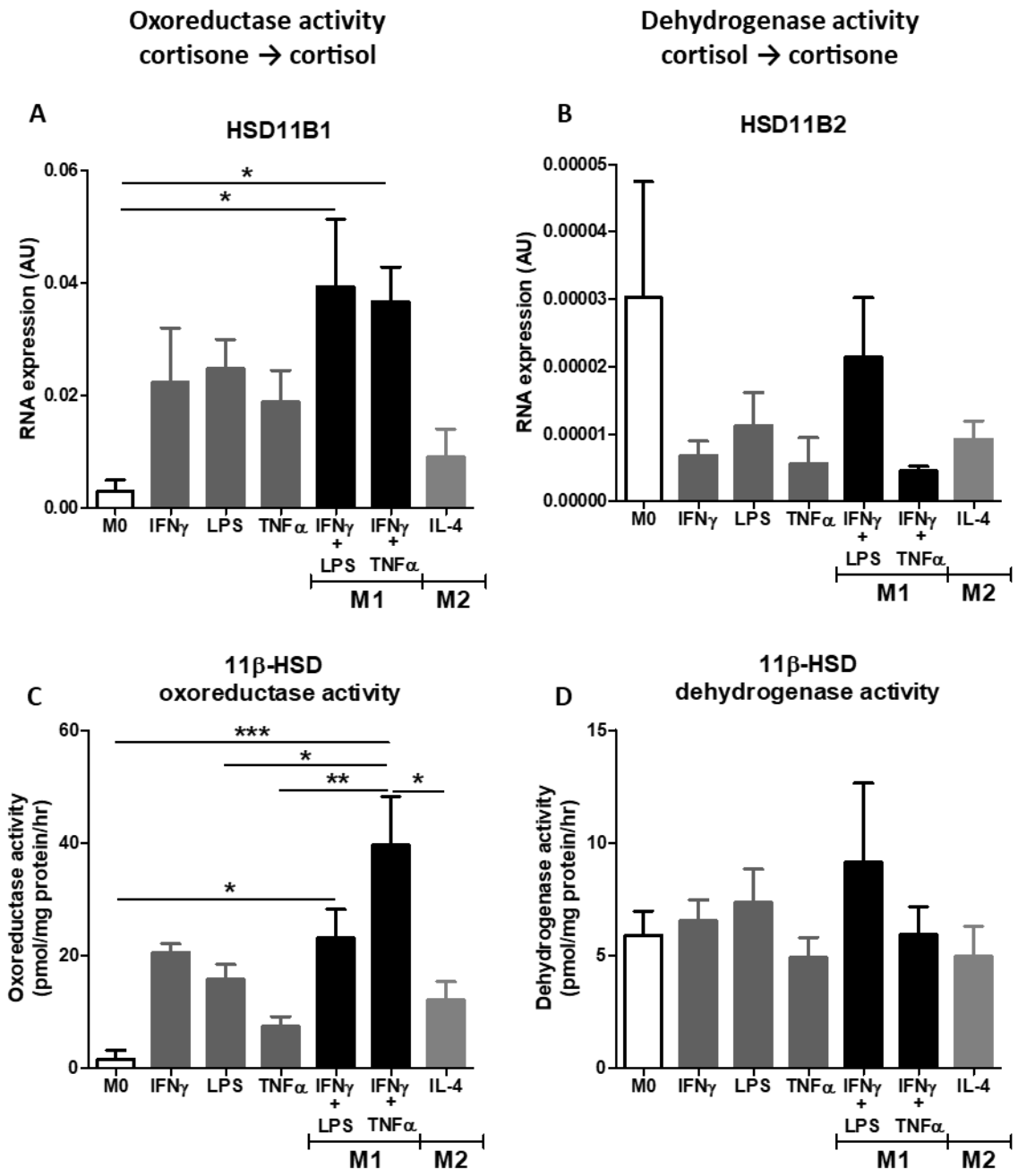

Figure 4-5 Pro-inflammatory polarisation induces 11β-HSD1 gene expression and enzyme activity in macrophages

mRNA expression (AU) of (A) *HSD11B1* and (B) *HSD11B2* measured by qPCR in macrophages polarised for 24h (n=4). 11β-HSD (C) oxoreductase (GC activating) and (D) dehydrogenase (GC inactivating) activity (pmol/mg protein/hr) quantified by scanning TLC assays in macrophages polarised for 48h (n=3). Data are presented as mean ± SEM and statistical significance was determined using one-way ANOVA with Tukey's multiple comparisons test (* p≤0.05, ** p≤0.01, *** p≤0.001).

4.3.3 The 11β-HSD isozymes are further modulated in macrophages by GCs

In order to examine the role of GCs in the inflammatory regulation of the 11β-HSD enzymes in macrophages, we examined expression and activity following M1 and M2 polarisation in combination with treatment with the endogenous GC cortisol (1000 nM) or vehicle during 48h polarisation.

The addition of cortisol downregulated *HSD11B1* gene expression in IFNγ/TNFα (4.6-fold, P≤0.05) and IFNγ/LPS (3.0-fold, P≤0.05) M1-like polarised macrophages compared to those treated with vehicle (Figure 4-6 A). Whilst not significant, a trend towards downregulation in M2 (6.7-fold, P≥0.9999) and M0 (5.0-fold, P≥0.9999) macrophages was also observed in response to cortisol treatment during polarisation (Figure 4-6 A). Conversely, a trend towards increased *HSD11B2* mRNA expression was observed following addition of cortisol during IFNγ/TNFα M1 polarisation (4.0-fold, P=0.9982) and M2 polarisation (3.3-fold, P=0.5687), but not in IFNγ/LPS M1 macrophages or unpolarised M0 macrophages (Figure 4-6 B).

These trends were mirrored in 11β-HSD1 enzyme activity only for IFNγ/TNFα M1 polarised macrophages, where rate of GC activation decreased on cortisol treatment (4.0-fold, P≤0.01) (Figure 4-6 C). In IFNγ/LPS M1 macrophages, there was a trend towards decreased oxo-reductase activity with addition of cortisol, but this was not significant (1.8-fold, P=0.5077). GC-inactivating dehydrogenase activity however was unchanged by cortisol treatment (Figure 4-6 D). This equilibration of cortisol-treated and untreated is likely the result of cortisol being converted by 11β-HSD2 into cortisone, which then fed into 11β-HSD1 to generate further cortisol. Therefore, it is very technically difficult to measure the change in enzyme activity of 11β-HSD by pre-treatment with substrates.

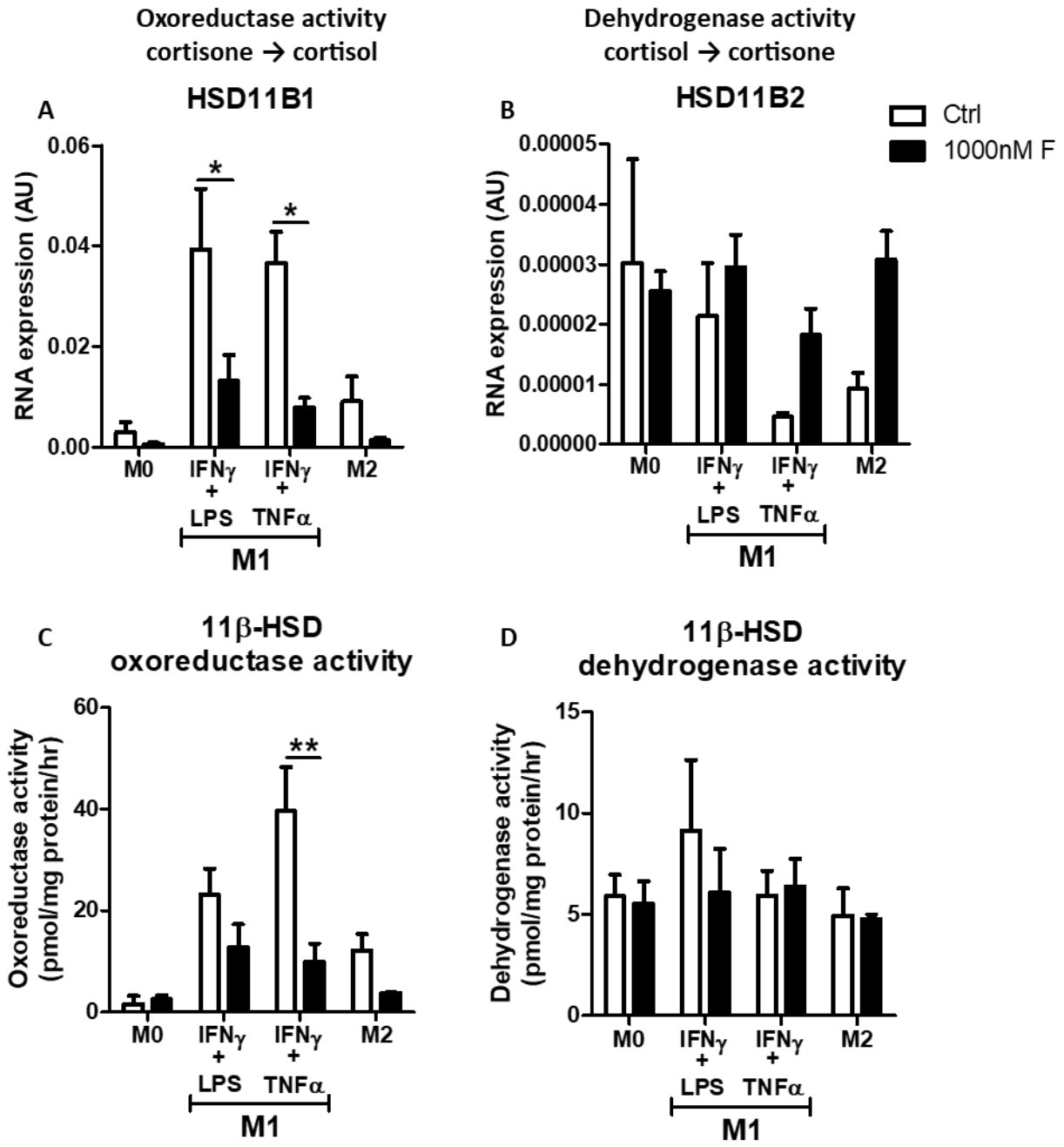

Figure 4-6 Cortisol stimulation downregulates 11β-HSD1 gene expression and enzyme activity

RNA expression (AU) of (A) *HSD11B1* and (B) *HSD11B2* measured by qPCR in macrophages polarised and treated with or without 1000 nM cortisol (F) for 24h (*HSD11B1* n=4; *HSD11B2* n=3, M2 n=2). 11β-HSD (C) oxo-reductase (GC activating) and (D) dehydrogenase (GC inactivating) activity (pmol/mg protein/hr) quantified by scanning TLC assays in macrophages polarised and treated with or without 1000 nM cortisol (F) for 48h (n=3; M2 n=2). Data are presented as mean ± SEM and statistical significance was determined using two-way ANOVA with Bonferroni multiple comparisons post-test (* p≤0.05, ** p≤0.01).

As cortisol downregulated 11β-HSD1 gene expression and activity, we next investigated whether the inactive GC cortisone could have similar effects following its intracrine metabolism and activation. As seen in Figure 4-6 D, pre-treatment with cortisol did not impact 11β-HSD2 activity, likely due to interconversion of cortisone and cortisol between 11β-HSD isozymes complicating the assay. Therefore, we assessed the ability of cortisone to downregulate mRNA expression of the 11β-HSD isozymes compared to cortisol. Macrophages were treated with 1000 nM cortisone during polarisation, and compared to high and low dose cortisol, 1000 nM and 100 nM respectively (Figure 4-7).

As before, high dose cortisol treatment during M1 polarisation dramatically downregulated *HSD11B1* gene expression (8.8-fold, P≤0.05; Figure 4-7 A). However, cortisone treatment did not affect *HSD11B1* expression. Both doses of cortisol upregulated *HSD11B2* expression (control vs 100 nM cortisol: 8.9-fold, P≤0.05; control vs 1000 nM cortisol: 18.6-fold, P≤0.001), while the effect of cortisone treatment again was equivalent to control (Figure 4-7 B). These trends were also seen in M2 polarised macrophages, with a cortisol-induced downregulation of *HSD11B1* and induction of *HSD11B2* however neither of these effects were significant (Figure 4-7 D-E).

We next assessed the effects of the PPARγ-activating compound rosiglitazone on 11β-HSD gene expression, as PPARγ agonists have previously been shown to enhance *HSD11B1* expression and activity, and we hypothesised this could overcome cortisol-induced downregulation of *HSD11B1* expression (293). Treatment with the PPARγ-activating drug rosiglitazone did not affect *HSD11B1* expression in M1 macrophages (Figure 4-7 C). Rosiglitazone treatment appeared to increase *HSD11B1* expression in M2 macrophages (M2

control vs rosiglitazone-treated M2: 3.2-fold, P=0.8453), however this was also not significant (Figure 4-7 F).

These findings suggest a reciprocal regulation of the 11β-HSD enzymes in macrophages; while inflammation upregulates *HSD11B1* expression in macrophages, stimulation with active, but not inactive, GCs downregulates this. Conversely, cortisol treatment upregulates the expression of its inactivating enzyme, *HSD11B2*, in inflammatory macrophages.

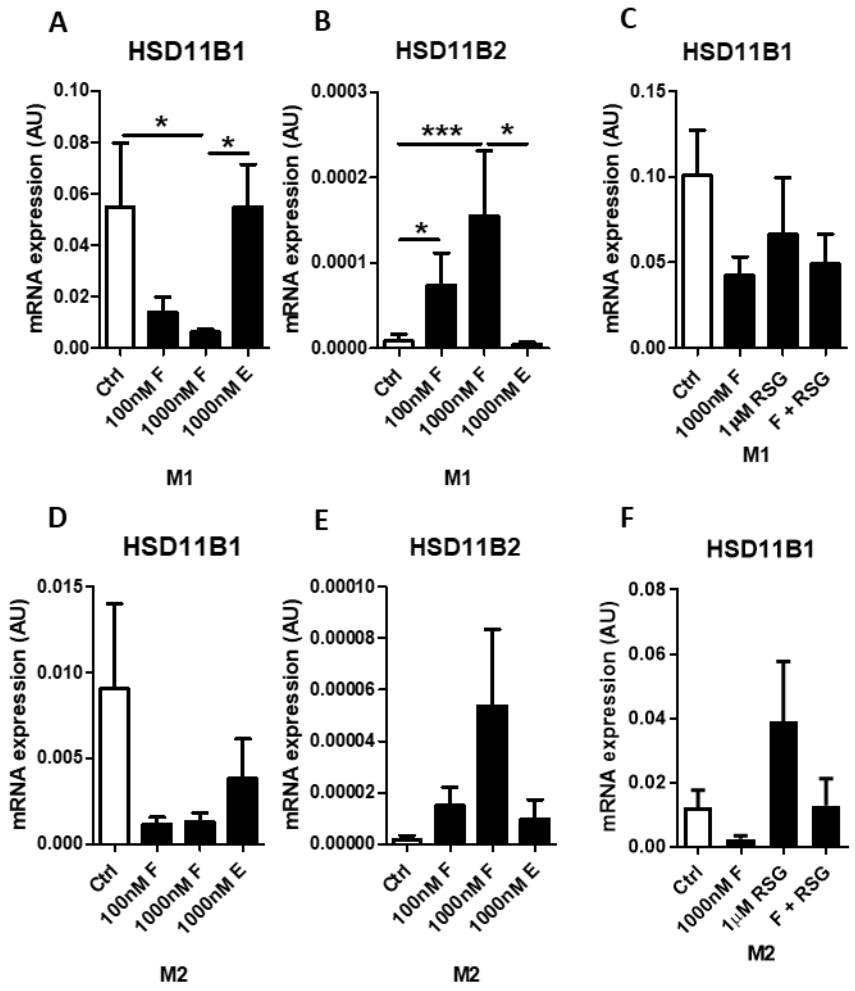

Figure 4-7 Cortisol, but not cortisone, drives reciprocal regulation of 11β-HSD isozymes

mRNA expression (AU) of *HSD11B1* and *HSD11B2* measured by qPCR in (A-B) M1 (IFNγ/LPS) macrophages and (C-D) M2 (IL-4) macrophages untreated (Ctrl) or treated with 100 nM or 1000 nM cortisol (F) or 1000 nM cortisone (E) for 24h (n=4). The effect of 1μM rosiglitazone (RSG) treatment during 24h polarisation with and without 1000 nM cortisol (F) on *HSD11B1* expression was assessed in (C) M1 (IFNγ/LPS) macrophages and (F) M2 (IL-4) polarised macrophages (n=3). Data are presented as mean ± SEM and statistical significance was determined using one-way ANOVA with Tukey's multiple comparisons test (* p≤0.05, *** p≤0.001).

4.3.4 GC pre-receptor metabolism regulation in alveolar macrophages as a tissue resident macrophage population

In order to assess whether the inflammation-induced upregulation of GC pre-receptor metabolism was present in macrophage populations aside from our blood monocyte-derived culture model, we investigated the expression of *HSD11B1* and *GILZ* in human alveolar macrophages (Figure 4-8).

Inflammatory polarisation of alveolar macrophages with LPS showed a trend towards upregulation of *HSD11B1* compared to M0 macrophages, although significance could not be assessed due to low sample size for M0 macrophages (Figure 4-8 A). There was also a trend towards downregulation of *HSD11B1* when M1 alveolar macrophages were treated with increasing concentrations of cortisol (control vs 100 nM cortisol: 2.1-fold, P=0.7336; control vs 1000 nM cortisol: 3.4-fold, P=0.5198), but not cortisone (control vs 1000 nM cortisone P=.09874; Figure 4-8 B). Similarly, the GC-inducible gene *GILZ* was slightly upregulated by GCs (control vs 100 nM cortisol: 4.9-fold, P=0.6328; control vs 1000 nM cortisol: 5.1-fold, P=0.6066), but again this was not significant (Figure 4-8 C).

These findings suggest that alveolar macrophages may have a similar reciprocal regulation of 11β-HSD1 by inflammatory activation and GC stimulation as seen with blood monocyte-derived macrophages, however there was considerable variability between the patient samples these cells were isolated from.

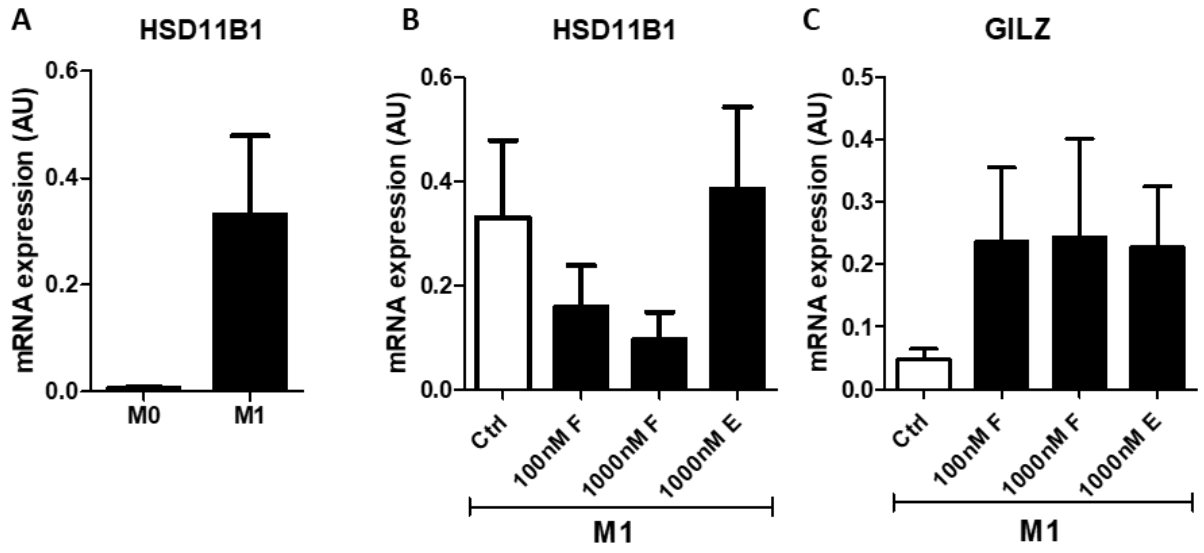

Figure 4-8 GC pre-receptor metabolism by 11β-HSD1 may be upregulated by inflammation and downregulated by cortisol in alveolar macrophages

RNA expression (AU) of (A) *HSD11B1* in alveolar macrophages unpolarised (M0) or M1-like polarised (LPS) for 24h as measured by qPCR (M0 n=2, M1-like n=3). RNA expression of (A) *HSD11B1* and (B) *GILZ* in alveolar macrophages polarised to M1 and untreated (Ctrl) or treated with 100 nM or 1000 nM cortisol (F) or 1000 nM cortisone (E) during 24h polarisation (n=3). Data are presented as mean ± SEM and statistical significance was determined using paired Student's t-test (A) or one-way ANOVA with Tukey's multiple comparisons test (B-C).

4.3.5 The functional effects of GC metabolism and activation on macrophage polarisation

Having characterised an inflammation-induced upregulation of 11β-HSD1 expression and activity in M1 inflammatory macrophages, we next investigated the functional effects of GC activation by 11β-HSD1 on acquisition of a polarised state by macrophages. To examine this, we treated macrophages with or without 1000 nM cortisone or cortisol during M1 or M2 polarisation (Figure 4-9).

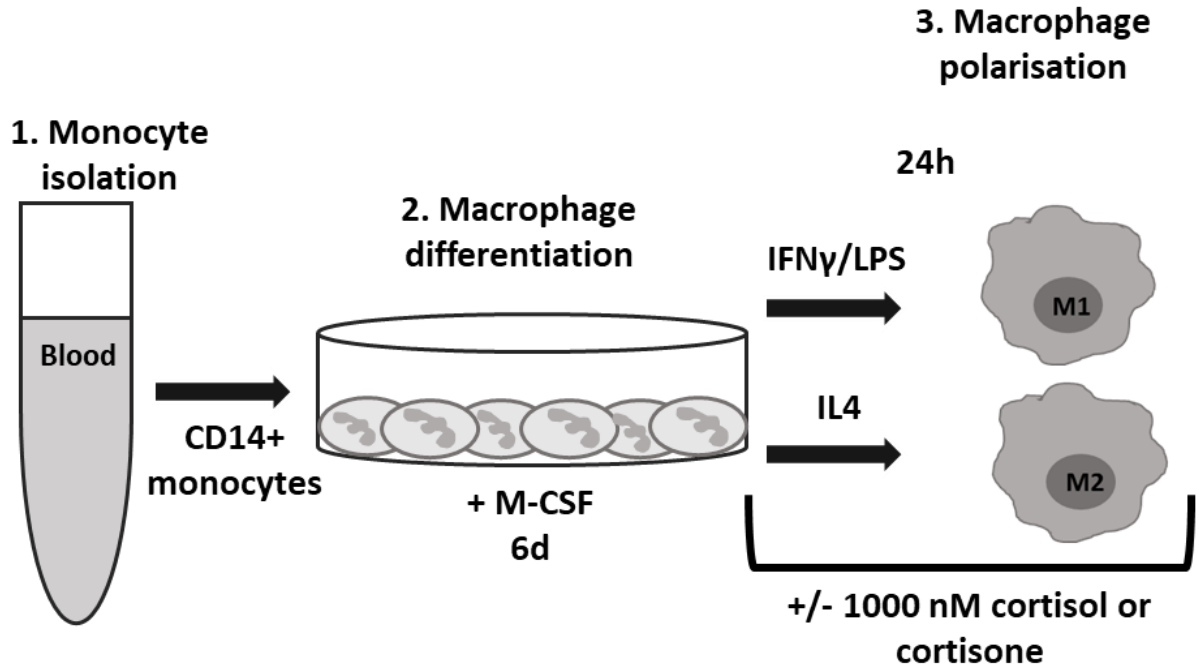

Figure 4-9 Schematic for analysis of GC stimulation during macrophage polarisation

1. Monocyte isolation – CD14+ monocytes isolated directly from whole blood with RosetteSep™ kit. 2. Macrophage differentiation – isolated monocytes differentiated into macrophages with d6 M-CSF treatment, with media changes on d2 and d5. 3. Macrophage polarisation – mature differentiated macrophages are polarised for 24h into M1 macrophages (20 ng/ml IFNγ and 10 ng/ml LPS) or M2 macrophages (20 ng/ml IL-4) with concurrent treatment with 1000 nM cortisol or cortisone or vehicle.

The mRNA expression of key genes involved in GC signalling metabolism were assessed following 24h polarisation, with or without cortisone or cortisol: the GRα gene *NR3C1*, the GC-responsive anti-inflammatory transcription factor *GILZ*, and the enzyme which generates the 11β-HSD1 cofactor NADPH, *H6PDH* (Figure 4-10). *NR3C1* and *H6PDH* expression were unaffected by GC treatment in M1 macrophages (Figure 4-10 A, C). Both cortisol and cortisone treatment increased *GILZ* expression in M1 macrophages compared to control, however the induction of *GILZ* was greater with cortisol (control vs cortisol: 7.0-fold, P≤0.001; cortisol vs cortisone: 1.7-fold, P≤0.05) than with cortisone (control vs cortisone: 4.1-fold, P≤0.001) (Figure 4-10 B). Although GC treatment appeared to decrease expression of *NR3C1* and *H6PDH*

in M2 macrophages, these changes were not significant (Figure 4-10 D, F). In M2 macrophages, cortisol and cortisone treatment similarly increased *GILZ* expression, with a greater induction again seen with cortisol (control vs cortisol: 8.1-fold, P≤0.001; cortisol vs cortisone: 2.4-fold, P≤0.05) than cortisone (control vs cortisone: 3.4-fold, P≤0.05) (Figure 4-10 E). These data confirm that our macrophage cultures are GC-sensitive, as shown by upregulation of the anti-inflammatory GC responsive gene *GILZ*.

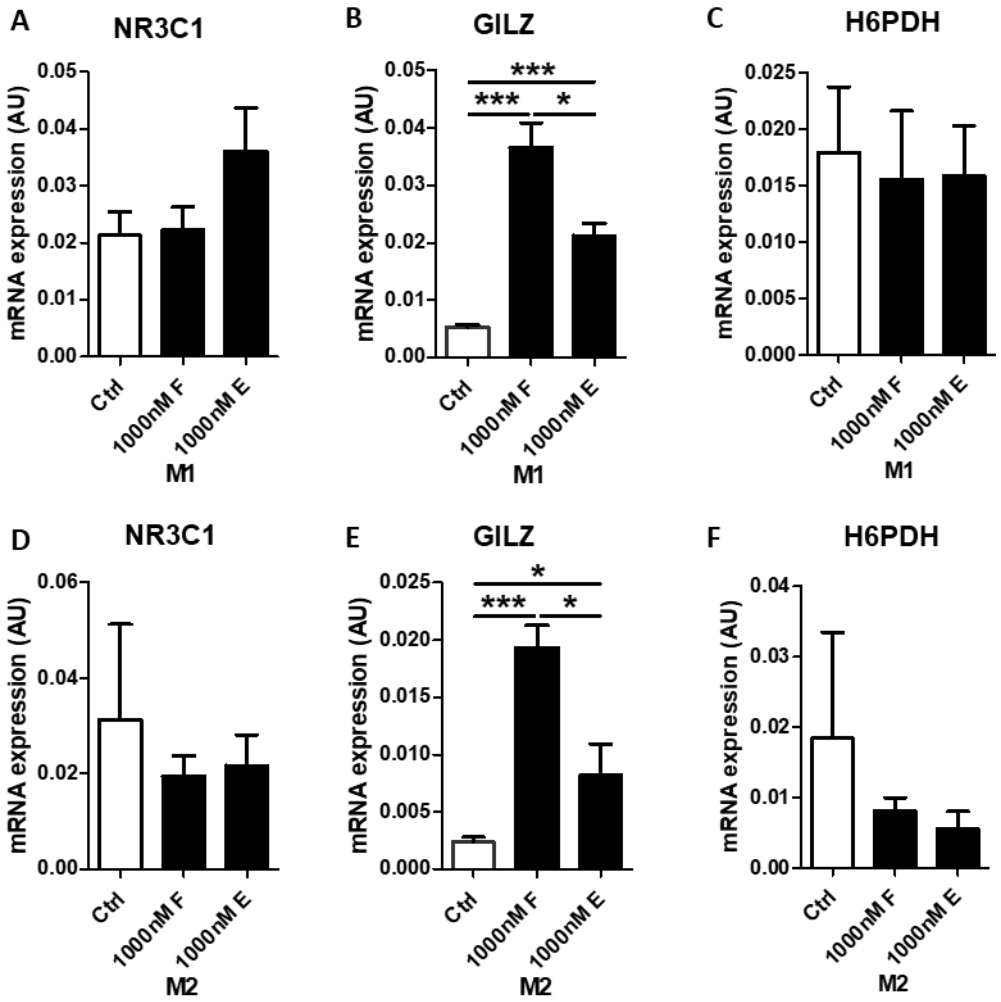

Figure 4-10 Glucocorticoid treatment upregulates GILZ but not other genes involved in glucocorticoid metabolism

RNA expression (AU) of (A) *NR3C1*, (B) *GILZ* and (C) *HDPDH* measured by qPCR in M1 (IFNγ/LPS) macrophages and M2 (IL-4) macrophages untreated (Ctrl) or treated during polarisation with 1000 nM cortisol (F) or 1000 nM cortisone (E) for 24h (n=4). Data are presented as mean ± SEM and statistical significance was determined using one-way ANOVA with Tukey's multiple comparisons test (* p≤0.05, *** p≤0.001).

4.3.5.1 The functional effects of GC metabolism and activation in M1 macrophages

The effect of GC treatment on acquisition of pro-inflammatory profiles was assessed by treating M1 macrophages with 1000 nM cortisol or cortisone during polarisation with IFNγ and LPS (Figure 4-11).

Whilst a marked downregulation of both *TNFα* and *IL-6* mRNA was observed in response to cortisol treatment, these were not significant (*TNFα* control vs cortisol: 5.6-fold, P= 0.0593; *IL-6* control vs cortisol: 2.7-fold, P= 0.1744) (Figure 4-11 A, B). Similarly, there was a trend towards decreased expression of the anti-inflammatory cytokine *IL-10* with cortisol treatment (control vs cortisol: 3.1-fold, P=0.4070) (Figure 4-11 C). Cortisol treatment increased expression of the pro-resolution scavenger receptor *CD163* (control vs cortisol: 10.4-fold, P≤0.01), however again cortisone had no effect compared to control (Figure 4-11 D). Expression of the high affinity IgG receptor *CD64* saw a nonsignificant increase with both cortisol (2.0-fold, P=0.0795) and cortisone (1.8-fold, P=0.1274) compared to control (Figure 4-11 E).

In contrast to gene expression, concurrent treatment with cortisol or cortisone during M1 polarisation significantly reduced secretion of the pro-inflammatory cytokine TNFα (control vs cortisol: 125.9-fold, P≤0.001; control vs cortisone: 16.3-fold, Figure 4-11 F). Secretion of the pro-inflammatory cytokine IL-12 p70 showed a trend towards decrease on treatment with both cortisol (25.5-fold, P=0.4510) and cortisone (11.7-fold, P=0.5759) compared to M1 polarised only, however this was not significant (Figure 4-11 G). As seen with gene expression, secretion of the anti-inflammatory cytokine IL-10 showed a slight decrease on cortisol

treatment compared to polarised only (5.5-fold, P=0.2079) (Figure 4-11 H). It was not possible to examine IL-6 cytokine secretion or *IL-12A (p35)* expression in these cells.

Together these data show that treatment with active cortisol impedes full acquisition of macrophage M1-like pro-inflammatory profiles, with induction of scavenger receptor *CD163* as previously reported (419). Cortisone treatment during polarisation had no effect on gene expression, likely due to the timepoint of treatments not allowing for sufficient conversion and GC-response. Nevertheless, cortisone was able to significantly decrease secretion of the potent pro-inflammatory cytokine TNFα, a key feature of inflammatory M1 macrophages.

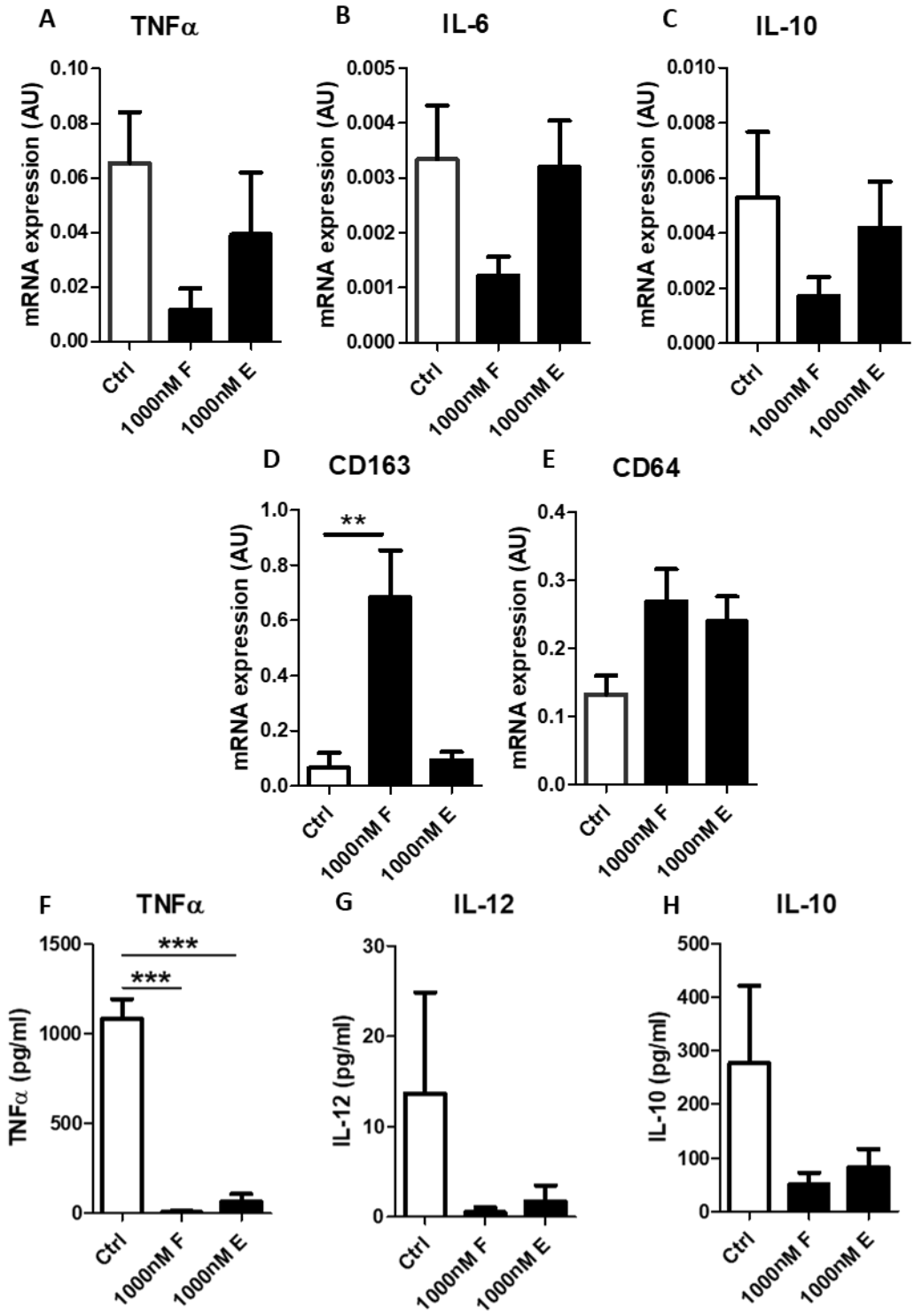

Figure 4-11 GC treatment during polarisation attenuates M1 pro-inflammatory profiles

RNA expression (AU) of (A) *TNFα*, (B) *IL-6*, (C) *CD64*, (D) *CD163* and (E) *IL-10* measured by qPCR, and cytokine concentration (pg/ml) of (F) TNFα, (G) IL-12 p70 and (H) IL-10 quantified by ELISA in M1 macrophages (IFNγ and LPS) untreated (Ctrl) or treated 1000 nM cortisol (F) or 1000 nM cortisone (E) for 24h during polarisation (qPCR n=4, ELISA n=3). Data are presented as mean ± SEM and statistical significance was determined using one-way ANOVA with Tukey's multiple comparisons test (* p≤0.05, *** p≤0.001).

4.3.5.2 The functional effects of GC metabolism and activation in M2 macrophages

The effect of GC treatment on expression of these polarisation-associated markers was then assessed to determine whether they would promote a similar more pro-resolution phenotype in more anti-inflammatory M2 macrophages (Figure 4-12).

Cortisol and cortisone treatment during polarisation both significantly downregulated *TNFα* expression in M2 macrophages, with a more potent decrease seen with cortisol (10.8-fold, P≤0.01) than cortisone (3.9-fold, P≤0.05) compared to control (Figure 4-12 A). GC treatment had no effect on *IL-6* expression (Figure 4-12 B). A trend towards increased *IL-10* expression was observed with cortisol treatment compared to both control (3.3-fold, P=0.0737) and cortisone treatment (2.4-fold, P=0.2926) (Figure 4-12 C). As in M1 macrophages, *CD163* expression was induced by cortisol, and here this was significantly higher than both control (5.3-fold, P≤0.01) and cortisone (4.9-fold, P≤0.05) treatment (Figure 4-12 D). There was no effect of GC treatment on *CD64* expression, save for a nonsignificant decrease in expression with cortisol (2.2-fold, P=0.7402) (Figure 4-12 E). Within M2 macrophages, GC treatment had no significant effect on TNFα or IL-12 p70 release, in line with their limited baseline secretion of these cytokines (Figure 4-12 F, G). There was a trend towards increase in release of IL-10 by cortisol treated M2 macrophages compared to control (1.8-fold, P=0.3178) and cortisone treatment (3.0-fold, P=0.1013), however this was not statistically significant (Figure 4-12 H).

Together these data show that GCs can help to promote the acquisition of a pro-resolution anti-inflammatory profile during M2 polarisation, via decrease in TNFα gene expression. However, as with M1 macrophages, cortisol had greater effects than cortisone during polarisation, as seen with a cortisol-induced increase in *CD163* expression

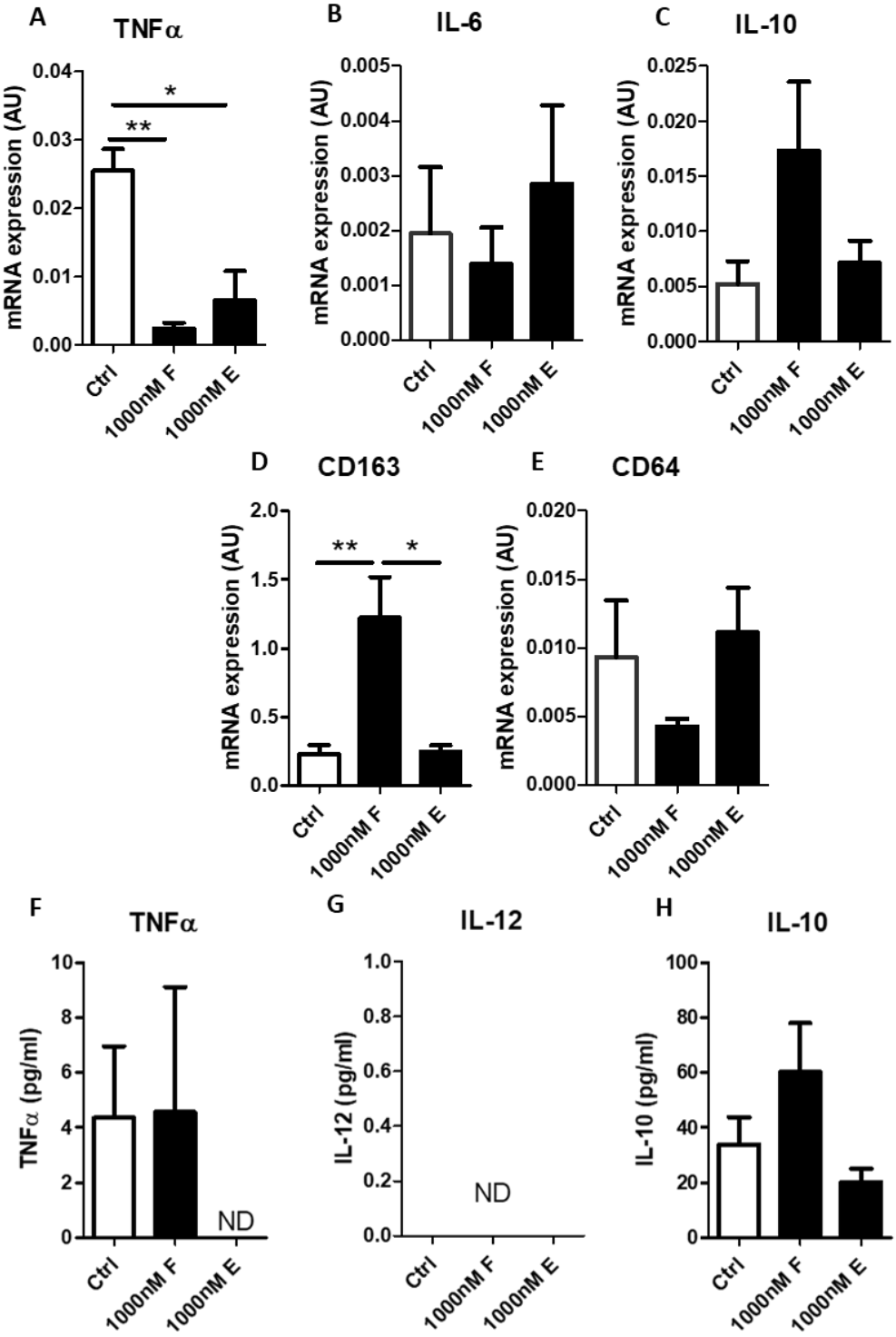

Figure 4-12 GC treatment augments acquisition of anti-inflammatory pro-resolution profile during M2 polarisation

RNA expression (AU) of (A) *TNFα*, (B) *IL-6*, (C) *CD64*, (D) *CD163* and (E) *IL-10* measured by qPCR, and cytokine concentration (pg/ml) of (F) TNFα, (G) IL-12 p70 and (H) IL-10 quantified by ELISA in M2 macrophages (IL-4) untreated (Ctrl) or treated 1000 nM cortisol (F) or 1000 nM cortisone (E) for 24h during polarisation (qPCR n=4, ELISA n=3). Data are presented as mean ± SEM and statistical significance was determined using one-way ANOVA with Tukey's multiple comparisons test (* p≤0.05, ** p≤0.01).

4.3.5.3 The functional effects of GCs on M2 macrophage phagocytosis

Phagocytosis is a key macrophage function known to be positively regulated by GCs, including via pre-receptor metabolism by 11β-HSD1 (278). We tested the effects of M2 polarisation, as these cells are known to possess phagocytic capabilities in line with their roles in tissue remodelling and resolution of inflammation. These cells were treated with cortisol, prior to testing inactive cortisone, as this was expected to give additive effects on phagocytosis (Figure 4-13) (111).

M2 macrophages were seen to phagocytose fluorescently-labelled *E. coli* particles, however cortisol treatment during polarisation did not enhance this and instead a nonsignificant decrease in phagocytosis was seen (1.7-fold, P=0.1565, Figure 4-13 A). We calculated an estimate of beads phagocytosed by macrophages by measuring fluorescence intensity of diluted beads and plotting the fluorescence intensity of M2 macrophages with and without cortisol (Figure 4-13 B). This suggested that less than 10% of the beads in each well were being phagocytosed by macrophages. These data imply that in this experimental setup phagocytosis was not affected by cortisol and therefore this setup was not suitable to examine regulation of this function by GC metabolism.

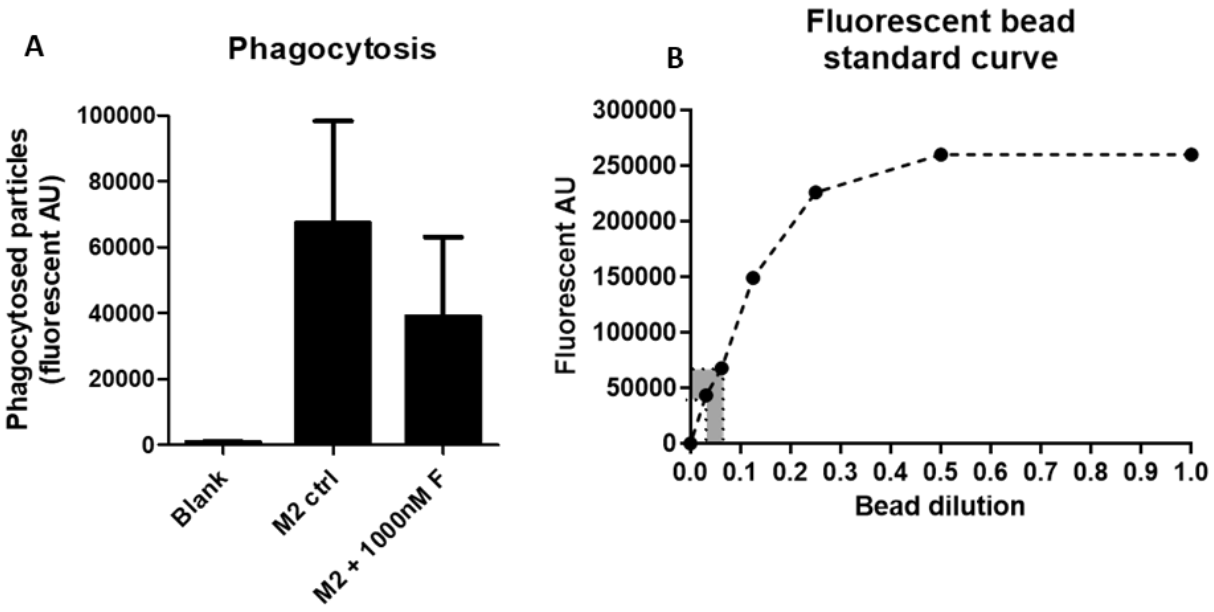

Figure 4-13 Cortisol did not have an effect on macrophage phagocytosis of *E. coli* particles

(A) Fluorescence intensity of FITC-labelled *E. coli* particles (AU) taken up by M2 (IL-4) polarised macrophages untreated (Ctrl) or treated with 1000 nM cortisol (F) (n=3). (B) Standard curve of fluorescence intensity (AU) of fluorescent bead dilutions, dotted lines and grey shading show average intensity of fluorescence from beads phagocytosed by macrophages (M2 control = 6,7344.27 AU; M2 + 1000 nM cortisol = 3,8849.42 AU) to calculate proportion of phagocytosed beads. Data are presented as (A) mean ± SEM or (B) individual datapoints and statistical significance was determined using Student's paired t-test to compare M2 polarised with M2 polarised treated with cortisol (A).

4.3.5.4 The functional effects of GC metabolism on macrophage viability

One of the most potent immunosuppressive effects GCs exert on immune cells is promotion of apoptosis in populations such as T and B cells (220-222). In order to confirm that the GC-induced decreases in pro-inflammatory profiles seen in our macrophages was not due to loss of cell viability, we measured viability and apoptosis in M0 and M1-like macrophages treated with 1000 nM cortisol or cortisone during 24h polarisation (Figure 4-14). GC treatment was not seen to have any effect on either viability (Figure 4-14 A) or apoptosis (Figure 4-14 B) of macrophages at the doses explored in this study.

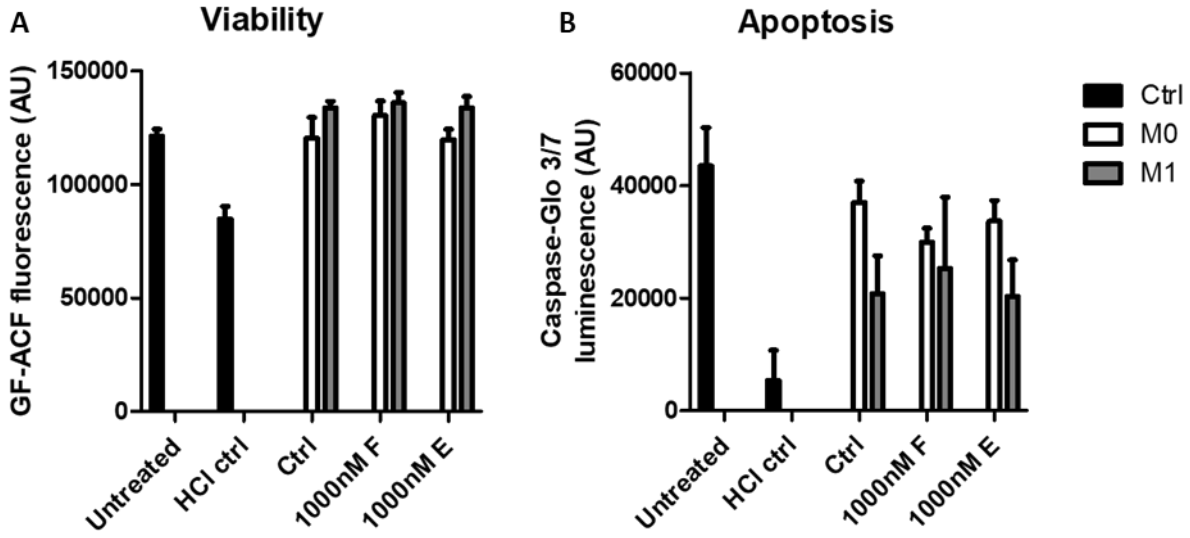

Figure 4-14 Downregulation of M1 macrophage pro-inflammatory profiles by glucocorticoids is not caused by loss of cell viability

(A) Cell viability as quantified by GF-AFC fluorescence (AU) and (B) apoptosis as quantified by Caspase-Glo 3/7 luminescence (AU) in untreated or 10mM HCl treated (HCl ctrl) M0 macrophages and M0 and M1-like (IFNγ and TNFα) polarised macrophages (Ctrl) treated with 1000 nM cortisol (F) or cortisone (E), using an ApoLive-Glo multiplex assay (n=3). Data are presented as mean ± SEM and statistical significance was determined using two-way ANOVA with Bonferroni's multiple comparisons test.

4.3.6 Pre-receptor metabolism of cortisone regulates inflammatory function of macrophages on subsequent inflammatory challenge

Simultaneous inflammatory polarisation and cortisone treatment likely didn't result in negative regulation of inflammatory profiles in M1 macrophages, as there was not sufficient time for inflammation-induced upregulation of 11β-HSD1 to metabolise inactive GCs. In order to assess the impact of pre-receptor metabolism of cortisone by 11β-HSD1 on macrophage inflammatory function, we tested the effect of cortisone treatment on inflammatory output of differentially polarised macrophages subjected to subsequent LPS inflammatory challenge (Figure 4-15).

Unpolarised M0 macrophages were compared to M1-like polarised with IFNγ and TNFα as these had been shown to possess the lowest and highest levels of *HSD11B1* mRNA expression (Figure 4-5 A; M0 v IFNγ/TNFα-polarised: 12.7-fold, $P \leq 0.05$) and enzyme activity respectively (Figure 4-5 C; M0 v IFNγ/TNFα-polarised: 25-fold, $P \leq 0.001$). Using IFNγ/TNFα-polarised allowed us to compare the response of LPS-naïve M0 and M1-like macrophages to acute LPS challenge to assess regulation of inflammatory function.

It was predicted that only the pro-inflammatory M1-like polarisation would drive sufficient 11β-HSD1 expression and activity to metabolise cortisone into active GCs and downregulate inflammatory responses on LPS challenge, compared to unpolarised M0 macrophages and M1 macrophages not treated with cortisone.

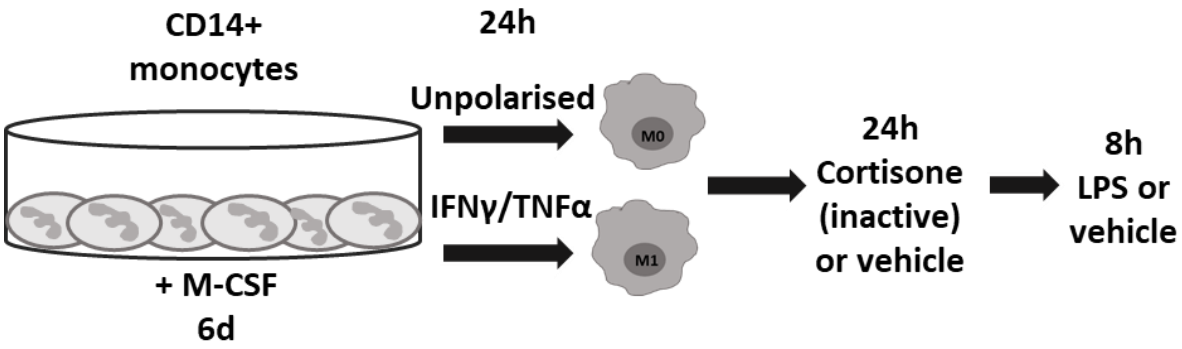

Figure 4-15 Schematic for analysis of regulation of inflammatory function by cortisone in an LPS challenge model

CD14+ monocytes isolated from whole blood by RosetteSep™ kit were differentiated into macrophages by 6d incubation with 20 ng/ml M-CSF. Macrophages were polarised into M0 unpolarised cells (untreated) or pro-inflammatory M1 (IFNγ and TNFα) for 24h. Medium was changed, and polarised cells were treated with 1000 nM cortisone (E) or vehicle for 24h. Then cells were treated with 10 ng/ml LPS for 8h and RNA and supernatants collected.

The gene expression of key pro-inflammatory cytokines and the pro-resolution scavenger receptor *CD163* was assessed by qPCR analysis of differentially polarised macrophages, treated with cortisone, and then stimulated with LPS for 8h (Figure 4-16).

As expected, since M0 unpolarised macrophages were previously shown to have very little *HSD11B1* expression (Figure 4-5 A), cortisone treatment prior to LPS stimulation of M0 macrophages had no impact on their expression of inflammatory cytokines compared to LPS treatment without cortisone (Figure 4-16 A-C). In IFNγ/TNFα M1-like polarised macrophages, there was a trend towards reduction of inflammatory cytokine gene expression in LPS-stimulated cells pre-treated with cortisone compared to LPS only, however these comparisons were not significant (*TNFα* LPS v cortisone/LPS: 2.6-fold, P=0.0594; *IL-6* LPS v cortisone/LPS, 4.2-fold, P=0.2772; *IL-12A* LPS v cortisone/LPS: 4.6-fold, P=0.7317; Figure 4-16 A-C). Although expression appeared blunted by cortisone treatment, the levels of *TNFα*, *IL-6* and *IL-12A* gene

expression were still higher than polarised-only controls. However, cortisone pre-treatment of LPS stimulated M1 macrophages was able to significantly upregulate the pro-resolution scavenger receptor *CD163* compared to LPS only treatment (14.0-fold, P≤0.05; Figure 4-16 D).

These data show that cortisone metabolism by 11β-HSD1 in M1-polarised cells may help to regulate pro-inflammatory gene expression on subsequent inflammatory challenge, however the stimulation timepoints chosen may not be the optimal time for capture of these effects at their greatest intensity.

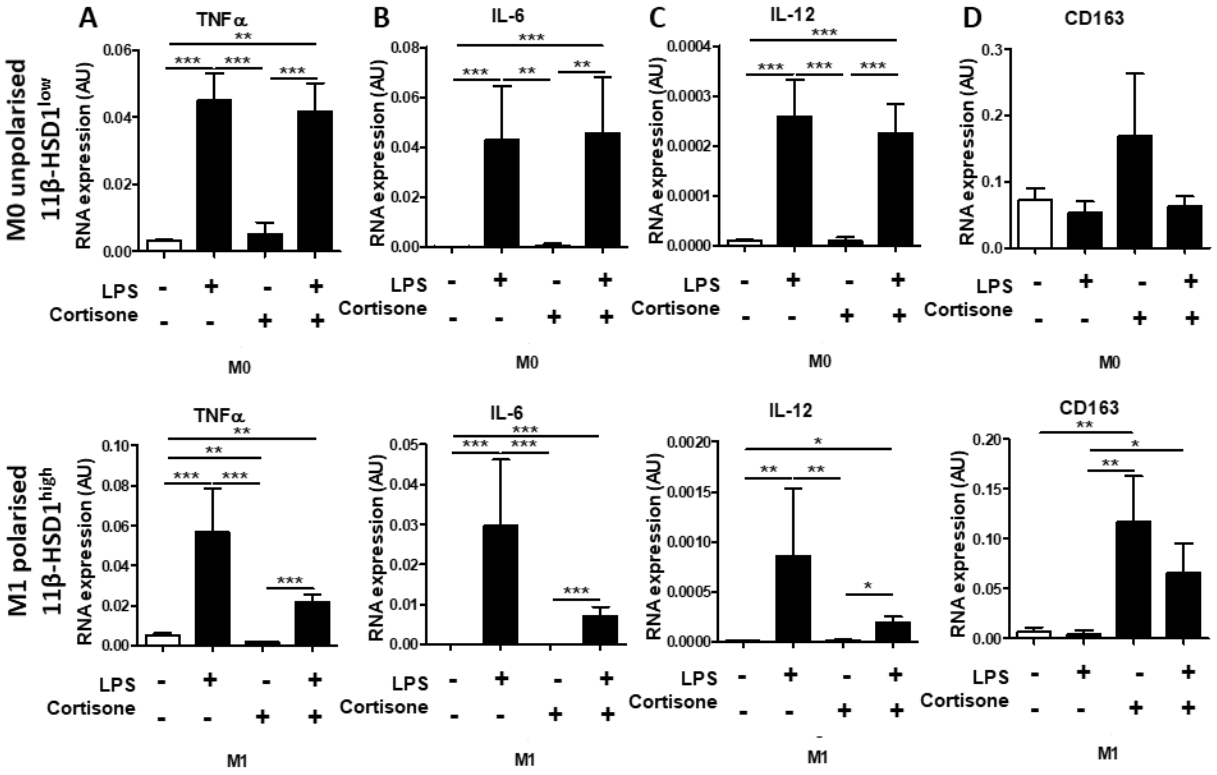

Figure 4-16 Pre-receptor metabolism of glucocorticoids regulates inflammatory gene expression in M1 macrophages

Macrophages were polarised for 24h into M0 unpolarised or IFNγ/TNFα M1-like macrophages, then treated with cortisone for 24h before 8h LPS stimulation. mRNA expression (AU) of (A) *TNFα*, (B) *IL-6*, (C) *IL-12A* and (D) *CD163* measured by qPCR (n=5, cortisone only n=4). Data are presented as mean ± SEM and statistical significance was determined using one-way ANOVA with Tukey's multiple comparisons test (* p≤0.05, ** p≤0.01, *** p≤0.001).

We then investigated the cytokine output of these cells, assessing production of the pro-inflammatory cytokines TNFα, IL-6 and IL-12 p70 by cortisone pre-treated M0 and M1-like macrophages challenged with LPS (Figure 4-17). As before, cortisone pre-treatment made no difference to the cytokine output of LPS stimulated M0 macrophages (Figure 4-17 A-C). M1-like macrophages however, produced significantly less TNFα (1.8-fold, LPS v cortisone/LPS $P \leq 0.001$; Figure 4-17 A) and IL-6 (2.9-fold, LPS v cortisone/LPS $P \leq 0.05$; Figure 4-17 B) on LPS stimulation when pre-treated with cortisone than those simulated with LPS without pre-treatment. Additionally, there was a trend towards decreased IL-12 p70 secretion from LPS treated M1-like macrophages that had been pre-treated with cortisone compared to those only stimulated with LPS (LPS v cortisone/LP: 1.6-fold, $P=0.2243$), however this was not significant (Figure 4-17 C).

These data show that GC pre-receptor metabolism is not only upregulated on inflammatory polarisation of macrophages, but that it also allows the metabolism of inactive cortisone to negatively regulate the inflammatory profiles of these cells on subsequent inflammatory challenge.

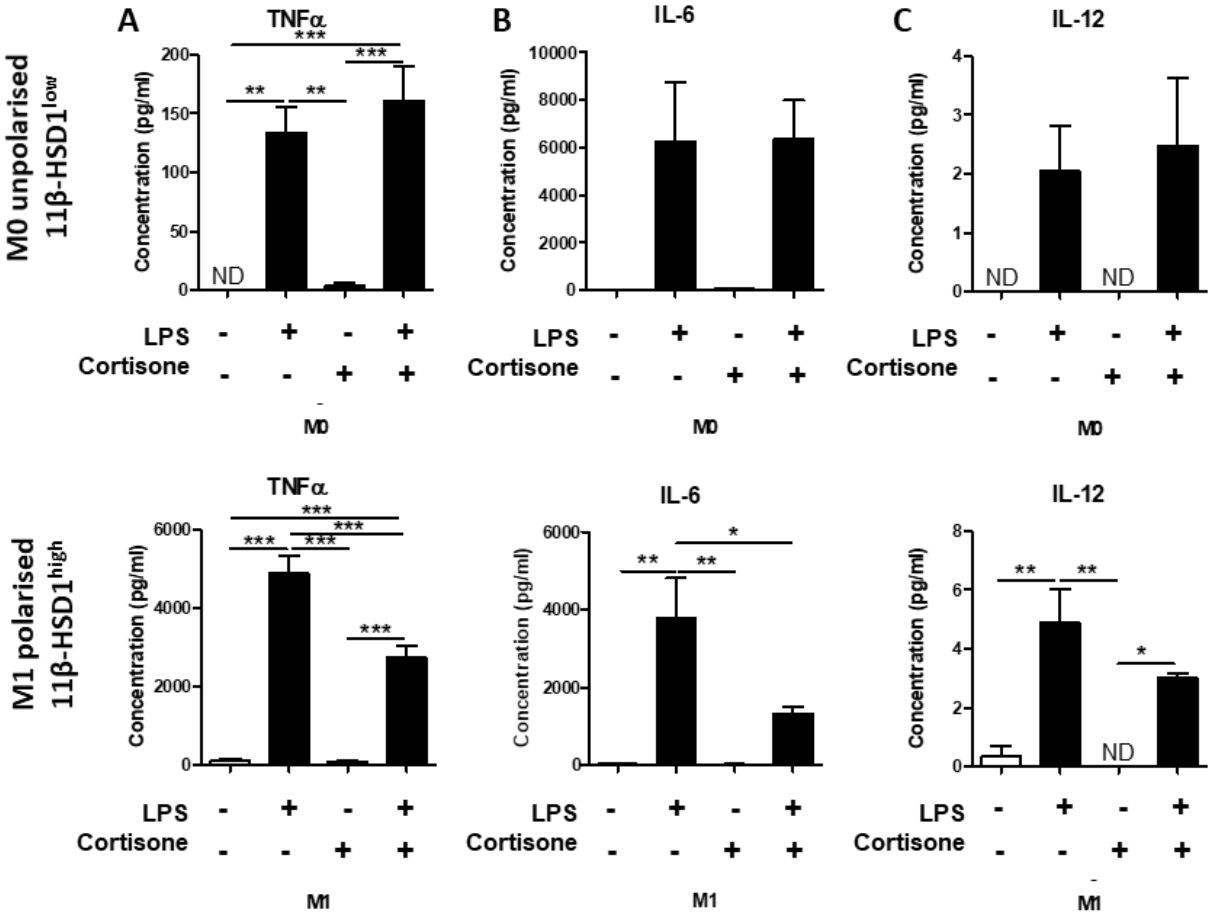

Figure 4-17 Pre-receptor metabolism of glucocorticoids regulates inflammatory cytokine production in M1 macrophages

Macrophages were polarised for 24h into M0 unpolarised or IFNγ/TNFα M1-like macrophages, then treated with cortisone for 24h before 8h LPS stimulation. Supernatants were assessed by ELISA to measure cytokine production (pg/ml): (A) TNFα, (B) IL-6 and (C) IL-12 p70 (n=5, cortisone only n=4). Data are presented as mean ± SEM and statistical significance was determined using one-way ANOVA with Tukey's multiple comparisons test (* p≤0.05, ** p≤0.01, *** p≤0.001). ND, not detected.

4.4 Discussion

RA synovial steroid metabolism profiles, assessed in Chapter 3, suggested that intracrine and paracrine metabolism of GCs and androgens by macrophages was more important to their function and impact on disease activity than contributions to tissue level steroid levels. Our group has previously explored paracrine GC signalling via 11β-HSD1 between macrophages and fibroblasts. Using conditioned media treatments of in vitro cell cultures, we found that loss of 11β-HSD1 by genetic knockout in fibroblasts could be compensated for by generation of active GCs by macrophages, resulting in downregulation of inflammatory fibroblast cytokine secretion. However, myeloid, but not mesenchymal, *Hsd11b1* knockout TNF-tg mice had worse disease than *Hsd11b1*-competent TNF-tg mice when treated with active corticosterone (290). Therefore, the GC-mediated regulation of inflammation in myeloid cells could not be fully compensated for by stromal cell paracrine signalling. We therefore investigated the role of intracrine GC activation by 11β-HSD1 in macrophages using in vitro cultures, which allowed us to focus solely on macrophages, and not other LysM+ populations affected by myeloid-targeting knockouts such as neutrophils (299).

Macrophages have previously been found to upregulate the expression and activity of 11β-HSD1 on inflammatory stimulation and polarisation, however there are conflicting reports of more anti-inflammatory factors, such as the M2 polarising cytokine IL-4, driving greater 11β-HSD1 induction than pro-inflammatory factors in myeloid cells (104, 273, 291). Additionally, many of these earlier studies used murine-derived macrophages or macrophage cell lines, which may respond differently to inflammatory stimulation compared with human macrophages.

We therefore investigated whether the inflammation-induced upregulation of 11β-HSD1 that we found in human RA synovial macrophages (Chapter 3) was also present in polarised human blood monocyte-derived macrophages, and whether intracrine activation of GCs by this enzyme served to regulate inflammatory functions. *HSD11B1* gene expression and cortisol generating activity were significantly increased in "classically" polarised M1 macrophages (IFNγ and LPS) and also in M1-like macrophages generated from IFNγ and TNFα (Figure 4-5), which have previously been reported to possess potent pro-inflammatory and anti-microbial functions (109, 418, 420). IFNγ and TNFα are key pro-inflammatory cytokines found in the synovium of RA patients, and are linked with intensity of synovitis (421). This supports our findings in the AMP bulk RNA-seq study, where increasing inflammation, both at the local synovial level as measured by leukocyte infiltration and at the systemic level with DAS28-CRP, induces higher expression of *HSD11B1* in macrophages.

We did not find significant induction of 11β-HSD1 expression or activity on M2 polarisation (Figure 4-5), conflicting with some earlier findings in monocyte-derived macrophages where IL-4 polarisation induced the highest expression of *HSD11B1* (273, 293). However, both of these studies treated isolated monocytes directly with IL-4 to drive M2 macrophage polarisation, rather than having temporally separated macrophage differentiation and stimulation stages. This likely represents a cell context specific regulation of 11β-HSD1 in macrophages and monocytes, with this method of differentiating macrophages from monocytes with concurrent cytokine stimulation perhaps driving a more monocyte-like cell rather than a macrophage. We also saw similar trends in inflammatory-activated alveolar macrophages (Figure 4-8), suggesting a conserved response across sites in tissue macrophages.

Reports of the regulation of the 11β-HSD enzymes by GCs in macrophages were not found in the literature. In stromal cells, simultaneous stimulation with inflammatory factors and GCs, such as TNFα and dexamethasone in fibroblasts and osteoblasts, additively increases 11β-HSD1 expression and activity (284, 285). However, we found that addition of cortisol during macrophage inflammatory polarisation significantly decreased *HSD11B1* expression, and also decreased cortisol generating oxo-reductase enzyme activity in IFNγ/TNFα M1-like polarised macrophages (Figure 4-6). This GC-induced downregulation is to be expected as osteoclasts, which like macrophages are myeloid-derived, show a similar inflammation-induced upregulation and GC-induced downregulation of 11β-HSD1 (282). This has important implications for our aim to target GCs more specifically to macrophages via 11β-HSD1 as it suggests that active GCs generated by macrophage metabolism of targeted inactive GCs will not lead to a positive feedback loop of GC generation and thus further harmful actions of GCs on off-target cells such as osteoblasts and myocytes.

Our findings on the effects of polarisation and GC treatment on *HSD11B2* expression are less clear, as we did not find significant changes in expression or activity of 11β-HSD2 when assessing macrophage polarisation and high dose cortisol treatment (Figure 4-6), however we did find a significant induction of *HSD11B2* in M1 (IFNγ/LPS) macrophages when assessing a cortisol dose response (Figure 4-7 B). Despite previous reports in the literature identifying 11β-HSD2 on synovial macrophages in RA, we did not find a high level of mRNA expression of this enzyme in synovial macrophages in the AMP RNA-seq dataset. Similarly, our qPCR analysis of the *HSD11B2* gene in monocyte-derived macrophages identified relatively low-level expression. Thus, our data implies a reciprocal regulation of the 11β-HSD enzymes in inflammatory polarised macrophages, in which active GCs downregulate 11β-HSD1 to prevent

further GC generation and may upregulate 11β-HSD2 to promote their inactivation. This represents the inherent plasticity of macrophages in their response to external stimuli, with pre-receptor GC metabolism by these enzymes similarly linked to changes in macrophage polarisation and function. However, there needs to be further analysis of 11β-HSD2 gene expression and activity to confirm this GC-mediated regulation. It may be that our timepoints for assessing gene expression (24h) and enzyme activity (48h polarisation/treatment then 18h dehydrogenase activity assay) are not suitable for this enzyme in macrophages, or macrophage 11β-HSD2 simply does not have as much functional relevance as 11β-HSD1. Finally, contrary to previous findings, we did not see any significant effects of PPARγ-activation on *HSD11B1* expression. However, Chinetti-Gbaguidi et al described a different method for generating macrophages from monocytes, instead differentiating monocytes directly into M2-like macrophages with long-term IL-4 treatment, which likely contributed to their finding of higher 11β-HSD1 activity (293). Further analysis using dose responses of rosiglitazone and other PPARγ-agonists, as well as confirmation of PPARγ-induced gene expression, would give a confirmation of whether the slight induction of *HSD11B1* in M2 macrophages (Figure 4-7 F) is indicative of regulation of *HSD11B1* expression by PPARγ.

Further supporting our aim of targeting 11β-HSD1 in inflammatory macrophages to improve anti-inflammatory functions of GCs are our findings that inactive GCs could drive functional changes in M1 macrophages. Treating macrophages with 24h GCs at the time of polarisation downregulated some cytokine production in M1 macrophages, although only TNFα significantly (Figure 4-11 F), while gene expression analysis did not yield any significant changes with cortisone treatment (Figure 4-11 A-E). Cortisone treatment however did drive a significant upregulation of the GC-inducible gene *GILZ*, implying that enough was converted

to activate GRα (Figure 4-10). In M2 macrophages, cortisone treatment unexpectedly and significantly downregulated *TNFα* mRNA expression (Figure 4-12 A); it may be that the very low-level induction of *TNFα* in this more anti-inflammatory cell type (as seen compared to M1 in Figure 4-3 C) was more easily suppressed by the low level of active GC generated from cortisone in these cells. Importantly, viability assays confirmed that this downregulation of inflammatory function was not simply due to cell death induced by GC treatment at the doses assessed in this study (Figure 4-14).

Active GC treatment with cortisol during polarisation promoted expression of the haemoglobin scavenger receptor CD163 in M1 and M2 macrophages (Figure 4-11 D, Figure 4-12 D) which has previously been shown to be GC-inducible on macrophages, and is associated with a pro-resolution macrophage phenotype (419). We did not, however, see other expected effects of GC treatment on macrophages, including enhanced phagocytosis of apoptotic cells and release of anti-inflammatory cytokines such as IL-10 (223, 224).

By temporally separating our inflammatory polarisation of macrophages from treatment with inactive GC and assessing the subsequent response to LPS inflammatory challenge, we were able to better discern the effects of cortisone treatment on macrophage inflammatory function. Unpolarised macrophages, shown to have very little 11β-HSD1 expression or activity (Figure 4-5), did not exhibit a suppression of LPS-induced inflammatory cytokine mRNA expression and production when pre-treated with cortisone (Figure 4-16 and Figure 4-17). However, IFNγ/TNFα-polarised M1 macrophages, with high 11β-HSD1 expression and activity, were able to significantly increase expression of *CD163* and decrease secretion of TNFα and IL-6 on LPS challenge when pre-treated with cortisone (Figure 4-16 and Figure 4-17). This

experiment shows the intracrine regulation of macrophage inflammatory function by 11β-HSD1-metabolised GCs, with pro-inflammatory polarisation priming these cells for responsiveness to inactive GCs. The effect of these metabolised GCs is a shift towards resolution of inflammation through downregulation of inflammatory cytokines and upregulation of the scavenger receptor *CD163*. Further studies should confirm the role of 11β-HSD1 in this process using inhibitors and assess acquisition of further pro-resolution functions such as other scavenger receptors and phagocytosis of apoptotic cells.

Due to time constraints and the low throughput method of macrophage generation from blood monocytes, a limitation of this thesis is that we were not able to investigate further macrophage functions and their regulation by inflammatory polarisation and GCs. These constraints limited our flow cytometry analysis, as large amounts of cells are required to assess the effects of GC treatment on expression of polarisation-associated surface marker expression. Instead, these markers were initially used to confirm and validate macrophage polarisation in pilot experiments (Figure 4-3 D). Additionally, we were unable to fully compare differences of GC treatment on polarised macrophage gene expression and cytokine secretion for the cytokines IL-6 and IL-12 p70 (Figure 4-11 and Figure 4-12).

Analysis of phagocytosis was not investigated further as active GCs did not regulate phagocytosis in the experimental setup assessed, and so we did not expect inactive GCs to have any effects. GCs are well known to promote phagocytosis of apoptotic cells but also phagosomal destruction of pathogens such as bacteria (422, 423). However, there are conflicting reports of GCs instead suppressing macrophage phagocytosis of pathogens (229, 424, 425). The outcome of GC treatment on phagocytosis is likely highly dependent on the

polarisation state of the macrophage and the potency of the GCs tested. As IL-4 polarised M2 macrophages have been characterised as a distinct subset to the GC-induced "M2c" macrophage, it is likely that each factor could antagonise functions promoted by the other. Although M2 macrophages have previously been reported to have a great phagocytic capacity for *E. coli*, as used in our assay, this function may be suppressed by cortisol in this context (426). As GCs have previously been shown to have key roles in clearance of apoptotic cells during the resolution of inflammation, investigation of this specific function may be more informative. This could be carried out using quantification of the uptake of fluorescently-labelled apoptotic cells by macrophages using imaging or flow cytometry. The use of a pH-sensitive dye such as pHrodo™ would detect acidification of the phagosome and thus confirm phagocytosis.

A further function that is known to be negatively regulated by GCs is antigen presentation. GC treatment downregulates the professional antigen presentation molecule MHCII (HLA in humans) which is a defined marker of M1-like pro-inflammatory polarisation of macrophages (226, 229, 230). This marker has been found to differentiate functionally distinct subsets of synovial macrophages in RA; with MHCII+ macrophages linked to disease progression and MHCII- associated instead with resolution of inflammation and disease activity (120). Previous work in the Hardy group identified a significant shift towards MHCII+ M1-like macrophage polarisation in *Hsd11b1*$^{-/-}$ TNF-tg mice, suggesting that GC metabolism by this enzyme helps to promote pro-resolution polarisation and functions of macrophages at the expense of the MHCII+ pro-inflammatory subset (314). This finding may link to the poor clinical response to therapeutic GCs seen in *11βflx/LysMcre* TNF-tg mice compared to *Hsd11b1*-competent mice; macrophage 11β-HSD1 may also mediate pro-resolution polarisation in response to

therapeutic GCs, and these are important for resolution of inflammation and disease (290). Further work using our in vitro macrophage cultures could examine effects of inactive GC treatment on expression of MHCII and costimulatory markers required for antigen presentation by qPCR and flow cytometry, as well as functional assays to measure ability of treated macrophages to activate T cells with cognate antigen.

It may also be important to further investigate the regulation of 11β-HSD1 in other macrophage populations, such as synovial tissue macrophages as these cells are highly heterogeneous and tissue specific. Although inflammatory activation and GC-treatment of alveolar macrophages showed trends toward induction and downregulation of *HSD11B1* respectively (Figure 4-8), mirroring findings in monocyte-derived macrophage cultures, these changes were not significant. This is likely due to the high level of variability between patient samples, particularly as these alveolar macrophages were isolated from patients with mild COPD, a disease in which macrophages play a key role in orchestration of inflammation (427). A comparison of these mild COPD macrophages with those isolated from healthy controls could suggest whether 11β-HSD1 is differentially regulated by inflammation in this disease and plays a role in macrophage inflammatory function here.

In conclusion, in this study we aimed to investigate how macrophage inflammatory function was regulated by 11β-HSD1 metabolism of GCs. We confirmed that inflammatory polarisation upregulates 11β-HSD1 metabolism in primary human blood monocyte derived macrophages, as seen in synovial RA macrophages. This inflammation-induced activation of the endogenous GC cortisol from cortisone enables anti-inflammatory regulation of macrophage function by changing inflammatory cytokine profiles and expression of pro-resolution scavenger

receptors. The downregulation of inflammatory functions and upregulation of pro-resolution markers represents a shift in polarisation towards a macrophage phenotype, which likely promotes resolution of inflammation and tissue repair, and may be beneficial in diseases such as RA.

Chapter 5 MACROPHAGE METABOLISM OF ANDROGENS AND FUNCTIONAL EFFECTS ON INFLAMMATORY PROFILES

5.1 Introduction

Androgens are known to have generally anti-inflammatory and immunosuppressant effects. This is believed to play a role in the marked sex imbalance of autoinflammatory diseases such as RA, where there is a higher proportion of female patients, and lower androgen levels are linked with increased incidence of RA and higher inflammatory measures such as ESR (351-353). However, dysregulation of androgen levels in RA may also present at the intracrine level, in which inactive precursors are activated to functional androgens within a cell, in immune cells such as synovial macrophages, which play a major role in dictating the inflammatory RA environment.

As discussed in Section 1.4.4, different populations of macrophages, including synovial and monocyte-derived macrophages, have been found to express various enzymes of the androgen metabolic pathway, and androgen stimulation appears to exert anti-inflammatory effects on macrophages (374, 375). However, most studies on the functional effects of androgen stimulation in macrophages have focused on the active androgens testosterone and DHT (371, 379-381, 383). Less is known about how androgen metabolism is regulated by inflammatory polarisation of macrophages and how this metabolism influences macrophage function.

Intracrine androgen metabolism by RA synovial macrophages may be involved in their inflammatory function, as these cells have been identified to metabolise testosterone into

both the potent active androgen DHT, but also the less active precursor androstenedione (390, 391). However, again, it is unknown how this is regulated with inflammation and whether this metabolism differs between distinct subsets of tissue macrophages.

Analysis of the AMP RNA-seq dataset in Chapter 3 identified an inflammation-induced differential expression of key androgen activating enzymes AKR1C3 and SRD5A1 in RA synovial macrophages. scRNA-seq dataset analysis found that the inflammatory-upregulated SRD5A1 was primarily expressed in the synovial macrophage subset associated with severe disease, while the inflammation-downregulated enzyme AKR1C3 was mainly expressed by a subset associated with remission and healthy synovial tissue. This, in line with our findings that overall ratios of active androgens and precursors in RA synovial fluid did not change with inflammation or disease severity suggests that macrophage intracrine androgen metabolism may have more of a role in defining the inflammatory status of the diseased joint.

To explore this further, in this chapter we investigate androgen metabolism in monocyte-derived macrophages, as previously carried out for GC pre-receptor metabolism in Chapter 4, in order to further characterise the regulatory relationship between macrophage inflammatory polarisation and function and intracrine androgen metabolism.

5.2 Materials and methods

5.2.1 Macrophage culture and polarisation

Monocytes were isolated from human blood cones by RosetteSep™ and differentiated into macrophages for 6d with 20 ng/ml M-CSF as previously described (section 2.3.1).

Macrophages were polarised for 24h into M0 (unpolarised) or M1-like (20 ng/ml IFNγ and 10 ng/ml TNFα) prior to treatment with androgens to assess effects of androgen metabolism on inflammatory profiles.

5.2.1.1 Steroid hormone quantification

Androgen metabolism was assessed in differentially polarised macrophages by treating cells with androgen precursors and assessing conversion into metabolites by LC-MS/MS. Following 24h polarisation, macrophages were treated with 100nM of DHEA, androstenedione or testosterone (all Sigma-Aldrich, UK) or ethanol vehicle for 48h. Supernatants were then collected and stored at -80°C.

Steroids were extracted from supernatants using liquid/liquid extraction as detailed in section 2.5.5. Dr Angela Taylor ran all samples on a Waters Xevo® mass spectrometer as detailed in section 2.5.5. The concentrations of androgens were quantified relative to a calibration series spanning the range 0.5-1000 ng/ml for each steroid.

5.2.2 Gene expression analysis

Following the appropriate treatment timepoint, RNA was isolated from macrophage cultures with an innuPREP RNA Mini kit (Analytik Jena, Germany), following manufacturer's protocol, as described in section 2.4.1. Yield and purity of samples, as determined by absorbance ratios at 260/280 and 260/230, was measured on a NanoDrop™ ND-1000 spectrophotometer (Wilmington, USA). 350ng of RNA per sample was reverse transcribed using Applied Biosystems reverse transcription reagents and a GeneAmp® PCR System 27000 machine (Applied Biosystems, UK), following the protocol detailed in section 2.4.2. qPCR analysis was carried out on a QuantStudio™ 5 Real-Time PCR System (Applied Biosystems, UK) with TaqMan probes, listed in section 2.4.3. Expression of genes of interest was normalised to that of 18S.

5.2.3 Cell viability assay

Viability was assessed using an ApoLive-Glo® Multiplex assay (Promega, UK) as detailed in section 2.9. Following differentiation from monocytes as before on Eppendorf® Cell Imaging 96 well glass bottom plates (Sigma-Aldrich, UK) macrophages were polarised to M0 (untreated) or M1-like (IFNγ and TNFα) for 24h with ethanol vehicle control or 10nM DHT (Sigma-Aldrich, UK) and then assessed for viability and apoptosis according to manufacturer's guidelines. M0 macrophages were treated with 10mM hydrochloric acid (HCl) 10min before assay as a positive cell death control.

5.2.4 Cytokine release analysis

Cytokine levels were measured by ELISA as detailed in section 2.6. Supernatants were collected from macrophage cultures following relevant stimulation time. ELISAs were carried out using Invitrogen Human Uncoated ELISA Kits for TNFα and IL-12 p70 (both Thermo Fisher Scientific, UK) and Precoated Quantikine® Human IL-6 ELISA Kit (R&D Systems, UK), following manufacturers' protocols, and ran on a FLUOstar® Omega Microplate Reader (BMG Labech, Germany).

5.2.5 Statistical analysis

Statistical significance was assessed with IBM SPSS Statistics v28.0.1.0 (IBM Analytics, USA) and GraphPad Prism v5.03 and v9.5 (GraphPad Software, USA). Normality of data was tested using a Shapiro-Wilk test for Gaussian distribution. One-way ANOVA with Tukey's post hoc analysis was used to test significance between all groups when multiple treatment groups were present. Two-way ANOVA analysis with Bonferroni multiple comparison post-test was used to compare between macrophage polarisation subsets and treatment groups. Statistical significance is presented as follows: * $P \leq 0.05$, ** $P \leq 0.01$ and *** $P \leq 0.001$.

5.3 Results

5.3.1 Differential expression of androgen activating enzymes *AKR1C3* and *SRD5A1* in pro-inflammatory monocyte-derived macrophages

As androgen levels in blood sera differ between males and females and could affect blood monocyte-derived macrophage responses to androgen stimulation in vitro, we assessed the baseline levels of androgens in blood samples used for macrophage culture by LC-MS/MS (Figure 5-1).

Baseline sera levels of testosterone were mostly within the healthy male reference range as previously published (410) (Figure 5-1 A). DHT levels were fully within the healthy male reference ranges (Figure 5-1 B). These data suggest that all these samples can be analysed together, as they all have similar baseline androgen levels.

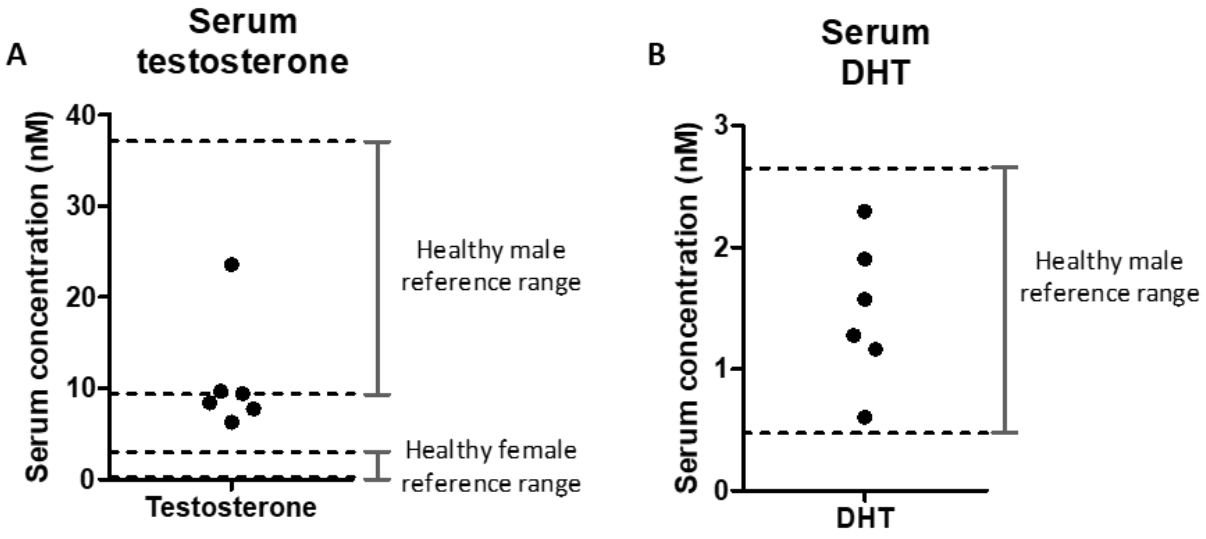

Figure 5-1 Androgen levels in in vitro macrophage samples

Concentration (nM) of (A) testosterone and (B) DHT in sera of whole blood samples used for macrophage generation quantified by LC-MS/MS (n=6). Dotted lines show healthy male reference ranges for serum testosterone and DHT as previously published by Kratz (410).

Analysis of the AMP bulk RNA-seq dataset identified that the androgen activating genes *AKR1C3* and *SRD5A1* were differentially regulated with inflammation and disease severity in RA synovial macrophages (Chapter 3). While the early-stage androgen activator *AKR1C3* was downregulated with increasing synovitis and DAS28-CRP, expression of the DHT-generating enzyme *SRD5A1* was upregulated. We therefore investigated whether similar changes in gene expression would be seen with differential inflammatory polarisation of monocyte-derived macrophages as measured by qPCR (Figure 5-2).

As with the AMP RNA-seq data, expression of *AKR1C3* was significantly lower in pro-inflammatory M1-like macrophages polarised with IFNγ and TNFα compared with unpolarised M0 (8.6-fold, P≤0.01; Figure 5-2 A). Similarly, expression of *SRD5A1* was higher in M1-like macrophages than in M0 (2.0-fold, P≤0.05, Figure 5-2 B).

These data show that human blood monocyte-derived macrophages have a similar transcriptional regulation of *AKR1C3* and *SRD5A1* with inflammation as previously identified synovial macrophages.

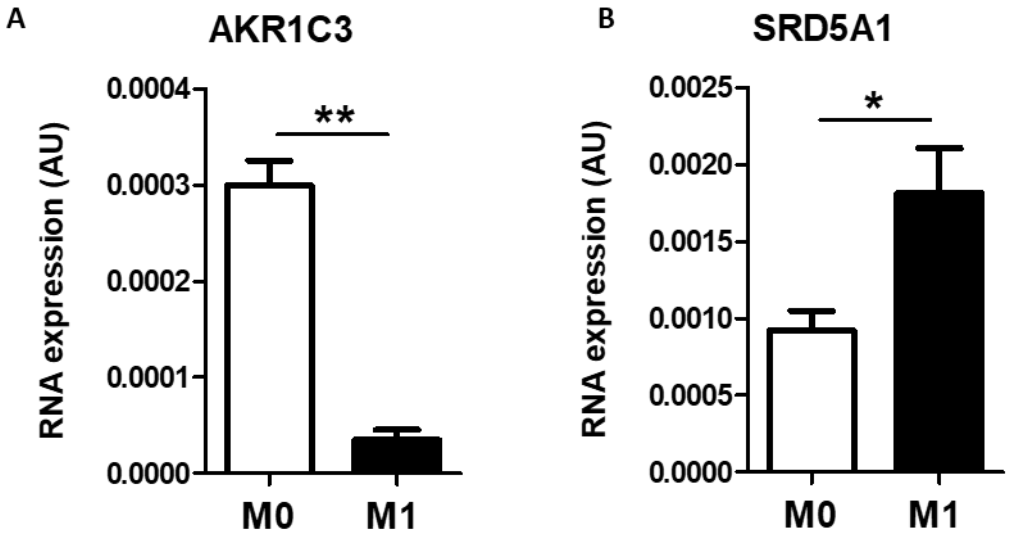

Figure 5-2 Androgen metabolism genes are differentially regulated in inflammatory human macrophages

RNA expression (AU) of the androgen activating enzymes (A) *ARK1C3* and (B) *SRD5A1* in macrophages polarised for 24h to unpolarised M0 or pro-inflammatory M1-like (IFNγ and TNFα) as measured by qPCR (n=4). Data are presented as mean ± SEM and statistical significance was determined using paired Student's t-test (* p≤0.05, ** p≤0.01).

5.3.2 Inflammatory macrophages have increased androgen activation

The metabolism of androgens was assessed by treating M0 or M1-like polarised macrophages with the precursors DHEA, androstenedione or testosterone and quantifying metabolite production by LC-MS/MS (Figure 5-3). These steroids have previously been shown to be metabolised by macrophage populations to yield downstream androgens (374, 375).

DHEA treatment of M0 macrophages resulted in negligible conversion of this precursor into other androgen metabolites (Figure 5-3 A). Treatment with androstenedione led to some conversion into 5α-androstanedione (31.1% [±6.5%]), androsterone (8.9% [±3.0%]) and some further metabolites (Figure 5-3 B). M0 macrophages also converted some testosterone into DHT but only marginally (10.2% [±3.4%]; Figure 5-3 C).

Similar to M0 macrophages, M1-like macrophages did not convert DHEA into further androgens (Figure 5-3 D). However, M1-like macrophages converted nearly all the androstenedione treatment into downstream metabolites, in particular 5α-androstanedione (49.5% [±2.1%]), androsterone (21.0% [±1.6%]) and active androgen DHT (11.8% [±1.1%]; Figure 5-3 E). 31.4% (±4.3%) of the testosterone treatment was converted into DHT but also some upstream inactive metabolites such as androstenediol (18.0% [±3.1%]; Figure 5-3 F).

We also assessed the baseline generation of androgens in M1-like polarised macrophages; however, androgens were only produced at very low to minimal levels and so were assumed to be negligible (Figure 5-3 G).

These data show that monocyte-derived macrophages are capable of metabolising inactive androgen precursors into active androgens, and suggest that this metabolism is upregulated in inflammatory polarised macrophages.

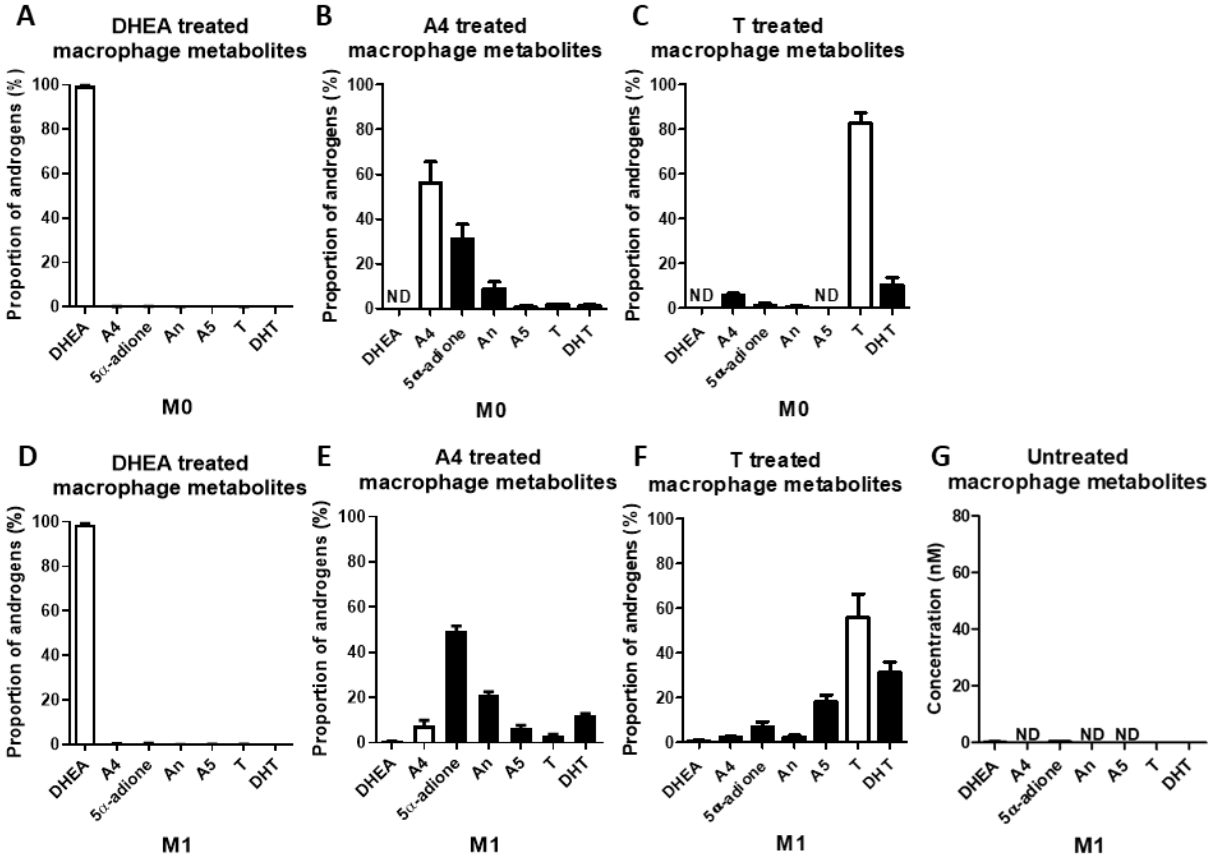

Figure 5-3 Macrophages can metabolise androgens from precursors

Proportion (percentage) of androgens in supernatants of macrophages polarised for 24h to unpolarised (M0) (A-C) or pro-inflammatory M1-like (IFNγ and TNFα) (D-F) and then treated for 48h with 100 nM DHEA, androstenedione (A4) or testosterone (T) and analysed by LC-MS/MS (n=5, DHEA treated n=3). White bars depict the androgen with which macrophages were treated. (G) Concentration (nM) of androgens in macrophages polarised to M1 for 48h without androgen treatment, as quantified by LC-MS/MS (n=5). Data are presented as mean ± SEM. 5α-adione, 5α-androstandione; A4, androstenedione; A5, androstenediol; An, androsterone; DHEA, dehydroepiandrosterone; DHT, dihydrotestosterone; ND, not detected; T, testosterone.

In order to assess whether inflammatory polarised macrophages had differences in androgen metabolism in line with their differing enzyme gene expression we calculated the generation of androgens from their precursors (Figure 5-4). It was not possible to calculate the AKR1C3-catalysed conversion of DHEA into androstenediol, as most of the samples contained androstenediol levels below the limit of detection. Therefore, we assessed the conversion of DHEA into testosterone, despite this not being a direct conversion step (Figure 5-4 A).

As expected, given the low conversion of DHEA in Figure 5-3, there were no differences in androstenedione/DHEA or testosterone/DHEA in DHEA treated M0 and M1-like macrophages (A4/DHEA: M0 v M1-like 2.4-fold, P=0.2793; T/DHEA: 2.2-fold, P=0.1100; Figure 5-4 B-C). There was a trend towards greater generation of DHT from testosterone in M1-like macrophages compared to M0 macrophages, in line with their increased SRD5A1 expression, but this was not significant (6.4-fold, P=0.0625; Figure 5-4 D).

In androstenedione treated macrophages, however, M1-like polarisation was found to increase the generation of 5α-androstanedione from androstenedione (28.4-fold, P≤0.01), in line with the greater level of SRD5A1 expression seen in these cells (Figure 5-4 E). M1-like macrophages also showed significantly higher generation of DHT from 5α-androstanedione (6.8-fold, P≤0.01; Figure 5-4 F) and conversion of androstenedione into testosterone (19.8-fold, P≤0.05; Figure 5-4 G), both of which were catalysed by AKR1C3.

Collectively these data show that despite inflammatory polarisation driving differential regulation of the SRD5A1 and AKR1C3 enzymes, the effects on metabolism appear to be a general increase in production of androgens from precursors compared to unpolarised macrophages.

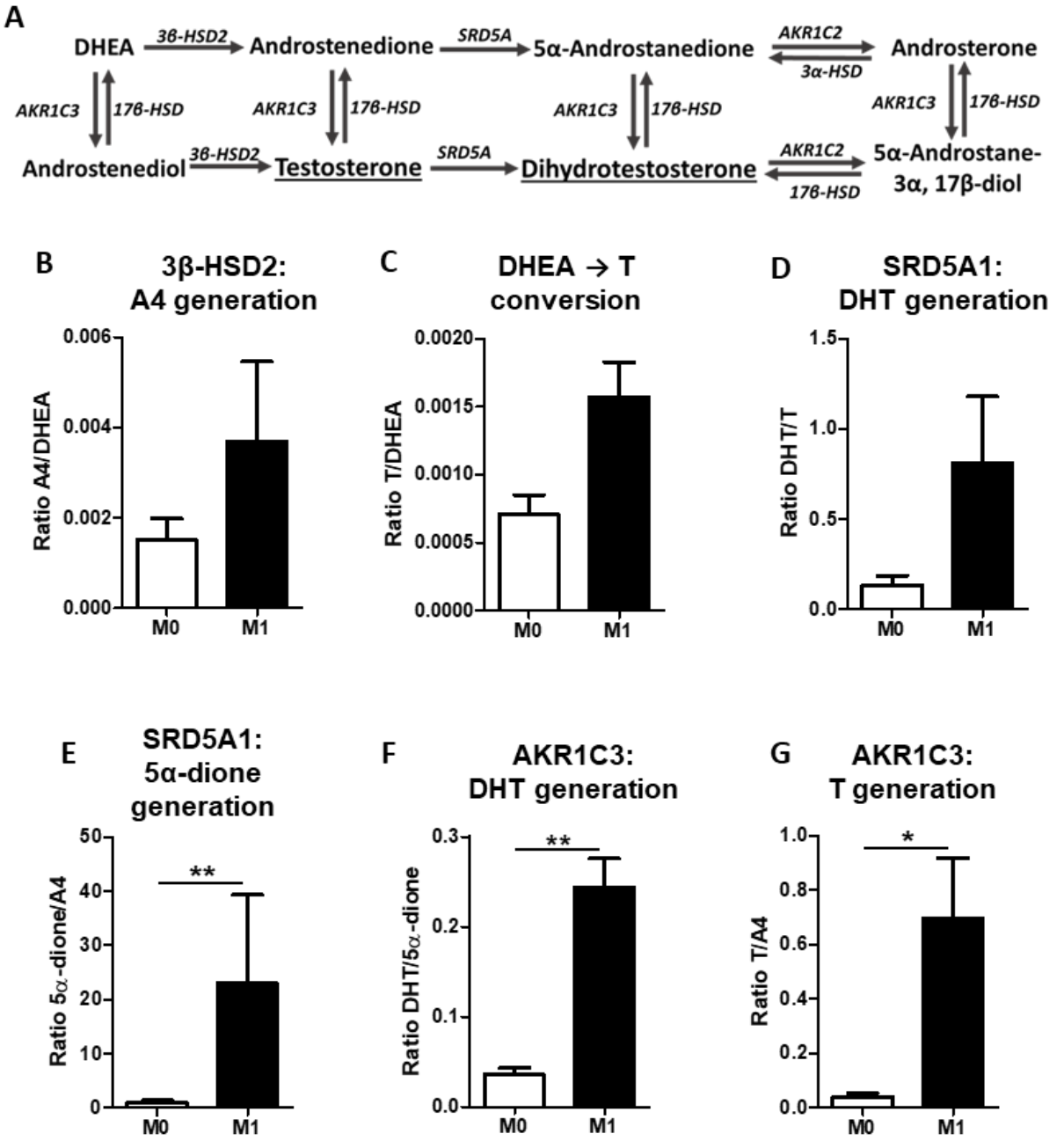

Figure 5-4 Inflammatory polarisation increases androgen activation in macrophages

(A) Pathway of androgen activation. Ratio of (B) androstenedione (A4) over DHEA and (C) testosterone (T) over DHEA in DHEA-treated cells, (D) dihydrotestosterone (DHT) over T in T treated cells, and (E) 5α-androstandione (5α-adione) over A4, (F) DHT over 5α-adione and (G) T over A4 in A4 treated cells, in macrophages polarised to M0 (unpolarised) or M1 (IFNγ and TNFα) for 24h and then treated with 100 nM DHEA, T or A4 and steroid levels in supernatants quantified by LC-MS/MS (n=5; DHEA-treated n=3). Data are presented as mean ± SEM and statistical significance was determined using Student's paired t-test (* p≤0.05, ** p≤0.01).

5.3.3 Differences in androgen metabolism between M0 and M1 macrophages are not due to changes in viability

We assessed the effects of androgen stimulation on viability of M0 and M1-like polarised macrophages to ensure that differences in metabolism were not caused by loss of cell viability (Figure 5-5). We treated macrophages with the potent androgen DHT, as this would have the strongest androgenic effects.

There were no differences in viability (Figure 5-5 A) for M0 and M1-like macrophages when treated with the active androgen DHT. Although there was a trend towards decreased apoptosis in M1-like macrophages compared to M0 for both control (1.8-fold, P=0.2190) and DHT treated (1.7-fold, P=0.2153), these were also not significant (Figure 5-5 B). These data suggest that the decreased androgen metabolism seen in M0 macrophages is not due to changes in viability compared to M1-like macrophages on androgen stimulation.

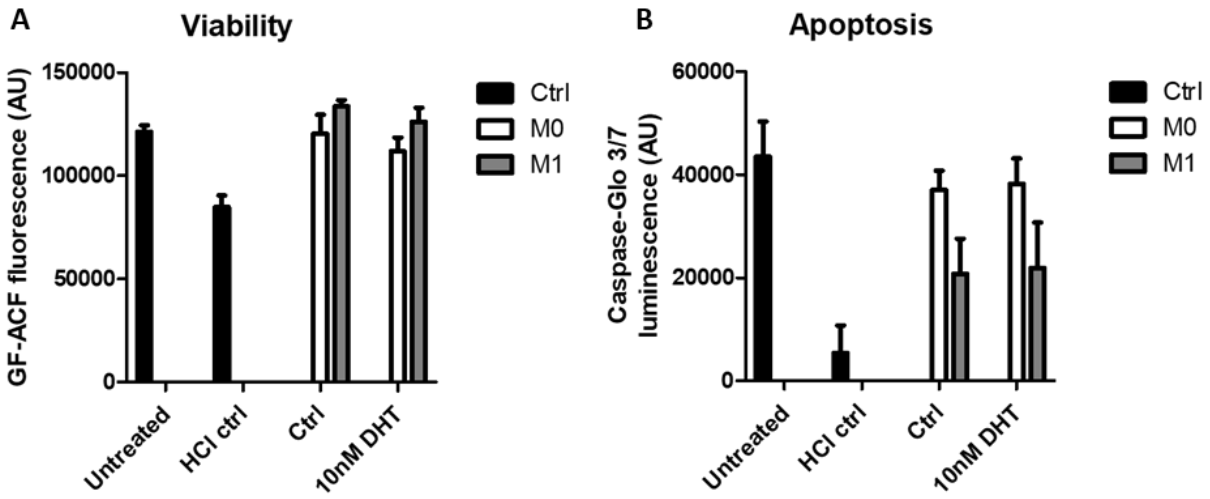

Figure 5-5 DHT treatment does not affect macrophage viability

(A) Cell viability as quantified by GF-AFC fluorescence (AU) and (B) apoptosis as quantified by Caspase-Glo 3/7 luminescence (AU) in untreated or HCl treated (HCl ctrl) M0 macrophages and M0 and M1-like (IFNγ and TNFα) polarised macrophages (Ctrl) treated with 10nM dihydrotestosterone (DHT), using an ApoLive-Glo multiplex assay (n=3). Data are presented as mean ± SEM and statistical significance was determined using two-way ANOVA with Bonferroni's multiple comparisons post-test.

5.3.4 Pre-receptor androgen metabolism does not influence inflammatory function of macrophages on subsequent inflammatory challenge

We assessed the impact of inflammatory polarisation induced differences in metabolism on regulation of macrophage inflammatory functions using the same LPS challenge methodology used in Chapter 4.

As shown in Figure 5-6, macrophages were polarised for 24h to yield unpolarised M0 or inflammatory M1-like macrophages (IFNγ/TNFα); these were each treated with androgens for 24h before acute LPS challenge for 8h to assess whether androgen pre-treatment would reduce subsequent inflammatory response to LPS. We assessed treatment with the inactive androgen precursor androstenedione and testosterone, which can function both as an active androgen and as a precursor to the more potent DHT. DHT pre-treatment was included to compare the anti-inflammatory effects of intracrine androgen metabolism to treatment with an active potent androgen. Cortisol pre-treatment was included as a positive control to assess regulation of LPS-induced inflammation, and to assess if cortisol and DHT stimulation could provide additive anti-inflammatory effects. As M1-like macrophages were confirmed to exhibit greater androgen activation than M0 macrophages, we predicted that we would see a greater downregulation of LPS-induced inflammatory responses in M1-like polarised macrophages.

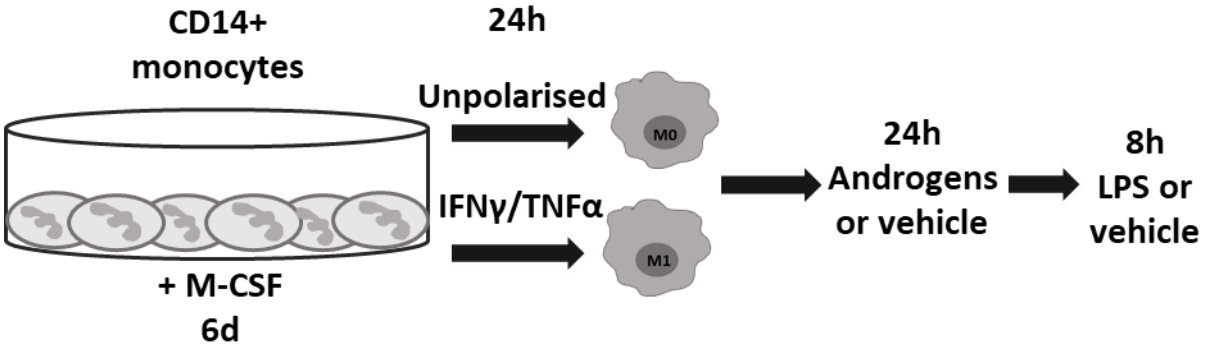

Figure 5-6 Schematic for analysis of regulation of inflammatory function by androgen metabolism

CD14+ monocytes isolated from whole blood by RosetteSepTM kit were differentiated into macrophages by 6h incubation with 20 ng/ml M-CSF. Macrophages were polarised into M0 unpolarised cells (untreated) or pro-inflammatory M1-like (IFNγ and TNFα) for 24h. Medium was changed, and polarised cells were treated with 10 nM DHT (with or without 1000 nM cortisol), 100 nM androstenedione or 100 nM testosterone or vehicle for 24h. Then cells were treated with 10 ng/ml LPS for 8h and RNA and supernatants collected.

The effects of intracrine androgen metabolism on macrophage inflammatory gene expression was assessed by qPCR in M0 and M1-like macrophages (Figure 5-7).

Cortisol pre-treatment downregulated LPS-induced expression of the pro-inflammatory cytokine genes *TNFα* (M0 LPS control vs cortisol LPS: 3.6-fold, P≤0.001; M1-like: 1.8-fold, P≤0.05; Figure 5-7 A), *IL-6* (M1-like: 3.6-fold, P≤0.05; Figure 5-7 B) and *IL-12A* (M1-like: 4.8-fold, P≤0.01; Figure 5-7 C) and increased expression of the pro-resolution gene *CD163* (M0 LPS control vs cortisol LPS: 2.5-fold, P≤0.001; M1-like: 8.6-fold, P≤0.001; Figure 5-7 D). Although there was a trend towards decrease of LPS-induced expression of *IL-6* and *IL-12A* with cortisol pre-treatment in M0 macrophages, these were not significant (*IL-6*: M0 LPS control vs cortisol LPS: 6.4-fold, P=0.0518; *IL-12A*: M0 LPS control vs cortisol LPS: 2.2-fold, P=0.3985).

Pre-treatment with androstenedione (A4), testosterone or DHT alone did not significantly regulate LPS-induced inflammatory gene expression profiles. When DHT was applied in combination with cortisol there was a significant decrease in LPS-induced expression of *TNFα* expression in M0 macrophages (M0 LPS control vs cortisol+DHT LPS: 3.0-fold, P≤0.01; Figure 5-7 A), *IL-6* in M1-like macrophages (M1-like LPS control vs cortisol+DHT LPS: 4.2-fold, P≤0.05; Figure 5-7 B) and *IL-12A* in M1-like macrophages (M1-like LPS control vs cortisol+DHT LPS: 6.0-fold, P≤0.01; Figure 5-7 C). There was also an increase in *CD163* expression on combined cortisol and DHT pre-treatment prior to LPS stimulation compared to LPS alone (M0 LPS control vs cortisol+DHT LPS: 2.7-fold, P≤0.001; M1-like LPS control vs cortisol+DHT LPS: 8.3-fold, P≤0.001; Figure 5-7 D). However, the gene expression changes seen with addition of DHT to cortisol pre-treatment were no different to cortisol pre-treatment alone: no additive changes in inflammatory regulation were seen.

Therefore, despite an inflammation-induced increase in androgen metabolism seen in M1-like macrophages, treating these cells with androgens did not decrease inflammatory gene responses to subsequent inflammatory challenge with LPS.

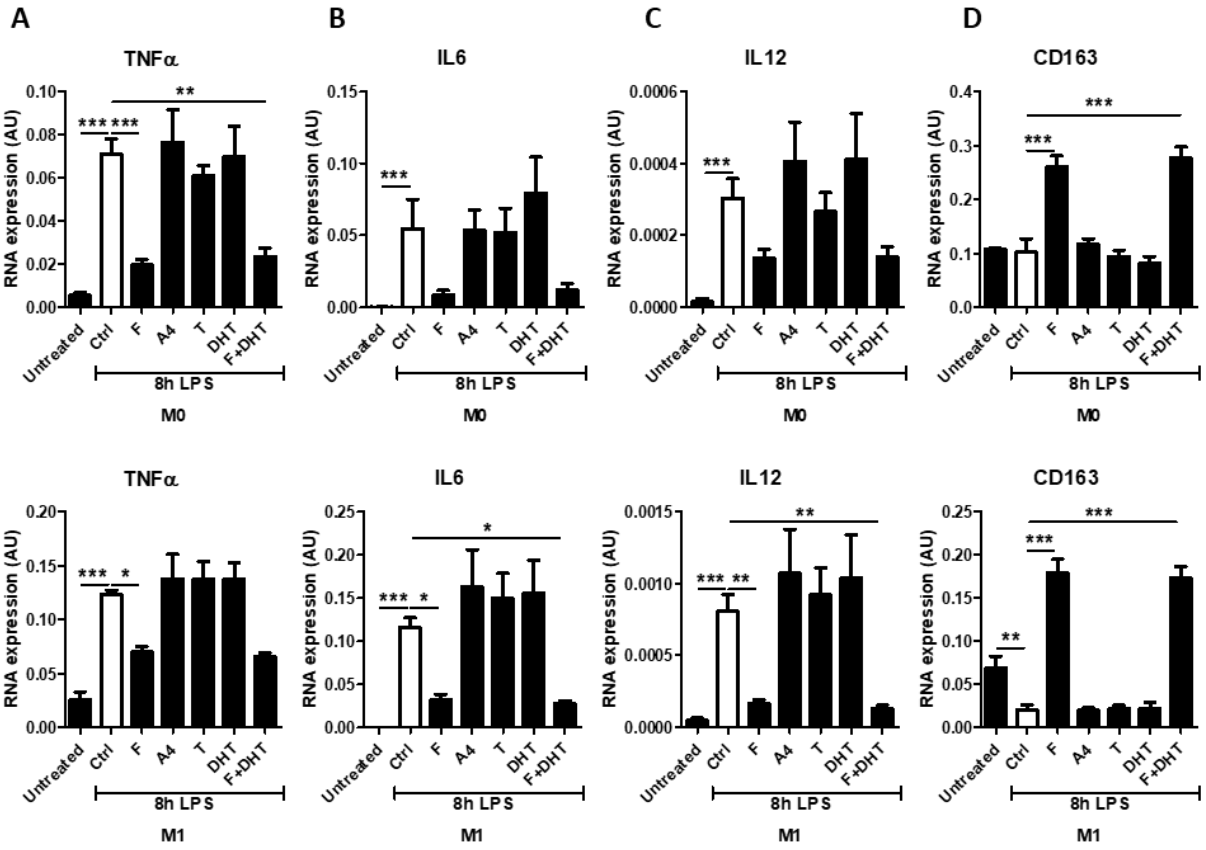

Figure 5-7 Androgen pre-treatment does not suppress inflammatory gene profiles from LPS stimulation

RNA expression (AU) of (A) *TNFα*, (B) *IL-6*, (C) *IL-12A* and (D) *CD163* in macrophages polarised for 24h to unpolarised (M0) or inflammatory M1-like (IFNγ/TNFα) and then untreated (Ctrl), treated with 8h LPS only (LPS) or pre-treated with 24h 1000 nM cortisol (F), 100 nM androstenedione (A4), 100 nM testosterone (T), 10 nM dihydrotestosterone (DHT) or combined 1000 nM cortisol and 10 nM DHT (F+DHT) as measured by qPCR (n=3). Data are presented as mean ± SEM and statistical significance was determined with one-way ANOVA with Dunnett's post-test to compare groups to LPS-only group (* p≤0.05, ** p≤0.01, *** p≤0.001).

The effects of androgen pre-treatment on regulation of LPS challenge-induced inflammatory cytokine release in M0 and M1-like polarised macrophages was assessed by ELISA analysis of supernatants (Figure 5-8).

As with gene expression, cortisol pre-treatment reduced the LPS-induced secretion of the inflammatory cytokines TNFα (M0 LPS control vs cortisol LPS: 2.2-fold, P≤0.01; M1-like: 11.3-fold, P≤0.001; Figure 5-8 A), IL-6 (M1-like: 2.1-fold, P≤0.05; Figure 5-8 B) and IL-12 p70 (M1-like: P≤0.05; Figure 5-7 C). There was a trend towards decrease of LPS-induced secretion of IL-6 with cortisol pre-treatment in M0 macrophages; this was not significant (M0 LPS control vs cortisol LPS: 3.8-fold, P=0.1550).

While concomitant DHT and cortisol pre-treatment prior to LPS stimulation did decrease release of TNFα (M0 LPS control vs cortisol+DHT LPS: 2.1-fold, P≤0.001; M1-like LPS control vs cortisol+DHT LPS: 13.2-fold, P≤0.001; Figure 5-8 A), IL-6 (M1-like LPS control vs cortisol+DHT LPS: 2.9-fold, P≤0.01; Figure 5-8 B) and IL-12 p70 (M1-like LPS control vs cortisol+DHT LPS: 23.9-fold, P≤0.05; Figure 5-8 C), again these were not dissimilar to level of decrease induced by cortisol pre-treatment alone. Pre-treatment with androgens also had no effect on LPS-induced cytokine secretion.

Together these data show that despite increased androgen metabolism occurring within inflammatory macrophages compared to unpolarised macrophages, this intracrine metabolism did not regulate their inflammatory functional response to LPS challenge.

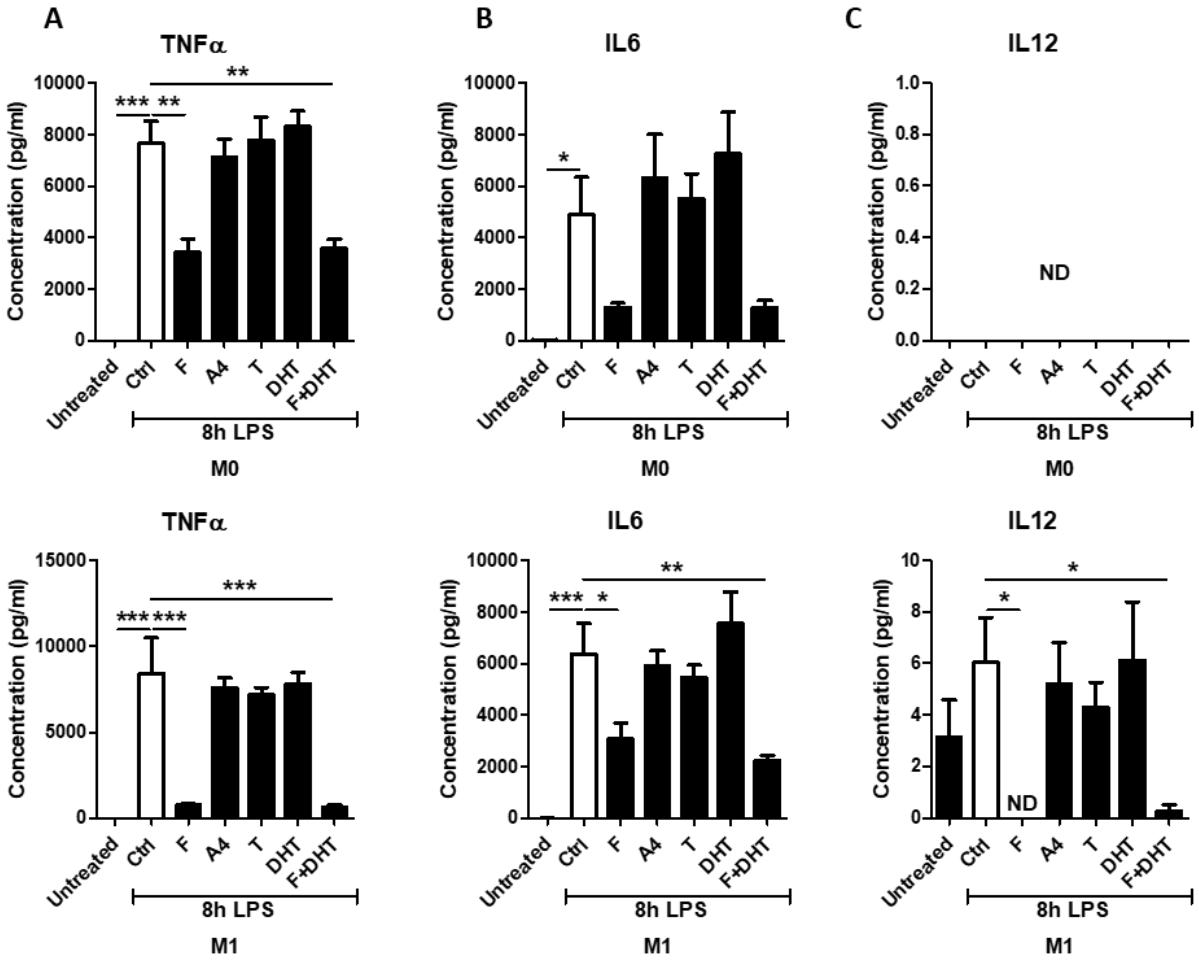

Figure 5-8 Androgen pre-treatment does not suppress inflammatory cytokines from LPS stimulation

Cytokine concentration (pg/ml) in supernatants of (A) TNFα, (B) IL-6 and (C) IL-12 p70 in macrophages polarised for 24h to unpolarised (M0) or inflammatory M1-like (IFNγ/TNFα) and then untreated (Ctrl), treated with 8h LPS only (LPS) or pre-treated with 24h 1000 nM cortisol (F), 100 nM androstenedione (A4), 100 nM testosterone (T), 10 nM dihydrotestosterone (DHT) or combined 1000 nM cortisol and 10 nM DHT (F+DHT) as measured by ELISA (n=3). Data are presented as mean ± SEM and statistical significance was determined with one-way ANOVA with Dunnett's post-test to compare groups to LPS-only group (* p≤0.05, ** p≤0.01, *** p≤0.001). ND, not detected.

5.4 Discussion

The dysregulation of systemic androgen metabolism has been strongly implicated in the pathophysiology of chronic inflammatory diseases such as RA (339, 356, 358, 359). However, the local availability of steroids is closely regulated by paracrine and intracrine metabolism, which facilitate active steroid signalling between and within cells respectively (333). Our lab has previously highlighted the importance of inflammatory GC pre-receptor metabolism by 11β-HSD1 in the pathology and resolution of arthritis (290, 314). Given the anti-inflammatory effects of androgens on immune cells and the previously reported expression of key androgenic enzymes in these cells, intracrine metabolism of androgens has been implicated in functional regulation of macrophages (334). Our analysis of the AMP RA RNA-seq dataset in Chapter 3 identified that the key extragonadal androgen activating enzymes, *AKR1C3* and *SRD5A1*, were amongst the most differentially regulated steroid metabolism genes in RA synovial macrophages. In Chapter 4, we found GC intracrine metabolism by 11β-HSD1 allowed for functional regulation of inflammatory macrophages. Therefore, we sought to identify whether androgen intracrine metabolism by *AKR1C3* and *SRD5A1* would regulate inflammatory macrophages in a similar manner.

Analysis of monocyte-derived macrophages confirmed a similar transcriptional regulation of the key rate limiting androgen activating enzymes *AKR1C3* and *SRD5A1* with inflammation as previously identified in RA synovial macrophages. *AKR1C3* was previously found to decrease expression in synovial macrophages with increasing DAS28-CRP and local synovitis, which was mirrored by the lower expression identified in unpolarised macrophages compared to inflammatory polarised macrophages (Figure 5-2 A). Meanwhile, the inverse was true for

SRD5A1, which instead increased with measures of inflammation in RA and with M1-like polarisation in vitro (Figure 5-2 B). These data imply a conserved regulation of androgen metabolism across tissue and monocyte-derived macrophage populations with inflammation.

Although androgen metabolism by SRD5A1 and AKR1C3 has been identified in numerous macrophage subsets, including synovial macrophages, alveolar macrophages, and monocyte-derived in vitro models, far less is known about the effects of inflammatory polarisation on androgen metabolism (374, 375, 390, 391). In mice, in vivo LPS challenge reduced the expression of *AKR1C3* and *SRD5A1* on isolated microglia compared to those from vehicle-treated animals, while treatment of ex vivo microglia with LPS after isolation instead upregulated both enzymes. This in vitro activation resulted in an increased generation of DHT, 5α-androstanedione and testosterone from androstenedione (428). Further investigation of the effects of androgen metabolism by inflammatory macrophages has instead focused more on the balance of androgen and estrogen production. Synovial macrophages were identified to increase aromatase activity, and therefore conversion of androgens to estrogens, in response to stimulation with GCs, IL-1, IL-6 or TNFα (429). However, this is highly cell context specific, as the monocyte-derived macrophage THP-1 line instead downregulates aromatase expression in response to TNFα stimulation (377). This androgen-estrogen metabolism balance could also be affected by the inflammatory regulation of androgen activating enzymes such as AKR1C3 and SRD5A1. This is beyond the scope of this thesis; however, given its links to androgen metabolism and more pro-inflammatory effects, estrogen metabolism in macrophages warrants further investigation. Finally, AKR1C3 is also involved in prostaglandin metabolism, generating the prostaglandin (PG) F isomers, PGF_2 and 9α,11β-PGF_2 (430). This function of AKR1C3 has been implicated in enhancing the pro-inflammatory functions of

macrophages and therefore metastasis of hepatocellular carcinoma (431). Therefore, further work should also take into consideration the other substrates of these enzymes, and the other metabolic pathways they incorporate and how these impact inflammatory function.

The differential regulation of AKR1C3 and SRD5A1 by inflammatory activation in macrophages does not appear to have been reported previously. The balance of these enzymes in inflammatory macrophages may shift androgen metabolism more towards activation of later stage potent androgens such as DHT from testosterone, while decreasing the activation of earlier androgen precursors such as DHEA. This would imply an overall decrease in intracrine androgen activation in inflammatory macrophages, as by decreasing *AKR1C3* expression macrophages would be expected to have reduced ability to generate testosterone from available DHEA or androstenedione, nor could they convert 5α-androstanedione into DHT via the alternative pathway of androgen synthesis (Figure 5-4 A). Reciprocal regulation of SRD5A1 and AKR1C3 has not previously been reported. As these enzymes are both reductases that use NADPH as a cofactor, it may be that transcriptional regulation is required for adequate NADPH availability, particularly also with its use as a substrate by inflammatory macrophage NADPH oxidase enzymes to generate ROS (432).

However, despite this differential transcriptional regulation with inflammation, on analysis of androgen metabolism by LC-MS/MS it was found that inflammatory M1-like polarised macrophages had generally higher levels of androgen activation than M0 unpolarised macrophages (Figure 5-4). This included the SRD5A1-catalysed generation of 5α-androstanedione from androstenedione and DHT from testosterone, but also the AKR1C3-catalysed conversion of 5α-androstanedione to DHT and androstenedione to testosterone

(Figure 5-4). As many genes are acutely regulated by inflammatory activation, it may be that the 24h timepoint used for our monocyte-derived macrophage cultures is missing a more dynamic regulation of these genes. However, this was the same trend seen with RNA-seq analysis of synovial macrophages in Chapter 3. There is likely further posttranscriptional regulation of these enzymes which is modulating their activity beyond their transcription in macrophages. In Rubinow's review of the role of intracrine sex steroid metabolism, synovial macrophages were noted to be more estrogenic while monocyte-derived macrophages appear more androgenic, based on analysis of metabolism following steroid treatments ex vivo (334). Therefore, we might expect differences in steroid metabolism between these cell types, despite the similar patterns of inflammation-induced gene expression we identified in this thesis. Further comparison is warranted, such as investigating the differences in steroid metabolism in ex vivo cell cultures of each, to assess whether inflammation-induced changes in androgen metabolism are conserved between different macrophage populations. This would be important given that analysis of synovial macrophages is primarily carried out on ex vivo samples from OA and RA patients, where increased inflammatory cytokines may be inducing aromatase expression to higher levels than that of healthy synovial macrophages (363, 365, 375, 429).

As we identified increased androgen activation in pro-inflammatory polarised macrophages compared to unpolarised, we assessed whether this would lead to anti-inflammatory regulation capable of driving differential responses to subsequent LPS challenge (Figure 5-6). In Chapter 4 we found that inflammatory polarisation allowed M1-like macrophages to respond to cortisone and limit subsequent inflammatory response to LPS. However, despite distinct differences in enzyme gene expression and androgen metabolism, androgen pre-

treatment did not affect response to LPS in either macrophage polarisation subset (Figure 5-7 and Figure 5-8). We postulated that a combination of cortisol and DHT stimulation could drive synergistic anti-inflammatory effects, particularly as these steroids share some regulatory mechanisms such as inhibition of NFκB by enhancement of IκBα (193, 381). However, no additive effect was seen when compared to cortisol pre-treatment alone. It may be that 24h was not sufficient time for macrophages to metabolise androgens, as our LC-MS/MS analysis used a 48h androgen treatment timepoint to ensure adequate time for measurable conversion. Previous work assessing androgen metabolism in macrophages has used treatment timings between 24h and 5d, however alveolar macrophages have been found to convert androstenedione into measurable quantities of testosterone and 5α-androstanedione in as little as 1-4h (374, 375, 390, 391). Therefore, further work should be carried out using our monocyte-derived macrophage cultures to determine the kinetics of androgen activation and identify the best timepoints for assessing impact of intracrine activation on functional responses.

Importantly, in our LC-MS/MS analysis of androgen treated macrophages, it was not possible to directly follow the metabolic fate of the precursors. More accurate analysis of androgen metabolism could be carried out using radioisotope tracer assays, in which macrophages would be treated with labelled precursors, which would be transferred to their resulting downstream metabolites. Anti-inflammatory effects of direct androgen stimulation on our macrophage polarisation models could also be explored, such as the previously reported testosterone-induced decrease in TNFα release on LPS challenge (372). This would be useful to replicate in our cultures as a positive control to assess relevance of intracrine androgen activation. We could additionally directly assess the relevance of intracrine androgen

metabolism to macrophage anti-inflammatory regulation by treating with enzyme inhibitors (433). For example, inhibition of the SRD5A1 enzyme with drugs such as finasteride would allow us to compare macrophage responses to testosterone treatment with and without its intracrine conversion to DHT.

Our study was limited by low sample sizes and limitations of working with NHS blood donor cones. Measurements of baseline serum androgen levels were used with the goal of separating biological replicates by high and low androgen levels, however these were all found to be within a similar male range and so were analysed together (410). Separation of blood samples by biological sex and age for monocyte-derived cultures would allow us to investigate whether macrophage androgen metabolism contributes to the sex and age differences identified in autoinflammatory diseases such as RA (352). Blood monocyte-derived macrophages from post-menopausal female and age-matched male donors were previously found to have equivalent levels of AR expression and anti-inflammatory response to testosterone treatment, however the higher levels of estrogens have been strongly linked to the enhanced inflammatory function of macrophages commonly measured in seen in pre-menopausal females (382, 434).

It may be that macrophage activation of androgens has more functional relevance in paracrine rather than intracrine signalling. This is supported by our findings in the AMP RA RNA-seq dataset, where synovial macrophages only expressed low levels of the *AR* gene, whilst FLS had moderate expression. Although monocyte-derived macrophages have been shown to express *AR*, further work should assess expression of and signalling at the AR in our monocyte-derived macrophage cultures to see if this differs with RA synovial macrophages (370, 382). Previously

our group confirmed the paracrine signalling of GCs between macrophages and FLS using transfer of conditioned media from one population treated with inactive GCs to the other population that had *Hsd11b1* knocked out (290). Similar work could be carried out using conditioned media from macrophages treated with androgens to assess whether they can generate active androgens capable of regulating fibroblast inflammatory functions, such as the previously reported decrease of IL-6 release by TNFα-activated fibroblasts treated with testosterone (435).

In conclusion, while an inflammation-induced regulation of androgen activating enzymes and androgen metabolism was identified in monocyte-derived macrophage cultures, these did not drive an anti-inflammatory functional shift via intracrine means in our experimental setup. This indicates that macrophages may function as paracrine activators of androgens to aid regulation of further inflammatory cell types. However, further work is required to assess the balance of intracrine and paracrine androgen metabolism in macrophage populations.

Chapter 6 TARGETING MACROPHAGE STEROID METABOLISM TO IMPROVE ANTI-INFLAMMATORY EFFECTS OF GLUCOCORTICOIDS

6.1 Introduction

Therapeutic GCs are widely utilised in the treatment of numerous chronic inflammatory diseases, but their application is limited by potent catabolic side effects on tissues such as bone and muscle (39). Administration of intra-articular (IA) GCs into inflamed RA joints reduces synovial T cells and inflammatory mediators including MMPs, RANKL and TNFα (254-256). In contrast, viability of synovial macrophages are generally unaffected and synovial macrophage numbers can positively predict success of IA GC therapy (45). This implies that rather than simply eliminating inflammatory macrophages, local GC therapy promotes phenotypic shifts in macrophage function, likely driving enhancement of the pro-resolution subsets of synovial tissue macrophages that have been associated with drug-free remission of RA (144, 146).

IA injection offers more site-specific targeting of GCs, with a reduction in systemic GC-associated side effects (247, 253). However, complications of IA GC injections include pain at the injection site, rapid drug elimination via capillary and lymphatic clearance and catabolic side effects on local tissues, as well as systemic effects, such as HPA downregulation, on release of GCs into systemic circulation (436-438). Therefore, there has been an unmet need to identify GC formulations that possess greater specificity for inflammatory cells with physical properties that facilitate IA injection into inflamed joints.

As reviewed extensively by Oliveira et al, numerous distinct formulations of hydrogels have emerged as valuable drug delivery vehicles in the treatment of RA, due to their chemical and mechanical biocompatibility (439). In this chapter, we examined sheared hydrogels made from the polysaccharide gellan as one such hydrogel formulation based on their reported favourable profile of physical properties. These include biocompatibility, improved ease of injectability, stability after injection and tuneable slow-release properties (440, 441).

In Chapter 3 we identified that expression of the GC-activating enzyme, *HSD11B1*, was elevated within inflammatory synovial macrophages in the joints of patients with RA. Then in Chapter 4 we confirmed that this enzyme is able to mediate the local amplification of GCs to downregulate macrophage pro-inflammatory polarisation and functions and upregulate pro-resolution markers. We identified that 11β-HSD1 expression could be used to more selectively target and activate GC precursors within pro-inflammatory macrophages in vitro, whilst in vivo studies previously demonstrated that 11β-HSD1 shapes macrophage polarisation and function within the inflamed arthritic joint (290, 314). Therefore, in this chapter we hypothesised that local inactive GC release from sheared hydrogels could selectively target increased GC metabolism in inflammatory macrophages to downregulate their tissue destructive and pro-inflammatory functions while promoting acquisition of a more pro-resolution phenotype. Furthermore, we hypothesised that sheared gellan hydrogels would be suitable vehicles for slow release of GCs to prolong steroid metabolism and efficacy of anti-inflammatory functions in macrophages.

6.2 Materials and methods

6.2.1 Macrophage culture and polarisation

Monocytes were isolated from human blood cones by RosetteSep™ and differentiated into macrophages for 6d with 20 ng/ml M-CSF as previously described (section 2.3.1).

To assess inactive GC formulations, macrophages were polarised for 24h into M0 (unpolarised), M1-like (20 ng/ml IFNγ and 10 ng/ml TNFα) or M2 (20 ng/ml IL-4) prior to treatment with compounds or soluble GC controls.

6.2.2 Generation of sheared hydrogels

Cortisone and ethanol vehicle loaded hydrogels were generated as detailed in section 2.10.1. Briefly, 1% w/v low acyl gellan gum (KELCOGEL®, USA), 17 ml deionised sterile water, 5% v/v PBS and 10 mM sodium chloride (Sigma-Aldrich, UK) were mixed in a Wheaton™ borosilicate glass spinner flask (Thermo Fisher, UK) and then autoclaved to dissolve and sterilise. 1ml 10mM cortisone or ethanol was added to the flask during gelation under shear on a magnetic stirrer at 100°C for 15 minutes, then stirring at 500 rpm for 2h. Gels were stored at 4°C until testing on cells or rheology.

500 µl of sheared hydrogel formulation was loaded into a 1 ml syringe with 25Gx25mm BD Microlance™ 3 needle (both Fisher Scientific Ltd, UK and 100 µl injected onto a strip of Parafilm® to assess ease of injectability.

Soluble GCs and hydrogels were added at a dilution of 1/100 to polarised macrophages and incubated for 24h. Sheared hydrogels were pipetted into culture media above adherent cell

layer, where they were seen to remain without contact with macrophages. Supernatants were collected carefully by pipette to avoid disrupting or taking up hydrogel, and hydrogels were removed from culture wells with a cell scraper before RNA isolation as detailed below.

6.2.2.1 Rheological analysis

Rheological properties of ethanol vehicle loaded hydrogels were measured as detailed in section 2.10.2 using the Viscometry Shear Rate Ramp programme on a Kinexus Ultra rheometer with 40 mm parallel plates at 1 mm gap (Malvern Panalytical, UK). Data were analysed with rSpace software v1.75.2326 (Malvern Panalytical, UK). Rheological measurements were carried out at 37°C to mimic in vitro cell culture conditions.

6.2.3 Gene expression analysis

Following the appropriate treatment timepoint, RNA was isolated from macrophage cultures with an innuPREP RNA Mini kit (Analytik Jena, Germany), following manufacturer's protocol, as described in section 2.4.1. Yield and purity of samples, as determined by absorbance ratios at 260/280 and 260/230, were measured on a NanoDrop™ ND-1000 spectrophotometer (Wilmington, USA). 350 ng of RNA per sample were reverse transcribed using Applied Biosystems reverse transcription reagents and a GeneAmp® PCR System 27000 machine (Applied Biosystems, UK), following the protocol detailed in section 2.4.2. qPCR analysis was carried out on a QuantStudio™ 5 Real-Time PCR System (Applied Biosystems, UK) with TaqMan probes, listed in section 2.4.3. Expression of genes of interest were normalised to that of 18S.

6.2.4 Cytokine release analysis

Cytokine levels were measured by Ana Crastin, using ELISA as detailed in section 2.6. Supernatants were collected from macrophage cultures following relevant stimulation time. ELISAs were carried out using Invitrogen Human Uncoated ELISA Kits for TNFα and IL-12 p70 (both Thermo Fisher Scientific, UK) and Precoated Quantikine® Human IL-6 ELISA Kit (R&D Systems, UK), following manufacturers' protocols, and ran on a FLUOstar® Omega Microplate Reader (BMG Labech, Germany).

6.2.5 Statistical analysis

Statistical significance was assessed with IBM SPSS Statistics v28.0.1.0 (IBM Analytics, USA) and GraphPad Prism v5.03 and v9.5 (GraphPad Software, USA). Normality of data was tested using a Shapiro-Wilk test for Gaussian distribution. One-way ANOVA with Tukey's post hoc analysis was used to test significance between all groups when multiple treatment groups were present. Two-way ANOVA analysis with Bonferroni multiple comparison post-test was used to compare between macrophage polarisation subsets and treatment groups. Statistical significance is presented as follows: * $P \leq 0.05$, ** $P \leq 0.01$ and *** $P \leq 0.001$.

6.3 Results

6.3.1 Sheared hydrogels possess shear-thinning properties

Different formulations of ethanol vehicle loaded sheared gellan hydrogels were developed to investigate their suitability for injection into arthritic joints. Gels were made with either 1% or 2% of the gelling-agent gellan and 10-50 mM sodium chloride, a crosslinker which facilitates covalent bond formation in the gels.

Injectability of gels was briefly assessed by loading gels into a 1 ml syringe with a 25G needle, the smallest gauge typically used for IA injections, and 100 µl gel injected onto Parafilm® (Figure 6-1) (442). At 1% gellan gels were readily injectable by hand to form a straight line. Conversely, 2% gels were difficult to inject by hand and formed fragmented lines on the Parafilm®.

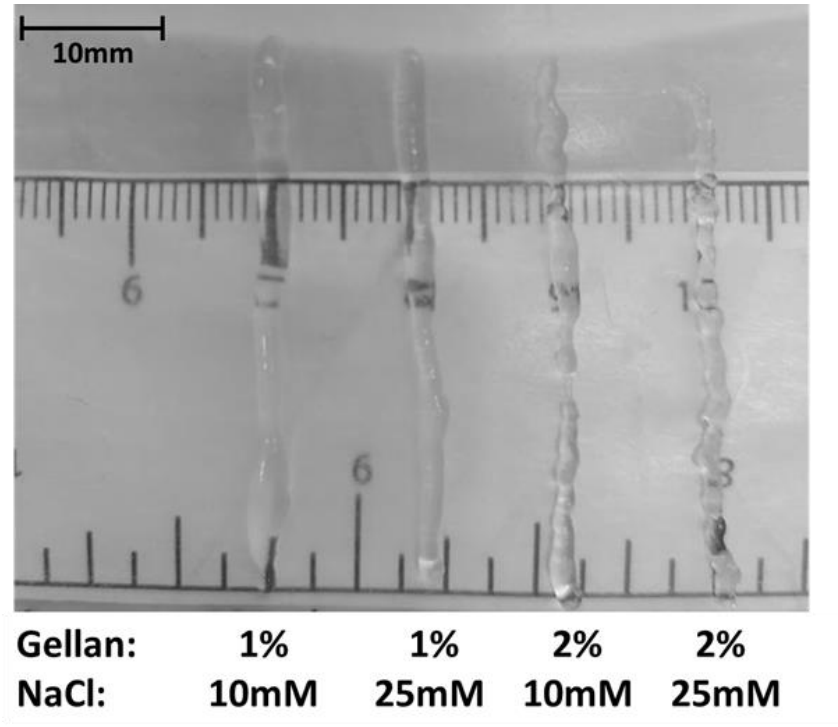

Figure 6-1 1% gellan gels have better injectability than 2% gels

Representative image of 100 µl sheared hydrogels (1% or 2% gellan and 10 mM or 25 mM sodium chloride [NaCl]) injected using a 25G syringe onto Parafilm®.

The effects of gellan, crosslinker concentration and ethanol vehicle on physical viscometric properties of hydrogels were further assessed by rheological analysis (Figure 6-2). This was done to select the best formulation of hydrogel for greater shear-thinning behaviour and ease of injectability.

To assess shear-thinning properties, we tested the relationship between shear rate and shear stress. All gels showed a non-linear relationship between shear rate and shear stress (Figure 6-2 A). While all of the 1% gellan gels showed similar shear stress with applied shear rate despite differences in sodium chloride concentration, the 2% gellan gels required far higher shear stress, in line with their poor injectability. Similarly, although all gels showed a non-linear relationship between shear rate and shear viscosity, the 2% gels possessed greater shear viscosity than 1% gels (Figure 6-2 B). Shear rate ramp analysis (Figure 6-2 C) showed that the viscosity of all gels decreased as shear rate was increased (ramp up). This relationship was also seen with application of decreasing shear rates (ramp down) following ramp up, showing that this shear-thinning behaviour is reversible and therefore should be retained in synovial joints following IA injection.

These data show that 1% gellan gels are more suitable for application in IA injection, as they possessed greater shear-thinning behaviour than 2% gellan gels. Sodium chloride concentration did not have any measurable effect on this behaviour, nor did ethanol vehicle appear to impede this behaviour.

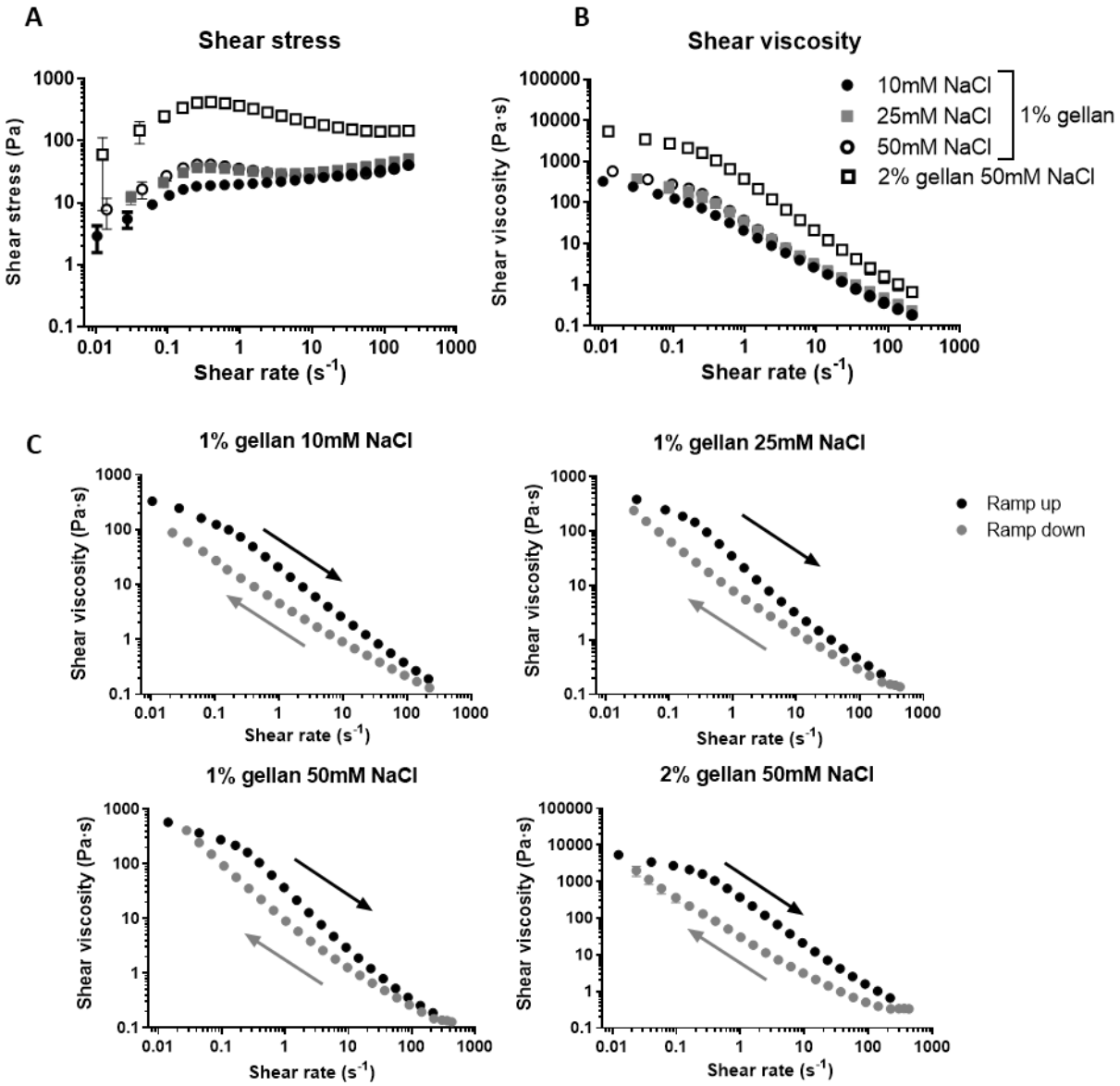

Figure 6-2 Sheared gellan hydrogels have reversible shear-thinning behaviour

Rheological properties of sheared hydrogels were assessed using a Kinexus rheometer. (A) Shear stress (pascals, Pa) and (B) shear viscosity (pascal seconds, Pa·s) of gels at applied shear rates (s^{-1}) during shear rate ramp up. (C) Shear viscosity of each gel during shear rate ramp up (black circles) and ramp down (grey circles). Data are presented as mean ± SEM of 3 technical repeats of each gel.

6.3.2 Cortisone-loaded hydrogels induce pro-resolution gene expression

Cortisone-loaded sheared hydrogels were generated to examine targeting of inflammatory macrophage pre-receptor GC metabolism with a slow-release injectable hydrogel. Macrophages were polarised for 24h to drive differential 11β-HSD1 expression and activity (as confirmed previously in Chapter 4) and then incubated for 24h with hydrogels or soluble cortisone (Figure 6-3). As it was not known how much drug would be released from formulations, the maximum dose of cortisone was loaded into hydrogels, resulting in an assumed maximum treatment dose of 5 μM, and this was compared to treatment with 1 μM soluble cortisone as assessed previously.

Assessment of gene expression by qPCR showed that both M1-like (IFNγ/TNFα) and M2 macrophages upregulated the GC-inducible gene *GILZ* on soluble cortisol treatment as expected (M1-like control vs cortisone gel treated: 4.1-fold, P≤0.001; M2: control vs cortisone gel treated: 4.2-fold, P≤0.05; Figure 6-3 A). However, only M1-like macrophages showed *GILZ* induction on cortisone hydrogel treatment (control vs cortisone gel treated: 5.4-fold, P≤0.001).

Treatment with soluble cortisone (M1-like control vs cortisone: 2.1-fold, P=0.5995) and cortisone hydrogels (M1-like control vs cortisone: 2.2-fold, P=0.3578; M1-like cortisone hydrogel vs blank hydrogel: 2.3-fold, P=0.5695) lead to a nonsignificant downregulation in *TNFα* expression in M1-like macrophages (Figure 6-3 B).

Soluble cortisone and cortisone-hydrogels significantly induced expression of the scavenger receptor *CD163* in M1-like macrophages (control vs cortisone treated: 5.7-fold, P≤0.001; control vs cortisone gel treated: 8.4-fold, P≤0.001) although there was no significant

difference in expression between soluble and hydrogel cortisone stimulation (P≥0.9999; Figure 6-3 C). In contrast, no changes in expression for either *TNFα* or *CD163* were observed in M0 or M2 macrophages with soluble or hydrogel cortisone.

These data show that cortisone hydrogels are able to release their GC content such that pro-inflammatory polarised macrophages can metabolise and respond to GCs. This promoted the upregulation of anti-inflammatory genes, implying a shift in polarisation to pro-resolution functions.

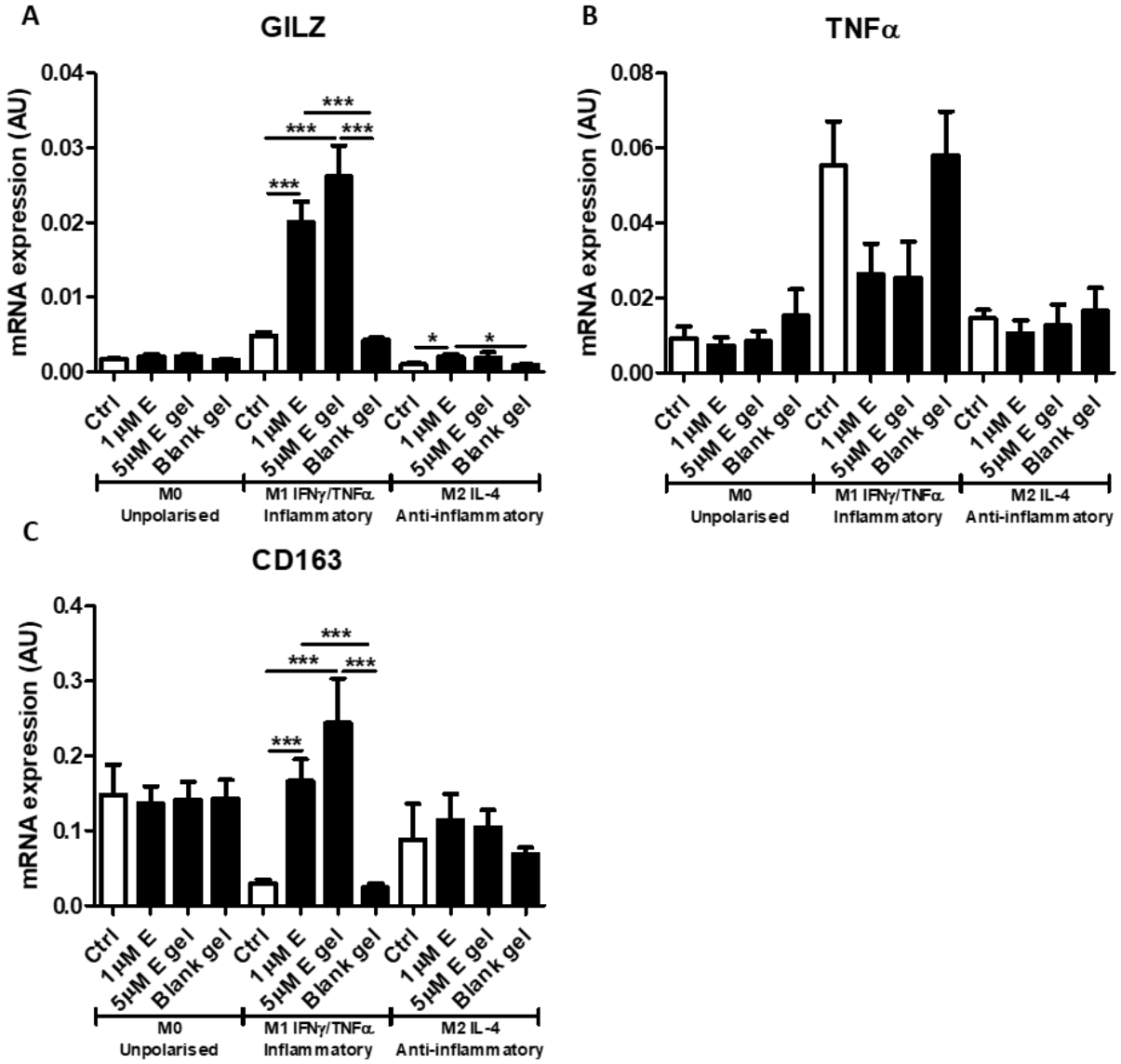

Figure 6-3 Cortisone-loaded hydrogels upregulate pro-resolution gene profiles selectively in M1 macrophages

RNA expression (AU) of (A) *GILZ*, (B) *TNFα* and (C) *CD163* in macrophages polarised for 24h to unpolarised (M0), pro-inflammatory M1-like (IFNγ and TNFα) and M2 (IL-4) and then treated for 24h with vehicle (Ctrl), 1000 nM cortisone (E), 5000 nM cortisone loaded in sheared hydrogel formulation (E gel) or ethanol vehicle loaded sheared hydrogel (Blank gel) as measured by qPCR (n=4, blank gel groups n=3, M2 groups n=3). Data are presented as mean ± SEM and statistical significance was determined using two-way ANOVA with Bonferroni multiple comparisons post-test. * P≤0.05 and *** P≤0.001.

Expression of the pro-inflammatory cytokine genes *IL-6* and *IL-12A* were assessed in M1-like macrophages following incubation with hydrogel cortisone, compared to those treated with soluble cortisone (Figure 6-4). However, expression of neither cytokine was decreased by cortisone treatments, likely due to the timing of stimulations.

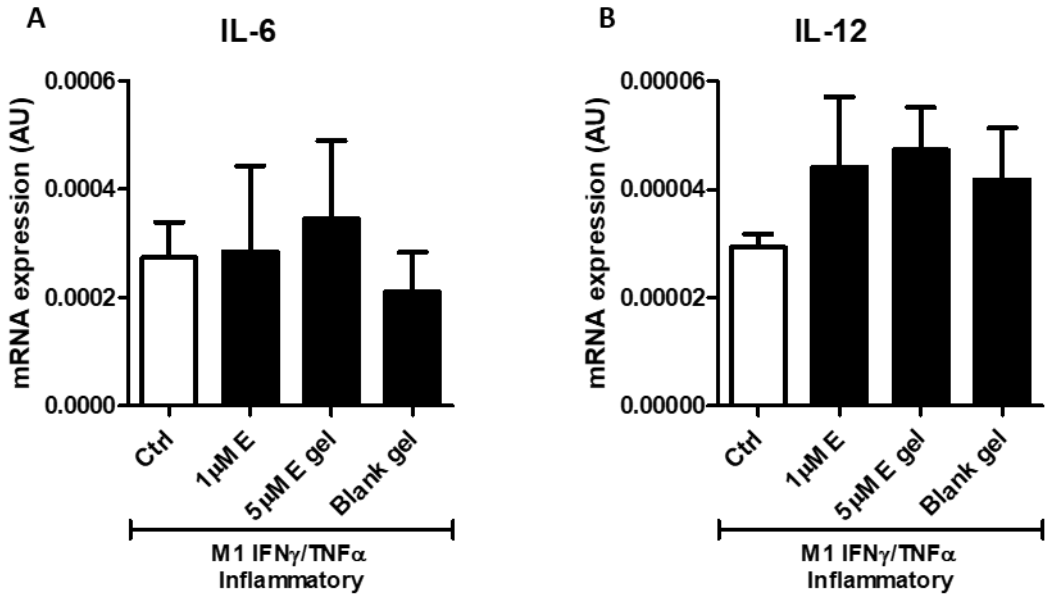

Figure 6-4 Optimisation is required for further inflammatory cytokine gene expression readouts in cortisone hydrogel bioassay

RNA expression (AU) of (A) *IL-6* and (B) *IL-12A* in macrophages polarised for 24h to pro-inflammatory M1-like (IFNγ and TNFα) and then treated for 24h with ethanol vehicle (Ctrl), 1000 nM cortisone (E), 5000 nM cortisone loaded in sheared hydrogel formulation (E gel) or ethanol vehicle loaded sheared hydrogel (Blank gel) as measured by qPCR (n=4, blank gel group n=3). Data are presented as mean ± SEM and statistical significance was determined using one-way ANOVA with Tukey's multiple comparisons test.

6.3.3 Blank hydrogel formulations have pro-inflammatory properties

The effects of cortisone hydrogel formulations on secretion of pro-inflammatory cytokines were assessed by ELISA in M0 and M1-like macrophages (Figure 6-5).

There was a trend towards decreased secretion of TNFα in M1-like macrophages treated with cortisone hydrogels though this was not significant (control vs cortisone hydrogel: 2.0-fold, P≥0.9999), however the ethanol vehicle-loaded blank gels drove strong and significant release of this cytokine compared to all other groups (control vs blank gel: 2.4-fold, P≤0.01; Figure 6-5 A).

A similar effect was seen with IL-6 (Figure 6-5 B). Blank gel treatment of M0 macrophages drove significant secretion of IL-6 (control vs blank gel: 6.0-fold, P≤0.01), while in M1-like macrophages a similar trend was seen although this was not significant (control vs blank gel: 6.5-fold, P=0.1960).

Both M0 and M1-like macrophages saw increased secretion of IL-12 p70 (Figure 6-5 C) following treatment with blank hydrogels (M0: control vs blank gel P≤0.001; M1-like: control vs blank gel: 4.5-fold, P≤0.001). A trend towards decreased IL-12 p70 output was seen with cortisone hydrogel treatment in M1-like macrophages however this was not significant (control vs cortisone hydrogel P≥0.9999).

Collectively these data show that while cortisone-loaded sheared hydrogels can upregulate expression of pro-resolution markers in M1 macrophages, the pro-inflammatory effects of blank gels on cytokine release emphasise the need for further optimisation to promote anti-inflammatory functions of GCs, such as improved sterilisation procedures during hydrogel generation.

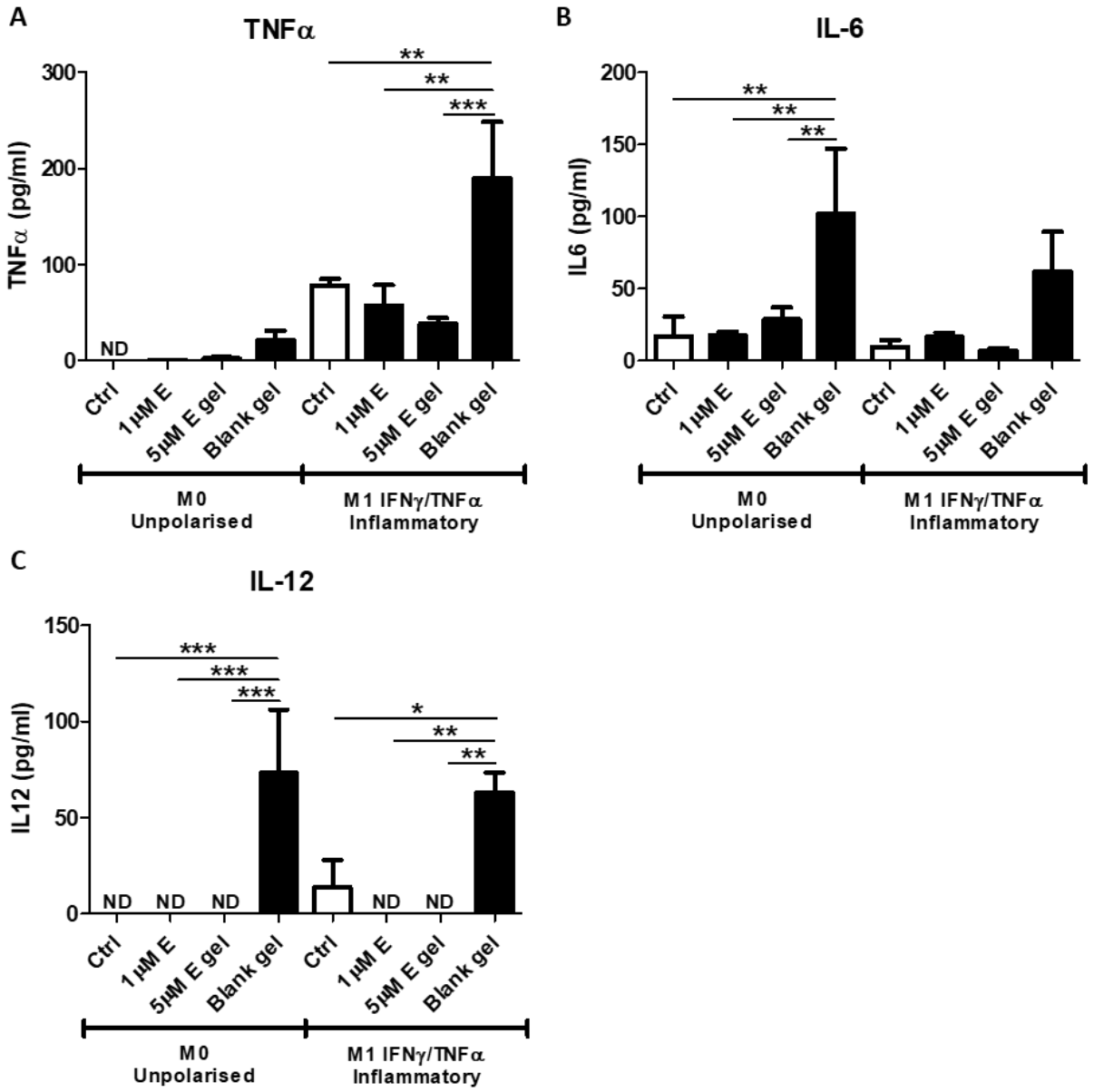

Figure 6-5 Current sheared hydrogel formulations induce pro-inflammatory cytokine output

Cytokine concentration (pg/ml) of (A) TNFα , (B) IL-6 and (C) IL-12A in macrophages polarised for 24h to unpolarised (M0) or pro-inflammatory M1-like (IFNγ and TNFα) and then treated for 24h with vehicle (Ctrl), 1000 nM cortisone (E), 5000 nM cortisone loaded in sheared hydrogel formulation (E gel) or ethanol vehicle loaded sheared hydrogel (Blank gel) as measured by qPCR (n=4, blank gel groups n=3). Data are presented as mean ± SEM and statistical significance was determined using two-way ANOVA with Bonferroni multiple comparisons post-test. * P≤0.05, P≤0.01 and *** P≤0.001. ND, not detected.

6.4 Discussion

Given the role of macrophages in inflammatory disease pathophysiology, they represent important targets for cellular anti-inflammatory interventions. Earlier work focused on depletion of synovial macrophages in RA, using compounds such as clodronate, however in-depth transcriptomic analyses have revealed distinct populations of protective synovial macrophages vital for disease resolution (120, 146, 443). Thus, more recent macrophage targeted novel therapeutics have explored shifting synovial macrophage polarisation from pro-inflammatory and tissue destructive to anti-inflammatory and tissue reparative.

Previous novel therapeutics targeting GCs to macrophages have included liposomes, drug carriers formed of phospholipid bilayers. These have been used to deliver primarily active GCs such as prednisolone intravenously, where they were more selectively taken up by macrophages via phagocytosis and reduced symptoms in arthritic models (444, 445). However while these were found to promote M2-like pro-resolution markers such as CD163 and CD206 in vitro, these compounds only drove decrease in M1-like macrophages, and sometimes also M2-like, in vivo using murine models of arthritis (446). This implies that this intervention would not be successful in promoting resolution of arthritis in more chronic human disease, where pro-resolution macrophages have been shown to be important for disease remission.

Compartmentalised delivery of therapeutics, such as IA, decreases systemic exposure to drugs such as GCs. It is also possible to target GCs in a temporal manner, such as “flare-responsive” hydrogels containing the active synthetic GC triamcinolone acetonide that were broken down to release steroid by MMPs in the RA synovial fluid or thermo-responsive gels structurally

sensitive to the increased heat of the inflamed joint (447, 448). However, this still risks exposing local bone and cartilage to GCs and associated catabolic effects, as this mechanism does not target GCs to selective populations. Inactive GCs such as cortisone offer targeting of GCs to cell populations expressing the activating enzyme 11β-HSD1. We have previously shown that synovial macrophages upregulate the gene *HSD11B1* with increasing inflammation in RA (Chapter 3) and that, in vitro, this enables metabolism of inactive GCs to drive a functional shift in macrophages from pro-inflammatory M1-like to more pro-resolution anti-inflammatory M2-like characterised by decrease in pro-inflammatory cytokines and increase in expression of pro-resolution and anti-inflammatory markers (Chapter 4). Therefore, targeting inactive GCs to this population in the inflamed RA joint could promote the anti-inflammatory pro-resolution effects of GCs, while limiting the deleterious catabolic effects on stromal cells.

Gellan is a hydrophilic polysaccharide derived from glucose metabolism by the bacterium *Sphingomonas elodea* (449). This compound is an approved food additive due to its proven biocompatibility, heat- and pH-stability and its ability to gel in solution at a lower concentration than other polysaccharides such as carrageenan. These key properties also make it suitable for pharmaceutical use. Gellan can also be used to form hydrogels: polymer chain networks with potent hydrophilic properties. These provide improved biocompatibility and biodegradability due to water content and tuneable encapsulation properties for slow drug release (450). Slow release of GCs into the arthritic joint space could alleviate the undesired catabolic side effects of GCs while minimising loss of drug from the site due to rapid turnover of synovial fluid (413, 414).

The injection of GC-hydrogels into the articular space, while allowing site-specific delivery of drug, poses further problems including the painful discomfort of IA injection and the potential impact of long-lasting drug formulations on joint movement. These issues can be overcome by applying shear forces to hydrogels during gelation. These resulting sheared "fluid gels" possess a higher viscosity at rest, but a lower viscosity on application of shear. Consequently, the forces applied during injection should cause the gel to liquify, improving injectability and patient comfort and reducing time taken to inject (440, 451). Additionally, the shear-thinning properties of fluid hydrogels should prevent the gel impeding movement, as shear forces within the joint induced by movement should promote decreased viscosity, and therefore malleability, of the gel. These properties have been shown in in vivo models of osteoarthritis, however have not yet been assessed in targeting inactive GCs to synovial RA macrophages (452, 453).

As part of a collaboration with Professor Liam Grover's group at the University of Birmingham Health Technologies Institute we generated sheared gellan hydrogels that demonstrated shear-thinning properties (Figure 6-3). 2% gellan gels proved too thick to easily inject with a 25G syringe, but 1% gellan hydrogels could be injected smoothly, and so these were investigated further. The ability of gellan to form gels at low concentrations is dependent on cations present in solution, such as Na^+ from sodium chloride (454). Therefore, the concentration of this crosslinker added to solution should allow finetuning of gel properties such as viscosity. We did not see any differences in properties such as shear viscosity or injectability with the 1% gellan gels on changing sodium chloride concentration, however the crosslinker concentration could further modify properties affecting gel suitability not yet investigated, such as drug release.

The gellan hydrogels demonstrate shear-thinning behaviour, however at lower shear rates (around ≤0.1s^{-1}) they all appear to exhibit Newtonian behaviour characterised by relatively unchanging shear viscosity with increasing shear rate. This strongly implies the gels have viscoelastic properties as expected in sheared hydrogels, presenting with an elastic phase characterised by resistance to deformation and a viscous phase characterised by increased flow (455). While increasing the gellan content from 1% to 2% increased the viscosity of hydrogels and made them difficult to inject by hand, changing the crosslinker content did not appear to affect this. Further rheological characterisation is needed to confirm this and how these properties affect injectability, as the shear rate applied to the hydrogel during injection would need to be within this shear-thinning range for sufficient improvement to injectability. The viscoelastic properties can be further interrogated using rheological analysis of the elastic and viscous modulus by frequency sweeps to understand the behaviour of the hydrogels (455). The proportion of gellan, concentration of crosslinker and conditions of shearing and gelation (time, temperature and shear force applied) should all be further investigated to determine their effects on viscoelastic properties for injection and also their impact on GC drug loading and release to ensure steady release of drug.

Although there was insufficient time to investigate GC release in this study, this could be carried out by ELISA analysis of loaded hydrogels incubated for set timepoints. Additionally, although we tested cortisone as we previously investigated the role of pre-receptor metabolism of this endogenous steroid in macrophage functions, other GC formulations may be more suitable for hydrogel formulations and drug delivery into synovial fluid. A water-soluble GC such as prednisone sodium succinate would have higher affinity for the hydrogel formulation and so would likely provide slower release into the synovial fluid, while GCs with

hydrophobic highly branched esters such as hexacetonide residues would instead have higher affinity for synovial fluid and be retained there (247). Although ethanol loaded hydrogels were confirmed to have shear-thinning behaviour (Figure 6-2), we did not test other vehicles such as water. The use of water-soluble GCs could improve viscoelastic properties of sheared hydrogels as the water vehicle may better facilitate shear-thinning behaviour of the gellan hydrogel than ethanol.

In this study we were only able to investigate the effects of cortisone hydrogels on macrophages at a 24h stimulation timepoint, however longer-term stimulations would be important in showing the effects of long-term cortisone release on macrophage functions. Although we predict that with the reciprocal regulation of 11β-HSD1 by inflammation and GC stimulation (discussed in Chapter 4) inflammatory macrophages will initially respond to cortisone and downregulate inflammatory functions, including ability to respond to inactive GCs, further characterisation is needed. Previous research has shown that longer-term GC stimulation promotes different macrophage functions, such as preferentially enhancing further macrophage recruitment on LPS stimulation (230). Furthermore, the effect of cortisone hydrogel treatment on other cell populations present in the inflamed synovia should also be assessed. As reviewed in introduction section 1.3.3, GC stimulation affects cells in diverse ways depending on cell type and stimulation context. Of particular importance is the effect of inactive GC hydrogels on stromal cell populations. Although RA synovial fibroblasts were shown to express *HSD11B1* (Chapter 3), this expression was not inflammation-responsive, as was seen in macrophages. While GC-induced anti-inflammatory regulation of pathogenic synovial fibroblasts may be beneficial, we are aiming to develop hydrogels that

preferentially target macrophages to avoid the catabolic effects of GCs on the stromal cells of muscle and bone, and fibroblast 11β-HSD1 may enhance this.

In this chapter, we generated cortisone-loaded hydrogels which drove induction of GC-responsive gene *GILZ* (Figure 6-3 A) and scavenger receptor *CD163* (Figure 6-3 C) selectively in M1-like polarised macrophages. This confirms that inactive GC-loaded sheared hydrogels are a potential novel route for more selectively targeting GCs to inflammatory macrophages during RA flares, where their expression of 11β-HSD1 is upregulated (as shown in synovial tissue in Chapter 3 and in vitro in Chapter 4). The upregulation of *CD163* is particularly interesting as this implies these inflammatory macrophages are shifting to a more pro-resolution M2-like phenotype in addition to downregulation of inflammatory factors (419). As *CD163* is one of the genes enriched in clusters of synovial tissue macrophages previously identified in healthy and remission-associated synovium, it would be important to investigate the modulation of further markers of this protective cluster such as CD206 and MerTK (146).

Despite these promising data, we were unable to see successful downregulation of inflammatory cytokine expression or output (Figure 6-3; 6-4; 6-5). The timepoints assessed may not be suitable for measuring acute inflammatory cytokines. However, more critical is the induction of inflammatory cytokine secretion by our blank hydrogel formulation (Figure 6-5). Gellan is an FDA-approved food additive and is currently being investigated in numerous drug delivery and tissue engineering mechanisms, where it has been reported not to cause cytotoxicity in multiple cell types (456, 457). The mechanical properties of hydrogels such as gellan have previously been reported to affect macrophage function, as stiffness of hydrogels was shown to promote either inflammatory or anti-inflammatory functions of macrophages

(458, 459). However, while only the ethanol vehicle loaded blank gels were assessed for rheological properties, we would expect the cortisone loaded gels to have the same viscoelastic properties, as the cortisone is fully soluble in ethanol. The cortisone-loaded hydrogels did not show these inflammatory effects. This may be because the 11β-HSD1^{high} M1-like macrophages able to metabolise cortisone into anti-inflammatory cortisol and cancel out pro-inflammatory effects of the gel formulation. However, this was not expected within the 11β-HSD1^{low} unpolarised M0 macrophages, which, as shown in Chapter 4, were unable to meaningfully metabolise to cortisone in order to limit response to an inflammatory challenge. It is unlikely that they would be able to respond sufficiently to cortisone in hydrogels and so we would expect similar inflammatory effects in M0 macrophages from both cortisone and vehicle hydrogels. Therefore, the pro-inflammatory effects of the ethanol gels could be due to a contaminant introduced during gel generation, despite autoclaving of the hydrogel prior to shearing. As this was an initial pilot study to assess feasibility of targeting inflammatory macrophage GC metabolism with sheared hydrogels, there is considerable scope to optimise the method of hydrogel generation.

Further functional assays are required to assess suitability of gellan hydrogels as a vehicle for targeting inactive GCs to macrophages. This includes additional analysis of the effects of these hydrogels on macrophages, including viability assays to ensure hydrogels do not cause cell death and also imaging to investigate whether macrophages directly interact with gellan. Previous research into betamethasone loaded gellan hydrogels found they did not promote death of THP-1 macrophages, however they did not look further into the interactions between macrophages and gellan (460). Macrophages can recognise numerous polysaccharide species via different receptors, including scavenger receptors, mannose receptors and TLRs, with the

particular saccharide units defining receptor specificity and resulting functional outcome. For example, TLR4 ligation of chitosan induces inflammatory activation of macrophages, while β-glucan polysaccharides bind to the receptor dectin-1 to instead promote macrophage phagocytic activity (461, 462). In our in vitro stimulation assays, macrophages were not in contact with the gellan hydrogels, however future work involving cultures of monocyte-derived macrophages seeded on top of layers of gellan hydrogel would allow for investigation of macrophage interactions with gellan.

The interactions between macrophages and gellan hydrogels are particularly important when considering the application of these hydrogels in the inflamed arthritic joint. As gellan is a polysaccharide, gellan hydrogels are sensitive to degradation by the enzyme lysozyme, which is produced by macrophages (463). Moreover, the levels of lysozyme in the RA synovia can be far higher than in healthy synovia, which may result in degradation of gellan hydrogels and rapid release of encapsulated GCs. Additionally, the pH of RA synovial fluid is lower than that of healthy synovial fluid, and lower pH values have been found to increase gellan hydrogel rigidity and slow release of drugs (466-468). Therefore, further in vitro work assessing the impact of macrophage and synovial fluid interaction with gellan hydrogels should be carried out to assess kinetics of GC drug release, such as the effects of hydrogel incubation in synovial fluid as previously carried out by Joshi et al in their investigation of MMP-sensitive GC loaded hydrogels (447).

The next stage of this research is in vivo testing to examine the efficacy of inactive GC loaded sheared hydrogels in arthritic disease. There is ongoing work being carried out in our group to test IA injection of similar gellan sheared hydrogels in the knee joints of TNF-tg arthritis model

mice. This work will also determine the longevity of steroid release in vivo and how decreasing rate of GC release improves anti-inflammatory function of inactive GCs on macrophages and other cells of the inflamed synovia.

In conclusion, in this chapter we carried out initial proof of principle research into the feasibility of sheared gellan hydrogels as inactive GC drug carriers to target synovial macrophage inflammatory GC metabolism. We were able to generate shear-thinning injectable hydrogels which could selectively induce GC signalling and pro-resolution polarisation in inflammatory macrophages with these cortisone gels. Further refinement of gel generation and formulation is required prior to in vivo testing in arthritis model mice; this should focus on optimising GC release kinetics, macrophage anti-inflammatory functional assays and stimulation effects on further cell types.

Chapter 7 GENERAL DISCUSSION

Rheumatoid arthritis is a complex and heterogenous inflammatory disease affecting around 1% of the Western population, where it drives mortality and comorbidities such as CVD and cancer (1, 2, 41). Because of their central role in mediating synovitis and joint destruction, macrophages represent important drug targets for RA (120, 121, 130). An inflammation-induced dysregulation of steroid hormones, including increased GCs and decreased androgens, has been linked to the onset and severity of RA (358, 359, 363, 365). As macrophages are known to be acutely regulated by these steroids, and in some cases metabolise them, we hypothesised that inflammatory steroid metabolism within macrophages may contribute to RA inflammatory pathology and represent a novel therapeutic target (273, 278, 374, 375). Therefore, in this thesis we investigated the interplay between macrophage inflammatory function and steroid metabolism: exploring how macrophage polarisation influences intracrine steroid metabolism and assessing its impact on inflammatory function.

Our research found that key GC and androgen activating enzymes were differentially regulated in distinct inflammatory macrophage subsets in RA. In vitro investigation revealed that this metabolism in macrophages is acutely regulated by inflammatory stimulation. Intracrine GC metabolism promoted anti-inflammatory regulation of macrophages, while analysis of androgen metabolism suggested that macrophages likely play a role in paracrine activation and action of androgens. As these changes appear to relate to distinct macrophage subsets involved in RA disease resolution and promotion, further work should more intricately

interrogate metabolic function of these subsets in synovial tissue to identify their significance to disease.

7.1 Macrophage inflammatory steroid metabolism

Previous studies have highlighted a dysregulation of steroid hormones in RA at both the systemic level, in terms of adrenal production, and the local synovial tissue level, using isolated synoviocytes. Collectively these data show a shift towards decreased androgen production at the apparent expense of increased GCs (339, 356, 358, 359, 361, 365). GC-activation by 11β-HSD1 has been shown to mediate macrophage anti-inflammatory responses, and myeloid 11β-HSD1 action is important for the endogenous and physiological GC-mediated resolution of murine arthritis models (272, 290, 314). As such we hypothesised that synovial macrophages are central to steroid dysregulation in the inflamed RA synovium, with expression of *HSD11B1* and further steroidogenic enzymes changing with inflammation and disease severity. Therefore, we first examined the expression of steroidogenic enzymes in a bulk RNA-seq dataset of FACS-sorted human RA synoviocytes and then assessed the contribution of these enzymes to inflammatory profiles using in vitro macrophage cultures.

HSD11B1 expression is known to be induced on inflammatory polarisation of macrophages, and higher 11β-HSD1 activity has been found to predict progression to persistent disease and to correlate with measures of systemic inflammation in RA patients (309, 310). The importance of myeloid 11β-HSD1 has been demonstrated in numerous murine polyarthritis models, including the K/BxN serum transfer and TNF-tg models. Here, LysM-cre mediated knockout of *Hsd11b1* exacerbated inflammatory disease, delayed resolution, and reduced therapeutic response to GCs (272, 290, 314). Previous analysis of synovial samples from RA patients has provided conflicting data on the expression of 11β-HSD1 in macrophages, with some studies showing minimal expression, or higher expression of the GC inactivator 11β-

HSD2 (289, 309). Our data suggests that 11β-HSD1 expression in synovial macrophages is closely linked to inflammatory disease state, which aligns with previous in vitro studies that showed the impact of polarisation on expression (104, 273, 291, 292). Furthermore, this expression was identified in a synovial tissue subset linked with progression of severe RA: those expressing *SPP1*, the gene for the protein osteopontin known to have multiple pro-inflammatory effects on immune cells (145, 146). Therefore, synovial macrophage GC pre-receptor metabolism in distinct inflammatory subsets could have as important of a role in human RA disease pathology and therapeutic response to GC as shown in murine studies.

As RNA-seq data implied that macrophages could be contributing to intracrine and paracrine GC and androgen metabolism, we used monocyte-derived macrophage cultures to investigate the relationship between inflammatory polarisation and function and steroid metabolism. Our lab group has previously shown the importance of 11β-HSD1 in paracrine signalling of GCs between macrophages and FLS, however we hypothesised that this enzyme would also facilitate intracrine metabolism of GCs in inflammatory macrophages (290). As previously reported, inflammatory polarised macrophages upregulated 11β-HSD1, and this enabled them to respond to inactive GCs and regulate inflammatory profiles (104, 278, 295). We identified a shift from pro-inflammatory functions, such as release of TNFα, towards a more pro-resolution phenotype with expression of the scavenger receptor *CD163*. This phenotypic shift is relevant in the context of RA as a reduction of TNFα levels is considered a successful outcome of IA GCs (254). Additionally, CD163 is a known marker of synovial tissue macrophage subsets associated with maintenance of healthy synovium, and with remission from RA and protection from disease in animal models of arthritis (120, 141, 142, 146). These data strongly suggests that inflammatory macrophage 11β-HSD1 could be a therapeutic target to maximise

the anti-inflammatory actions of GCs by promoting a shift in macrophage polarisation towards more pro-resolution subsets. This targeting could reduce the catabolic actions of GCs on muscle and bone cells, while also avoiding the excess activation of GCs by inflammatory- and GC-activated fibroblasts (284, 285).

Our analysis of the AMP RA RNA-seq dataset identified that androgen activating enzymes were differentially regulated in inflammatory macrophages, including the two major extragonadal androgen activators *AKR1C3* and *SRD5A1* (336). We used our monocyte-derived macrophage cultures to investigate whether intracrine androgen metabolism could regulate inflammatory macrophage function in a similar manner as GCs. Pro-inflammatory polarisation drove a decrease in *AKR1C3* expression and an increase in *SRD5A1* expression compared to unpolarised macrophages, similar to the changes seen with inflammation in the AMP dataset. Despite these transcriptional changes, pro-inflammatory polarisation led to a general increase in androgen metabolism by macrophages, including greater generation of androgens via AKR1C3. Although previous studies of in vitro treatment of macrophages with androgens has noted general anti-inflammatory effects, such as decreased pro-inflammatory cytokines and ROS, there do not appear to be reports of the effects of inflammatory activation of macrophages on androgen metabolism (380, 383). Interestingly, inflammatory treatment of macrophages was found to decrease both the cholesterol transporting protein StAR, the first stage of de novo steroid synthesis, and the estrogen activator aromatase (377, 469). This may help to facilitate the increased androgen metabolism we identified with inflammatory M1-like polarisation, however further research would be needed to confirm this.

An important feature of steroidogenesis that was not addressed in this work is the capacity of many steroidogenic enzymes for conversion of multiple steroids. Most pertinent to our exploration of GC and androgen activation is the ability of SRD5A enzymes to generate 5α-reduced forms of GCs that have a far lower affinity for the GR. The high expression of SRD5A isozymes in the liver facilitates the clearance of GCs, with 5α-reduced GCs converted by 3α-HSDs into the tetrahydro- forms excreted from the body (170). Inhibition of 5α-reductases have been shown to enhance local tissue levels of GCs in patients with benign prostatic hyperplasia, and in vitro 5α-reductase inhibition was seen to promote GC-mediated regulation of lipogenesis in hepatocytes (470, 471). The inflammatory induction of *SRD5A1* identified in this thesis may function to clear GCs following their activation by the similarly inflammation-induced 11β-HSD1. Whether this mechanism is present in macrophages does not yet appear to have been studied, therefore the functional relevance of the SRD5A enzymes in macrophages and their different GC or androgen substrates remain to be determined. Furthermore, analysis of the AMP RNA-seq dataset showed that multiple components of the androgen and estrogen pathways were found to be modulated in macrophages with inflammation, such as the steroid transporter protein *SLCO4A1*, estrogen inactivator *HSD17B14* and androgen inactivator *AKR1C2*. Given the important cross-regulation of androgen and estrogen metabolism with inflammation, and within the RA synovia, these pathways should be investigated in more detail (361). This is of particular importance as androgens can be converted to estrogens via aromatase, an enzyme known to be upregulated by inflammatory stimulation in many cell types, with conflicting reports in macrophages (364, 375, 377, 378).

We were unable to demonstrate that metabolism of androgens could downregulate macrophage inflammatory responses to LPS challenge and therefore could not prove our hypothesis that intracrine androgen metabolism regulates macrophage inflammatory function. Our data suggests that macrophages could instead function as paracrine androgen activators, with inflammatory stimuli promoting the metabolism of inactive precursors into active androgens that can act on neighbouring AR-expressing cells. From our analysis of the AMP RNA-seq data this population is likely to be fibroblasts as they expressed higher levels of AR compared to synovial leukocyte populations, though this expression was not affected by disease severity or inflammation. There is limited data in the literature on the effects of androgen treatment on fibroblasts, particularly RA FLS, however testosterone was reported to downregulate the TNFα-induced secretion of IL-1β and IL-6 in a study of FLS isolated from CIA model rats and similar results were seen with a DHT-treated FLS cell line (362, 435). Paracrine androgen metabolism may also influence further cell types in the inflamed RA synovia. This includes T and B cells, which are known to express AR, with androgens having broadly anti-inflammatory actions including decreasing autoantibody production in systemic lupus erythematosus (SLE) (472, 473). However T and B cells also possess the enzymes necessary for intracrine androgen metabolism, such as SRD5A1, therefore care would need to be taken during investigation of paracrine signalling between macrophages and lymphocytes (346).

Our analysis of the RNA-seq data in Chapter 3 implies that androgen metabolism is distinctly regulated in different synovial macrophages, with *SRD5A1* expression concentrated particularly in pathogenic S100A12+ macrophages, while *AKR1C3* expression was found in the protective TREM2+ subset. This finding, recapitulated in our qPCR analysis of M0 and M1-like

polarised macrophages, suggests that pro-resolving synovial macrophages could act as activators of early-stage androgens by AKR1C3, while pro-inflammatory macrophages generate more late-stage potent androgens or inactivation of GCs via SRD5A1. Therefore, it may be that upregulating actions of AKR1C3 while decreasing those of SRD5A1 promotes a polarisation shift in inflammatory macrophages towards more pro-resolution functions. However, whether this would be through a cell-autonomous regulation of phenotype via intracrine steroid signalling or transcriptional regulation, or through crosstalk with neighbouring cells such as fibroblasts remains to be determined.

7.2 Translational application of our findings

Based on the established anti-inflammatory role of 11β-HSD1 within inflammatory macrophages, we hypothesised that this inflammation-induced GC metabolism could be used to target novel GC formulations to promote pro-resolution macrophage function. During this project we considered multiple approaches to achieving successful packaging of inactive GCs for macrophage uptake. This included liposomal packaging of GCs, which should allow selective macrophage targeting by phagocytic uptake (444). Similarly, we assessed conjugation of GCs to an inflammatory chemokine, which aimed to target that GC to inflammatory macrophages expressing that chemokine receptor (474). We chose to focus on sheared gellan hydrogels as their proven biocompatibility, tuneability and injectability makes them an attractive option for IA injection (440). Although we confirmed shear-thinning behaviour and selective modulation of gene expression in inflammatory M1-like macrophages via 11β-HSD1, the induction of pro-inflammatory cytokine secretion induced by vehicle-loaded gels shows further optimisation is required prior to in vivo testing. While this can likely be rectified in the short-term by improvements to hydrogel synthesis in our lab, there are further issues for application for IA injection that need to be considered in future work.

Current IA GC formulations used in UK clinical practice are fluid suspensions of active GCs resistant to 11β-HSD metabolism such as methylprednisolone acetate. These have a maximum therapeutic duration of around 2-4 weeks and their use is strictly limited to 4 times per year with an interval of 21 days between injections (37, 438). Gellan hydrogels have been shown to retain stability for up to 18 days following subcutaneous injection and 90 days in in vitro culture, however their stability in the inflamed RA synovial environment remains to be

determined (441). We predict that this stability and an extended half-life of GC release will reduce the need for repeated painful IA injections in patients. However, future work should be done to assess slow-release properties of GCs from sheared hydrogels and effects on macrophages, and effects on synoviocytes susceptible to the catabolic effects of IA GCs such as osteoblasts.

Following generation of inactive GC-loaded sheared hydrogels with suitable release properties, in vivo testing in mouse models of arthritis can be used to demonstrate whether these formulations decrease catabolic effects such as bone degradation compared to standard IA GCs. This will also inform the biocompatibility of gellan hydrogels in the synovial environment and kinetics of therapeutic efficacy. If these gels are shown to be unsuitable, then alternative methods of GC targeting could be investigated. These include antibody-conjugated GCs for more specific macrophage targeting, similar to the anti-CD163-antibody-dexamethasone conjugates currently being assessed to target CD163+ M2-like macrophages in non-alcoholic steatohepatitis (475). This technique could be used in RA using antibodies specific to markers of pathogenic synovial macrophage subsets, such as SPP1 or S100A12A, to target GCs selectively to them.

Although not the focus of our study, we identified differences in steroid metabolism between male and female RA patients that suggests there is sexual dimorphism in inflammatory steroid metabolism in diseases such as RA. Changes in *AKR1C3* and *SRD5A1* expression with DAS28-CRP were significant for female RA patients in the AMP study, but this was not significant in male patients. Although the far larger sample size for female patients than male (23 vs 7) likely contributed to this, it may also be that these metabolic changes are starker in female patients,

perhaps as they tend to have lower serum androgen levels (410). Previous research into the roles of sex steroids in RA did not find differences in synovial fluid steroid levels with sex nor expression of AR, whereas in this thesis we report a higher ratio of testosterone/androstenedione as catalysed by AKR1C3 in synovial fluid of male RA patients compared to female (334, 363, 388). This could be due to improvements in sensitivity of steroid quantification or larger sample size in our study, although our study did not have similar male and female sample sizes nor control for steroidal therapeutics as carried out in previous studies. The increase in AKR1C3-mediated generation of androgens seen in our monocyte-derived macrophage cultures on inflammatory polarisation may be a result of them predominantly originating from male blood donors. It may be that inflammation-induced downregulation of AKR1C3 activity primarily occurs within females, with this perhaps representing part of the sexual dimorphism seen in RA. The activity of AKR1C3 may depend on substrate availability, with a backdrop of lower serum androgen levels leading to reduced AKR1C3 at sites such as the synovium. This may also explain why males with lower serum androgen levels, as well as females, are more prone to developing RA (351, 353). As other autoimmune inflammatory diseases present with a high F:M patients ratio, such as Sjögren's syndrome and SLE, this mechanism may be present across conditions of chronic inflammation (317).

Despite evidence of anti-inflammatory actions in RA, therapeutic effects of androgens in clinical trials have been limited. Mouse models have shown a decrease in synovial hyperplasia and cartilage destruction following IA testosterone or DHT, at levels comparable to dexamethasone (393). However, this has not translated to human RA. One trial of intramuscular testosterone in postmenopausal female RA patients did decrease ESR, pain and

general disease score, however the majority of clinical trials have shown little to no benefit (476). Testosterone adjunct therapy in male RA patients was found to significantly increase serum testosterone and DHT, but did not drive any benefits in term of improving disease activity or bone mineral density (353). Additionally, an increase in serum estradiol was found, which implies the systemic excess androgens provided therapeutically were aromatised into estrogens, which may be driving pro-inflammatory effects. This, in turn, implies that the anti-inflammatory effects of androgens may be better targeted therapeutically to distinct cell populations where they would have the most benefit. Targeting androgens to macrophages may allow for paracrine activation of androgens to increase local synovial levels of androgens for anti-inflammatory effects on other cells such as fibroblasts or lymphocytes. Additionally, supplementation of androgens such as testosterone which are ligands for SRD5A1 may switch the activity of this enzyme towards androgen activation and away from GC inactivation, provided androgens are a preferential ligand. Screening of newly diagnosed RA patients for baseline androgen levels may indicate those who could be likely to benefit from this supplementation.

7.3 Future directions

An important limitation of this thesis was a focus on in vitro macrophage cultures. This research used blood cones from the Birmingham NHS Blood and Transplant centre. These consist of the leukocyte reduction filter from platelet donations and therefore are enriched for PBMCs compared to whole blood (477). We chose this option as it was a reliable source of high yield monocytes, which have been shown to generate high quality functional myeloid cells (478). However, the limitations of this approach are the lack of knowledge of donor characteristics, including sex and age, known to affect steroid metabolism and inflammatory response. In addition, there is no control over when samples were taken, meaning that baseline serum steroid levels were subject to diurnal variations, which also likely impacted our synovial fluid study (411, 479). While use of medications such as 5α-reductase inhibitors preclude blood donation, donors could be on other drugs affecting circulating steroid levels such as hormonal contraception or hormone replacement therapy (480).

Nevertheless, this in vitro model allowed us to assess steroid metabolism directly within macrophages, using M1-like polarisation with IFNγ and TNFα to recapitulate some key inflammatory functions of pathogenic RA synovial macrophage subsets. This work identified the importance of inflammatory macrophage intracrine GC signalling and implied a role for these cells in paracrine activation of androgens, which should now be investigated in greater detail in the context of the RA synovium to define its contribution to disease pathophysiology. This could be carried out using culture of synovial tissue macrophages isolated from the synovium of RA patients. As the synovial joints contain distinct macrophage subsets with differing contributions to disease, comparison of the steroidogenic profiles of these different

macrophage subsets would be valuable to understanding their contribution to disease pathology (145, 146). This is particularly important as monocyte-derived macrophage populations, similar to our in vitro culture model, have been shown to be the major driver of arthritic disease in animal models, while tissue resident populations may retain some pro-resolution capacity, and steroid metabolism may play roles in their differential functions (120). FACS-mediated separation of different cell populations of the synovium would allow us to culture and individually investigate steroidogenesis and inflammatory regulation of these distinct macrophage subsets in vitro. This technique would also facilitate analysis of paracrine signalling between macrophages and other synoviocytes, such as fibroblasts. Furthermore, analysis of the impact of macrophage steroid metabolism on stromal cells such as osteoblasts and myocytes would also be vital to assess the contribution of macrophages to the catabolic and anabolic effects of GCs and androgens respectively. This would be an essential step to investigating the feasibility and safety of therapeutic targeting of macrophage inflammatory steroid metabolism.

Using ex vivo synoviocytes would also allow us to overcome the difficulties in identifying changes in synovial fluid GC and androgen activation with measures of disease severity or inflammation in OA and RA patients due to rapid synovial fluid turnover and highly porosity of the synovial membrane to lipophilic steroids (414). A more accurate analysis of steroidogenesis at the tissue-specific and paracrine level could be carried out by analysing the steroid conversion of ex vivo mixed synoviocytes from patients, as has been carried out by previously published studies (363, 365). Future studies should therefore incorporate synovial tissue samples from RA patients, strengthened by age- and sex-matching, larger sample sizes and stricter exclusion criteria to exclude patients currently taking steroidal therapies.

Use of patient synovial tissue samples would allow analysis of the contribution and regulation of other cells of the inflamed RA synovium including fibroblasts and lymphocytes. However, more in depth analysis is likely only possible using animal models and tissues. Our group has previously investigated GC paracrine signalling using conditioned media transfer between macrophages and FLS isolated from global *Hsd11b1*$^{-/-}$ mice (290). Similar work could be carried out to assess paracrine signalling of androgens between these populations using transfer of conditioned media from androgen-treated macrophages on to FLS from *Srd5a1*$^{-/-}$ or *Akr1c3*$^{-/-}$ FLS, and vice versa.

The contribution of steroid metabolism by AKR1C3 and SRD5A1 to disease pathology could be investigated using animal models of arthritis. Importantly however, many mouse models of arthritis, including the TNF-tg model using the Tg197 transcript utilised by our group, are known not to reflect the sexual dimorphism present in human RA. In this model, arthritic disease begins prior to sexual maturity and so would likely not show full effects of sex steroids (27, 286, 481). It has been shown that the TNF-tg Tg3647 strain may better represent human sexual dimorphism, with female mice developing arthritic disease earlier than males (481). These features of RA could be important to recapitulate in animal models given their likely link to differential sex steroid metabolism, therefore this may be a better model for us to assess the role of androgen metabolism in disease-associated synovial macrophages. As discussed above, 5α-reductase inhibition may help to promote anti-inflammatory actions of GCs in macrophages by limiting their clearance, however this may impede any anti-inflammatory actions from intracrine or paracrine androgen metabolism. This could be tested using the TNF-tg mouse model of polyarthritis by assessing the efficacy of 5α-reductase inhibition therapy as an adjunct to therapeutic GCs.

7.4 Summary

We have identified a complex regulation of GC and androgen metabolism in macrophages, acutely governed by their inflammatory activation state. Intracrine GC metabolism was found to have functional relevance in regulating macrophage inflammatory functions, while macrophages may also act as paracrine activators of androgens as part of their interactions with immune and stromal cells. Furthermore, we have shown that inflammatory macrophage 11β-HSD1 may be a novel therapeutic target to enhance anti-inflammatory and pro-resolution functions of macrophages while limiting catabolic GC effects. The full significance of this steroid metabolism in synovial macrophages remains to be discovered, in particular how this varies between tissue subsets and contributes to pathophysiology of human disease. However, this research suggests that targeting components of inflammatory steroid metabolism in macrophages may be a promising route for future clinical interventions in chronic inflammatory diseases such as RA.

Chapter 8 SUPPLEMENTARY

CYP1A1	*CYP2D7*	*CYP11A1*	*RDH5*	*GUSB*	*PAPSS1*
CYP1A2	*CYP2D8P*	*CYP17A1*	*HSD17B10*	*SULT1A1*	*PAPSS2*
CYP1B1	*CYP2E1*	*CYP11B1*	*HSD17B11*	*SULT1E1*	*SUMF1*
CYP1D1P	*CYP2F1*	*CYP11B2*	*HSD17B12*	*SULT2A1*	*SUMF2*
CYP2A13	*CYP2F2P*	*CYP19A1*	*HSD17B13*	*SULT2B1*	*RXRA*
CYP2AB1P	*CYP2G1P*	*CYP21A2*	*HSD17B14*	*SULT1C4*	*RXRB*
CYP2AC1P	*CYP2G2P*	*CYP27A1*	*RDH11*	*STS*	*RXRG*
CYP2A6	*CYP2J2*	*AKR1C4*	*AKR1C1*	*AR*	*NR3C1*
CYP2A7	*CYP2R1*	*HSD3B1*	*AKR1C2*	*ESR1*	*NR3C2*
CYP2A7P1	*CYP2S1*	*HSD3B2*	*SRD5A1*	*ESR2*	
CYP2B6	*CYP2T1P*	*HSD11B1*	*SRD5A2*	*GPER1*	
CYP2B7P	*CYP2T3P*	*HSD11B2*	*SRD5A3*	*PGR*	
CYP2C8	*CYP2U1*	*HSD17B1*	*AKR1D1*	*SLCO1A2*	
CYP2C9	*CYP2W1*	*HSD17B2*	*UGT2B4*	*SLCO1B1*	
CYP2C18	*CYP3A4*	*HSD17B3*	*UGT2B7*	*SLCO1B3*	
CYP2C19	*CYP3A5*	*HSD17B4*	*UGT2B10*	*SLCO2B1*	
CYP2C56P	*CYP3A7*	*AKR1C3*	*UGT2B11*	*SLCO3A1*	
CYP2C58P	*CYP3A43*	*HSD17B6*	*UGT2B15*	*SLCO4A1*	
CYP2C61P	*CYP3A51P*	*HSD17B7*	*UGT2B17*	*SOAT1*	
CYP2D6	*CYP3A52P*	*HSD17B8*	*UGT2B28*	*SOAT2*	

Supplementary Table 1 Steroid metabolism genes analysed in AMP RNA-seq dataset

Progestogens	Glucocorticoids & mineralocorticoids	Androgens	Alternative pathway androgens
DHEA	Deoxycorticosterone	Androsterone	5α-DHP
Pregnenolone	Corticosterone	3α-Diol	Allopregnanolone
Progesterone	11-Deoxycortisol	Androstanedione	17OH-Allo
17OH-Preg	Cortisol	A4	17OH-DHP
17OH-Prog	Cortisone	Testosterone	
	Aldosterone	DHT	
		11Keto A4	
		11Keto T	
		11OH-A4	
		11OH-T	

Supplementary Table 2 Steroids quantified in synovial fluid by LC-MS/MS

Abbreviations: 3α-diol, 3α-androstanediol; 5α-DHP, 5α-dihydroprogesterone; 11OH-A4, 11β-hydroxyandrostenedione; 11OH-T, 11β-hydroxytestosterone; 11keto A4, 11-ketoandrostenedione; 11keto T, 11ketotestosterone; 17OH-allo, 17α-hydroxyallopregnanolone; 17OH-DHP, 17α-hydroxydihydroprogesterone; 17OH-preg, 17α-hydroxypregnenolone; 17OH-prog, 17α-hydroxyprogesterone; A4, androstenedione; DHEA, dehydroepiandrosterone; DHT, dihydrotestosterone.

Chapter 9 REFERENCES

1. Crowson CS, Matteson EL, Myasoedova E, Michet CJ, Ernste FC, Warrington KJ, et al. The Lifetime Risk of Adult-Onset Rheumatoid Arthritis and Other Inflammatory Autoimmune Rheumatic Diseases. Arthritis and Rheumatism. 2011;63(3):633-9.
2. McInnes IB, Schett G. MECHANISMS OF DISEASE The Pathogenesis of Rheumatoid Arthritis. New England Journal of Medicine. 2011;365(23):2205-19.
3. Navarro-Cano G, del Rincon I, Pogosian S, Roldan JF, Escalante A. Association of mortality with disease severity in rheumatoid arthritis, independent of comorbidity. Arthritis and Rheumatism. 2003;48(9):2425-33.
4. Gonzalez-Gay MA, Gonzalez-Juanatey C, Lopez-Diaz MJ, Pineiro A, Garcia-Porrua C, Miranda-Filloy JA, et al. HLA-DRB1 and persistent chronic inflammation contribute to cardiovascular events and cardiovascular mortality in patients with rheumatoid arthritis. Arthritis & Rheumatism-Arthritis Care & Research. 2007;57(1):125-32.
5. Kay J, Upchurch KS. ACR/EULAR 2010 rheumatoid arthritis classification criteria. Rheumatology. 2012;51:5-9.
6. Anderson J, Caplan L, Yazdany J, Robbins ML, Neogi T, Michaud K, et al. Rheumatoid Arthritis Disease Activity Measures: American College of Rheumatology Recommendations for Use in Clinical Practice. Arthritis Care & Research. 2012;64(5):640-7.
7. Taruc-Uy RL, Lynch SA. Diagnosis and Treatment of Osteoarthritis. Primary Care. 2013;40(4):821-+.
8. Sokolove J, Lepus CM. Role of inflammation in the pathogenesis of osteoarthritis: latest findings and interpretations. Ther Adv Musculoskelet Dis. 2013;5(2):77-94.
9. Smith MD. The normal synovium. The open rheumatology journal. 2011;5:100-6.
10. Smith MD, Barg E, Weedon H, Papengelis V, Smeets T, Tak PP, et al. Microarchitecture and protective mechanisms in synovial tissue from clinically and arthroscopically normal knee joints. Annals of the Rheumatic Diseases. 2003;62(4):303-7.
11. Bartok B, Firestein GS. Fibroblast-like synoviocytes: key effector cells in rheumatoid arthritis. Immunological Reviews. 2010;233:233-55.
12. Knab K, Chambers D, Krönke G. Synovial Macrophage and Fibroblast Heterogeneity in Joint Homeostasis and Inflammation. Frontiers in Medicine. 2022;9.
13. Culemann S, Gruneboom A, Nicolas-Avila JA, Weidner D, Lammle KF, Rothe T, et al. Locally renewing resident synovial macrophages provide a protective barrier for the joint. Nature. 2019;572(7771):670-+.
14. Bottini N, Firestein GS. Duality of fibroblast-like synoviocytes in RA: passive responders and imprinted aggressors. Nature Reviews Rheumatology. 2013;9(1):24-33.
15. Lefevre S, Knedla A, Tennie C, Kampmann A, Wunrau C, Dinser R, et al. Synovial fibroblasts spread rheumatoid arthritis to unaffected joints. Nature Medicine. 2009;15(12):1414-U10.
16. Filer A, Ward LSC, Kemble S, Davies CS, Munir H, Rogers R, et al. Identification of a transitional fibroblast function in very early rheumatoid arthritis. Annals of the Rheumatic Diseases. 2017;76(12):2105-12.
17. Humby F, Bombardieri M, Manzo A, Kelly S, Blades MC, Kirkham B, et al. Ectopic Lymphoid Structures Support Ongoing Production of Class-Switched Autoantibodies in Rheumatoid Synovium. Plos Medicine. 2009;6(1):59-75.

18. Cascao R, Rosario HS, Souto-Carneiro MM, Fonseca JE. Neutrophils in rheumatoid arthritis: More than simple final effectors. Autoimmunity Reviews. 2010;9(8):531-5.
19. Wei S, Kitaura H, Zhou P, Ross FP, Teitelbaum SL. IL-1 mediates TNF-induced osteoclastogenesis. Journal of Clinical Investigation. 2005;115(2):282-90.
20. Kotake S, Udagawa N, Takahashi N, Matsuzaki K, Itoh K, Ishiyama S, et al. IL-17 in synovial fluids from patients with rheumatoid arthritis is a potent stimulator of osteoclastogenesis. Journal of Clinical Investigation. 1999;103(9):1345-52.
21. Tsuboi M, Kawakami A, Nakashima T, Matsuoka N, Urayama S, Kawabe Y, et al. Tumor necrosis factor-alpha and interleukin-1 beta increase the Fas-mediated apoptosis of human osteoblasts. Journal of Laboratory and Clinical Medicine. 1999;134(3):222-31.
22. Yatsugi N, Tsukazaki T, Osaki M, Koji T, Yamashita S, Shindo H. Apoptosis of articular chondrocytes in rheumatoid arthritis and osteoarthritis: correlation of apoptosis with degree of cartilage destruction and expression of apoptosis-related proteins of p53 and c-myc. Journal of orthopaedic science : official journal of the Japanese Orthopaedic Association. 2000;5(2):150-6.
23. Barksby HE, Hui W, Wappler I, Peters HH, Milner JM, Richards CD, et al. Interleukin-1 in combination with oncostatin M up-regulates multiple genes in chondrocytes - Implications for cartilage destruction and repair. Arthritis and Rheumatism. 2006;54(2):540-50.
24. Mauri C, Williams RO, Walmsley M, Feldmann M. Relationship between Th1/Th2 cytokine patterns and the arthritogenic response in collagen-induced arthritis. European Journal of Immunology. 1996;26(7):1511-8.
25. Boissier MC, Feng XZ, Carlioz A, Roudier R, Fournier C. EXPERIMENTAL AUTOIMMUNE ARTHRITIS IN MICE .1. HOMOLOGOUS TYPE-II COLLAGEN IS RESPONSIBLE FOR SELF-PERPETUATING CHRONIC POLYARTHRITIS. Annals of the Rheumatic Diseases. 1987;46(9):691-700.
26. Malfait AM, Williams RO, Malik AS, Maini RN, Feldmann M. Chronic relapsing homologous collagen-induced arthritis in DBA/1 mice as a model for testing disease-modifying and remission-inducing therapies. Arthritis and Rheumatism. 2001;44(5):1215-24.
27. Keffer J, Probert L, Cazlaris H, Georgopoulos S, Kaslaris E, Kioussis D, et al. TRANSGENIC MICE EXPRESSING HUMAN TUMOR-NECROSIS-FACTOR - A PREDICTIVE GENETIC MODEL OF ARTHRITIS. Embo Journal. 1991;10(13):4025-31.
28. Li P, Schwarz EM. The TNF-alpha transgenic mouse model of inflammatory arthritis. Springer Seminars in Immunopathology. 2003;25(1):19-33.
29. Probert L, Plows D, Kontogeorgos G, Kollias G. THE TYPE-I INTERLEUKIN-1 RECEPTOR ACTS IN SERIES WITH TUMOR-NECROSIS-FACTOR (TNF) TO INDUCE ARTHRITIS IN TNF-TRANSGENIC MICE. European Journal of Immunology. 1995;25(6):1794-7.
30. Schett G, Hayer S, Tohidast-Akrad M, Schmid BJ, Lang S, Turk B, et al. Adenovirus-based overexpression of tissue inhibitor of metalloproteinases 1 reduces tissue damage in the joints of tumor necrosis factor alpha transgenic mice. Arthritis and Rheumatism. 2001;44(12):2888-98.
31. Hayer S, Redlich K, Korb A, Hermann S, Smolen J, Schett G. Tenosynovitis and osteoclast formation as the initial preclinical changes in a murine model of inflammatory arthritis. Arthritis and Rheumatism. 2007;56(1):79-88.
32. Basu D, Horvath S, Matsumoto I, Fremont DH, Allen PM. Molecular basis for recognition of an arthritic peptide and a foreign epitope on distinct MHC molecules by a single TCR. Journal of Immunology. 2000;164(11):5788-96.
33. Kouskoff V, Korganow AS, Duchatelle V, Degott C, Benoist C, Mathis D. Organ-specific disease provoked by systemic autoimmunity. Cell. 1996;87(5):811-22.
34. Asquith DL, Miller AM, McInnes IB, Liew FY. Animal models of rheumatoid arthritis. European Journal of Immunology. 2009;39(8):2040-4.
35. Smolen JS, Landewe RBM, Bijlsma JWJ, Burmester GR, Dougados M, Kerschbaumer A, et al. EULAR recommendations for the management of rheumatoid arthritis with synthetic and biological

disease-modifying antirheumatic drugs: 2019 update. Annals of the Rheumatic Diseases. 2020;79(6):685-99.
36. Bukhari MAS, Wiles NJ, Lunt M, Harrison BJ, Scott DGI, Symmons DPM, et al. Influence of disease-modifying therapy on radiographic outcome in inflammatory polyarthritis at five years - Results from a large observational inception study. Arthritis and Rheumatism. 2003;48(1):46-53.
37. Smolen JS, Landewe R, Bijlsma J, Burmester G, Chatzidionysiou K, Dougados M, et al. EULAR recommendations for the management of rheumatoid arthritis with synthetic and biological disease-modifying antirheumatic drugs: 2016 update. Annals of the Rheumatic Diseases. 2017;76(6):960-77.
38. Kirwan JR, Bijlsma JWJ, Boers M, Shea BJ. Effects of glucocorticoids on radiological progression in rheumatoid arthritis. Cochrane Database of Systematic Reviews. 2007(1).
39. Wilson JC, Sarsour K, Gale S, Petho-Schramm A, Jick SS, Meier CR. Incidence and Risk of Glucocorticoid-Associated Adverse Effects in Patients With Rheumatoid Arthritis. Arthritis Care & Research. 2019;71(4):498-511.
40. Stacy JM, Greenmyer JR, Beal JR, Sahmoun AE, Diri E. The efficacy of low dose short-term prednisone therapy for remission induction in newly diagnosed rheumatoid arthritis patients. Advances in Rheumatology. 2021;61(1).
41. Smolen JS, Aletaha D, Barton A, Burmester GR, Emery P, Firestein GS, et al. Rheumatoid arthritis. Nature Reviews Disease Primers. 2018;4.
42. Nagy G, Roodenrijs NMT, Welsing PMJ, Kedves M, Hamar A, van der Goes MC, et al. EULAR definition of difficult-to-treat rheumatoid arthritis. Annals of the Rheumatic Diseases. 2021;80(1):31-5.
43. Becede M, Alasti F, Gessl I, Haupt L, Kerschbaumer A, Landesmann U, et al. Risk profiling for a refractory course of rheumatoid arthritis. Seminars in Arthritis and Rheumatism. 2019;49(2):211-7.
44. Haringman JJ, Gerlag DM, Zwinderman AH, Smeets TJM, Kraan MC, Baeten D, et al. Synovial tissue macrophages: a sensitive biomarker for response to treatment in patients with rheumatoid arthritis. Annals of the Rheumatic Diseases. 2005;64(6):834-8.
45. Jahangier ZN, Jacobs JWG, Kraan MC, Wenting MJG, Smeets TJ, Bijlsma JWJ, et al. Pretreatment macrophage infiltration of the synovium predicts the clinical effect of both radiation synovectomy and intra-articular glucocorticoids. Annals of the Rheumatic Diseases. 2006;65(10):1286.
46. Metchnikoff E. Leçons sur la pathologie comparée de l'inflammation: faites à l'Institut Pasteur en avril et mai 1891: G. Masson; 1892.
47. Murray PJ, Wynn TA. Protective and pathogenic functions of macrophage subsets. Nature Reviews Immunology. 2011;11(11):723-37.
48. van Furth R. 27 - IDENTIFICATION OF MONONUCLEAR PHAGOCYTES: OVERVIEW AND DEFINITIONS. In: Adams DO, Edelson PJ, Koren HS, editors. Methods for Studying Mononuclear Phagocytes: Academic Press; 1981. p. 243-51.
49. Guilliams M, Ginhoux F, Jakubzick C, Naik SH, Onai N, Schraml BU, et al. Dendritic cells, monocytes and macrophages: a unified nomenclature based on ontogeny. Nature Reviews Immunology. 2014;14(8):571-8.
50. Vanfurth R, Cohn ZA. ORIGIN AND KINETICS OF MONONUCLEAR PHAGOCYTES. Journal of Experimental Medicine. 1968;128(3):415-+.
51. van Furth R. Production and migration of monocytes and kinetics of macrophages. In: van Furth R, editor. Mononuclear Phagocytes: Biology of Monocytes and Macrophages. Dordrecht: Springer Netherlands; 1992. p. 3-12.
52. Volkman A. THE ORIGIN AND TURNOVER OF MONONUCLEAR CELLS IN PERITONEAL EXUDATES IN RATS. Journal of Experimental Medicine. 1966;124(2):241-54.
53. Sawyer RT, Strausbauch PH, Volkman A. Resident macrophage proliferation in mice depleted of blood monocytes by strontium-89. Lab Invest. 1982;46(2):165-70.

54. Yamada M, Naito M, Takahashi K. KUPFFER CELL-PROLIFERATION AND GLUCAN-INDUCED GRANULOMA-FORMATION IN MICE DEPLETED OF BLOOD MONOCYTES BY SR-89. Journal of Leukocyte Biology. 1990;47(3):195-205.
55. Hashimoto D, Chow A, Noizat C, Teo P, Beasley MB, Leboeuf M, et al. Tissue-Resident Macrophages Self-Maintain Locally throughout Adult Life with Minimal Contribution from Circulating Monocytes. Immunity. 2013;38(4):792-804.
56. Ginhoux F, Greter M, Leboeuf M, Nandi S, See P, Gokhan S, et al. Fate Mapping Analysis Reveals That Adult Microglia Derive from Primitive Macrophages. Science. 2010;330(6005):841-5.
57. Schulz C, Perdiguero EG, Chorro L, Szabo-Rogers H, Cagnard N, Kierdorf K, et al. A Lineage of Myeloid Cells Independent of Myb and Hematopoietic Stem Cells. Science. 2012;336(6077):86-90.
58. Guilliams M, De Kleer I, Henri S, Post S, Vanhoutte L, De Prijck S, et al. Alveolar macrophages develop from fetal monocytes that differentiate into long-lived cells in the first week of life via GM-CSF. Journal of Experimental Medicine. 2013;210(10):1977-92.
59. Aziz A, Soucie E, Sarrazin S, Sieweke MH. MafB/c-Maf Deficiency Enables Self-Renewal of Differentiated Functional Macrophages. Science. 2009;326(5954):867-71.
60. Soucie EL, Weng ZM, Geirsdottir L, Molawi K, Maurizio J, Fenouil R, et al. Lineage-specific enhancers activate self-renewal genes in macrophages and embryonic stem cells. Science. 2016;351(6274).
61. Passlick B, Flieger D, Zieglerheitbrock HWL. IDENTIFICATION AND CHARACTERIZATION OF A NOVEL MONOCYTE SUBPOPULATION IN HUMAN PERIPHERAL-BLOOD. Blood. 1989;74(7):2527-34.
62. Ziegler-Heitbrock L, Ancuta P, Crowe S, Dalod M, Grau V, Hart DN, et al. Nomenclature of monocytes and dendritic cells in blood. Blood. 2010;116(16):E74-E80.
63. Patel AA, Zhang Y, Fullerton JN, Boelen L, Rongvaux A, Maini AA, et al. The fate and lifespan of human monocyte subsets in steady state and systemic inflammation. Journal of Experimental Medicine. 2017;214(7):1913-23.
64. Geissmann F, Jung S, Littman DR. Blood monocytes consist of two principal subsets with distinct migratory properties. Immunity. 2003;19(1):71-82.
65. Auffray C, Fogg D, Garfa M, Elain G, Join-Lambert O, Kayal S, et al. Monitoring of blood vessels and tissues by a population of monocytes with patrolling behavior. Science. 2007;317(5838):666-70.
66. Cros J, Cagnard N, Woollard K, Patey N, Zhang SY, Senechal B, et al. Human CD14(dim) Monocytes Patrol and Sense Nucleic Acids and Viruses via TLR7 and TLR8 Receptors. Immunity. 2010;33(3):375-86.
67. Gautier EL, Shay T, Miller J, Greter M, Jakubzick C, Ivanov S, et al. Gene-expression profiles and transcriptional regulatory pathways that underlie the identity and diversity of mouse tissue macrophages. Nature Immunology. 2012;13(11):1118-28.
68. Jakubzick C, Gautier EL, Gibbings SL, Sojka DK, Schlitzer A, Johnson TE, et al. Minimal Differentiation of Classical Monocytes as They Survey Steady-State Tissues and Transport Antigen to Lymph Nodes. Immunity. 2013;39(3):599-610.
69. Chimen M, Yates CM, McGettrick HM, Ward LSC, Harrison MJ, Apta B, et al. Monocyte Subsets Coregulate Inflammatory Responses by Integrated Signaling through TNF and IL-6 at the Endothelial Cell Interface. Journal of Immunology. 2017;198(7):2834-43.
70. Bystrom J, Evans I, Newson J, Stables M, Toor I, van Rooijen N, et al. Resolution-phase macrophages possess a unique inflammatory phenotype that is controlled by cAMP. Blood. 2008;112(10):4117-27.
71. Zigmond E, Varol C, Farache J, Elmaliah E, Satpathy AT, Friedlander G, et al. Ly6C(hi) Monocytes in the Inflamed Colon Give Rise to Proinflammatory Effector Cells and Migratory Antigen-Presenting Cells. Immunity. 2012;37(6):1076-90.

72. Komano Y, Nanki T, Hayashida K, Taniguchi K, Miyasaka N. Identification of a human peripheral blood monocyte subset that differentiates into osteoclasts. Arthritis Research & Therapy. 2006;8(5).
73. Yona S, Kim KW, Wolf Y, Mildner A, Varol D, Breker M, et al. Fate Mapping Reveals Origins and Dynamics of Monocytes and Tissue Macrophages under Homeostasis. Immunity. 2013;38(1):79-91.
74. Epelman S, Lavine KJ, Beaudin AE, Sojka DK, Carrero JA, Calderon B, et al. Embryonic and Adult-Derived Resident Cardiac Macrophages Are Maintained through Distinct Mechanisms at Steady State and during Inflammation. Immunity. 2014;40(1):91-104.
75. Ghosn EEB, Cassado AA, Govoni GR, Fukuhara T, Yang Y, Monack DM, et al. Two physically, functionally, and developmentally distinct peritoneal macrophage subsets. Proceedings of the National Academy of Sciences of the United States of America. 2010;107(6):2568-73.
76. Okabe Y, Medzhitov R. Tissue-Specific Signals Control Reversible Program of Localization and Functional Polarization of Macrophages. Cell. 2014;157(4):832-44.
77. Bain CC, Hawley CA, Garner H, Scott CL, Schridde A, Steers NJ, et al. Long-lived self-renewing bone marrow-derived macrophages displace embryo-derived cells to inhabit adult serous cavities. Nature Communications. 2016;7.
78. Davies LC, Rosas M, Smith PJ, Fraser DJ, Jones SA, Taylor PR. A quantifiable proliferative burst of tissue macrophages restores homeostatic macrophage populations after acute inflammation. European Journal of Immunology. 2011;41(8):2155-64.
79. Gilroy DW, Colville-Nash PR, McMaster S, Sawatzky DA, Willoughby DA, Lawrence T. Inducible cyclooxygenase-derived 15deoxy Delta(12-14)PGJ(2) brings about acute inflammatory resolution in rat pleurisy by inducing neutrophil and macrophage apoptosis. Faseb Journal. 2003;17(13):2269-+.
80. Arnold L, Henry A, Poron F, Baba-Amer Y, van Rooijen N, Plonquet A, et al. Inflammatory monocytes recruited after skeletal muscle injury switch into antiinflammatory macrophages to support myogenesis. Journal of Experimental Medicine. 2007;204(5):1057-69.
81. Swirski FK, Libby P, Aikawa E, Alcaide P, Luscinskas FW, Weissleder R, et al. Ly-6C(hi) monocytes dominate hypercholesterolemia-associated monocytosis and give rise to macrophages in atheromata. Journal of Clinical Investigation. 2007;117(1):195-205.
82. Aran D, Looney AP, Liu LQ, Wu E, Fong V, Hsu A, et al. Reference-based analysis of lung single-cell sequencing reveals a transitional profibrotic macrophage. Nature Immunology. 2019;20(2):163-+.
83. Kamada N, Hisamatsu T, Okamoto S, Chinen H, Kobayashi T, Sato T, et al. Unique CD14(+) intestinal macrophages contribute to the pathogenesis of Crohn disease via lL-23/IFN-gamma axis. Journal of Clinical Investigation. 2008;118(6):2269-80.
84. Medzhitov R. Origin and physiological roles of inflammation. Nature. 2008;454(7203):428-35.
85. Kolaczkowska E, Kubes P. Neutrophil recruitment and function in health and inflammation. Nature Reviews Immunology. 2013;13(3):159-75.
86. Fullerton JN, Gilroy DW. Resolution of inflammation: a new therapeutic frontier. Nature Reviews Drug Discovery. 2016;15(8):551-67.
87. Serhan CN, Levy BD. Resolvins in inflammation: emergence of the pro-resolving superfamily of mediators. Journal of Clinical Investigation. 2018;128(7):2657-69.
88. Sansbury BE, Spite M. Resolution of Acute Inflammation and the Role of Resolvins in Immunity, Thrombosis, and Vascular Biology. Circulation Research. 2016;119(1):113-30.
89. Walker J, Dichter E, Lacorte G, Kerner D, Spur B, Rodriguez A, et al. LIPOXIN A4 INCREASES SURVIVAL BY DECREASING SYSTEMIC INFLAMMATION AND BACTERIAL LOAD IN SEPSIS. Shock. 2011;36(4):410-6.
90. Savill JS, Wyllie AH, Henson JE, Walport MJ, Henson PM, Haslett C. MACROPHAGE PHAGOCYTOSIS OF AGING NEUTROPHILS IN INFLAMMATION - PROGRAMMED CELL-DEATH IN THE

NEUTROPHIL LEADS TO ITS RECOGNITION BY MACROPHAGES. Journal of Clinical Investigation. 1989;83(3):865-75.
91. Huynh MLN, Fadok VA, Henson PM. Phosphatidylserine-dependent ingestion of apoptotic cells promotes TGF-beta 1 secretion and the resolution of inflammation. Journal of Clinical Investigation. 2002;109(1):41-50.
92. Newson J, Stables M, Karra E, Arce-Vargas F, Quezada S, Motwani M, et al. Resolution of acute inflammation bridges the gap between innate and adaptive immunity. Blood. 2014;124(11):1748-64.
93. Buckley CD, Pilling D, Lord JM, Akbar AN, Scheel-Toellner D, Salmon M. Fibroblasts regulate the switch from acute resolving to chronic persistent inflammation. Trends in Immunology. 2001;22(4):199-204.
94. Ehlers S, Schaible UE. The granuloma in tuberculosis: dynamics of a host-pathogen collusion. Frontiers in Immunology. 2013;3.
95. Kokkola R, Li J, Sundberg E, Aveberger AC, Palmblad K, Yang H, et al. Successful treatment of collagen-induced arthritis in mice and rats by targeting extracellular high mobility group box chromosomal protein 1 activity. Arthritis and Rheumatism. 2003;48(7):2052-8.
96. Fredman G, Li YS, Dalli J, Chiang N, Serhan CN. Self-Limited versus Delayed Resolution of Acute Inflammation: Temporal Regulation of Pro-Resolving Mediators and MicroRNA. Scientific Reports. 2012;2.
97. Mills CD, Kincaid K, Alt JM, Heilman MJ, Hill AM. M-1/M-2 macrophages and the Th1/Th2 paradigm. Journal of Immunology. 2000;164(12):6166-73.
98. Stein M, Keshav S, Harris N, Gordon S. INTERLEUKIN-4 POTENTLY ENHANCES MURINE MACROPHAGE MANNOSE RECEPTOR ACTIVITY - A MARKER OF ALTERNATIVE IMMUNOLOGICAL MACROPHAGE ACTIVATION. Journal of Experimental Medicine. 1992;176(1):287-92.
99. Munder M, Eichmann K, Modolell M. Alternative metabolic states in murine macrophages reflected by the nitric oxide synthase arginase balance: Competitive regulation by CD4(+) T cells correlates with Th1/Th2 phenotype. Journal of Immunology. 1998;160(11):5347-54.
100. Akagawa KS. Functional heterogeneity of colony-stimulating factor-induced human monocyte-derived macrophages. International Journal of Hematology. 2002;76(1):27-34.
101. Stanley ER, Berg KL, Einstein DB, Lee PSW, Pixley FJ, Wang Y, et al. Biology and action of colony-stimulating factor-1. Molecular Reproduction and Development. 1997;46(1):4-10.
102. Lacey DC, Achuthan A, Fleetwood AJ, Dinh H, Roiniotis J, Scholz GM, et al. Defining GM-CSF- and Macrophage-CSF Dependent Macrophage Responses by In Vitro Models. Journal of Immunology. 2012;188(11):5752-65.
103. Jaguin M, Houlbert N, Fardel O, Lecureur V. Polarization profiles of human M-CSF-generated macrophages and comparison of M1-markers in classically activated macrophages from GM-CSF and M-CSF origin. Cellular Immunology. 2013;281(1):51-61.
104. Martinez FO, Gordon S, Locati M, Mantovani A. Transcriptional profiling of the human monocyte-to-macrophage differentiation and polarization: New molecules and patterns of gene expression. Journal of Immunology. 2006;177(10):7303-11.
105. Rodriguez-Prados JC, Traves PG, Cuenca J, Rico D, Aragones J, Martin-Sanz P, et al. Substrate Fate in Activated Macrophages: A Comparison between Innate, Classic, and Alternative Activation. Journal of Immunology. 2010;185(1):605-14.
106. Yu Q, Wang Y, Dong L, He Y, Liu R, Yang Q, et al. Regulations of Glycolytic Activities on Macrophages Functions in Tumor and Infectious Inflammation. Frontiers in Cellular and Infection Microbiology. 2020;10.
107. Xue J, Schmidt SV, Sander J, Draffehn A, Krebs W, Quester I, et al. Transcriptome-Based Network Analysis Reveals a Spectrum Model of Human Macrophage Activation. Immunity. 2014;40(2):274-88.

108. Whyte CS, Bishop ET, Rueckerl D, Gaspar-Pereira S, Barker RN, Allen JE, et al. Suppressor of cytokine signaling (SOCS)1 is a key determinant of differential macrophage activation and function. Journal of Leukocyte Biology. 2011;90(5):845-54.
109. Martinez FO, Gordon S. The M1 and M2 paradigm of macrophage activation: time for reassessment. F1000prime reports. 2014;6:13-.
110. Tiemessen MM, Jagger AL, Evans HG, van Herwijnen MJC, John S, Taams LS. CD4(+)CD25(+)Foxp3(+) regulatory T cells induce alternative activation of human monocytes/macrophages. Proceedings of the National Academy of Sciences of the United States of America. 2007;104(49):19446-51.
111. Balce DR, Li B, Allan ERO, Rybicka JM, Krohn RM, Yates RM. Alternative activation of macrophages by IL-4 enhances the proteolytic capacity of their phagosomes through synergistic mechanisms. Blood. 2011;118(15):4199-208.
112. Martinez FO, Sica A, Mantovani A, Locati M. Macrophage activation and polarization. Frontiers in Bioscience-Landmark. 2008;13:453-61.
113. Devilliers WJS, Fraser IP, Hughes DA, Doyle AG, Gordon S. MACROPHAGE-COLONY-STIMULATING FACTOR SELECTIVELY ENHANCES MACROPHAGE SCAVENGER RECEPTOR EXPRESSION AND FUNCTION. Journal of Experimental Medicine. 1994;180(2):705-9.
114. Schif-Zuck S, Gross N, Assi S, Rostoker R, Serhan CN, Ariel A. Saturated-efferocytosis generates pro-resolving CD11b(low) macrophages: Modulation by resolvins and glucocorticoids. European Journal of Immunology. 2011;41(2):366-79.
115. Sutterwala FS, Noel GJ, Salgame P, Mosser DM. Reversal of proinflammatory responses by ligating the macrophage Fc gamma receptor type I. Journal of Experimental Medicine. 1998;188(1):217-22.
116. Varga T, Mounier R, Horvath A, Cuvellier S, Dumont F, Poliska S, et al. Highly Dynamic Transcriptional Signature of Distinct Macrophage Subsets during Sterile Inflammation, Resolution, and Tissue Repair. Journal of Immunology. 2016;196(11):4771-82.
117. Stanley ER, Chitu V. CSF-1 Receptor Signaling in Myeloid Cells. Cold Spring Harbor Perspectives in Biology. 2014;6(6).
118. Cauli A, Yanni G, Panayi GS. Interleukin-1, interleukin-1 receptor antagonist and macrophage populations in rheumatoid arthritis synovial membrane. Rheumatology. 1997;36(9):935-40.
119. Hogg N, Palmer DG, Revell PA. MONONUCLEAR PHAGOCYTES OF NORMAL AND RHEUMATOID SYNOVIAL-MEMBRANE IDENTIFIED BY MONOCLONAL-ANTIBODIES. Immunology. 1985;56(4):673-81.
120. Misharin AV, Cuda CM, Saber R, Turner JD, Gierut AK, Haines GK, et al. Nonclassical Ly6C(-) Monocytes Drive the Development of Inflammatory Arthritis in Mice. Cell Reports. 2014;9(2):591-604.
121. Mulherin D, Fitzgerald O, Bresnihan B. Synovial tissue macrophage populations and articular damage in rheumatoid arthritis. Arthritis and Rheumatism. 1996;39(1):115-24.
122. Herenius MMJ, Thurlings RM, Wijbrandts CA, Bennink RJ, Dohmen SE, Voermans C, et al. Monocyte migration to the synovium in rheumatoid arthritis patients treated with adalimumab. Annals of the Rheumatic Diseases. 2011;70(6):1160-2.
123. Yeo L, Adlard N, Biehl M, Juarez M, Smallie T, Snow M, et al. Expression of chemokines CXCL4 and CXCL7 by synovial macrophages defines an early stage of rheumatoid arthritis. Annals of the Rheumatic Diseases. 2016;75(4):763-71.
124. Chu CQ, Field M, Feldmann M, Maini RN. LOCALIZATION OF TUMOR-NECROSIS-FACTOR-ALPHA IN SYNOVIAL TISSUES AND AT THE CARTILAGE PANNUS JUNCTION IN PATIENTS WITH RHEUMATOID-ARTHRITIS. Arthritis and Rheumatism. 1991;34(9):1125-32.
125. Koch AE, Kunkel SL, Harlow LA, Johnson B, Evanoff HL, Haines GK, et al. ENHANCED PRODUCTION OF MONOCYTE CHEMOATTRACTANT PROTEIN-1 IN RHEUMATOID-ARTHRITIS. Journal of Clinical Investigation. 1992;90(3):772-9.

126. Koch AE, Kunkel SL, Burrows JC, Evanoff HL, Haines GK, Pope RM, et al. Synovial tissue macrophage as a source of the chemotactic cytokine IL-8. The Journal of Immunology. 1991;147(7):2187-95.
127. Kemble S, Croft AP. Critical Role of Synovial Tissue-Resident Macrophage and Fibroblast Subsets in the Persistence of Joint Inflammation. Frontiers in Immunology. 2021;12.
128. Croft AP, Campos J, Jansen K, Turner JD, Marshall J, Attar M, et al. Distinct fibroblast subsets drive inflammation and damage in arthritis. Nature. 2019;570(7760):246-+.
129. Saeki N, Imai Y. Reprogramming of synovial macrophage metabolism by synovial fibroblasts under inflammatory conditions. Cell Communication and Signaling. 2020;18(1).
130. Kuo D, Ding J, Cohn IS, Zhang F, Wei K, Rao DA, et al. HBEGF(+) macrophages in rheumatoid arthritis induce fibroblast invasiveness. Science Translational Medicine. 2019;11(491).
131. Iguchi T, Kurosaka M, Ziff M. Electron microscopic study of HLA-DR and monocyte/macrophage staining cells in the rheumatoid synovial membrane. Arthritis Rheum. 1986;29(5):600-13.
132. Tsark EC, Wang W, Teng YC, Arkfeld D, Dodge GR, Kovats S. Differential MHC class, II-mediated presentation of rheumatoid arthritis autoantigens by human dendritic cells and macrophages. Journal of Immunology. 2002;169(11):6625-33.
133. Michaelsson E, Holmdahl M, Engstrom A, Burkhardt H, Scheynius A, Holmdahl R. MACROPHAGES, BUT NOT DENDRITIC CELLS, PRESENT COLLAGEN TO T-CELLS. European Journal of Immunology. 1995;25(8):2234-41.
134. Sokolove J, Zhao XY, Chandra PE, Robinson WH. Immune Complexes Containing Citrullinated Fibrinogen Costimulate Macrophages via Toll-like Receptor 4 and Fc gamma Receptor. Arthritis and Rheumatism. 2011;63(1):53-62.
135. Laurent L, Anquetil F, Clavel C, Ndongo-Thiam N, Offer G, Miossec P, et al. IgM rheumatoid factor amplifies the inflammatory response of macrophages induced by the rheumatoid arthritis-specific immune complexes containing anticitrullinated protein antibodies. Annals of the Rheumatic Diseases. 2015;74(7):1425-31.
136. Egan PJ, van Nieuwenhuijze A, Campbell IK, Wicks IP. Promotion of the Local Differentiation of Murine Th17 Cells by Synovial Macrophages During Acute Inflammatory Arthritis. Arthritis and Rheumatism. 2008;58(12):3720-9.
137. Tetlow LC, Lees M, Ogata Y, Nagase H, Woolley DE. DIFFERENTIAL EXPRESSION OF GELATINASE-B (MMP-9) AND STROMELYSIN-1 (MMP-3) BY RHEUMATOID SYNOVIAL-CELLS IN-VITRO AND IN-VIVO. Rheumatology International. 1993;13(2):53-9.
138. Yokota K, Sato K, Miyazaki T, Kitaura H, Kayama H, Miyoshi F, et al. Combination of Tumor Necrosis Factor alpha and Interleukin-6 Induces Mouse Osteoclast-like Cells With Bone Resorption Activity Both In Vitro and In Vivo. Arthritis & Rheumatology. 2014;66(1):121-9.
139. Genovese MC, Becker J, Schiff M, Luggen M, Sherrer Y, Kremer J, et al. Abatacept for rheumatoid arthritis refractory to tumor necrosis factor alpha inhibition. New England Journal of Medicine. 2005;353(11):1114-23.
140. Smeets TJM, Kraan MC, van Loon ME, Tak PP. Tumor necrosis factor a blockade reduces the synovial cell infiltrate early after initiation of treatment, but apparently not by induction of apoptosis in synovial tissue. Arthritis and Rheumatism. 2003;48(8):2155-62.
141. Fonseca JE, Edwards JCW, Blades S, Gouldin NJ. Macrophage subpopulations in rheumatoid synovium - Reduced CD163 expression in CD4+ T lymphocyte-rich microenviroments. Arthritis and Rheumatism. 2002;46(5):1210-6.
142. De Rycke L, Baeten D, Foell D, Kruithof E, Veys EM, Roth J, et al. Differential expression and response to anti-TNF alpha treatment of infiltrating versus resident tissue macrophage subsets in autoimmune arthritis. Journal of Pathology. 2005;206(1):17-27.

143. Zwadlo G, Voegeíi R, Osthoff KS, Sorg C. A Monoclonal Antibody to a Novel Differentiation Antigen on Human Macrophages Associated with the Down-Regulatory Phase of the Inflammatory Process. Pathobiology. 1987;55(6):295-304.
144. Mandelin AM, Homan PJ, Shaffer AM, Cuda CM, Dominguez ST, Bacalao E, et al. Transcriptional Profiling of Synovial Macrophages Using Minimally Invasive Ultrasound-Guided Synovial Biopsies in Rheumatoid Arthritis. Arthritis & Rheumatology. 2018;70(6):841-54.
145. Zhang F, Wei K, Slowikowski K, Fonseka CY, Rao DA, Kelly S, et al. Defining inflammatory cell states in rheumatoid arthritis joint synovial tissues by integrating single-cell transcriptomics and mass cytometry. Nature Immunology. 2019;20(7):928-+.
146. Alivernini S, MacDonald L, Elmesmari A, Finlay S, Tolusso B, Gigante MR, et al. Distinct synovial tissue macrophage subsets regulate inflammation and remission in rheumatoid arthritis. Nature Medicine. 2020;26(8):1295-+.
147. Sun ST, Liu WL, Li YF. CADM1 enhances intestinal barrier function in a rat model of mild inflammatory bowel disease by inhibiting the STAT3 signaling pathway. Journal of Bioenergetics and Biomembranes. 2020;52(5):343-54.
148. Cole TJ, Blendy JA, Monaghan AP, Krieglstein K, Schmid W, Aguzzi A, et al. TARGETED DISRUPTION OF THE GLUCOCORTICOID RECEPTOR GENE BLOCKS ADRENERGIC CHROMAFFIN CELL-DEVELOPMENT AND SEVERELY RETARDS LUNG MATURATION. Genes & Development. 1995;9(13):1608-21.
149. Exton JH, Friedmann N, Wong EHA, Brineaux JP, Corbin JD, Park CR. INTERACTION OF GLUCOCORTICOIDS WITH GLUCAGON AND EPINEPHRINE IN CONTROL OF GLUCONEOGENESIS AND GLYCOGENOLYSIS IN LIVER AND OF LIPOLYSIS IN ADIPOSE-TISSUE. Journal of Biological Chemistry. 1972;247(11):3579-+.
150. Exton JH, Miller TB, Harper SC, Park CR. CARBOHYDRATE-METABOLISM IN PERFUSED LIVERS OF ADRENALECTOMIZED AND STEROID-REPLACED RATS. American Journal of Physiology. 1976;230(1):163-70.
151. Bloom SR, Edwards AV, Hardy RN, Malinowska KW, Silver M. ENDOCRINE RESPONSES TO INSULIN HYPOGLYCEMIA IN YOUNG CALF. Journal of Physiology-London. 1975;244(3):783-803.
152. Bayo P, Sanchis A, Bravo A, Cascallana JL, Buder K, Tuckermann J, et al. Glucocorticoid receptor is required for skin barrier competence. Endocrinology. 2008;149(3):1377-88.
153. Goodwin JE, Zhang JH, Geller DS. A critical role for vascular smooth muscle in acute glucocorticoid-induced hypertension. Journal of the American Society of Nephrology. 2008;19(7):1291-9.
154. Hench PS, Kendall EC, Slocumb CH, Polley HF. THE EFFECT OF A HORMONE OF THE ADRENAL CORTEX (17-HYDROXY-11-DEHYDROCORTICOSTERONE - COMPOUND-E) AND OF PITUITARY ADRENOCORTICOTROPHIC HORMONE ON RHEUMATOID ARTHRITIS - PRELIMINARY REPORT. Annals of the Rheumatic Diseases. 1949;8(2):97-104.
155. Nader N, Chrousos GP, Kino T. Interactions of the circadian CLOCK system and the HPA axis. Trends in Endocrinology and Metabolism. 2010;21(5):277-86.
156. Berkenbosch F, Vanoers J, Delrey A, Tilders F, Besedovsky H. CORTICOTROPIN-RELEASING FACTOR PRODUCING NEURONS IN THE RAT ACTIVATED BY INTERLEUKIN-1. Science. 1987;238(4826):524-6.
157. Bernardini R, Kamilaris TC, Calogero AE, Johnson EO, Gomez MT, Gold PW, et al. INTERACTIONS BETWEEN TUMOR NECROSIS FACTOR-ALPHA, HYPOTHALAMIC CORTICOTROPIN-RELEASING HORMONE, AND ADRENOCORTICOTROPIN SECRETION IN THE RAT. Endocrinology. 1990;126(6):2876-81.
158. Fukata J, Usui T, Naitoh Y, Nakai Y, Imura H. EFFECTS OF RECOMBINANT HUMAN INTERLEUKIN-1-ALPHA, INTERLEUKIN-1-BETA, 2 AND 6 ON ACTH SYNTHESIS AND RELEASE IN THE MOUSE PITUITARY-TUMOR CELL-LINE ATT-20. Journal of Endocrinology. 1989;122(1):33-9.

159. Jefcoate C. High-flux mitochondrial cholesterol trafficking, a specialized function of the adrenal cortex. Journal of Clinical Investigation. 2002;110(7):881-90.
160. Miller WL, Auchus RJ. The Molecular Biology, Biochemistry, and Physiology of Human Steroidogenesis and Its Disorders. Endocrine Reviews. 2011;32(1):81-151.
161. Stewart PM, Murry BA, Mason JI. Human kidney 11 beta-hydroxysteroid dehydrogenase is a high affinity nicotinamide adenine dinucleotide-dependent enzyme and differs from the cloned type I isoform. J Clin Endocrinol Metab. 1994;79(2):480-4.
162. Munck A, Brinckjo.T. SPECIFIC AND NONSPECIFIC PHYSIOCHEMICAL INTERACTIONS OF GLUCOCORTICOIDS AND RELATED STEROIDS WITH RAT THYMUS CELLS IN VITRO. Journal of Biological Chemistry. 1968;243(21):5556-&.
163. Hollenberg SM, Weinberger C, Ong ES, Cerelli G, Oro A, Lebo R, et al. Primary structure and expression of a functional human glucocorticoid receptor cDNA. Nature. 1985;318(6047):635-41.
164. Weinberger C, Hollenberg SM, Ong ES, Harmon JM, Brower ST, Cidlowski J, et al. IDENTIFICATION OF HUMAN GLUCOCORTICOID RECEPTOR COMPLEMENTARY-DNA CLONES BY EPITOPE SELECTION. Science. 1985;228(4700):740-2.
165. Erkut ZA, Pool C, Swaab DF. Glucocorticoids suppress corticotropin-releasing hormone and vasopressin expression in human hypothalamic neurons. Journal of Clinical Endocrinology & Metabolism. 1998;83(6):2066-73.
166. Perry MG, Kirwan JR, Jessop DS, Hunt LP. Overnight variations in cortisol, interleukin 6, tumour necrosis factor alpha and other cytokines in people with rheumatoid arthritis. Annals of the Rheumatic Diseases. 2009;68(1):63-8.
167. Dunn JF, Nisula BC, Rodbard D. TRANSPORT OF STEROID-HORMONES - BINDING OF 21 ENDOGENOUS STEROIDS TO BOTH TESTOSTERONE-BINDING GLOBULIN AND CORTICOSTEROID-BINDING GLOBULIN IN HUMAN-PLASMA. Journal of Clinical Endocrinology & Metabolism. 1981;53(1):58-68.
168. Mendel CM. THE FREE HORMONE HYPOTHESIS - A PHYSIOLOGICALLY BASED MATHEMATICAL-MODEL. Endocrine Reviews. 1989;10(3):232-74.
169. Hammond GL, Smith CL, Paterson NAM, Sibbald WJ. A ROLE FOR CORTICOSTEROID-BINDING GLOBULIN IN DELIVERY OF CORTISOL TO ACTIVATED NEUTROPHILS. Journal of Clinical Endocrinology & Metabolism. 1990;71(1):34-45.
170. Stewart PM, Newell-Price JDC. Chapter 15 - The Adrenal Cortex. In: Melmed S, Polonsky KS, Larsen PR, Kronenberg HM, editors. Williams Textbook of Endocrinology (Thirteenth Edition). Philadelphia: Elsevier; 2016. p. 489-555.
171. Leung DYM, Hamid Q, Vottero A, Szefler SJ, Surs W, Minshall E, et al. Association of glucocorticoid insensitivity with increased expression of glucocorticoid receptor beta. Journal of Experimental Medicine. 1997;186(9):1567-74.
172. Morgan DJ, Poolman TM, Williamson AJK, Wang ZC, Clark NR, Ma'ayan A, et al. Glucocorticoid receptor isoforms direct distinct mitochondrial programs to regulate ATP production. Scientific Reports. 2016;6.
173. Ding XF, Anderson CM, Ma H, Hong H, Uht RM, Kushner PJ, et al. Nuclear Receptor-Binding Sites of Coactivators Glucocorticoid Receptor Interacting Protein 1 (GRIP1) and Steroid Receptor Coactivator 1 (SRC-1): Multiple Motifs with Different Binding Specificities. Molecular Endocrinology. 1998;12(2):302-13.
174. Hard T, Kellenbach E, Boelens R, Maler BA, Dahlman K, Freedman LP, et al. SOLUTION STRUCTURE OF THE GLUCOCORTICOID RECEPTOR DNA-BINDING DOMAIN. Science. 1990;249(4965):157-60.
175. Danielian PS, White R, Lees JA, Parker MG. IDENTIFICATION OF A CONSERVED REGION REQUIRED FOR HORMONE DEPENDENT TRANSCRIPTIONAL ACTIVATION BY STEROID-HORMONE RECEPTORS. Embo Journal. 1992;11(3):1025-33.

176. Picard D, Yamamoto KR. 2 SIGNALS MEDIATE HORMONE-DEPENDENT NUCLEAR-LOCALIZATION OF THE GLUCOCORTICOID RECEPTOR. Embo Journal. 1987;6(11):3333-40.
177. Wu BL, Li PY, Liu YW, Lou ZY, Ding Y, Shu CL, et al. 3D structure of human FK506-binding protein 52: Implications for the assembly of the glucocorticoid receptor/Hsp90/immunophilin heterocomplex. Proceedings of the National Academy of Sciences of the United States of America. 2004;101(22):8348-53.
178. Pratt WB. The role of heat shock proteins in regulating the function, folding, and trafficking of the glucocorticoid receptor. Journal of Biological Chemistry. 1993;268(29):21455-8.
179. Abraham SM, Lawrence T, Kleiman A, Warden P, Medghalchi M, Tuckermann J, et al. Antiinflammatory effects of dexamethasone are partly dependent on induction of dual specificity phosphatase 1. Journal of Experimental Medicine. 2006;203(8):1883-9.
180. Yang YH, Morand EF, Getting SJ, Paul-Clark M, Liu DL, Yona S, et al. Modulation of inflammation and response to dexamethasone by annexin 1 in antigen-induced arthritis. Arthritis and Rheumatism. 2004;50(3):976-84.
181. Lim HW, Uhlenhaut NH, Rauch A, Weiner J, Hubner S, Hubner N, et al. Genomic redistribution of GR monomers and dimers mediates transcriptional response to exogenous glucocorticoid in vivo. Genome Research. 2015;25(6):836-44.
182. Drouin J, Sun YL, Chamberland M, Gauthier Y, Delean A, Nemer M, et al. NOVEL GLUCOCORTICOID RECEPTOR COMPLEX WITH DNA ELEMENT OF THE HORMONE-REPRESSED POMC GENE. Embo Journal. 1993;12(1):145-56.
183. Surjit M, Ganti KP, Mukherji A, Ye T, Hua G, Metzger D, et al. Widespread Negative Response Elements Mediate Direct Repression by Agonist-Liganded Glucocorticoid Receptor. Cell. 2011;145(2):224-41.
184. Uhlenhaut NH, Barish GD, Yu RT, Downes M, Karunasiri M, Liddle C, et al. Insights into Negative Regulation by the Glucocorticoid Receptor from Genome-wide Profiling of Inflammatory Cistromes. Molecular Cell. 2013;49(1):158-71.
185. Weikum ER, de Vera IMS, Nwachukwu JC, Hudson WH, Nettles KW, Kojetin DJ, et al. Tethering not required: the glucocorticoid receptor binds directly to activator protein-1 recognition motifs to repress inflammatory genes. Nucleic Acids Research. 2017;45(14):8596-608.
186. Ray A, Prefontaine KE. PHYSICAL ASSOCIATION AND FUNCTIONAL ANTAGONISM BETWEEN THE P65 SUBUNIT OF TRANSCRIPTION FACTOR NF-KAPPA-B AND THE GLUCOCORTICOID RECEPTOR. Proceedings of the National Academy of Sciences of the United States of America. 1994;91(2):752-6.
187. Miner JN, Yamamoto KR. THE BASIC REGION OF AP-1 SPECIFIES GLUCOCORTICOID RECEPTOR ACTIVITY AT A COMPOSITE RESPONSE ELEMENT. Genes & Development. 1992;6(12B):2491-501.
188. Sasse SK, Gruca M, Allen MA, Kadiyala V, Song TY, Gally F, et al. Nascent transcript analysis of glucocorticoid crosstalk with TNF defines primary and cooperative inflammatory repression. Genome Research. 2019;29(11):1753-65.
189. Leis H, Page A, Ramirez A, Bravo A, Segrelles C, Paramio J, et al. Glucocorticoid receptor counteracts tumorigenic activity of Akt in skin through interference with the phosphatidylinositol 3-kinase signaling pathway. Molecular Endocrinology. 2004;18(2):303-11.
190. Duval D, Durant S, Homo-Delarche F. Non-genomic effects of steroids Interactions of steroid molecules with membrane structures and functions. Biochimica et Biophysica Acta (BBA) - Reviews on Biomembranes. 1983;737(3):409-42.
191. Deng Q, Riquelme D, Trinh L, Low MJ, Tomic M, Stojilkovic S, et al. Rapid Glucocorticoid Feedback Inhibition of ACTH Secretion Involves Ligand-Dependent Membrane Association of Glucocorticoid Receptors. Endocrinology. 2015;156(9):3215-27.
192. Galon J, Franchimont D, Hiroi N, Frey G, Boettner A, Ehrhart-Bornstein M, et al. Gene profiling reveals unknown enhancing and suppressive actions of glucocorticoids on immune cells. Faseb Journal. 2002;16(1):61-71.

193. Auphan N, Didonato JA, Rosette C, Helmberg A, Karin M. IMMUNOSUPPRESSION BY GLUCOCORTICOIDS - INHIBITION OF NF-KAPPA-B ACTIVITY THROUGH INDUCTION OF I-KAPPA-B SYNTHESIS. Science. 1995;270(5234):286-90.
194. Brostjan C, Anrather J, Csizmadia V, Stroka D, Soares M, Bach FH, et al. Glucocorticoid-mediated repression of NF kappa B activity in endothelial cells does not involve induction of I kappa B alpha synthesis. Journal of Biological Chemistry. 1996;271(32):19612-6.
195. Konig H, Ponta H, Rahmsdorf HJ, Herrlich P. INTERFERENCE BETWEEN PATHWAY-SPECIFIC TRANSCRIPTION FACTORS - GLUCOCORTICOIDS ANTAGONIZE PHORBOL ESTER-INDUCED AP-1 ACTIVITY WITHOUT ALTERING AP-1 SITE OCCUPATION INVIVO. Embo Journal. 1992;11(6):2241-6.
196. Zhang C, Baumgartner RA, Yamada K, Beaven MA. Mitogen-activated protein (MAP) kinase regulates production of tumor necrosis factor-alpha and release of arachidonic acid in mast cells - Indications of communication between p38 and p42 MAP kinases. Journal of Biological Chemistry. 1997;272(20):13397-402.
197. Ayroldi E, Migliorati G, Bruscoli S, Marchetti C, Zollo O, Cannarile L, et al. Modulation of T-cell activation by the glucocorticoid-induced leucine zipper factor via inhibition of nuclear factor kappa B. Blood. 2001;98(3):743-53.
198. Ayroldi E, Zollo O, Macchiarulo A, Di Marco B, Marchetti C, Riccardi C. Glucocorticoid-induced leucine zipper inhibits the raf-extracellular signal-regulated kinase pathway by binding to Raf-1. Molecular and Cellular Biology. 2002;22(22):7929-41.
199. Mittelstadt PR, Ashwell JD. Inhibition of AP-1 by the glucocorticoid-inducible protein GILZ. Journal of Biological Chemistry. 2001;276(31):29603-10.
200. McArthur S, Gobbetti T, Kusters DHM, Reutelingsperger CP, Flower RJ, Perretti M. Definition of a Novel Pathway Centered on Lysophosphatidic Acid To Recruit Monocytes during the Resolution Phase of Tissue Inflammation. Journal of Immunology. 2015;195(3):1139-51.
201. Sawmynaden P, Perretti M. Glucocorticoid upregulation of the annexin-A1 receptor in leukocytes. Biochemical and Biophysical Research Communications. 2006;349(4):1351-5.
202. Kassel O, Sancono A, Kratzschmar J, Kreft B, Stassen M, Cato ACB. Glucocorticoids inhibit MAP kinase via increased expression and decreased degradation of MKP-1. Embo Journal. 2001;20(24):7108-16.
203. Tabardel Y, Duchateau J, Schmartz D, Marecaux G, Shahla M, Barvais L, et al. Corticosteroids increase blood interleukin-10 levels during cardiopulmonary bypass in men. Surgery. 1996;119(1):76-80.
204. Franco LM, Gadkari M, Howe KN, Sun J, Kardava L, Kumar P, et al. Immune regulation by glucocorticoids can be linked to cell type-dependent transcriptional responses. Journal of Experimental Medicine. 2019;216(2):384-406.
205. Perretti M, Ahluwalia A. The microcirculation and inflammation: Site of action for glucocorticoids. Microcirculation. 2000;7(3):147-61.
206. Cronstein BN, Kimmel SC, Levin RI, Martiniuk F, Weissmann G. A MECHANISM FOR THE ANTIINFLAMMATORY EFFECTS OF CORTICOSTEROIDS - THE GLUCOCORTICOID RECEPTOR REGULATES LEUKOCYTE ADHESION TO ENDOTHELIAL-CELLS AND EXPRESSION OF ENDOTHELIAL LEUKOCYTE ADHESION MOLECULE-1 AND INTERCELLULAR-ADHESION MOLECULE-1. Proceedings of the National Academy of Sciences of the United States of America. 1992;89(21):9991-5.
207. Grosman N, Jensen SM. INFLUENCE OF GLUCOCORTICOIDS ON HISTAMINE-RELEASE AND CA-45 UPTAKE BY ISOLATED RAT MAST-CELLS. Agents and Actions. 1984;14(1):21-30.
208. Zhou J, Liu DF, Liu C, Kang ZM, Shen XH, Chen YZ, et al. Glucocorticoids inhibit degranulation of mast cells in allergic asthma via nongenomic mechanism. Allergy. 2008;63(9):1177-85.
209. Filep JG, Delalandre A, Payette Y, FoldesFilep E. Glucocorticoid receptor regulates expression of L-selectin and CD11/CD18 on human neutrophils. Circulation. 1997;96(1):295-301.

210. Cox G. GLUCOCORTICOID TREATMENT INHIBITS APOPTOSIS IN HUMAN NEUTROPHILS - SEPARATION OF SURVIVAL AND ACTIVATION OUTCOMES. Journal of Immunology. 1995;154(9):4719-25.
211. Ehrchen J, Steinmuller L, Barczyk K, Tenbrock K, Nacken W, Eisenacher M, et al. Glucocorticoids induce differentiation of a specifically activated, anti-inflammatory subtype of human monocytes. Blood. 2007;109(3):1265-74.
212. Larsson S, Linden M. Effects of a corticosteroid, budesonide, on production of bioactive IL-12 by human monocytes. Cytokine. 1998;10(10):786-9.
213. Mozo L, Suarez A, Gutierrez C. Glucocorticoids up-regulate constitutive interleukin-10 production by human monocytes. Clinical and Experimental Allergy. 2004;34(3):406-12.
214. Van den Heuvel MM, Van Beek NMA, Broug-Holub E, Postmus PE, Hoefsmit ECM, Beelen RHJ, et al. Glucocorticoids modulate the development of dendritic cells from blood precursors. Clinical and Experimental Immunology. 1999;115(3):577-83.
215. Chamorro S, Garcia-Vallejo JJ, Unger WWJ, Fernandes RJ, Bruijns SCM, Laban S, et al. TLR Triggering on Tolerogenic Dendritic Cells Results in TLR2 Up-Regulation and a Reduced Proinflammatory Immune Program. Journal of Immunology. 2009;183(5):2984-94.
216. Lowenberg M, Verhaar AP, van den Brink GR, Hommes DW. Glucocorticoid signaling: a nongenomic mechanism for T-cell immunosuppression. Trends in Molecular Medicine. 2007;13(4):158-63.
217. Cupps TR, Gerrard TL, Falkoff RJM, Whalen G, Fauci AS. EFFECTS OF INVITRO CORTICOSTEROIDS ON B-CELL ACTIVATION, PROLIFERATION, AND DIFFERENTIATION. Journal of Clinical Investigation. 1985;75(2):754-61.
218. Franchimont D, Galon J, Gadina M, Visconti R, Zhou YJ, Aringer M, et al. Inhibition of Th1 immune response by glucocorticoids, dexamethasone selectively inhibits IL-12-induced Stat4 phosphorylation in T lymphocytes. Journal of Immunology. 2000;164(4):1768-74.
219. Schleimer RP, Jacques A, Shin HS, Lichtenstein LM, Plaut M. INHIBITION OF T-CELL-MEDIATED CYTO-TOXICITY BY ANTI-INFLAMMATORY STEROIDS. Journal of Immunology. 1984;132(1):266-71.
220. Reichardt HM, Kaestner KH, Tuckermann J, Kretz O, Wessely O, Bock R, et al. DNA binding of the glucocorticoid receptor is not essential for survival. Cell. 1998;93(4):531-41.
221. Migliorati G, Pagliacci C, Moraca R, Crocicchio F, Nicoletti I, Riccardi C. Glucocorticoid-induced apoptosis of natural killer cells and cytotoxic T lymphocytes. Pharmacol Res. 1992;26 Suppl 2:26-7.
222. Lill-Elghanian D, Schwartz K, King L, Fraker P. Glucocorticoid-induced apoptosis in early B cells from human bone marrow. Experimental Biology and Medicine. 2002;227(9):763-70.
223. Zizzo G, Hilliard BA, Monestier M, Cohen PL. Efficient Clearance of Early Apoptotic Cells by Human Macrophages Requires M2c Polarization and MerTK Induction. Journal of Immunology. 2012;189(7):3508-20.
224. Giles KM, Ross K, Rossi AG, Hotchin NA, Haslett C, Dransfield I. Glucocorticoid augmentation of macrophage capacity for phagocytosis of apoptotic cells is associated with reduced p130Cas expression, loss of paxillin/pyk2 phosphorylation, and high levels of active Rac. Journal of Immunology. 2001;167(2):976-86.
225. Barish GD, Downes M, Alaynick WA, Yu RT, Ocampo CB, Bookout AL, et al. A nuclear receptor atlas: Macrophage activation. Molecular Endocrinology. 2005;19(10):2466-77.
226. Snyder DS, Unanue ER. CORTICOSTEROIDS INHIBIT MURINE MACROPHAGE-IA EXPRESSION AND INTERLEUKIN-1 PRODUCTION. Journal of Immunology. 1982;129(5):1803-5.
227. Zanker B, Walz G, Wieder KJ, Strom TB. EVIDENCE THAT GLUCOCORTICOSTEROIDS BLOCK EXPRESSION OF THE HUMAN INTERLEUKIN-6 GENE BY ACCESSORY CELLS. Transplantation. 1990;49(1):183-5.
228. Beutler B, Krochin N, Milsark IW, Luedke C, Cerami A. Control of cachectin (tumor necrosis factor) synthesis: mechanisms of endotoxin resistance. Science. 1986;232(4753):977-80.

229. Long F, Wang YX, Liu L, Zhou J, Cui RY, Jiang CL. Rapid nongenomic inhibitory effects of glucocorticoids on phagocytosis and superoxide anion production by macrophages. Steroids. 2005;70(1):55-61.
230. van de Garde MDB, Martinez FO, Melgert BN, Hylkema MN, Jonkers RE, Hamann J. Chronic Exposure to Glucocorticoids Shapes Gene Expression and Modulates Innate and Adaptive Activation Pathways in Macrophages with Distinct Changes in Leukocyte Attraction. Journal of Immunology. 2014;192(3):1196-208.
231. Zhou JY, Zhong HJ, Yang C, Yan J, Wang HY, Jiang JX. Corticosterone exerts immunostimulatory effects on macrophages via endoplasmic reticulum stress. British Journal of Surgery. 2010;97(2):281-93.
232. Lim HY, Muller N, Herold MJ, van den Brandt J, Reichardt HM. Glucocorticoids exert opposing effects on macrophage function dependent on their concentration. Immunology. 2007;122(1):47-53.
233. Bhattacharyya S, Brown DE, Brewer JA, Vogt SK, Muglia LJ. Macrophage glucocorticoid receptors regulate toll-like receptor 4-mediated inflammatory responses by selective inhibition of p38 MAP kinase. Blood. 2007;109(10):4313-9.
234. Bhattacharyya S, Ratajczak CK, Vogt SK, Kelley C, Colonna M, Schreiber RD, et al. TAK1 targeting by glucocorticoids determines JNK and I kappa B regulation in Toll-like receptor-stimulated macrophages. Blood. 2010;115(10):1921-31.
235. Hu XY, Li WP, Meng C, Ivashkiv LB. Inhibition of IFN-gamma signaling by glucocorticoids. Journal of Immunology. 2003;170(9):4833-9.
236. Stifel U, Wolfschmitt EM, Vogt J, Wachter U, Vettorazzi S, Tews D, et al. Glucocorticoids coordinate macrophage metabolism through the regulation of the tricarboxylic acid cycle. Molecular Metabolism. 2022;57.
237. Sauvage MAD, Maatouk L, Arnoux I, Pasco M, Diez AS, Delahaye M, et al. Potent and multiple regulatory actions of microglial glucocorticoid receptors during CNS inflammation. Cell Death and Differentiation. 2013;20(11):1546-57.
238. Galuppo P, Vettorazzi S, Hovelmann J, Scholz CJ, Tuckermann JP, Bauersachs J, et al. The glucocorticoid receptor in monocyte-derived macrophages is critical for cardiac infarct repair and remodeling. Faseb Journal. 2017;31(11):5122-32.
239. Cech AC, Shou J, Gallagher H, Daly JM. Glucocorticoid Receptor Blockade Reverses Postinjury Macrophage Suppression. Archives of Surgery. 1994;129(12):1227-32.
240. Kleiman A, Hubner S, Parkitna JMR, Neumann A, Hofer S, Weigand MA, et al. Glucocorticoid receptor dimerization is required for survival in septic shock via suppression of interleukin-1 in macrophages. Faseb Journal. 2012;26(2):722-9.
241. Vettorazzi S, Bode C, Dejager L, Frappart L, Shelest E, Klassen C, et al. Glucocorticoids limit acute lung inflammation in concert with inflammatory stimuli by induction of SphK1. Nature Communications. 2015;6.
242. Meers GK, Bohnenberger H, Reichardt HM, Luhder F, Reichardt SD. Impaired resolution of DSS-induced colitis in mice lacking the glucocorticoid receptor in myeloid cells. Plos One. 2018;13(1).
243. Barnes PJ. Corticosteroids: The drugs to beat. European Journal of Pharmacology. 2006;533(1-3):2-14.
244. Pickup ME. CLINICAL PHARMACOKINETICS OF PREDNISONE AND PREDNISOLONE. Clinical Pharmacokinetics. 1979;4(2):111-28.
245. Czock D, Keller F, Rasche FM, Haussler U. Pharmacokinetics and pharmacodynamics of systemically administered glucocorticoids. Clinical Pharmacokinetics. 2005;44(1):61-98.
246. Diederich S, Scholz T, Eigendorff E, Bumke-Vogt C, Quinkler M, Exner P, et al. Pharmacodynamics and pharmacokinetics of synthetic mineralocorticoids and glucocorticoids: Receptor transactivation and prereceptor metabolism by 11 beta-hydroxysteroid-dehydrogenases. Hormone and Metabolic Research. 2004;36(6):423-9.

247. Caldwell JR. Intra-articular corticosteroids - Guide to selection and indications for use. Drugs. 1996;52(4):507-14.
248. Sapolsky RM, Romero LM, Munck AU. How do glucocorticoids influence stress responses? Integrating permissive, suppressive, stimulatory, and preparative actions. Endocrine reviews. 2000;21(1):55-89.
249. Swanson C, Lorentzon M, Conaway HH, Lerner UH. Glucocorticoid regulation of osteoclast differentiation and expression of receptor activator of nuclear factor-kappa B (NF-kappa B) ligand, osteoprotegerin, and receptor activator of NF-kappa B in mouse calvarial bones. Endocrinology. 2006;147(7):3613-22.
250. Humphrey EL, Williams JHH, Davie MWJ, Marshall MJ. Effects of dissociated glucocorticoids on OPG and RANKL in osteoblastic cells. Bone. 2006;38(5):652-61.
251. Troncoso R, Paredes F, Parra V, Gatica D, Vasquez-Trincado C, Quiroga C, et al. Dexamethasone-induced autophagy mediates muscle atrophy through mitochondrial clearance. Cell Cycle. 2014;13(14):2281-95.
252. Ortega E, Rodriguez C, Strand LJ, Segre E. EFFECTS OF CLOPREDNOL AND OTHER CORTICOSTEROIDS ON HYPOTHALAMIC-PITUITARY-ADRENAL AXIS FUNCTION. Journal of International Medical Research. 1976;4(5):326-37.
253. Hetland ML, Stengaard-Pedersen K, Junker P, Lottenburger T, Hansen I, Andersen LS, et al. Aggressive combination therapy with intra-articular glucocorticoid injections and conventional disease-modifying anti-rheumatic drugs in early rheumatoid arthritis: second-year clinical and radiographic results from the CIMESTRA study. Annals of the Rheumatic Diseases. 2008;67(6):815-22.
254. af Klint E, Grundtman C, Engstrom M, Catrina AI, Makrygiannakis D, Klareskog L, et al. Intraarticular glucocorticoid treatment reduces inflammation in synovial cell infiltrations more efficiently than in synovial blood vessels. Arthritis and Rheumatism. 2005;52(12):3880-9.
255. Green MJ, Gough AKS, Devlin J, Smith J, Astin P, Taylor D, et al. Serum MMP-3 and MMP-1 and progression of joint damage in early rheumatoid arthritis. Rheumatology. 2003;42(1):83-8.
256. Makrygiannakis D, af Klint E, Catrina SB, Botusan IR, Klareskog E, Klareskog L, et al. Intraarticular corticosteroids decrease synovial RANKL expression in inflammatory arthritis. Arthritis and Rheumatism. 2006;54(5):1463-72.
257. Stewart PM, Krozowski ZS. 11 beta-Hydroxysteroid dehydrogenase. Vitamins and hormones. 1999;57:249-324.
258. Dzyakanchuk AA, Balaza Z, Nashev LG, Amrein KE, Odermatt A. 11 beta-Hydroxysteroid dehydrogenase 1 reductase activity is dependent on a high ratio of NADPH/NADP(+) and is stimulated by extracellular glucose. Molecular and Cellular Endocrinology. 2009;301(1-2):137-41.
259. Maser E, Volker B, Friebertshauser J. 11 beta-hydroxysteroid dehydrogenase type 1 from human liver: Dimerization and enzyme cooperativity support its postulated role as glucocorticoid reductase. Biochemistry. 2002;41(7):2459-65.
260. Lavery GG, Walker EA, Draper N, Jeyasuria P, Marcos J, Shackleton CHL, et al. Hexose-6-phosphate dehydrogenase knock-out mice lack 11 beta-hydroxysteroid dehydrogenase type 1-mediated glucocorticoid generation. Journal of Biological Chemistry. 2006;281(10):6546-51.
261. Kotelevtsev Y, Holmes MC, Burchell A, Houston PM, Schmoll D, Jamieson P, et al. 11beta-hydroxysteroid dehydrogenase type 1 knockout mice show attenuated glucocorticoid-inducible responses and resist hyperglycemia on obesity or stress. Proceedings of the National Academy of Sciences of the United States of America. 1997;94(26):14924-9.
262. Basu R, Singh RJ, Basu A, Chittilapilly EG, Johnson CM, Toffolo G, et al. Splanchnic cortisol production occurs in humans - Evidence for conversion of cortisone to cortisol via the 11-beta hydroxysteroid dehydrogenase (11 beta-HSD) type 1 pathway. Diabetes. 2004;53(8):2051-9.
263. Siiteri PK, Murai JT, Hammond GL, Nisker JA, Raymoure WJ, Kuhn RW. THE SERUM TRANSPORT OF STEROID-HORMONES. Recent Progress in Hormone Research. 1982;38:457-503.

264. Whorwood CB, Ricketts ML, Stewart PM. Epithelial cell localization of type 2 11 beta-hydroxysteroid dehydrogenase in rat and human colon. Endocrinology. 1994;135(6):2533-41.
265. Smith RE, Maguire JA, SteinOakley AN, Sasano H, Takahashi KI, Fukushima K, et al. Localization of 11 beta-hydroxysteroid dehydrogenase type II in human epithelial tissues. Journal of Clinical Endocrinology & Metabolism. 1996;81(9):3244-8.
266. Morgan SA, McCabe EL, Gathercole LL, Hassan-Smith ZK, Larner DP, Bujalska IJ, et al. 11beta-HSD1 is the major regulator of the tissue-specific effects of circulating glucocorticoid excess. Proc Natl Acad Sci U S A. 2014;111(24):E2482-91.
267. Morgan SA, Sherlock M, Gathercole LL, Lavery GG, Lenaghan C, Bujalska IJ, et al. 11 beta-Hydroxysteroid Dehydrogenase Type 1 Regulates Glucocorticoid-Induced Insulin Resistance in Skeletal Muscle. Diabetes. 2009;58(11):2506-15.
268. Masuzaki H, Paterson J, Shinyama H, Morton NM, Mullins JJ, Seckl JR, et al. A transgenic model of visceral obesity and the metabolic syndrome. Science. 2001;294(5549):2166-70.
269. Rosenstock J, Banarer S, Fonseca VA, Inzucchi SE, Sun W, Yao WQ, et al. The 11-beta-Hydroxysteroid Dehydrogenase Type 1 Inhibitor INCB13739 Improves Hyperglycemia in Patients With Type 2 Diabetes Inadequately Controlled by Metformin Monotherapy. Diabetes Care. 2010;33(7):1516-22.
270. Feig PU, Shah S, Hermanowski-Vosatka A, Plotkin D, Springer MS, Donahue S, et al. Effects of an 11 beta-hydroxysteroid dehydrogenase type 1 inhibitor, MK-0916, in patients with type 2 diabetes mellitus and metabolic syndrome. Diabetes Obesity & Metabolism. 2011;13(6):498-504.
271. Martin CS, Cooper MS, Hardy RS. Endogenous Glucocorticoid Metabolism in Bone: Friend or Foe. Frontiers in Endocrinology. 2021;12.
272. Coutinho AE, Gray M, Brownstein DG, Salter DM, Sawatzky DA, Clay S, et al. 11 beta-Hydroxysteroid Dehydrogenase Type 1, But Not Type 2, Deficiency Worsens Acute Inflammation and Experimental Arthritis in Mice. Endocrinology. 2012;153(1):234-40.
273. Thieringer R, Le Grand CB, Carbin L, Cai TQ, Wong BM, Wright SD, et al. 11 beta-hydroxysteroid dehydrogenase type 1 is induced in human monocytes upon differentiation to macrophages. Journal of Immunology. 2001;167(1):30-5.
274. Zhang TY, Ding XH, Daynes RA. The expression of 11 beta-hydroxysteroid dehydrogenase type I by lymphocytes provides a novel means for intracrine regulation of glucocorticoid activities. Journal of Immunology. 2005;174(2):879-89.
275. Coutinho AE, Brown JK, Yang F, Brownstein DG, Gray M, Seckl JR, et al. Mast Cells Express 11 beta-hydroxysteroid Dehydrogenase Type 1: A Role in Restraining Mast Cell Degranulation. Plos One. 2013;8(1).
276. Coutinho AE, Kipari TMJ, Zhang ZG, Esteves CL, Lucas CD, Gilmour JS, et al. 11 beta-Hydroxysteroid Dehydrogenase Type 1 Is Expressed in Neutrophils and Restrains an Inflammatory Response in Male Mice. Endocrinology. 2016;157(7):2928-36.
277. Freeman L, Hewison M, Hughes SV, Evans KN, Hardie D, Means TK, et al. Expression of 11 beta-hydroxysteroid dehydrogenase type 1 permits regulation of glucocorticoid bioavailability by human dendritic cells. Blood. 2005;106(6):2042-9.
278. Gilmour JS, Coutinho AE, Cailhier JF, Man TY, Clay M, Thomas G, et al. Local amplification of Glucocorticoids by 11 beta-hydroxysteroid dehydrogenase type 1 promotes macrophage phagocytosis of apoptotic leukocytes. Journal of Immunology. 2006;176(12):7605-11.
279. Soulier A, Blois SM, Sivakumaran S, Fallah-Arani F, Henderson S, Flutter B, et al. Cell-intrinsic regulation of murine dendritic cell function and survival by prereceptor amplification of glucocorticoid. Blood. 2013;122(19):3288-97.
280. Lee NR, Kim BJ, Lee CH, Lee YB, Lee S, Hwang HJ, et al. Role of 11 beta-hydroxysteroid dehydrogenase type 1 in the development of atopic dermatitis. Scientific Reports. 2020;10(1).
281. Cooper MS, Bujalska I, Rabbitt E, Walker EA, Bland R, Sheppard MC, et al. Modulation of 11 beta-hydroxysteroid dehydrogenase isozymes by proinflammatory cytokines in osteoblasts: An

autocrine switch from glucocorticoid inactivation to activation. Journal of Bone and Mineral Research. 2001;16(6):1037-44.
282. Fenton CG, Crastin A, Martin CS, Suresh S, Montagna I, Hussain B, et al. 11 beta-Hydroxysteroid Dehydrogenase Type 1 within Osteoclasts Mediates the Bone Protective Properties of Therapeutic Corticosteroids in Chronic Inflammation. International Journal of Molecular Sciences. 2022;23(13).
283. Cooper MS, Rabbitt EH, Goddard PE, Bartlett WA, Hewison M, Stewart PM. Osteoblastic 11 beta-hydroxysteroid dehydrogenase type 1 activity increases with age and glucocorticoid exposure. Journal of Bone and Mineral Research. 2002;17(6):979-86.
284. Kaur K, Hardy R, Ahasan MM, Eijken M, van Leeuwen JP, Filer A, et al. Synergistic induction of local glucocorticoid generation by inflammatory cytokines and glucocorticoids: implications for inflammation associated bone loss. Annals of the Rheumatic Diseases. 2010;69(6):1185-90.
285. Ahasan MM, Hardy R, Jones C, Kaur K, Nanus D, Juarez M, et al. Inflammatory regulation of glucocorticoid metabolism in mesenchymal stromal cells. Arthritis and Rheumatism. 2012;64(7):2404-13.
286. Hardy RS, Doig CL, Hussain Z, O'Leary M, Morgan SA, Pearson MJ, et al. 11-Hydroxysteroid dehydrogenase type 1 within muscle protects against the adverse effects of local inflammation. Journal of Pathology. 2016;240(4):472-83.
287. Zbankova S, Bryndova J, Leden P, Kment M, Svec A, Pacha J. 11 beta-hydroxysteroid dehydrogenase 1 and 2 expression in colon from patients with ulcerative colitis. Journal of Gastroenterology and Hepatology. 2007;22(7):1019-23.
288. Stegk JP, Ebert B, Martin HJ, Maser E. Expression profiles of human 11 beta-hydroxysteroid dehydrogenases type 1 and type 2 in inflammatory bowel diseases. Molecular and Cellular Endocrinology. 2009;301(1-2):104-8.
289. Hardy R, Rabbitt EH, Filer A, Emery P, Hewison M, Stewart PM, et al. Local and systemic glucocorticoid metabolism in inflammatory arthritis. Annals of the Rheumatic Diseases. 2008;67(9):1204-10.
290. Fenton C, Martin C, Jones R, Croft A, Campos J, Naylor AJ, et al. Local steroid activation is a critical mediator of the anti-inflammatory actions of therapeutic glucocorticoids. Ann Rheum Dis. 2021;80(2):250-60.
291. Ishii T, Masuzaki H, Tanaka T, Arai N, Yasue S, Kobayashi N, et al. Augmentation of 11 beta-hydroxysteroid LPS-activated J774.1 macrophages dehydrogenase type 1 in - Role of 11 beta-HSD1 in pro-inflammatory properties in macrophages. Febs Letters. 2007;581(3):349-54.
292. Susarla R, Liu L, Walker EA, Bujalska IJ, Alsalem J, Williams GP, et al. Cortisol Biosynthesis in the Human Ocular Surface Innate Immune Response. Plos One. 2014;9(4).
293. Chinetti-Gbaguidi G, Bouhlel MA, Copin C, Duhem C, Derudas B, Neve B, et al. Peroxisome Proliferator-Activated Receptor-gamma Activation Induces 11 beta-Hydroxysteroid Dehydrogenase Type 1 Activity in Human Alternative Macrophages. Arteriosclerosis Thrombosis and Vascular Biology. 2012;32(3):677-U342.
294. Peixoto R, Turban S, Battle JH, Chapman KE, Seckl JR, Morton NM. Preadipocyte 11 beta-hydroxysteroid dehydrogenase type 1 is a keto-reductase and contributes to diet-induced visceral obesity in vivo. Endocrinology. 2008;149(4):1861-8.
295. Zhang TY, Daynes RA. Macrophages from 11 beta-hydroxysteroid dehydrogenase type 1-deficient mice exhibit an increased sensitivity to lipopolysaccharide stimulation due to TGF-beta-Mediated up-regulation of SHIP1 expression. Journal of Immunology. 2007;179(9):6325-35.
296. Chapman KE, Coutinho AE, Gray M, Gilmour JS, Savill JS, Seckl JR. The role and regulation of 11 beta-hydroxysteroid dehydrogenase type 1 in the inflammatory response. Molecular and Cellular Endocrinology. 2009;301(1-2):123-31.

297. McSweeney SJ, Hadoke PWF, Kozak AM, Small GR, Khaled H, Walker BR, et al. Improved heart function follows enhanced inflammatory cell recruitment and angiogenesis in 11 beta HSD1-deficient mice post-MI. Cardiovascular Research. 2010;88(1):159-67.
298. Mylonas KJ, Turner NA, Bageghni SA, Kenyon CJ, White CI, McGregor K, et al. 11 beta-HSD1 suppresses cardiac fibroblast CXCL2, CXCL5 and neutrophil recruitment to the heart post MI. Journal of Endocrinology. 2017;233(3):315-27.
299. Clausen BE, Burkhardt C, Reith W, Renkawitz R, Forster I. Conditional gene targeting in macrophages and granulocytes using LysMcre mice. Transgenic Research. 1999;8(4):265-77.
300. Zhang Z, Coutinho AE, Man TY, Kipari TMJ, Hadoke PWF, Salter DM, et al. Macrophage 11 beta-HSD-1 deficiency promotes inflammatory angiogenesis. Journal of Endocrinology. 2017;234(3):291-9.
301. Pascual G, Fong AL, Ogawa S, Gamliel A, Li AC, Perissi V, et al. A SUMOylation-dependent pathway mediates transrepression of inflammatory response genes by PPAR-gamma. Nature. 2005;437(7059):759-63.
302. Doig CL, Bashir J, Zielinska AE, Cooper MS, Stewart PM, Lavery GG. TNF alpha-mediated Hsd11b1 binding of NF-kappa B p65 is associated with suppression of 11 beta-HSD1 in muscle. Journal of Endocrinology. 2014;220(3):389-96.
303. Sai S, Esteves CL, Kelly V, Michailidou Z, Anderson K, Coll AP, et al. Glucocorticoid regulation of the promoter of 11 beta-hydroxysteroid dehydrogenase type 1 is indirect and requires CCAAT/enhancer-binding protein-beta. Molecular Endocrinology. 2008;22(9):2049-60.
304. Yang Z, Zhu XO, Guo CM, Sun K. Stimulation of 11 beta-HSD1 expression by IL-1 beta via a C/EBP binding site in human fetal lung fibroblasts. Endocrine. 2009;36(3):404-11.
305. Esteves CL, Kelly V, Begay V, Man TY, Morton NM, Leutz A, et al. Regulation of Adipocyte 11 beta-Hydroxysteroid Dehydrogenase Type 1 (11 beta-HSD1) by CCAAT/Enhancer-Binding Protein (C/EBP) beta Isoforms, LIP and LAP. Plos One. 2012;7(5).
306. Ruffell D, Mourkioti F, Gambardella A, Kirstetter P, Lopez RG, Rosenthal N, et al. A CREB-C/EBP beta cascade induces M2 macrophage-specific gene expression and promotes muscle injury repair. Proceedings of the National Academy of Sciences of the United States of America. 2009;106(41):17475-80.
307. Tengku-Muhammad TS, Hughes TR, Ranki H, Cryer A, Ramji DP. Differential regulation of macrophage CCAAT-enhancer binding protein isoforms by lipopolysaccharide and cytokines. Cytokine. 2000;12(9):1430-6.
308. Chapman KE, Coutinho AE, Zhang Z, Kipari T, Savill JS, Seckl JR. Changing glucocorticoid action: 11 beta-Hydroxysteroid dehydrogenase type 1 in acute and chronic inflammation. Journal of Steroid Biochemistry and Molecular Biology. 2013;137:82-92.
309. Schmidt M, Weidler C, Naumann H, Anders S, Scholmerich R, Straub RH. Reduced capacity for the reactivation of glucocorticoids in rheumatoid arthritis synovial cells - Possible role of the sympathetic nervous system? Arthritis and Rheumatism. 2005;52(6):1711-20.
310. Nanus DE, Filer AD, Yeo L, Scheel-Toellner D, Hardy R, Lavery GG, et al. Differential glucocorticoid metabolism in patients with persistent versus resolving inflammatory arthritis. Arthritis Research & Therapy. 2015;17.
311. Edwards C. Sixty Years after Hench-Corticosteroids and Chronic Inflammatory Disease. Journal of Clinical Endocrinology & Metabolism. 2012;97(5):1443-51.
312. Olsen NJ, Sokka T, Seehorn CL, Kraft B, Maas K, Moore J, et al. A gene expression signature for recent onset rheumatoid arthritis in peripheral blood mononuclear cells. Annals of the Rheumatic Diseases. 2004;63(11):1387-92.
313. Hardy RS, Filer A, Cooper MS, Parsonage G, Raza K, Hardie DL, et al. Differential expression, function and response to inflammatory stimuli of 11 beta-hydroxysteroid dehydrogenase type 1 in human fibroblasts: a mechanism for tissue-specific regulation of inflammation. Arthritis Research & Therapy. 2006;8(4).

314. Hardy RS, Fenton C, Croft AP, Naylor AJ, Begum R, Desanti G, et al. 11 Beta-hydroxysteroid dehydrogenase type 1 regulates synovitis, joint destruction, and systemic bone loss in chronic polyarthritis. Journal of Autoimmunity. 2018;92:104-13.
315. Fenton CG, Webster JM, Martin CS, Fareed S, Wehmeyer C, Mackie H, et al. Therapeutic glucocorticoids prevent bone loss but drive muscle wasting when administered in chronic polyarthritis. Arthritis Research & Therapy. 2019;21.
316. Webster JM, Sagmeister MS, Fenton CG, Seabright AP, Lai YC, Jones SW, et al. Global Deletion of 11 beta-HSD1 Prevents Muscle Wasting Associated with Glucocorticoid Therapy in Polyarthritis. International Journal of Molecular Sciences. 2021;22(15).
317. Jacobson DL, Gange SJ, Rose NR, Graham NMH. Epidemiology and estimated population burden of selected autoimmune diseases in the United States. Clinical Immunology and Immunopathology. 1997;84(3):223-43.
318. Cutolo M, Straub RH. Sex steroids and autoimmune rheumatic diseases: state of the art. Nature Reviews Rheumatology. 2020;16(11):628-44.
319. Grino PB, Griffin JE, Wilson JD. TESTOSTERONE AT HIGH-CONCENTRATIONS INTERACTS WITH THE HUMAN ANDROGEN RECEPTOR SIMILARLY TO DIHYDROTESTOSTERONE. Endocrinology. 1990;126(2):1165-72.
320. Rege J, Nakamura Y, Satoh F, Morimoto R, Kennedy MR, Layman LC, et al. Liquid Chromatography-Tandem Mass Spectrometry Analysis of Human Adrenal Vein 19-Carbon Steroids Before and After ACTH Stimulation. Journal of Clinical Endocrinology & Metabolism. 2013;98(3):1182-8.
321. Kirschner MA, Bardin CW. ANDROGEN PRODUCTION AND METABOLISM IN NORMAL AND VIRILIZED WOMEN. Metabolism-Clinical and Experimental. 1972;21(7):667-+.
322. Turcu AF, Rege J, Auchus RJ, Rainey WE. 11-Oxygenated androgens in health and disease. Nature Reviews Endocrinology. 2020;16(5):284-96.
323. Schiffer L, Bossey A, Kempegowda P, Taylor AE, Akerman I, Scheel-Toellner D, et al. Peripheral blood mononuclear cells preferentially activate 11-oxygenated androgens. European Journal of Endocrinology. 2021;184(3):357-67.
324. Lee DK, Chang CS. Expression and degradation of androgen receptor: Mechanism and clinical implication. Journal of Clinical Endocrinology & Metabolism. 2003;88(9):4043-54.
325. Zhou ZX, Lane MV, Kemppainen JA, French FS, Wilson EM. SPECIFICITY OF LIGAND-DEPENDENT ANDROGEN RECEPTOR STABILIZATION - RECEPTOR DOMAIN INTERACTIONS INFLUENCE LIGAND DISSOCIATION AND RECEPTOR STABILITY. Molecular Endocrinology. 1995;9(2):208-18.
326. Benten WPM, Lieberherr M, Giese G, Wrehlke C, Stamm O, Sekeris CE, et al. Functional testosterone receptors in plasma membranes of T cells. Faseb Journal. 1999;13(1):123-33.
327. Benten WPM, Lieberherr M, Stamm O, Wrehlke C, Guo ZY, Wunderlich F. Testosterone signaling through internalizable surface receptors in androgen receptor-free macrophages. Molecular Biology of the Cell. 1999;10(10):3113-23.
328. Rosner W, Hryb DJ, Khan MS, Nakhla AM, Romas NA. Sex hormone-binding globulin mediates steroid hormone signal transduction at the plasma membrane. Journal of Steroid Biochemistry and Molecular Biology. 1999;69(1-6):481-5.
329. Mueller JW, Gilligan LC, Idkowiak J, Arlt W, Foster PA. The Regulation of Steroid Action by Sulfation and Desulfation. Endocrine Reviews. 2015;36(5):526-63.
330. Longcope C. ADRENAL AND GONADAL ANDROGEN SECRETION IN NORMAL FEMALES. Clinics in Endocrinology and Metabolism. 1986;15(2):213-28.
331. Siiteri PK, Wilson JD. TESTOSTERONE FORMATION AND METABOLISM DURING MALE SEXUAL DIFFERENTIATION IN HUMAN EMBRYO. Journal of Clinical Endocrinology & Metabolism. 1974;38(1):113-25.

332. Thigpen AE, Silver RI, Guileyardo JM, Casey ML, McConnell JD, Russell DW. TISSUE DISTRIBUTION AND ONTOGENY OF STEROID 5-ALPHA-REDUCTASE ISOZYME EXPRESSION. Journal of Clinical Investigation. 1993;92(2):903-10.
333. Labrie F. INTRACRINOLOGY. Molecular and Cellular Endocrinology. 1991;78(3):C113-C8.
334. Rubinow KB. An intracrine view of sex steroids, immunity, and metabolic regulation. Molecular Metabolism. 2018;15:92-103.
335. Kamrath C, Hochberg Z, Hartmann MF, Remer T, Wudy SA. Increased Activation of the Alternative "Backdoor" Pathway in Patients with 21-Hydroxylase Deficiency: Evidence from Urinary Steroid Hormone Analysis. Journal of Clinical Endocrinology & Metabolism. 2012;97(3):E367-E75.
336. Schiffer L, Arlt W, Storbeck KH. Intracrine androgen biosynthesis, metabolism and action revisited. Molecular and Cellular Endocrinology. 2018;465(C):4-26.
337. Samson M, Labrie F, Zouboulis CC, Luu-The V. Biosynthesis of Dihydrotestosterone by a Pathway that Does Not Require Testosterone as an Intermediate in the SZ95 Sebaceous Gland Cell Line. Journal of Investigative Dermatology. 2010;130(2):602-4.
338. Du CG, Khalil MW, Sriram S. Administration of dehydroepiandrosterone suppresses experimental allergic encephalomyelitis in SJL/J mice. Journal of Immunology. 2001;167(12):7094-101.
339. Straub RH, Konecna L, Hrach S, Rothe G, Kreutz M, Schölmerich J, et al. Serum Dehydroepiandrosterone (DHEA) and DHEA Sulfate Are Negatively Correlated with Serum Interleukin-6 (IL-6), and DHEA Inhibits IL-6 Secretion from Mononuclear Cells in Man in Vitro: Possible Link between Endocrinosenescence and Immunosenescence. The Journal of Clinical Endocrinology & Metabolism. 1998;83(6):2012-7.
340. Prall SP, Muehlenbein MP. DHEA Modulates Immune Function: A Review of Evidence. Dehydroepiandrosterone. 2018;108:125-44.
341. Mantalaris A, Panoskaltsis N, Sakai Y, Bourne P, Chang CS, Messing EM, et al. Localization of androgen receptor expression in human bone marrow. Journal of Pathology. 2001;193(3):361-6.
342. Chuang KH, Altuwaijri S, Li GH, Lai JJ, Chu CY, Lai KP, et al. Neutropenia with impaired host defense against microbial infection in mice lacking androgen receptor. Journal of Experimental Medicine. 2009;206(5):1181-99.
343. Malkin CJ, Pugh PJ, Jones RD, Kapoor D, Channer KS, Jones TH. The effect of testosterone replacement on endogenous inflammatory cytokines and lipid profiles in hypogonadal men. Journal of Clinical Endocrinology & Metabolism. 2004;89(7):3313-8.
344. Hepworth MR, Hardman MJ, Grencis RK. The role of sex hormones in the development of Th2 immunity in a gender-biased model of Trichuris muris infection. European Journal of Immunology. 2010;40(2):406-16.
345. Keller ET, Chang CS, Ershler WB. Inhibition of NF kappa B activity through maintenance of I kappa B alpha levels contributes to dihydrotestosterone-mediated repression of the interleukin-6 promoter. Journal of Biological Chemistry. 1996;271(42):26267-75.
346. Zhou ZF, Shackleton CHL, Pahwa S, White PC, Speiser PW. Prominent sex steroid metabolism in human lymphocytes. Molecular and Cellular Endocrinology. 1998;138(1-2):61-9.
347. Altuwaijri S, Chuang KH, Lai KP, Lai JJ, Lin HY, Young FM, et al. Susceptibility to Autoimmunity and B Cell Resistance to Apoptosis in Mice Lacking Androgen Receptor in B Cells. Molecular Endocrinology. 2009;23(4):444-53.
348. Zhu ML, Bakhru P, Conley B, Nelson JS, Free M, Martin A, et al. Sex bias in CNS autoimmune disease mediated by androgen control of autoimmune regulator. Nature Communications. 2016;7.
349. Malkin CJ, Pugh PJ, Jones RD, Jones TH, Channer KS. Testosterone as a protective factor against atherosclerosis-immunomodulation and influence upon plaque development and stability. Journal of Endocrinology. 2003;178(3):373-80.
350. Yao QM, Wang B, An XF, Zhang JA, Ding LM. Testosterone level and risk of type 2 diabetes in men: a systematic review and meta-analysis. Endocrine Connections. 2018;7(1):220-31.

351. Pikwer M, Giwercman A, Bergstrom U, Nilsson JA, Jacobsson LTH, Turesson C. Association between testosterone levels and risk of future rheumatoid arthritis in men: a population-based case-control study. Annals of the Rheumatic Diseases. 2014;73(3):573-9.
352. Goemaere S, Ackerman C, Goethals K, Dekeyser F, Vanderstraeten C, Verbruggen G, et al. ONSET OF SYMPTOMS OF RHEUMATOID-ARTHRITIS IN RELATION TO AGE, SEX AND MENOPAUSAL TRANSITION. Journal of Rheumatology. 1990;17(12):1620-2.
353. Hall GM, Larbre JP, Spector TD, Perry LA, DaSilva JAP. A randomized trial of testosterone therapy in males with rheumatoid arthritis. British Journal of Rheumatology. 1996;35(6):568-73.
354. Islander U, Jochems C, Lagerquist MK, Forsblad-d'Elia H, Carlsten H. Estrogens in rheumatoid arthritis; the immune system and bone. Molecular and Cellular Endocrinology. 2011;335(1):14-29.
355. Schmidt M, Hartung R, Capellino S, Cutolo M, Pfeifer-Leeg A, Straub RH. Estrone/17 beta-Estradiol Conversion to, and Tumor Necrosis Factor Inhibition by, Estrogen Metabolites in Synovial Cells of Patients With Rheumatoid Arthritis and Patients With Osteoarthritis. Arthritis and Rheumatism. 2009;60(10):2913-22.
356. Straub RH, Lehle K, Herfarth H, Weber M, Falk W, Preuner J, et al. Dehydroepiandrosterone in relation to other adrenal hormones during an acute inflammatory stressful disease state compared with chronic inflammatory disease: role of interleukin-6 and tumour necrosis factor. European journal of endocrinology. 2002;146(3):365-74.
357. Cutolo M, Foppiani L, Prete C, Ballarino P, Sulli A, Villaggio B, et al. Hypothalamic-pituitary-adrenocortical axis function in premenopausal women with rheumatoid arthritis not treated with glucocorticoids. Journal of Rheumatology. 1999;26(2):282-8.
358. Straub RH, Pongratz G, Scholmerich E, Kees F, Schaible TF, Antoni C, et al. Long-term anti-tumor necrosis factor antibody therapy in rheumatoid arthritis patients sensitizes the pituitary gland and favors adrenal androgen secretion. Arthritis and Rheumatism. 2003;48(6):1504-12.
359. Straub RH, Harle P, Yamana S, Matsuda T, Takasugi K, Kishimoto T, et al. Anti-interleukin-6 receptor antibody therapy favors adrenal androgen secretion in patients with rheumatoid arthritis - A randomized, double-blind, placebo-controlled study. Arthritis and Rheumatism. 2006;54(6):1778-85.
360. van der Goes MC, Straub RH, Wenting MJG, Capellino S, Jacobs JWG, Jahangier ZN, et al. Intra-articular glucocorticoid injections decrease the number of steroid hormone receptor positive cells in synovial tissue of patients with persistent knee arthritis. Annals of the Rheumatic Diseases. 2012;71(9):1552-8.
361. Cutolo M, Seriolo B, Villaggio B, Pizzorni C, Craviotto C, Sulli A. Androgens and estrogens modulate the immune and inflammatory responses in rheumatoid arthritis. Neuroendocrine Immune Basis of the Rheumatic Diseases Ii, Proceedings. 2002;966:131-42.
362. Xu J, Itoh Y, Hayashi H, Takii T, Miyazawa K, Onozaki K. Dihydrotestosterone Inhibits Interleukin-1 alpha or Tumor Necrosis Factor alpha-Induced Proinflammatory Cytokine Production via Androgen Receptor-Dependent Inhibition of Nuclear Factor-kappa B Activation in Rheumatoid Fibroblast-Like Synovial Cell Line. Biological & Pharmaceutical Bulletin. 2011;34(11):1724-30.
363. Castagnetta LA, Carruba G, Granata OM, Stefano R, Miele M, Schmidt M, et al. Increased estrogen formation and estrogen to androgen ratio in the synovial fluid of patients with rheumatoid arthritis. The Journal of Rheumatology. 2003;30(12):2597-605.
364. Macdiarmid F, Wang D, Duncan LJ, Purohit A, Ghilchik MW, Reed MJ. STIMULATION OF AROMATASE-ACTIVITY IN BREAST FIBROBLASTS BY TUMOR-NECROSIS-FACTOR-ALPHA. Molecular and Cellular Endocrinology. 1994;106(1-2):17-21.
365. Schmidt M, Weidler C, Naumann H, Anders S, Scholmerich J, Straub RH. Androgen conversion in osteoarthritis and rheumatoid arthritis synoviocytes - androstenedione and testosterone inhibit estrogen formation and favor production of more potent 5 alpha-reduced androgens. Arthritis Research & Therapy. 2005;7(5):R938-R48.

366. Li ZG, Danis VA, Brooks PM. EFFECT OF GONADAL-STEROIDS ON THE PRODUCTION OF IL-1 AND IL-6 BY BLOOD MONONUCLEAR-CELLS INVITRO. Clinical and Experimental Rheumatology. 1993;11(2):157-62.
367. Taneja V, Behrens M, Mangalam A, Griffiths MM, Luthra HS, David CS. New humanized HLA-DR4-transgenic mice that mimic the sex bias of rheumatoid arthritis. Arthritis and Rheumatism. 2007;56(1):69-78.
368. Kanda N, Tsuchida T, Tamaki K. Testosterone inhibits immunoglobulin production by human peripheral blood mononuclear cells. Clinical and Experimental Immunology. 1996;106(2):410-5.
369. Khalkhali-Ellis Z, Seftor EA, Nieva DRC, Handa RJ, Price RH, Kirschmann DA, et al. Estrogen and progesterone regulation of human fibroblast-like synoviocyte function in vitro: Implications in rheumatoid arthritis. Journal of Rheumatology. 2000;27(7):1622-31.
370. Lee GT, Kim JH, Kwon SJ, Stein MN, Hong JH, Nagaya N, et al. Dihydrotestosterone Increases Cytotoxic Activity of Macrophages on Prostate Cancer Cells via TRAIL. Endocrinology. 2019;160(9):2049-60.
371. Becerra-Diaz M, Strickland AB, Keselman A, Heller NM. Androgen and Androgen Receptor as Enhancers of M2 Macrophage Polarization in Allergic Lung Inflammation. Journal of Immunology. 2018;201(10):2923-33.
372. D'Agostino P, Milano S, Barbera C, Di Bella G, La Rosa M, Ferlazzo V, et al. Sex hormones modulate inflammatory mediators produced by macrophages. Neuroendocrine Immune Basis of the Rheumatic Diseases. 1999;876:426-9.
373. Hennebold JD, Daynes RA. REGULATION OF MACROPHAGE DEHYDROEPIANDROSTERONE-SULFATE METABOLISM BY INFLAMMATORY CYTOKINES. Endocrinology. 1994;135(1):67-75.
374. Milewich L, Kaimal V, Toews GB. ANDROSTENEDIONE METABOLISM IN HUMAN ALVEOLAR MACROPHAGES. Journal of Clinical Endocrinology & Metabolism. 1983;56(5):920-4.
375. Schmidt M, Kreutz M, Loffler G, Scholmerich J, Straub RH. Conversion of dehydroepiandrosterone to downstream steroid hormones in macrophages. Journal of Endocrinology. 2000;164(2):161-9.
376. Batty MJ, Chabrier G, Sheridan A, Gage MC. Metabolic Hormones Modulate Macrophage Inflammatory Responses. Cancers. 2021;13(18).
377. Shozu M, Zhao Y, Simpson ER. Estrogen biosynthesis in THP1 cells is regulated by promoter switching of the aromatase (CYP19) gene. Endocrinology. 1997;138(12):5125-35.
378. Watanabe M, Ohno S, Wachi H. Effect of beta-agonist on the dexamethasone-induced expression of aromatase by the human monocyte cells. Endocrine Connections. 2017;6(2):82-8.
379. Rettew JA, Huet-Hudson YM, Marriott I. Testosterone reduces macrophage expression in the mouse of toll-like receptor 4, a trigger for inflammation and innate immunity. Biology of Reproduction. 2008;78(3):432-7.
380. Benten WPM, Guo Z, Krucken J, Wunderlich F. Rapid effects of androgens in macrophages. Steroids. 2004;69(8-9):585-90.
381. Cutolo M, Capellino S, Montagna P, Ghiorzo P, Sulli A, Villaggio B. Sex hormone modulation of cell growth and apoptosis of the human monocytic/macrophage cell line. Arthritis Research & Therapy. 2005;7(5):R1124-R32.
382. Corcoran MP, Meydani M, Lichtenstein AH, Schaefer EJ, Dillard A, Lamon-Fava S. Sex hormone modulation of proinflammatory cytokine and C-reactive protein expression in macrophages from older men and postmenopausal women. Journal of Endocrinology. 2010;206(2):217-24.
383. Friedl R, Brunner M, Moeslinger T, Spieckermann PG. Testosterone inhibits expression of inducible nitric oxide synthase in murine macrophages. Life Sciences. 2000;68(4):417-29.
384. Liu LM, Benten WPM, Wang LY, Hao XF, Li QL, Zhang HP, et al. Modulation of Leishmania donovani infection and cell viability by testosterone in bone marrow-derived macrophages: Signaling via surface binding sites. Steroids. 2005;70(9):604-14.

385. Cao J, Li Q, Shen XH, Yao Y, Li LL, Ma HT. Dehydroepiandrosterone attenuates LPS-induced inflammatory responses via activation of Nrf2 in RAW264.7 macrophages. Molecular Immunology. 2021;131:97-111.
386. Cao J, Li LL, Yao Y, Xing YX, Ma HT. Dehydroepiandrosterone exacerbates nigericin-induced abnormal autophagy and pyroptosis via GPER activation in LPS-primed macrophages. Cell Death & Disease. 2022;13(4).
387. Rom WN, Harkin T. DEHYDROEPIANDROSTERONE INHIBITS THE SPONTANEOUS RELEASE OF SUPEROXIDE RADICAL BY ALVEOLAR MACROPHAGES INVITRO IN ASBESTOSIS. Environmental Research. 1991;55(2):145-56.
388. Cutolo M, Accardo S, Villaggio B, Barone A, Sulli A, Coviello DA, et al. Androgen and estrogen receptors are present in primary cultures of human synovial macrophages. Journal of Clinical Endocrinology & Metabolism. 1996;81(2):820-7.
389. Cutolo M, Accardo S, Villaggio B, Clerico P, Indiveri F, Carruba G, et al. EVIDENCE FOR THE PRESENCE OF ANDROGEN RECEPTORS IN THE SYNOVIAL TISSUE OF RHEUMATOID-ARTHRITIS PATIENTS AND HEALTHY CONTROLS. Arthritis and Rheumatism. 1992;35(9):1007-15.
390. Cutolo M, Accardo S, Villaggio B, Barone A, Sulli A, Balleari E, et al. ANDROGEN METABOLISM AND INHIBITION OF INTERLEUKIN-1 SYNTHESIS IN PRIMARY CULTURED HUMAN SYNOVIAL MACROPHAGES. Mediators of Inflammation. 1995;4(2):138-43.
391. Cutolo M, Villaggio B, Barone A, Sulli A, Accardo S, Granata OM, et al. Primary cultures of human synovial macrophages metabolize androgens. Basis for Cancer Management. 1996;784:534-41.
392. Rontzsch A, Thoss K, Petrow PK, Henzgen S, Brauer R. Amelioration of murine antigen-induced arthritis by dehydroepiandrosterone (DHEA). Inflammation Research. 2004;53(5):189-98.
393. Steward A, Bayley DL. EFFECTS OF ANDROGENS IN MODELS OF RHEUMATOID-ARTHRITIS. Agents and Actions. 1992;35(3-4):268-72.
394. Cutolo M, Giusti M, Villaggio B, Barone A, Accardo S, Sulli A, et al. Testosterone metabolism and cyclosporin A treatment in rheumatoid arthritis. British Journal of Rheumatology. 1997;36(4):433-9.
395. Attur MG, Patel R, Thakker G, Vyas P, Levartovsky D, Patel P, et al. Differential anti-inflammatory effects of immunosuppressive drugs: Cyclosporin, rapamycin and FK-506 on inducible nitric oxide synthase, nitric oxide, cyclooxygenase-2 and PGE(2) production. Inflammation Research. 2000;49(1):20-6.
396. Goodwin S, McPherson JD, McCombie WR. Coming of age: ten years of next-generation sequencing technologies. Nature Reviews Genetics. 2016;17(6):333-51.
397. National, Health If. Accelerating Medicines Partnership® (AMP®) 2014 [Available from: https://www.nih.gov/research-training/accelerating-medicines-partnership-amp.
398. Krenn V, Morawietz L, Haupl T, Neidel J, Petersen I, Konig A. Grading of chronic synovitis - A histopathological grading system for molecular and diagnostic pathology. Pathology Research and Practice. 2002;198(5):317-25.
399. Lash GE, Pinto LA. Multiplex cytokine analysis technologies. Expert Review of Vaccines. 2010;9(10):1231-7.
400. Manferdini C, Saleh Y, Dolzani P, Gabusi E, Trucco D, Filardo G, et al. Impact of Isolation Procedures on the Development of a Preclinical Synovial Fibroblasts/Macrophages in an In Vitro Model of Osteoarthritis. Biology-Basel. 2020;9(12).
401. Mahida RY, Scott A, Parekh D, Lugg ST, Belchamber KBR, Hardy RS, et al. Assessment of Alveolar Macrophage Dysfunction Using an in vitro Model of Acute Respiratory Distress Syndrome. Frontiers in Medicine. 2021;8.
402. Fenske M. Determination of cortisol and cortisone in human morning and overnight urine by thin-layer chromatography and fluorescence derivatisation with isonicotinic acid hydrazide. Chromatographia. 2000;52(11-12):810-4.

403. Want EJ, Cravatt BF, Siuzdak G. The expanding role of mass spectrometry in metabolite profiling and characterization. Chembiochem. 2005;6(11):1941-51.
404. Malvern Instruments Limited L. A Basic Introduction to Rheology 2016.
405. Tamai I, Nezu J, Uchino H, Sai Y, Oku A, Shimane M, et al. Molecular identification and characterization of novel members of the human organic anion transporter (OATP) family. Biochemical and Biophysical Research Communications. 2000;273(1):251-60.
406. Nobel CSI, Dunas F, Abrahmsen LB. Purification of full-length recombinant human and rat type 1 11 beta-hydroxysteroid dehydrogenases with retained oxidoreductase activities. Protein Expression and Purification. 2002;26(3):349-56.
407. Andersson S, Russell DW. STRUCTURAL AND BIOCHEMICAL-PROPERTIES OF CLONED AND EXPRESSED HUMAN AND RAT STEROID 5-ALPHA-REDUCTASES. Proceedings of the National Academy of Sciences of the United States of America. 1990;87(10):3640-4.
408. Lukacik P, Keller B, Bunkoczi G, Kavanagh K, Lee WH, Adamski J, et al. Structural and biochemical characterization of human orphan DHRS10 reveals a novel cytosolic enzyme with steroid dehydrogenase activity. Biochemical Journal. 2007;402:419-27.
409. Steckelbroeck S, Jin Y, Gopishetty S, Oyesanmi B, Penning TM. Human cytosolic 3 alpha-hydroxysteroid dehydrogenases of the aldo-keto reductase superfamily display significant 3 beta-hydroxysteroid dehydrogenase activity - Implications for steroid hormone metabolism and action. Journal of Biological Chemistry. 2004;279(11):10784-95.
410. Kratz A, Lewandrowski KB. Normal reference laboratory values. New England Journal of Medicine. 1998;339(15):1063-72.
411. Qian XX, Droste SK, Lightman SL, Reul J, Linthorst ACE. Circadian and Ultradian Rhythms of Free Glucocorticoid Hormone Are Highly Synchronized between the Blood, the Subcutaneous Tissue, and the Brain. Endocrinology. 2012;153(9):4346-53.
412. Khoromi S, Muniyappa R, Nackers L, Gray N, Baldwin H, Wong KA, et al. Effects of chronic osteoarthritis pain on neuroendocrine function in men. Journal of Clinical Endocrinology & Metabolism. 2006;91(11):4313-8.
413. Brown TJ, Laurent UBG, Fraser JRE. TURNOVER OF HYALURONAN IN SYNOVIAL JOINTS - ELIMINATION OF LABELED HYALURONAN FROM THE KNEE-JOINT OF THE RABBIT. Experimental Physiology. 1991;76(1):125-34.
414. Levick JR, McDonald JN. FLUID MOVEMENT ACROSS SYNOVIUM IN HEALTHY JOINTS - ROLE OF SYNOVIAL-FLUID MACROMOLECULES. Annals of the Rheumatic Diseases. 1995;54(5):417-23.
415. Oster H, Challet E, Ott V, Arvat E, de Kloet ER, Dijk DJ, et al. The Functional and Clinical Significance of the 24-Hour Rhythm of Circulating Glucocorticoids. Endocrine Reviews. 2017;38(1):3-45.
416. Turcu AF, Nanba AT, Chomic R, Upadhyay SK, Giordano TJ, Shields JJ, et al. Adrenal-derived 11-oxygenated 19-carbon steroids are the dominant androgens in classic 21-hydroxylase deficiency. European Journal of Endocrinology. 2016;174(5):601-9.
417. McWhorter FY, Wang TT, Nguyen P, Chung T, Liu WF. Modulation of macrophage phenotype by cell shape. Proceedings of the National Academy of Sciences of the United States of America. 2013;110(43):17253-8.
418. Mantovani A, Sica A, Sozzani S, Allavena P, Vecchi A, Locati M. The chemokine system in diverse forms of macrophage activation and polarization. Trends in Immunology. 2004;25(12):677-86.
419. Buechler C, Ritter M, Orso E, Langmann T, Klucken J, Schmitz G. Regulation of scavenger receptor CD163 expression in human monocytes and macrophages by pro- and antiinflammatory stimuli. Journal of Leukocyte Biology. 2000;67(1):97-103.
420. Mosser DM, Edwards JP. Exploring the full spectrum of macrophage activation. Nature Reviews Immunology. 2008;8(12):958-69.

421. Sakito S, Ueki Y, Eguchi K, Kawabe Y, Nagataki S. SERUM CYTOKINES IN PATIENTS WITH RHEUMATOID-ARTHRITIS - CORRELATION OF INTERFERON-GAMMA AND TUMOR-NECROSIS-FACTOR-ALPHA WITH THE CHARACTERISTICS OF PERIPHERAL-BLOOD MONONUCLEAR-CELLS. Rheumatology International. 1995;15(1):31-7.
422. van der Goes A, Hoekstra K, van den Berg TK, Dijkstra CD. Dexamethasone promotes phagocytosis and bacterial killing by human monocytes/macrophages in vitro. Journal of Leukocyte Biology. 2000;67(6):801-7.
423. Taylor AE, Finney-Hayward TK, Quint JK, Thomas CMR, Tudhope SJ, Wedzicha JA, et al. Defective macrophage phagocytosis of bacteria in COPD. European Respiratory Journal. 2010;35(5):1039-47.
424. Zwet TL, Thompson J, Furth R. Effect of glucocorticosteroids on the phagocytosis and intracellular killing by peritoneal macrophages. Infect Immun. 1975;12(4):699-705.
425. Olivares-Morales MJ, De la Fuente MK, Dubois-Camacho K, Parada D, Diaz-Jimenez D, Torres-Riquelme A, et al. Glucocorticoids Impair Phagocytosis and Inflammatory Response Against Crohn's Disease-Associated Adherent-Invasive Escherichia coli. Frontiers in Immunology. 2018;9.
426. Schulz D, Severin Y, Zanotelli VRT, Bodenmiller B. In-Depth Characterization of Monocyte-Derived Macrophages using a Mass Cytometry-Based Phagocytosis Assay. Scientific Reports. 2019;9.
427. Vlahos R, Bozinovski S. Role of alveolar macrophages in chronic obstructive pulmonary disease. Frontiers in Immunology. 2014;5.
428. Gottfried-Blackmore A, Sierra A, Jellinck PH, McEwen BS, Bulloch K. Brain microglia express steroid-converting enzymes in the mouse. Journal of Steroid Biochemistry and Molecular Biology. 2008;109(1-2):96-107.
429. Capellino S, Straub RH, Cutolo M. Aromatase and regulation of the estrogen-to-androgen ratio in synovial tissue inflammation: common pathway in both sexes. Steroids in Neuroendocrine Immunology and Therapy of Rheumatic Diseases I. 2014;1317:24-31.
430. Suzuki-Yamamoto T, Nishizawa M, Fukui M, Okuda-Ashitaka E, Nakajima T, Ito S, et al. cDNA cloning, expression and characterization of human prostaglandin F synthase. Febs Letters. 1999;462(3):335-40.
431. Zhou QQ, Tian W, Jiang ZY, Huang TT, Ge C, Liu TF, et al. A Positive Feedback Loop of AKR1C3-Mediated Activation of NF-kappa B and STAT3 Facilitates Proliferation and Metastasis in Hepatocellular Carcinoma. Cancer Research. 2021;81(5):1361-74.
432. Wink DA, Hines HB, Cheng RYS, Switzer CH, Flores-Santana W, Vitek MP, et al. Nitric oxide and redox mechanisms in the immune response. Journal of Leukocyte Biology. 2011;89(6):873-91.
433. Xu WW, Schiffer L, Qadir MMF, Zhang YQ, Hawley J, De Sa PM, et al. Intracrine Testosterone Activation in Human Pancreatic beta-Cells Stimulates Insulin Secretion. Diabetes. 2020;69(11):2392-9.
434. Scotland RS, Stables MJ, Madalli S, Watson P, Gilroy DW. Sex differences in resident immune cell phenotype underlie more efficient acute inflammatory responses in female mice. Blood. 2011;118(22):5918-27.
435. Ganesan K, Balachandran C, Manohar BM, Puvanakrishnan R. Effects of testosterone, estrogen and progesterone on TNF-alpha mediated cellular damage in rat arthritic synovial fibroblasts. Rheumatology International. 2012;32(10):3181-8.
436. Habib G, Jabbour A, Artul S, Hakim G. Intra-articular methylprednisolone acetate injection at the knee joint and the hypothalamic-pituitary-adrenal axis: a randomized controlled study. Clinical Rheumatology. 2014;33(1):99-103.
437. Owen SG, Francis HW, Roberts MS. DISAPPEARANCE KINETICS OF SOLUTES FROM SYNOVIAL-FLUID AFTER INTRAARTICULAR INJECTION. British Journal of Clinical Pharmacology. 1994;38(4):349-55.

438. Uson J, Rodriguez-Garcia SC, Castellanos-Moreira R, O'Neill TW, Doherty M, Boesen M, et al. EULAR recommendations for intra-articular therapies. Annals of the Rheumatic Diseases. 2021;80(10):1299-305.
439. Oliveira IM, Fernandes DC, Cengiz IF, Reis RL, Oliveira JM. Hydrogels in the treatment of rheumatoid arthritis: drug delivery systems and artificial matrices for dynamic in vitro models. Journal of Materials Science-Materials in Medicine. 2021;32(7).
440. Cooke ME, Jones SW, ter Horst B, Moiemen N, Snow M, Chouhan G, et al. Structuring of Hydrogels across Multiple Length Scales for Biomedical Applications. Advanced Materials. 2018;30(14).
441. Silva-Correia J, Zavan B, Vindigni V, Silva TH, Oliveira JM, Abatangelo G, et al. Biocompatibility Evaluation of Ionic- and Photo-Crosslinked Methacrylated Gellan Gum Hydrogels: In Vitro and In Vivo Study. Advanced Healthcare Materials. 2013;2(4):568-75.
442. Rastogi AK, Davis KW, Ross A, Rosas HG. Fundamentals of Joint Injection. American Journal of Roentgenology. 2016;207(3):484-94.
443. Barrera P, Blom A, van Lent P, van Bloois L, Beijnen JH, van Rooijen N, et al. Synovial macrophage depletion with clodronate-containing liposomes in rheumatoid arthritis. Arthritis and Rheumatism. 2000;43(9):1951-9.
444. Hofkens W, Grevers LC, Walgreen B, de Vries TJ, Leenen PJM, Everts V, et al. Intravenously delivered glucocorticoid liposomes inhibit osteoclast activity and bone erosion in murine antigen-induced arthritis. Journal of Controlled Release. 2011;152(3):363-9.
445. Metselaar JM, van den Berg WB, Holthuysen AEM, Wauben MHM, Storm G, van Lent PLEM. Liposomal targeting of glucocorticoids to synovial lining cells strongly increases therapeutic benefit in collagen type II arthritis. Annals of the rheumatic diseases. 2004;63(4):348-53.
446. Hofkens W, Schelbergen R, Storm G, van den Berg WB, van Lent PL. Liposomal Targeting of Prednisolone Phosphate to Synovial Lining Macrophages during Experimental Arthritis Inhibits M1 Activation but Does Not Favor M2 Differentiation. Plos One. 2013;8(2).
447. Joshi N, Yan J, Levy S, Bhagchandani S, Slaughter KV, Sherman NE, et al. Towards an arthritis flare-responsive drug delivery system. Nature Communications. 2018;9.
448. Abou-ElNour M, Soliman ME, Skouras A, Casettari L, Geneidi AS, Ishak RAH. Microparticles-in-Thermoresponsive/Bioadhesive Hydrogels as a Novel Integrated Platform for Effective Intra-articular Delivery of Triamcinolone Acetonide. Molecular Pharmaceutics. 2020;17(6):1963-78.
449. Kang KS, Veeder GT, Mirrasoul PJ, Kaneko T, Cottrell IW. AGAR-LIKE POLYSACCHARIDE PRODUCED BY A PSEUDOMONAS SPECIES - PRODUCTION AND BASIC PROPERTIES. Applied and Environmental Microbiology. 1982;43(5):1086-91.
450. Hoffman AS. Hydrogels for biomedical applications. Advanced Drug Delivery Reviews. 2002;54(1):3-12.
451. Garrec DA, Norton IT. Understanding fluid gel formation and properties. Journal of Food Engineering. 2012;112(3):175-82.
452. Lei YT, Wang XK, Liao JY, Shen JL, Li YL, Cai ZW, et al. Shear-responsive boundary-lubricated hydrogels attenuate osteoarthritis. Bioactive Materials. 2022;16:472-84.
453. Cai ZX, Zhang HB, Wei Y, Wu M, Fu AL. Shear-thinning hyaluronan-based fluid hydrogels to modulate viscoelastic properties of osteoarthritis synovial fluids. Biomaterials Science. 2019;7(8):3143-57.
454. Grasdalen H, Smidsrod O. GELATION OF GELLAN GUM. Carbohydrate Polymers. 1987;7(5):371-93.
455. Chen MH, Wang LL, Chung JJ, Kim YH, Atluri P, Burdick JA. Methods To Assess Shear-Thinning Hydrogels for Application As Injectable Biomaterials. Acs Biomaterials Science & Engineering. 2017;3(12):3146-60.

456. Oliveira JT, Santos TC, Martins L, Picciochi R, Marques AP, Castro AG, et al. Gellan Gum Injectable Hydrogels for Cartilage Tissue Engineering Applications: In Vitro Studies and Preliminary In Vivo Evaluation. Tissue Engineering Part A. 2010;16(1):343-53.
457. ter Horst B, Moakes RJA, Chouhan G, Williams RL, Moiemen NS, Grover LM. A gellan-based fluid gel carrier to enhance topical spray delivery. Acta Biomaterialia. 2019;89:166-79.
458. Zhuang ZM, Zhang Y, Sun SN, Li Q, Chen KW, An CF, et al. Control of Matrix Stiffness Using Methacrylate-Gelatin Hydrogels for a Macrophage-Mediated Inflammatory Response. Acs Biomaterials Science & Engineering. 2020;6(5):3091-102.
459. Li ZQ, Bratlie KM. How Cross-Linking Mechanisms of Methacrylated Gellan Gum Hydrogels Alter Macrophage Phenotype. Acs Applied Bio Materials. 2019;2(1):217-25.
460. Oliveira IM, Goncalves C, Shin ME, Lee S, Reis RL, Khang G, et al. Enzymatically crosslinked tyramine-gellan gum hydrogels as drug delivery system for rheumatoid arthritis treatment. Drug Delivery and Translational Research. 2021;11(3):1288-300.
461. Zhang P, Liu WZ, Peng YF, Han BQ, Yang Y. Toll like receptor 4 (TLR4) mediates the stimulating activities of chitosan oligosaccharide on macrophages. International Immunopharmacology. 2014;23(1):254-61.
462. Herre J, Marshall ASJ, Caron E, Edwards AD, Williams DL, Schweighoffer E, et al. Dectin-1 uses novel mechanisms for yeast phagocytosis in macrophages. Blood. 2004;104(13):4038-45.
463. Xu ZH, Li ZQ, Jiang S, Bratlie KM. Chemically Modified Gellan Gum Hydrogels with Tunable Properties for Use as Tissue Engineering Scaffolds. Acs Omega. 2018;3(6):6998-7007.
464. Torsteinsdottir I, Hakansson L, Hallgren R, Gudbjornsson B, Arvidson NG, Venge P. Serum lysozyme: a potential marker of monocyte/macrophage activity in rheumatoid arthritis. Rheumatology. 1999;38(12):1249-54.
465. Bennett RM, Skosey JL. LACTOFERRIN AND LYSOZYME LEVELS IN SYNOVIAL-FLUID - DIFFERENTIAL INDEXES OF ARTICULAR INFLAMMATION AND DEGRADATION. Arthritis and Rheumatism. 1977;20(1):84-90.
466. Goldie I, Nachemson A. SYNOVIAL PH IN RHEUMATOID KNEE-JOINTS .I. EFFECT OF SYNOVECTOMY. Acta Orthopaedica Scandinavica. 1969;40(5):634-+.
467. Picone CSF, Cunha RL. Influence of pH on formation and properties of gellan gels. Carbohydrate Polymers. 2011;84(1):662-8.
468. Zhou SW, Zheng XM, Yi K, Du XC, Wang C, Cui PF, et al. Temperature-Ion-pH Triple Responsive Gellan Gum as In Situ Hydrogel for Long-Acting Cancer Treatment. Gels. 2022;8(8).
469. Ma Y, Ren S, Pandak WM, Li X, Ning Y, Lu C, et al. The effects of inflammatory cytokines on steroidogenic acute regulatory protein expression in macrophages. Inflammation Research. 2007;56(12):495-501.
470. Nasiri M, Nikolaou N, Parajes S, Krone NP, Valsamakis G, Mastorakos G, et al. 5 alpha-Reductase Type 2 Regulates Glucocorticoid Action and Metabolic Phenotype in Human Hepatocytes. Endocrinology. 2015;156(8):2863-71.
471. Jin RJ, Forbes C, Miller NL, Strand D, Case T, Cates JM, et al. Glucocorticoids are induced while dihydrotestosterone levels are suppressed in 5-alpha reductase inhibitor treated human benign prostate hyperplasia patients. Prostate. 2022;82(14):1378-88.
472. Kanda N, Tsuchida T, Tamaki K. Testosterone suppresses anti-DNA antibody production in peripheral blood mononuclear cells from patients with systemic lupus erythematosus. Arthritis and Rheumatism. 1997;40(9):1703-11.
473. Araneo BA, Dowell T, Diegel M, Daynes RA. DIHYDROTESTOSTERONE EXERTS A DEPRESSIVE INFLUENCE ON THE PRODUCTION OF INTERLEUKIN-4 (IL-4), IL-5, AND GAMMA-INTERFERON, BUT NOT IL-2 BY ACTIVATED MURINE T-CELLS. Blood. 1991;78(3):688-99.
474. Barth ND, Van Dalen FJ, Karmakar U, Bertolini M, Mendive-Tapia L, Kitamura T, et al. Enzyme-Activatable Chemokine Conjugates for In Vivo Targeting of Tumor-Associated Macrophages. Angewandte Chemie-International Edition. 2022;61(41).

475. Svendsen P, Graversen JH, Etzerodt A, Hager H, Roge R, Gronbaek H, et al. Antibody-Directed Glucocorticoid Targeting to CD163 in M2-type Macrophages Attenuates Fructose-Induced Liver Inflammatory Changes. Molecular Therapy-Methods & Clinical Development. 2017;4:50-61.
476. Booij A, Biewengabooij CM, HuberBruning O, Cornelis C, Jacobs JWG, Bijlsma JWJ. Androgens as adjuvant treatment in postmenopausal female patients with rheumatoid arthritis. Annals of the Rheumatic Diseases. 1996;55(11):811-5.
477. Dietz AB, Bulur PA, Emery RL, Winters JL, Epps DE, Zubair AC, et al. A novel source of viable peripheral blood mononuclear cells from leukoreduction system chambers. Transfusion. 2006;46(12):2083-9.
478. Pfeiffer IA, Zinser E, Strasser E, Stein MF, Dorrie J, Schaft N, et al. Leukoreduction system chambers are an efficient, valid, and economic source of functional monocyte-derived dendritic cells and lymphocytes. Immunobiology. 2013;218(11):1392-401.
479. Brambilla DJ, Matsumoto AM, Araujo AB, McKinlay JB. The Effect of Diurnal Variation on Clinical Measurement of Serum Testosterone and Other Sex Hormone Levels in Men. Journal of Clinical Endocrinology & Metabolism. 2009;94(3):907-13.
480. Wang Q, Wurtz P, Auro K, Morin-Papunen L, Kangas AJ, Soininen P, et al. Effects of hormonal contraception on systemic metabolism: cross-sectional and longitudinal evidence. International Journal of Epidemiology. 2016;45(5):1445-57.
481. Bell RD, Wu EK, Rudmann CA, Forney M, Kaiser CRW, Wood RW, et al. Selective Sexual Dimorphisms in Musculoskeletal and Cardiopulmonary Pathologic Manifestations and Mortality Incidence in the Tumor Necrosis Factor-Transgenic Mouse Model of Rheumatoid Arthritis. Arthritis & Rheumatology. 2019;71(9):1512-23.